Fall 2014

Synthesis of inhibitors targeting the downstream enzymes in the isoprenoid biosynthetic pathways

Xiang Zhou
University of Iowa

SYNTHESIS OF INHIBITORS TARGETING THE DOWNSTREAM ENZYMES IN THE ISOPRENOID BIOSYNTHETIC PATHWAYS

by

Xiang Zhou

A thesis submitted in partial fulfillment
of the requirements for the
Doctor of Philosophy degree in Chemistry
in the Graduate College of
The University of Iowa

December 2014

Thesis Supervisor: Professor David F. Wiemer

Graduate College
The University of Iowa
Iowa City, Iowa

CERTIFICATE OF APPROVAL

PH.D. THESIS

This is to certify that the Ph.D. thesis of

Xiang Zhou

has been approved by the Examining Committee
for the thesis requirement for the Doctor of Philosophy
degree in Chemistry at the December 2014 graduation.

Thesis Committee:
David F. Wiemer, Thesis Supervisor

Sarah A. Holstein

James B. Gloer

F. Christopher Pigge

M. Lei Geng

To my parents and grandparents

A single sunbeam is enough to drive away many shadows
St. Francis of Assisi

ACKNOWLEDGEMENTS

It has been a long journey to grow from an elementary school student with curiosity about everything in this world to a Ph.D. student who has finally been well educated. For an international student, such as me, to pursue a degree and a career overseas, I have found many challenges, including different languages, cultures, environments, and especially the long distance back to my home. However, on the other hand, it has been such an exciting experience to live in a very different country to make great friends and have a brand new life. When I look back over the past few years, I have many people to thank for their generous help, encouragement, and friendship.

The first and the most important people I want to thank are my parents. Although I am not patient enough to follow all of their cautions for me, in my heart, I know that they are always my most powerful supporters. They have been trying to solve all my troubles, leaving me to pursue my desired career without worries. One thing I deeply regret is that I cannot visit them more often. But completion of my doctoral degree will be the best present to return their love.

Another important person that I would like to thank is my Ph.D. mentor, Dr. David Wiemer. As an advisor, he is intelligent and gives me tremendously helpful suggestions and ideas to guide me to solve my research projects. As a colleague, he always tries to understand and offers his generous help. Without Dr. Wiemer, I cannot image how I would have obtained my doctoral degree today. The same appreciation is given to my advisor at University of San Francisco, Dr. Hyunshun Shin. Not only did she bring me from China to the U.S., but I was well trained by her in many lab skills. She encouraged my interest in organic synthesis and led me to this career pathway.

I also want to express my appreciation to Dr. James Gloer, Dr. Chris Pigge, Dr. Sarah Holstein, Dr. Lei Geng, and Dr. Alexei Tivanski for serving as my committee members. Beside my academic advisors, I have learned much from my supervisors in industry as well, including Dr. Jiangbing Zhang (Novartis), Dr. Brian Lawhorn (GlaxoSmithKline) and Dr. David Washburn (GlaxoSmithKline). In this tough job market, they have acted as a "catalyst" to help me transfer from an academic environment to pharmaceutical industry and to develop my future career. I also have made great friends in the lab. I will never forget how Rocky Barney, Natalie Ulrich, Rebekah Richardson, and John Kodet helped me when I first joined Dr. Wiemer's group as a freshman. I also have a great friendship with Jaci Smits; she took care of me as if she was a big sister. With these friends, we spent many good times, both in lab and off work. I never felt I was lonely even in a foreign country. In my last couple of years in the lab, I also enjoyed working with my lab mates, Veronica Wills and Katie Loerch. Both of them shared fun times with me and made great contributions to my research as noted in my thesis. I want to express the same appreciation to Dr. Hohl's group, including Brian Wasko, Jacki Reilly, and to Dr. Holstein's group, including Ella Born, and Sarah Ferree, for running bioassays on my compounds. At the end, I would like to especially thank my girlfriend, Yan Hu. She jumped into my tedious single life, sparked the light of my future and brought me to happiness.

When I first time stepped onto the land of United States seven years ago, I could never image I would obtain a doctoral degree and enjoy a life with the blazing colors of today. This thesis is written for all the remarkable people I would like to acknowledge.

ABSTRACT

The nitrogenous bisphosphonates pamidronate, alendronate, risedronate, and zoledronate are used clinically in the treatment of bone disease. All of these drugs inhibit the enzyme farnesyl diphosphate synthase (FDPS), which mediates production of farnesyl diphosphate (FPP). However, because it is a branch point in isoprenoid biosynthesis, FPP is involved in the biosynthesis of several different substrates at the same time.

One key enzyme downstream of FDPS in isoprenoid biosynthesis is geranylgeranyl diphosphate synthase (GGDPS) which affords the geranylgeranyl diphosphate (GGPP) necessary for prenylation of the small GTPases such as Ras, Rab, Rho and Rac, that are important signaling proteins. Non-nitrogenous analogues of the clinical drugs, including mono- and bisisoprenoid bisphosphonates, have been developed more recently. These new analogues have been found to inhibit GGDPS selectively. Because it is important to inhibit the generation of GGPP, selective inhibition of GGDPS is highly desirable. In previous research, digeranyl bisphosphonate (DGBP) was discovered to show good inhibition of GGDPS. In order to obtain more potent analogues of the compound DGBP**,** and to study the biological effect of an α–alkoxy group on bisphosphonate compounds, a series of ether bisphosphonates has been prepared and studied.

A second important enzyme in isoprenoid biosynthesis is geranylgeranyl transferase II (GGTase II). This enzyme transfers GGPP to Rab proteins, and thus converts the parent proteins to lipoproteins which are essential for their proper cellular

localization. One known inhibitor of this enzyme is the chemical 3-PEHPC, but a high concentration of this compound is necessary to generate any cellular effects. In an effort to study the cellular effects that result from inhibition of this enzyme, and to develop more potent inhibitors, my research has focused on modification of 3-PEHPC to obtain derivatives that may have improved biological activity. Both the known compounds 3-PEHPC and 3-PEPC, and new structures, including the first generation PEHPC *N*-oxides and the second-generation compounds prepared through click chemistry, have been prepared and tested for activity in this system.

PUBLIC ABSTRACT

The nitrogenous bisphosphonates pamidronate, alendronate, risedronate, and zoledronate are used clinically in the treatment of bone disease. All of these drugs inhibit the enzyme farnesyl diphosphate synthase (FDPS), which mediates production of farnesyl diphosphate (FPP). However, FPP is involved in the biosynthesis of multiple other isoprenoids.

One key enzyme downstream of FDPS in isoprenoid biosynthesis is geranylgeranyl diphosphate synthase (GGDPS) which affords the geranylgeranyl diphosphate (GGPP) necessary for prenylation of the small GTPases that are important signaling proteins. Recently, non-nitrogenous analogues of the clinically used bisphosphonates have been found to inhibit GGDPS selectively, and are of interest because of their activity in biological systems. In order to obtain more potent analogues of the compound digeranyl bisphosphonate (DGBP), which has demonstrated a strong potency against GGDPS**,** a series of ether bisphosphonates has been prepared and studied.

A second important enzyme involving isoprenoids is geranylgeranyl transferase II (GGTase II). This enzyme transfers GGPP to Rab proteins, and thus converts the parent proteins to lipoproteins which are essential for their proper cellular localization. One known inhibitor of this enzyme is the chemical 3-PEHPC, but a high concentration of this compound is necessary to generate any cellular effects. In an effort to study the cellular effects that result from inhibition of this enzyme, my research has focused on modification of 3-PEHPC to obtain derivatives that may have improved biological activity.

More potent inhibitors have been developed to selectively target GGDPS or GGTase II that will lead to a better understanding of the mevalonate pathways.

TABLE OF CONTENTS

LIST OF TABLES

Table

LIST OF FIGURES

Figure

LIST OF ABBREVIATIONS

Ac	acetate
Anal.	analysis
Aq	aqueous
ATP	adenosine triphosphate
BINAP	2,2’-bis(diphenylphosphino)-1,1’-binaphthyl
br	broad
BRSM	based on recovered starting material
Bu	butyl
C	Celsius
cal	calories
calcd	calculated
COX	cyclooxygenase
DBU	1,8-diazabicylco[5.4.0]undec-7-ene
d	doublet
dba	dibenzylideneacetone
dd	doublet of doublets
DDQ	2,3–dichloro–5,6–dicyano–1,4–benzoquinone
DEAD	diethyl azodicarboxylate
DFP	diisopropyl phosphofluoridate
DIBAL	diisobutylaluminum hydride
DIPEA	diisopropylethylamine
DMAP	dimethylallyl pyrophosphate
DMF	dimethylformamide
DMS	dimethyl sulfide
DNA	deoxyribonucleic acid

DoM	directed *ortho*–metalation
dt	doublet of triplets
EAS	electrophilic aromatic substitution
ee	enantiomeric excess
EI	electron impact
ES	electrospray
Et	ethyl
g	gram
GC-MS	gas chromatography-mass spectrometry
hr	hour
HIV	human immunodeficiency virus
HPLC	high performance liquid chromatography
HRMS	high resolution mass spectroscopy
HWE	Horner–Wadsworth–Emmons
Hz	hertz
IPP	isopentenyl pyrophosphate
iPr	isopropyl
J	coupling constant
KB	oral carcinoma cell line
KHMDS	potassium hexamethyldisilyl azide
LA	Lewis acid
5-LOX	5-lipooxygenase
m	multiplet
M	molar
MCP	2-methylcinnolinium-4-(*o*-methylphosphonate)
Me	methyl
mg	milligram

min.	minutes
mL	milliliter
mmol	millimole
MOM	methoxymethyl
Ms	methanesulfonyl
m/*z*	mass/charge
NADH	nicotinamide adenine dinucleotide
n–BuLi	*n*–butyl lithium
NMMO	*N*-methylmorpholine *N*-oxide
NMR	nuclear magnetic resonance
NO	nitric oxide
NOE	nuclear overhauser enhancement
NOESY	nuclear overhauser enhancement spectroscopy
P-338	murine lyphocytic leukemia cell line
Ph	phenyl
PIV	pivaloyl
POM	pivaloyloxymethyl
ppm	parts per million
*p*TsOH	*p*–toluene sulfonic acid
q	quartet
quant.	quantitative
RNA	ribonucleic acid
rt	room temperature
s	singlet
s–BuLi	*sec*–butyl lithium
SM	starting material
sat.	saturated

t	triplet
TBABr	tetrabutylammonium bromide
TBDPS	*tert*–butyldiphenylsilyl
TBS	*tert*–butyldimethylsilyl
^{t}BuOK	potassium *tert*–butoxide
TEA	triethylamine
TMG	1,1,3,3-tetramethylguanidine
Tf	triflate
TFA	trifluoroacetic acid
THF	tetrahydrofuran
TLC	thin layer chromatography
TMEDA	tetramethylethylenediamine
TMS	trimethylsilyl
Ts	*p*–toluene sulfonyl

CHAPTER I

A BRIEF INTRODUCTION TO PHOSPHORUS

Phosphorus was discovered by a merchant, Dr. Hennig Brand of Hamburg, around the seventeenth century during the process of urine distillation. This new substance emitted light and thus was named as “cold fire”. Within the first years of its discovery, it was exhibited in the courts and fairs in Europe as a wonder that people had never seen.[1,2]

Phosphorus is a stable element with only one isotope form, ^{31}P, which loses electrons with great difficulty and never exists as an elemental cation. There are two major phosphorus forms, white and red. White phosphorus consists of P_4 molecules which are in tetrahedral arrangement. It can be converted to P_2 molecules by treatment with high temperature. This white form phosphorus is highly reactive, toxic, and flammable. It converts to red form phosphorus during a spontaneous process that can be accelerated by heat and light if protected from air. Although red phosphorus is still in a tetrahedral form, it is in a polymeric structure and therefore more stable compared with the white form.

White phosphorus was used in the match industry in the early nineteenth century. Due to its high toxicity, a small amount of white phosphorus is enough to kill an adult and people died from it due to either illegal or incautious use. Although it was lethal and extremely dangerous to use, because of the big demand for fire it was still needed in industry and daily life. In 1855, Swedish chemist Johan Lundstrom discovered a new method to use the more stable and less poisonous red phosphorus in the match

manufacturing process. As the safe production and application of matches was developed and enhanced, they were used more widely to accelerate the Industrial Revolution.

Phosphorus does not exist as a free element in nature. Instead, it usually forms a phosphate salt with calcium.[3] In older times, the original source of phosphorus was bone ash. The production process includes heating bone ash first and then decomposing it from phosphate of lime to sulphate of lime to give a crude liquid which could be further distilled by a clay retort in a heating furnace.[4] After the electronic arc furnace was introduced in 1890, phosphate ore, which is usually $Ca_5(PO_4)_3F$ or $Ca_5(PO_4)_3OH$, replaced bone ash as the major source of phosphorus production. In modern industry, to produce elemental phosphorus, phosphate ore is mixed with quartz sand (SiO_2) in an electronic arc furnace and heated to 1200 °C to 1500 °C to be reduced according to the equation:

$$2Ca_2(PO_4)_2 + 6SiO_2 + 10C = 6CaSiO_3 + P_4 + 10CO$$

The resulting vapor containing phosphorus and carbon monoxide is condensed to yield phosphorus as a white solid.[2,3] The dominant application of phosphorus at this time is as a fertilizer in agriculture. Nonetheless, it is also widely used in the fields of pharmaceuticals, organic synthesis, steel production, and even the weapon industry.[5]

Phosphorus is an essential element needed by all living cells in both animals and plants. For example, it is involved in the nucleotide, adenosine triphosphate (ATP), a high energy intermediate needed for life. The hydrolysis reaction of ATP catalysed by adenylpyrophosphatase (ATPase) can generate adenosine diphosphate (ADP), orthophosphate (P_i) and free energy which is used in biological processes such as

biosynthesis and active transport.[6,7] ADP can also release a significant amount of energy upon hydrolysis to give adenosine monophosphate (AMP) and P_i. At the same time, the conversion of ATP to ADP and AMP is a reversible process. By absorbing energy from light or the metabolism of food, the latter two lower energy nucleotides can serve as the starting materials to react with phosphate to reform ATP under conditions of enzyme catalysis.

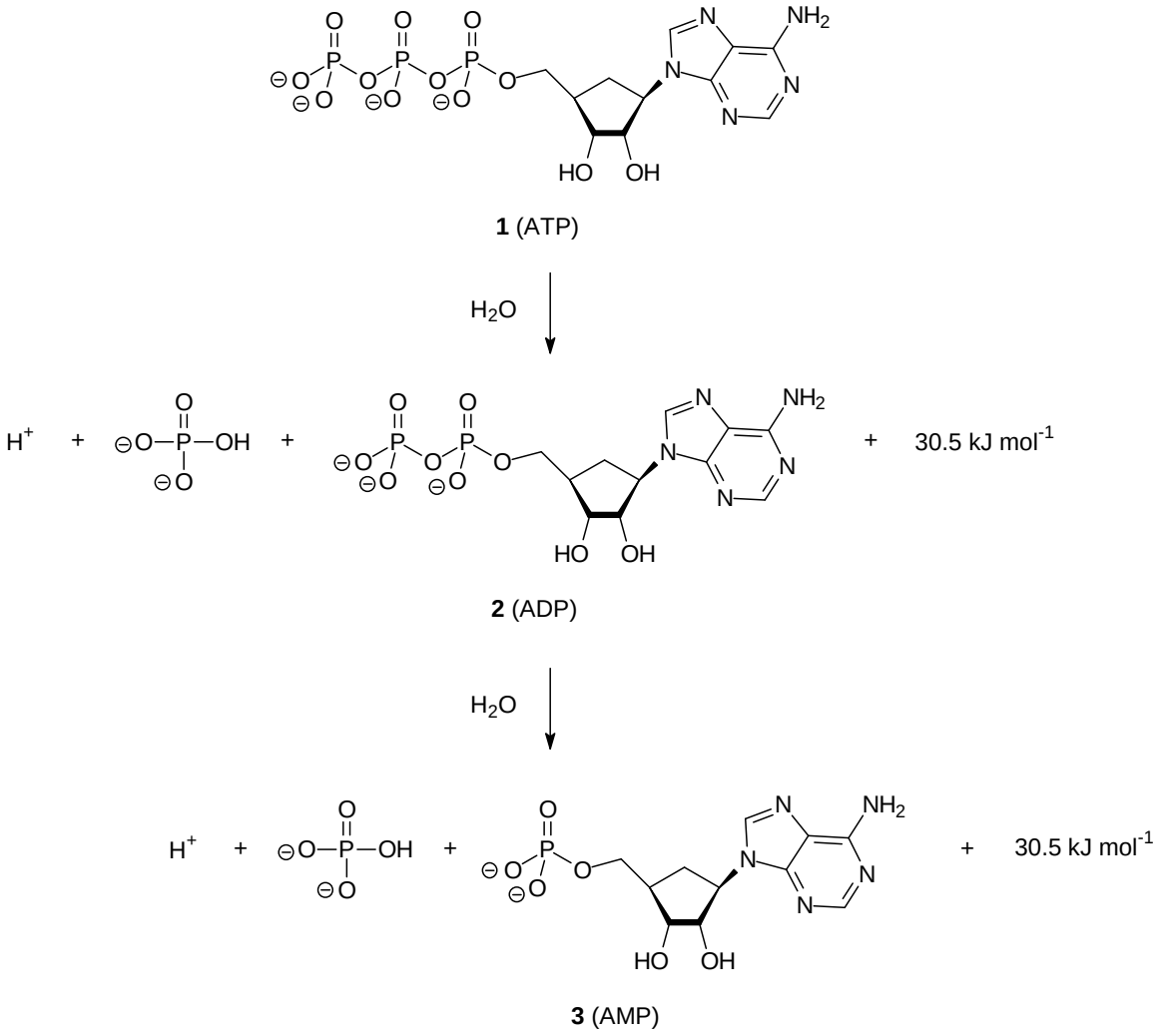

Figure 1. Hydrolysis of ATP[7]

The phosphate group also plays key roles in important cellular metabolic pathways to provide cells necessary substrates. One example is the mevalonate pathway which converts mevalonate to *isoprenoids* and *steroids*, including cholesterol. Mevalonate also is a starting material for hormones, bile acids, and vitamin D. Other quantities of mevalonate are converted to *nonsterol isoprenoids* which are important for posttranslational modification of many proteins , including those in the Ras superfamily of small GTPases. These proteins are involved in intracellular signaling pathways which are associated with cell growth, differentiation, and gene expression. [8-11]

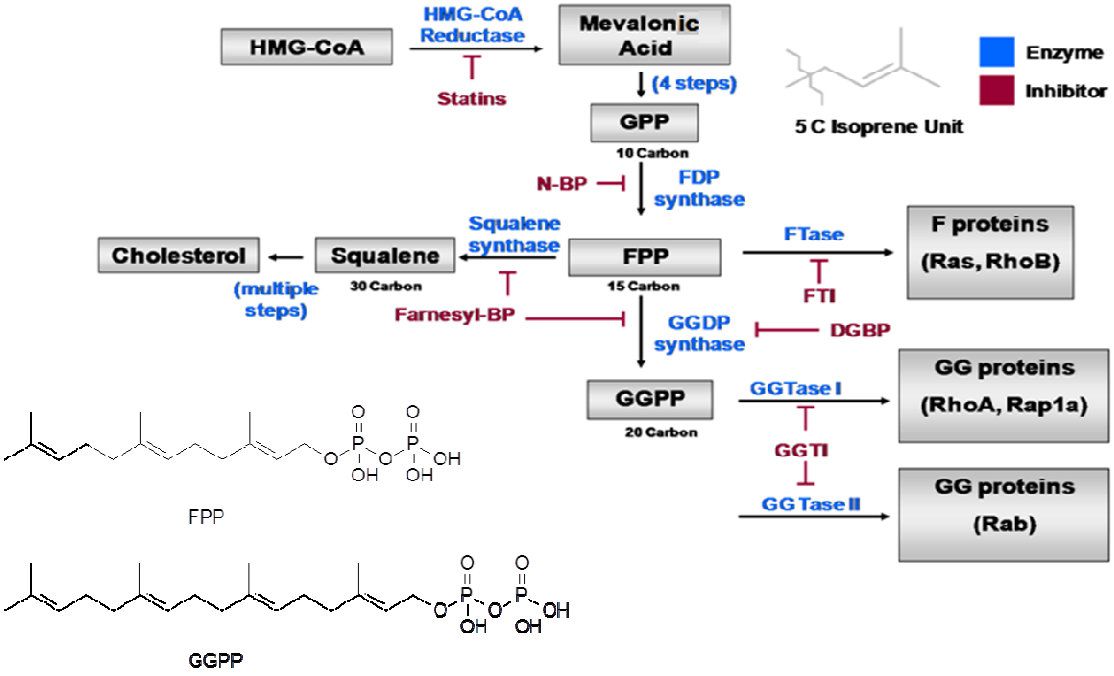

Figure 2. Isoprenoid biosynthesis pathway[12]

More detailed information about the the mevalonate pathway in mammals is shown in Figure 2. It begins with 3-hydroxy-3-methylglutaryl-COA (HMG-CoA) which is synthesized from acetyl CoA and acetoacetyl CoA by HMG-CoA synthase. The reduction reaction of HMG-CoA is catalysed by HMG-CoA reductase, the rate-limiting

enzyme of the mevalonate pathway, and leads to the generation of mevalonic acid. It then undergoes a phosphorylation reaction catalysed by mevalonate kinase (MK) which requires ATP to transfer a phosphate group to mevalonic acid to yield mevalonate-5-phosphate, a phosphomevalonate. The next reaction also is mediated by an enzyme, phosphomevalonate kinase (PMK) and ATP, which converts the mono-phosphate starting material to a pyrophosphate product, mevalonate-5-diphosphate, that subsequently undergoes a decarboxylation reaction to give an important intermediate, 3-isopentenyl pyrophosphate (IPP). The IPP formed is in an equilibrium with its isomer, dimethylallyl pyrophosphate (DMAPP). In plants, geranyl pyrophosphate synthase (GDPS) catalyses the reaction of one equivalent of the five carbon molecule, IPP, with another equivalent of its isomer, DMAPP, to generate the ten carbon adduct, geranyl diphosphate (GPP). GPP can undergo a parallel reaction with IPP in the presence of the enzyme, farnesyl pyrophosphate synthase (FDPS), to afford an important fifteen-carbon intermediate, farnesyl diphosphate (FPP). In animals, FDPS catalyses both reactions to convert three molecules of IPP to FPP as the ultimate product.[8]

As shown in Figure 2, FPP is at a branch point in the mevalonate pathway. A two-step head-to-head condensation of two identical molecules of FPP catalysed by squalene synthase (SQS) which leads to the generation of squalene, which contains a thirty-carbon structure.[13] Squalene can be converted to cholesterol through a multi-step process.[8] In addition, FPP can be directly transferred by farnesyl transferase (FTase) to proteins, including Ras and RhoB, in a process termed farnesylation. Furthermore, FPP can also react with one molecule of IPP to generate the twenty-carbon intermediate geranylgeranyl diphosphate (GGPP), a reaction which is mediated by geranylgeranyl

diphosphate synthase (GGDPS).[14,15] GGPP is involved in biosynthesis of many natural products, including the taxanes and gibberellins.[16] Furthermore, it can be transferred by either geranylgeranyl transferase I (GGTase I) to proteins such as RhoA and Rap1a, or by geranylgeranyl transferase II (GGTase II) to bring about geranylgeranylation of the Rab proteins.[10] Once these proteins are isoprenylated, they become functional signaling proteins after insertion into cellular membrane and participate in intracellular signaling pathways.[17,18,19] In addition, this post-translational prenylation process is important to signal transduction, cytoskeletal formation, and cell growth regulation.[20]

Statins are competitive inhibitors targeting HMG-CoA reductase and they are used to lower cholesterol.[21] However, since they interrupt the mevalonate pathway at the first step, they also reduce the synthesis of FPP and GGPP and induce apoptosis.[17,20,22,23] As discussed, FPP can be transferred by FTase to cause protein farnesylation which will activate p21, a ras oncogene product.[24,25] Once this post-translational modification is initiated, ras protein can be switched on to engage cell proliferation.[20] To inhibit protein prenylation more specifically, bisphosphonates have been widely used as drugs.[26] As shown in Figure 3, bisphosphonic acid is a close analogue of pyrophosphoric acid. Changing the central oxygen to a carbon not only stabilizes the entire structure, but also provides various possibilities to modify the molecule on this central carbon. For example, the nitrogenous bisphosphonates, alendronate, risedronate and zoledronate which are inhibitors targeting FDPS are used clinically in the treatment of bone disease.[27-29] In addition to depletion of farnesylation, inhibition of FDPS also results in reduced generation of GGPP. It has been reported that the addition of exogenous geranylgeraniol can reverse the inhibition of osteoclast-mediated bone resorption, which

suggests that agents that inhibit FDPS may exert activity through GGPP depletion.[30] Cellular GGPP also plays a critical role in post-translational modification. Therefore, it also will be of benefit to develop phosphonate inhibitors that target enzymes downstream of FDPS to deplete the generation of GGPP.[31,32]

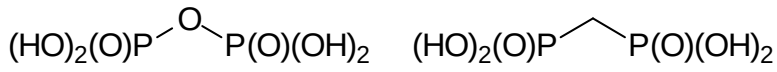

4 **5**

Figure 3. Pyrophosphoric acid (**4**), and bisphosphonic acid (**5**)

Phosphorus has a critical role in living organisms. More importantly to an organic synthetic chemist, it also is involved in many reactions to help to construct complex molecule structures. The most well-known application of phosphorus in organic synthesis is the Wittig reaction to form carbon-carbon double bonds. In 1954, Wittig and Schöllkopf discovered a methodology to use phosphorus ylides to react with a ketone or aldehyde to form olefins,[33,34] and this reaction still is widely used in natural product synthesis. They were awarded the Nobel Prize in Chemistry in 1979 for this discovery.

As shown in Figure 4, the electronegative carbon adjacent to triphenylphosphine in ylide **7** attacks the carbonyl group in compound **6** in a [2+2] cycloaddition to form either intermediate **8** or **9**, which will lead to the generation of a *cis* olefin or a *trans* olefin product. However, in the twisted transition state, intermediate **8** is more favored than **9** due to the van der Waals repulsion between R_1 and ylide groups. Therefore, the formation of **8** is faster than **9**, which results in the *cis* isomer as the dominant product.

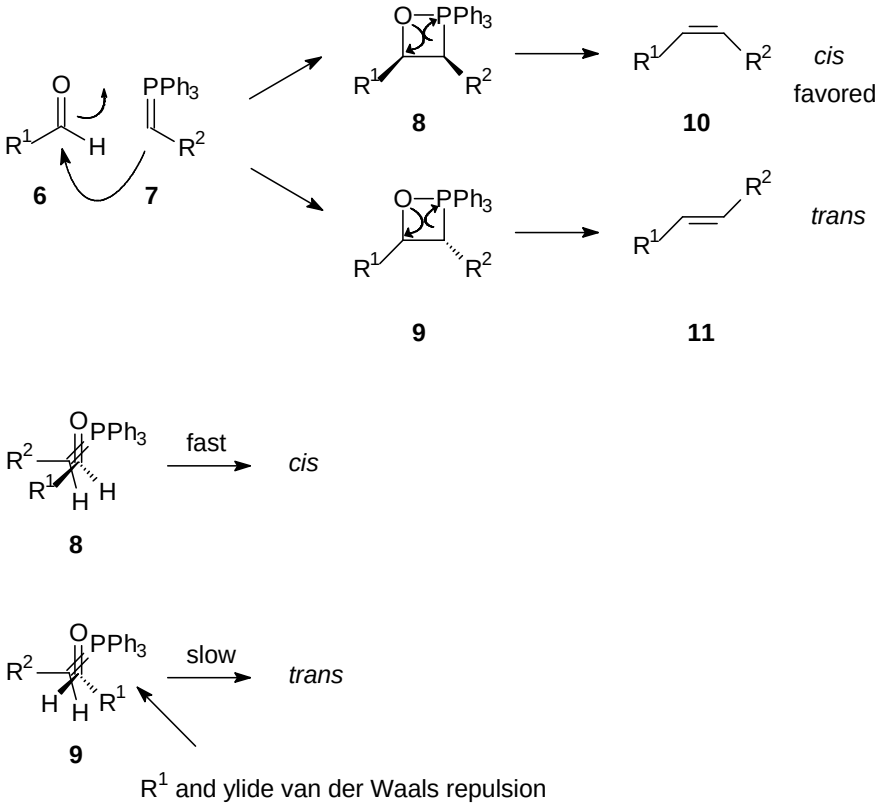

Figure 4. Wittig Reaction[35]

In an effort to synthesize the *trans* olefin, Dr. Leopold Horner modified the Wittig reaction in 1958, using phosphonate stabilized carbanions (Figure 5).[36-38] Phosphonate anion **12** can be formed by addition of base, such as NaH. The anion was added to aldehyde **6** to form transition states **13** or **14** in a rapid equilibration. The transition states **13** and **14** further rearrange to four membered ring intermediates **15** and **16**. Elimination of phosphate as a by-product affords the *trans* product **17**, and the *cis* product **18**. Because there is a steric interaction effect existing in the transition state **16**, it is less favored compared with its geometric isomer **15**. Therefore, the Horner-Wadsworth-Emmons reaction is widely employed for *trans* olefin preparation.[39-44]

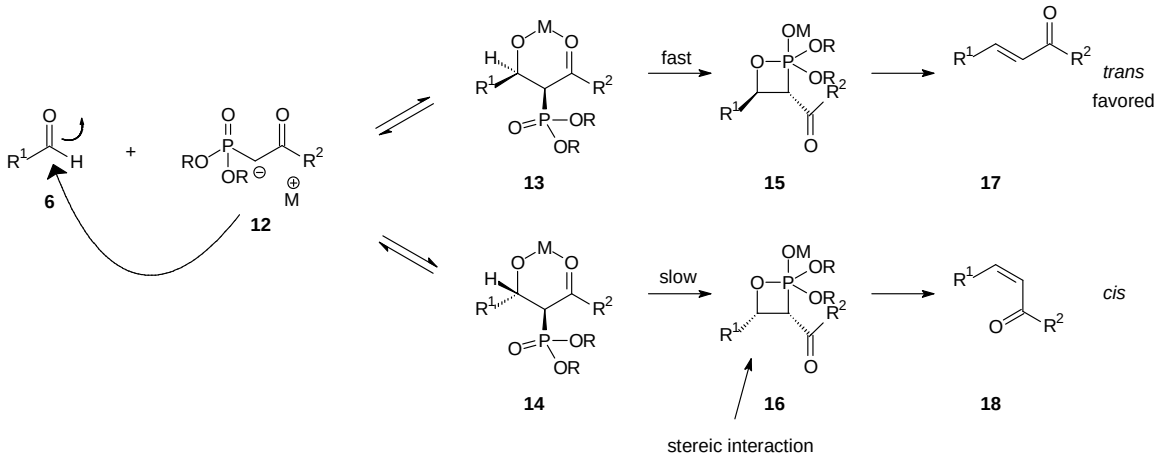

Figure 5. Horner-Wadsworth-Emmons Reaction[35]

Because phosphonate is an important functional group which has a wide range of applications in organic synthesis, methodologies to prepare alkyl phosphonates are highly respected. One incredibly useful reaction among them is the Michaelis-Arbuzov Reaction.[45] For example, when trialkyl phosphite **19** is treated with the alkyl halide **20**, the electron rich phosphorus atom attacks the electron deficient carbon atom adjacent to the halide to form intermediate **21**. The halide anion generated in the previous step reaction can further attack R' group on the phosphonate to cleave the C-O bond. As a result, the lone pair electrons form a P-O double bond to give alkyl phosphonate **22** as the desired product.

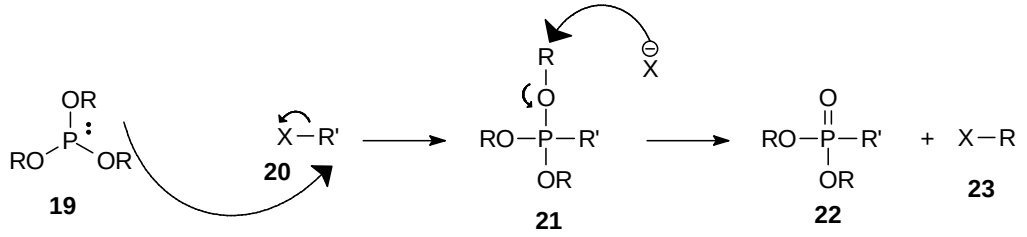

Figure 6. Michaelis-Arbuzov Reaction

Phosphonate hydrolysis is also an important and widely used reaction to convert a phosphonate ester to the phosphonic acid.[46-48] In McKenna's conditions, TMSBr is treated with 2,4,6-collidine to form a bromide salt **26**. After the addition of phosphonate **22**, the oxygen of the P=O group will attack the TMS group to form a silyl ether **27** which exists in three different resonance forms (**27A**-**27C**). A bromide anion will then attack the ester group of phosphonate **27C** to give neutral phosphonate silyl ester intermediate **27D** which further reacts with MeOH or water to cleave the trimethyl silyl group and form the phosphonic acid.[49]

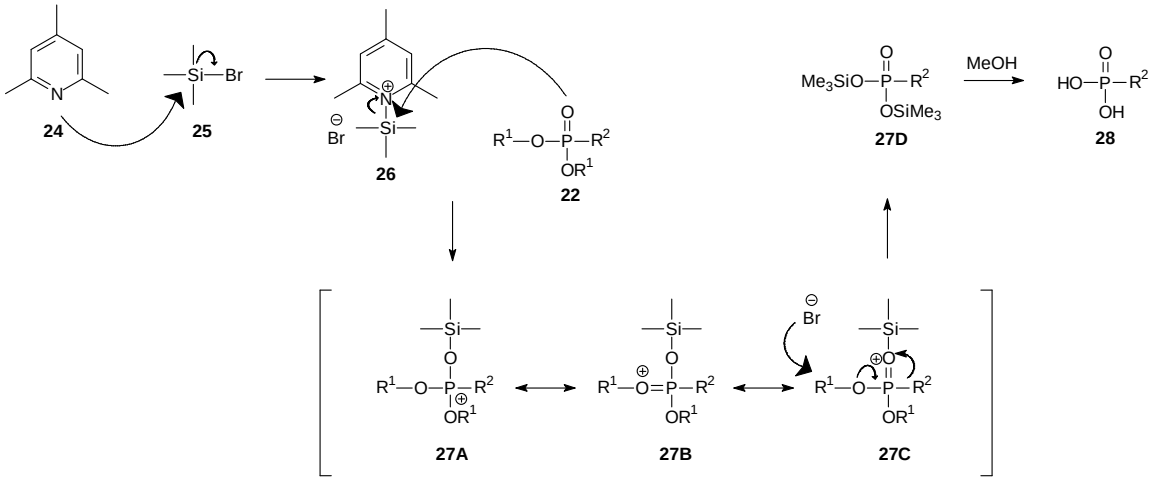

Figure 7. Proposed mechanism of phosphonate hydrolysis

More recently, in our group we developed a synthetic protocol to convert benzylic and allylic alcohols to phosphonates in the presence of ZnI_2.[50-52] The proposed mechanism is shown in Figure 8. Both triethyl phosphite and benzyl alcohol complex with ZnI_2 to form the transition state **30**. The electron rich phosphorus atom then attacks the electron deficient methylene group in benzyl alcohol to break the C-O bond and yield intermediate **31** and zinc oxide as by-product. It then undergoes Michaelis-Arbuzov reaction with iodide to afford phosphonate **32** as the final product.

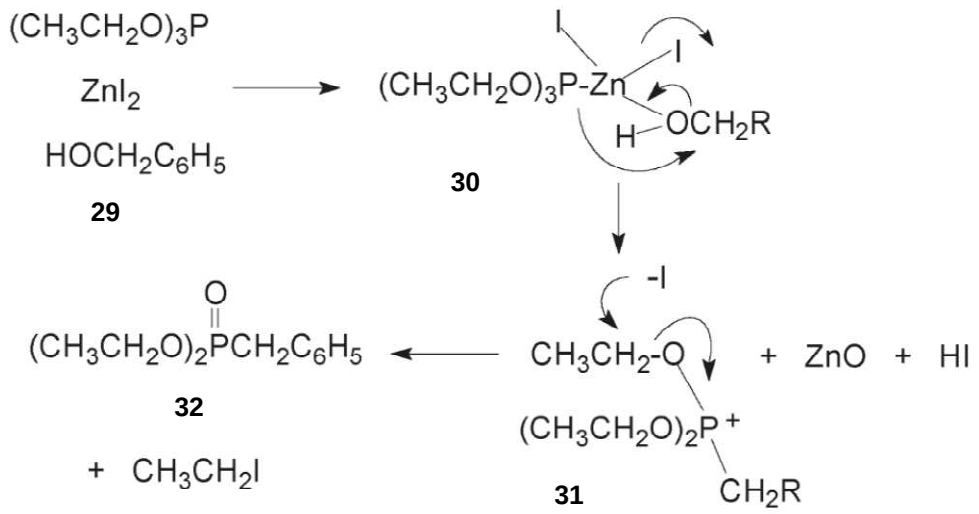

Figure 8. Proposed mechanism of alcohol-phosphonate conversion[50]

As has been related above, phosphorus is an important element which was discovered over 300 years ago and now is widely used in industry, agriculture, organic synthesis, and pharmaceutical research. Our group has a strong interest in phosphorus research, including using phosphorus as a tool in natural product synthesis and studying phosphonates as inhibitors of the mevalonate pathway. Some detailed research related to phosphonate inhibitor development will be discussed in the following chapters.

CHAPTER II

SYNTHESIS OF DIGERANYL BISPHOSPHONATE ANALOGUES

The nitrogenous bisphosphonates, pamidronate, alendronate, risedronate and zoledronate (Figure 9) are used clinically in the treatment of bone disease.[27,28] These drugs inhibit farnesyl diphosphate synthase (FDPS), a key enzyme at a branch point in the mevalonate pathway which is responsible for the production of farnesyl diphosphate (FPP).[29] Inhibition of FDPS will also interrupt cholesterol synthesis and protein geranylgeranylation as well. Another key enzyme, geranylgeranyl diphosphate synthase (GGDPS), is responsible for the biosynthesis of geranylgeranyl diphosphate (GGPP) which leads to protein geranylgeranylation of small GTPases such as Rab, Rho and Rac, which are important signaling proteins for osteoclast function. With the depletion of protein geranylgeranylation, both osteoclastic bone resorption and proliferation of cancer cells can be inhibited.[31,53,54] Because it is important to inhibit the generation of GGPP, a way to selectively inhibit GGDPS is highly desirable.

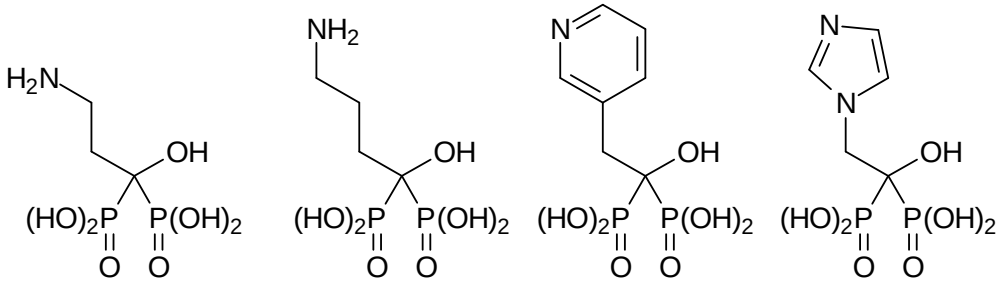

Figure 9. Nitrogenous bisphosphonates used as clinical drugs

Non-nitrogenous analogues of these four compounds, including monoalkyl bisphosphonates and dialkyl bisphosphonates which are shown in Figure 10, have been developed more recently. These new analogues have been found to selectively inhibit GGDPS.[31,32,55]

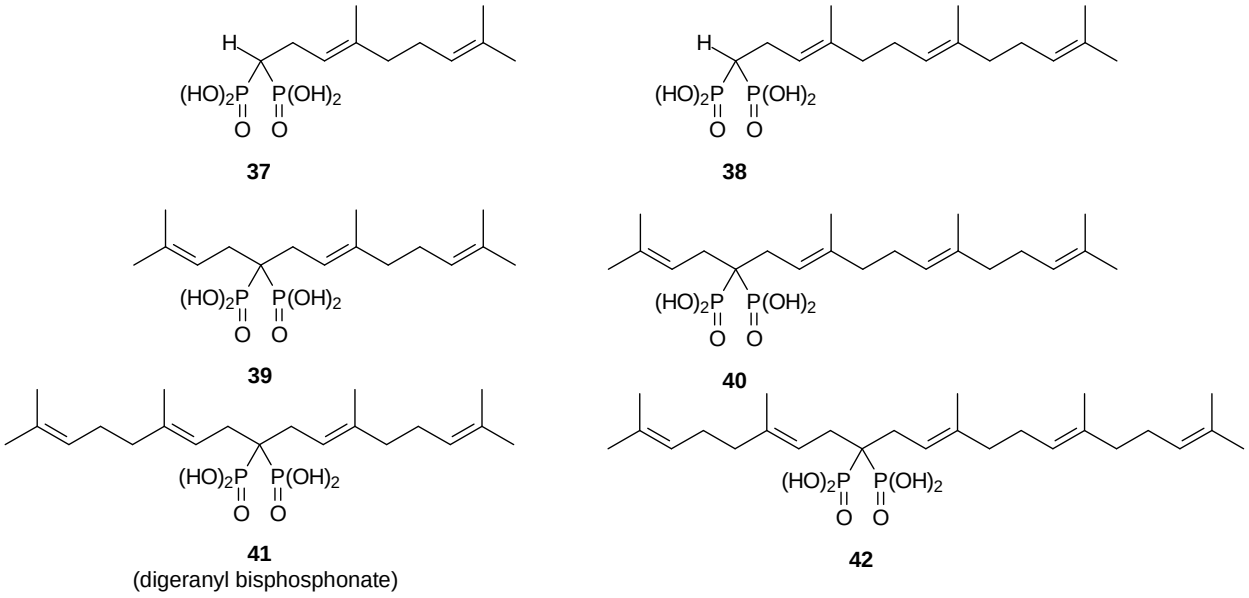

Figure 10. Non-nitrogenous bisphosphonates developed by the Wiemer group

The IC_{50} value against GGDPS *in vitro* of the lead compound in this family, digeranyl bisphosphonate **41** (DGBP), is approximately 0.2 μM.[31] Furthermore, the crystal structure of the GGDPS dimer and its binding motifs have been reported by Oldfield et al.[16] As is shown in Figure 11B, three magnesium metal cations coordinate with the pyrophosphate head group of the substrate pyrophosphate. There are two other sites which were identified in the enzyme, the hydrophobic site that is occupied by the farnesyl fragment of the substrate shown in the blue color, and the GGPP site that is occupied by the product resulting from the addition of one isopentenyl (IPP) unit to FPP (pink color structure). When GGDPS was incubated with DGBP, the polar

bisphosphonate head group also coordinated with the magnesium cations. One of the geranyl side chains occupied the FPP site while the other C-10 side chain was found in the GGPP site (green color structure). Therefore, this important "V-shape" of the inhibitor allows for competition with the natural substrate in binding to the enzyme.[16]

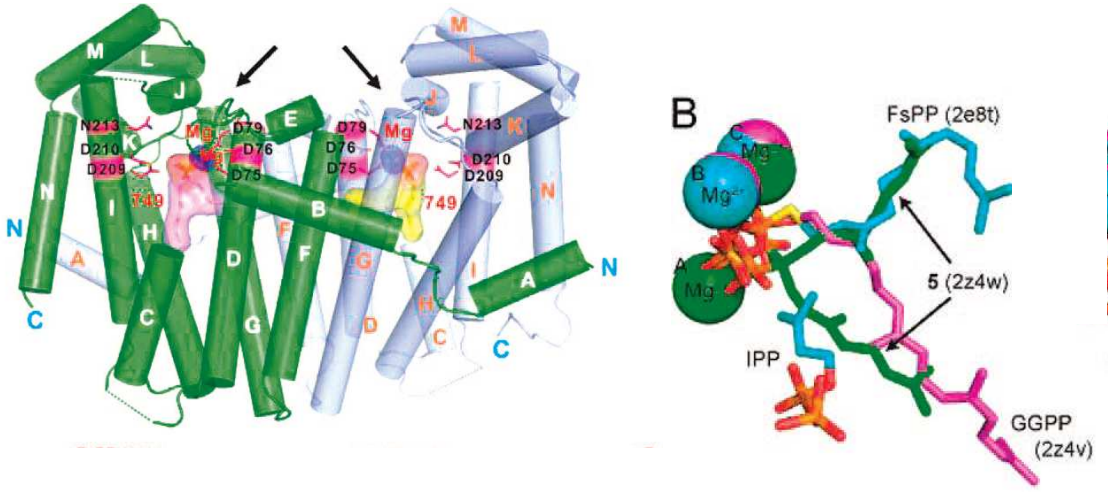

Figure 11. Structure of inhibitor-GGDPS complex[16]

According to previous studies, bisphosphonates bearing an α-hydroxy group attached to the germinal carbon will increase the bone affinity of the compound, because it can strengthen chelation with calcium cations.[56] Therefore, bisphosphonate head groups along with this α-hydroxy group were regarded as key features to enable the compound to rapidly localize to the surface of the bone. It was reported that the insertion of an α-hydroxy group boosts the compounds' bioactivity significantly.[57,58] Furthermore, compared with the bisphosphonate head group, the pyrophosphate group of the natural substrate has one more oxygen atom which may cause a slight difference in pKa by an inductive effect. Therefore, by introducing one α-oxygen atom, we predicted it would

help to mimic the physiological pKa more accurately[59] and thus increase binding ability with the enzyme.[60] On the other hand, according to the crystal structure of the enzyme bound to DGBP, it is very important for the inhibitor to carry two side chains to preserve the "V-shape".[16] Combining all these important features listed above, we designed compound **44** as an interesting analogue to the parent compound, DGBP (Figure 12). We hypothesized that it would be very interesting to investigate the biological effects that this α-oxygen atom brings to the structure. By modifying the length of two side chains, it also will help us to better understand the specific way this inhibitor binds to the enzyme.

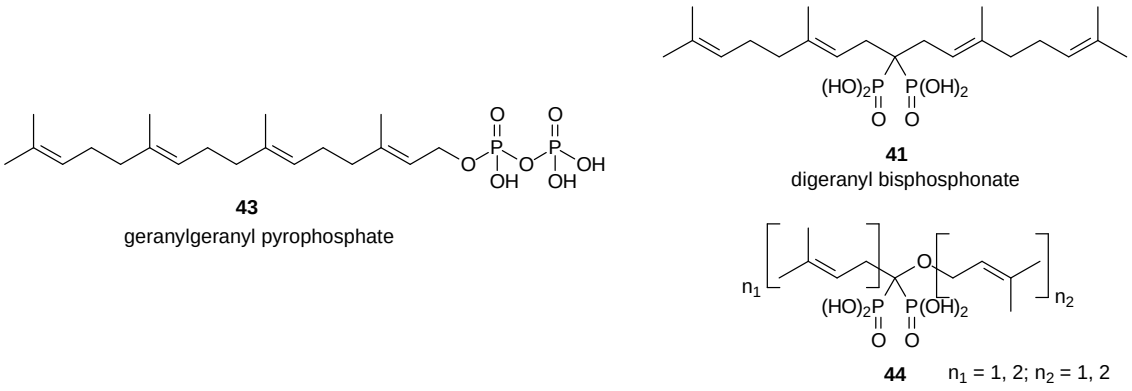

43 geranylgeranyl pyrophosphate

41 digeranyl bisphosphonate

44 $n_1 = 1, 2; n_2 = 1, 2$

Figure 12. Comparison of GGPP, DGBP and a DGBP analogue

Synthesis of *O,C*-dialkylbisphosphonates

The first generation retrosynthesis is shown in Figure 13. The tetra sodium salt **45** can be obtained from the hydrolysis of the tetraethyl ester **46**[49] which could arise from the alkylation reaction of the α-hydroxy bisphosphonate **47**. Therefore, compound **47** would be a very important intermediate to prepare for this synthetic route.

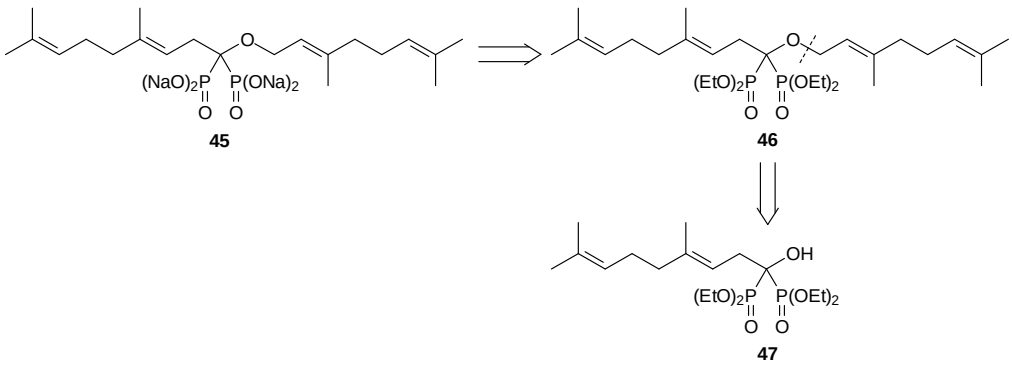

Figure 13. The retrosynthesis of *C*-geranyl-*O*-geranyl bisphosphonate **45**

Compound **48**, which has a much simpler structure and can be prepared from an inexpensive commercially available starting material, was selected as a model compound to study synthesis of a family of α-hydroxy bisphosphonates.

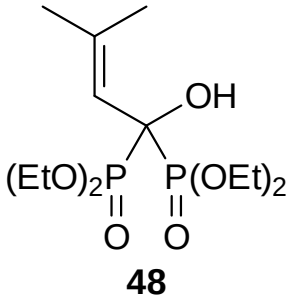

Figure 14. Model study target

The attempted synthesis of compound **48** is shown in Figure 15. The starting material 3, 3-dimethylacrylic acid (**49**) was treated with oxalyl chloride to prepare the acid chloride **50** in good yield.[61] The next two steps of the sequence were carried out in one flask. Michaelis-Arbuzov reaction occurred with acid chloride **50** when it was treated with triethyl phosphite to produce acyl phosphonate **51**.[62] Following completion of the reaction as monitored by ^{31}P NMR, a Pudovik reaction was applied with addition of one equivalent of diethylphosphite. In theory, the α-hydroxy bisphosphonate **48**

should have been formed. However, two peaks at 18.5 and −0.8 ppm with a 36.7 Hz coupling constant were observed in the ^{31}P NMR spectrum (Figure 16), indicative of the presence of both phosphonate and phosphate groups in the molecule. Based on these spectral data, it appeared that instead of the desired target molecule **48**, the rearrangement product **52** was obtained.

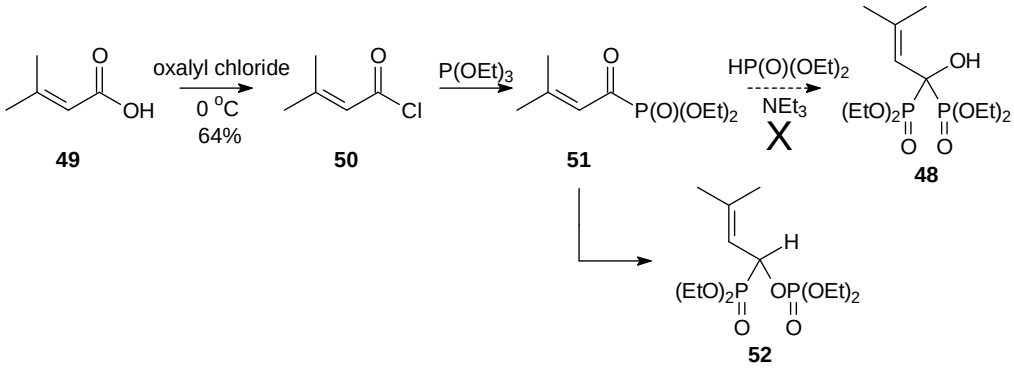

Figure 15. Attempted synthesis of intermediate **48**

This rapid rearrangement that leads to compound **52** may be driven by the strong bonding between oxygen and phosphorus atoms. The mechanism of this rearrangement reaction involves attack on the carbonyl group of compound **51** by diethyl phosphite. The resulting oxygen anion will further attack one of the phosphonate groups to cleave the C-P bond and form the new O-P bond. Further intermolecular proton transfer would lead to the formation of the final product **52**. Even though the desired α-hydroxy bisphosphonate **48** is generated, the acidic α-hydroxy group could be deprotonated easily by base and subsequent rearrangement forms the by-product **52** (Figure 17). This phenomenon was reported first by Fitch and Moedritzer[63] in 1962 and studied and supported more recently by numerous groups.[64-67] The structure of compound **52** was further confirmed by 2D NMR which is shown in Figure 16. Therefore, based on what

has been observed and what has been reported in the past, α-hydroxy bisphosphonate **48** is unstable under basic conditions. In addition, the allylic nature of the bisphosphonate head group may cause it to be even more reactive than saturated alkyl systems.

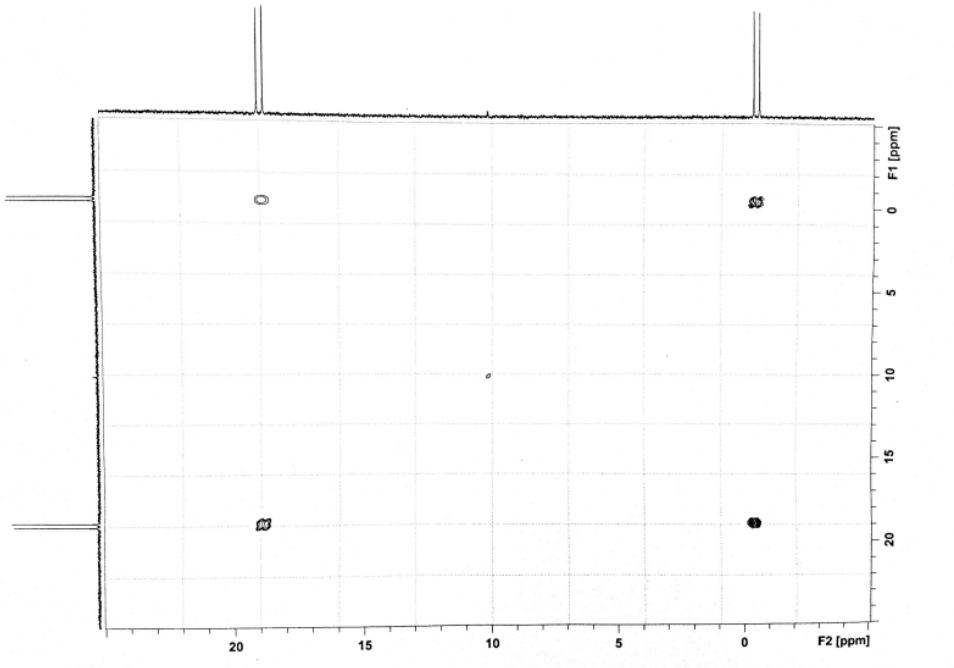

Figure 16. 2D phosphorus NMR of compound **52**

The next attempted synthesis started from the carboxylic acid **53** (Figure 18). It was converted to the acid chloride **54** upon treatment with oxalyl chloride and then further allowed to react with triethyl phosphite to assemble acyl phosphonate **55**. When the reaction mixture for the second step was monitored by ^{31}P NMR, the resonances for the α-hydroxy bisphosphonate **56** and rearrangement product **57** were observed along with trace amounts of the target molecule, and compound **56** was successfully isolated in low yield.

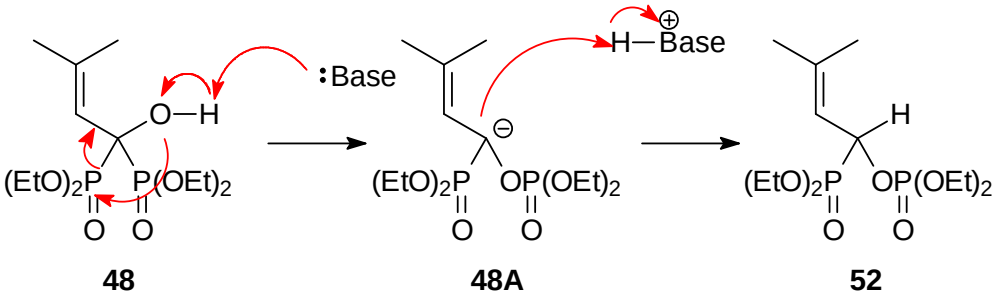

Figure 17. Rearrangement mechanism

Treatment of an acid chloride with multiple equivalents of triethyl phosphite can result in addition of two phosphonate groups in one flask. Furthermore, inspired by Kolodyazhnaya and Kolodyazhnyi's work, if a proton source can be added to the reaction mixture, the resulting oxygen anion might be trapped rapidly to avoid the undesired rearrangement reaction.[68,69]

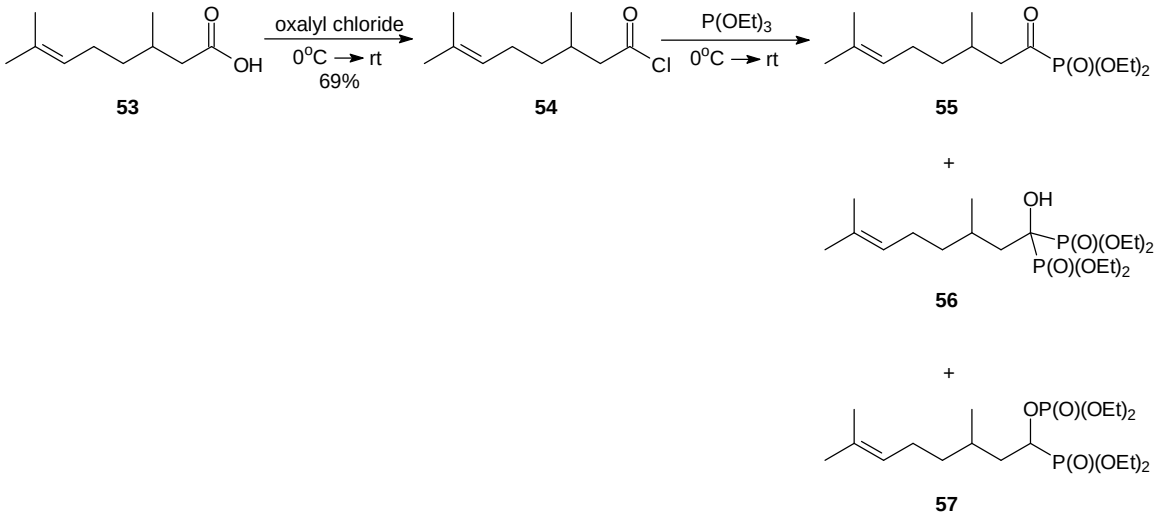

Figure 18. Attempted synthesis starting from acid **53**

The new synthetic strategy was carried out with intermediate acid chloride **54** (Figure 19). This compound was treated with 2.5 equivalents of triethyl phosphite and

pyridine hydrochloride was used as a proton source. The desired product, α-hydroxy bisphosphonate **56**, was thus obtained in 14% yield from this one flask reaction.

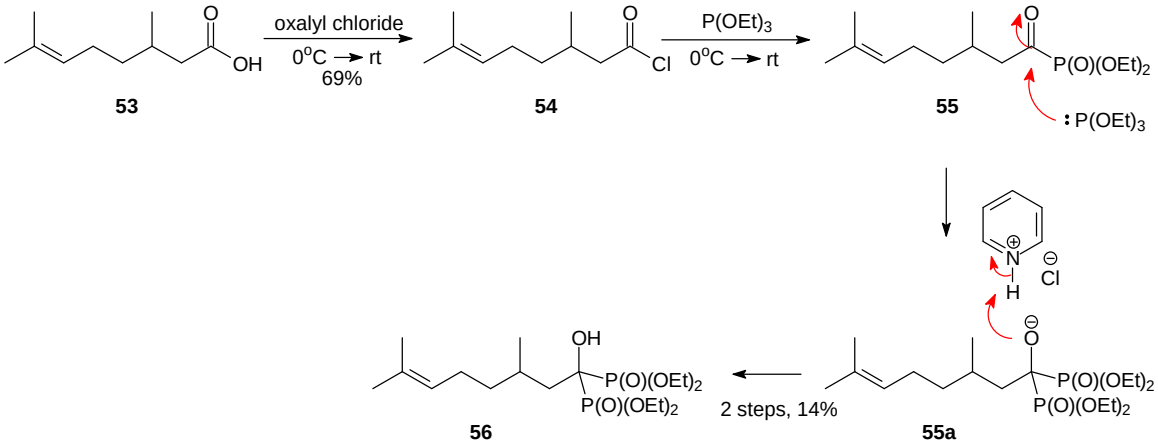

Figure 19. Synthesis of bisphosphonate **56**

Although a methodology to prepare the α-hydroxy bisphosphonates intermediates has been developed, there is still a serious synthetic limitation. The most important is that α-hydroxy bisphosphonates needed for our studies are not stable. These compounds undergo a rapid rearrangement reaction even when stored in a freezer. This unexpected feature not only lowers the yield of the α-hydroxy bisphosphonates, but also eliminates the possibility of alkylation of the α-hydroxy group because it cannot be treated with base. Therefore, development of a new strategy to synthesize the target molecule **44** was necessary.

The second generation retrosynthesis is shown in Figure 20. Tetra sodium salt **45** could be derived from the hydrolysis reaction of tetraethyl ester **46**.[49] The dialkylated compound **46** can be constructed by C−alkylation of the ether **58**[70] which can be further assembled by phosphorylation reaction of mono phosphonate **59**.[70-74] The *O*-alkylation of alcohol **60** will lead to the formation of intermediate **59**.[70,75]

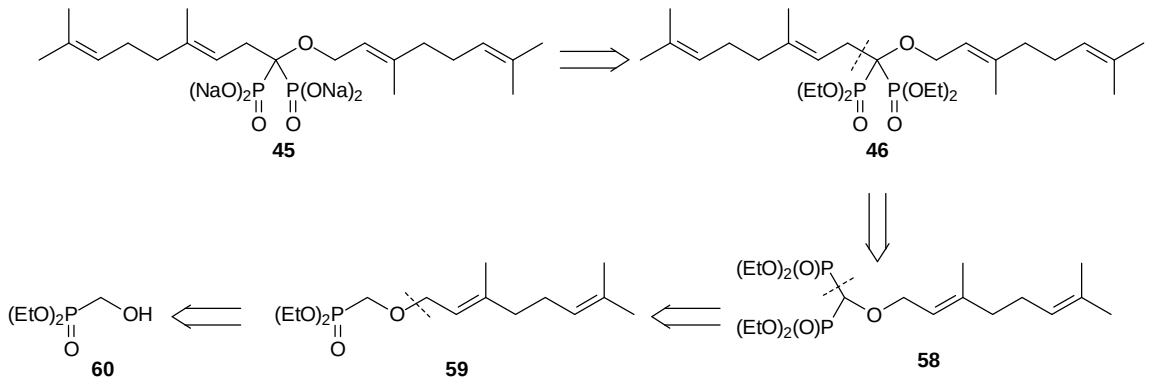

Figure 20. The second generation retrosynthesis

The synthesis started from commercial diethyl (hydroxymethyl)phosphonate **60**. This compound was treated with NaH followed by the addition of geranyl bromide to form the ether **59** which was further treated with LDA and diethyl chlorophosphate to lead to the generation of the key intermediate, the mono alkylated bisphosphonate **58** in moderate yield.[70] Once the key intermediate **58** was in hand, it was of interest to investigate whether compounds with the length of the *O*-alkyl side chain varied and constant lengths of the *C*-terminal side chain would demonstrate different bioactivities. Therefore, intermediate **58** was first treated with NaH to deprotonate the α-position and then separately with prenyl bromide and geranyl bromide to give the *C*-prenyl-*O*-geranyl bisphosphonate **62** and the *C*-geranyl-*O*-geranyl bisphosphonate **46**. Standard hydrolysis conditions with TMSBr and NaOH then afforded the corresponding salts **63** and **45**. Because the primary objective was to obtain the salts for biological studies, intermediate **58** also was directly hydrolysed to the mono alkylated bisphosphonate salt **61** (Figure 21).

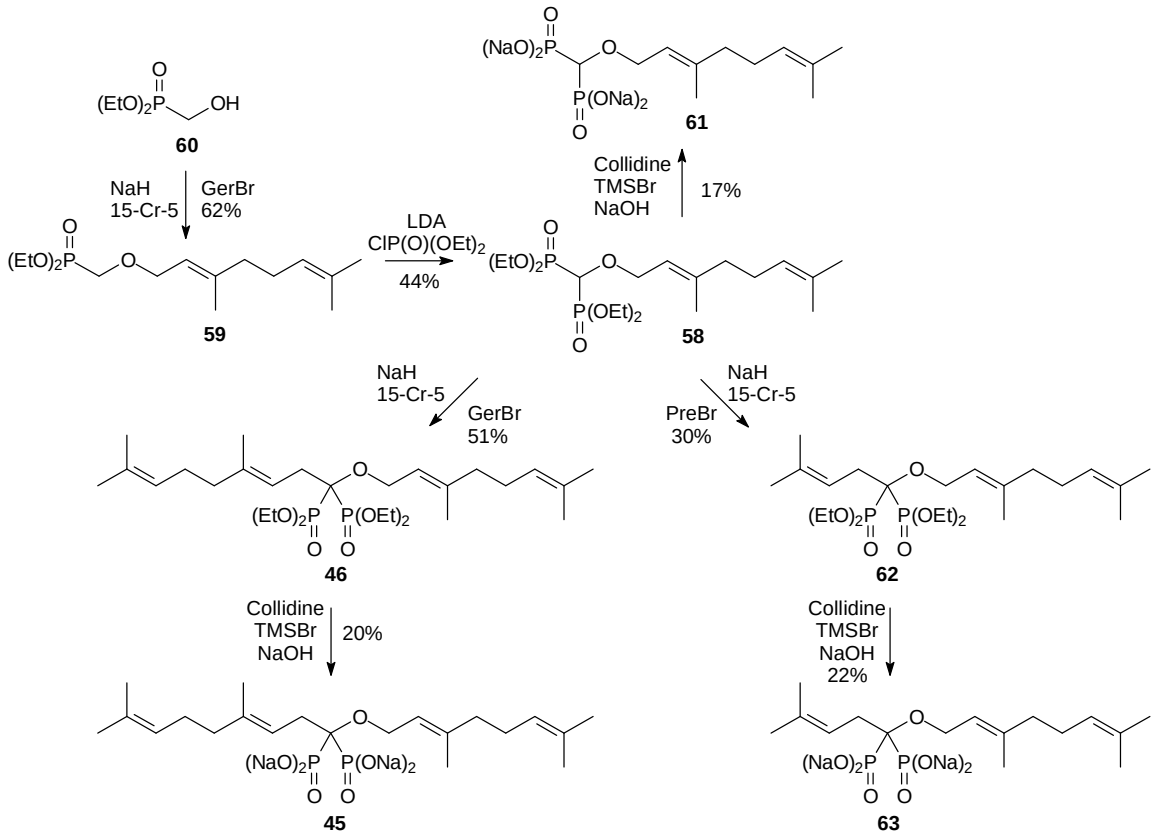

Figure 21. Synthesis of *O*-geranyl DGBP analogues

It also would be interesting to study the effect of modification of the alkyl group length on the oxygen substituent. Therefore, a series of analogues with a geranyl chain on the oxygen terminal and different isoprenoid chain lengths on the *C* terminal has been prepared as well. Diethyl (hydroxymethyl)phosphonate **60** was converted to the prenyl ether **64** through treatment with NaH and prenyl bromide. The phosphorylation reaction of mono phosphonate **64** afforded the desired intermediate, bisphosphonate **65**. Following the same synthetic strategy, attempted alkylation reactions of intermediate **65** gave the expected *C*-prenyl-*O*-prenyl bisphosphonate **69** and *C*-geranyl-*O*-prenyl bisphosphonate **66**. Hydrolysis of both of these two ethyl esters yielded their

corresponding salts compounds **70** and **67**. Intermediate **65** also was hydrolysed to provide the salt **68** as well (Figure 22).

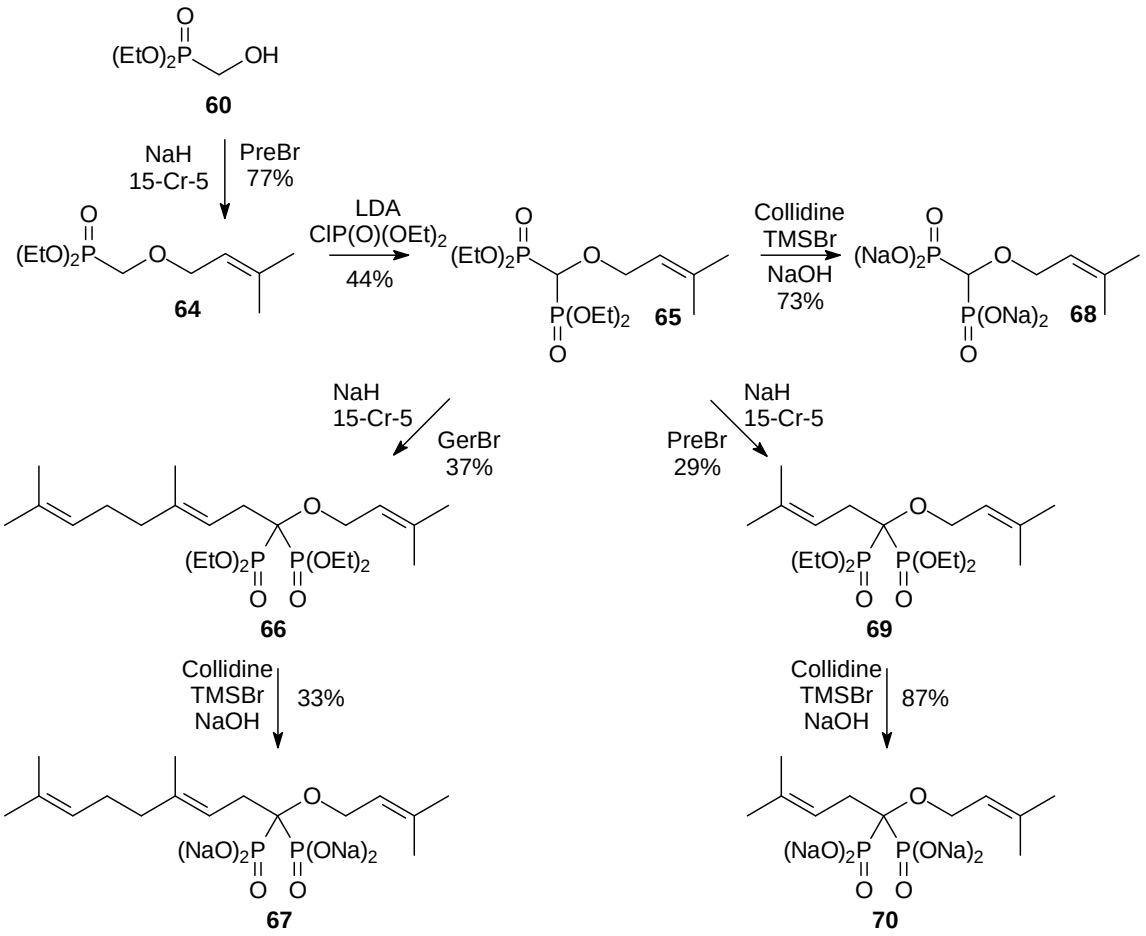

Figure 22. Synthesis of *O*-prenyl DGBP analogues

All the compounds that have been prepared at this stage are achiral molecules. It was of interest to attempt the synthesis of an analogue in this family that carries a stereogenic center. One 10-carbon side chain which bears a stereogenic center is the citronellyl group. Furthermore, both pure (*S*)-(□)-β-citronellol and (*R*)-(+)-β-citronellol are commercially available with the former more economical. Thus, as shown in Figure 23, the first target molecule was the *C*-(*S*)-citronellyl-*O*-geranyl bisphosphonate **71**.

However, the alkylation reaction of mono alkylated bisphosphonate **58** was not successful, perhaps due to the crowded carbon center at the α-position of the two bulky phosphonate moieties as well as the less reactive primary bromide in the citronellyl reagent. Increasing the reaction temperature caused the fragile ether chain to decompose. Therefore, reversing the reaction sequence to put on the less reactive side chain first was explored. Inspired by this idea, diethyl (hydroxymethyl)phosphonate **60** was allowed to react with citronellyl bromide first to give ether **72**, which was then treated under phosphorylation conditions to introduce the second phosphonate moiety and generate bisphosphonate **73**. Alkylation of intermediate **73** with the more reactive reagent, geranyl bromide, proceeded smoothly to yield dialkylated bisphosphonate **74** in moderate yield. A standard hydrolysis reaction of the ethyl ester **74** afforded the corresponding salt **75**.

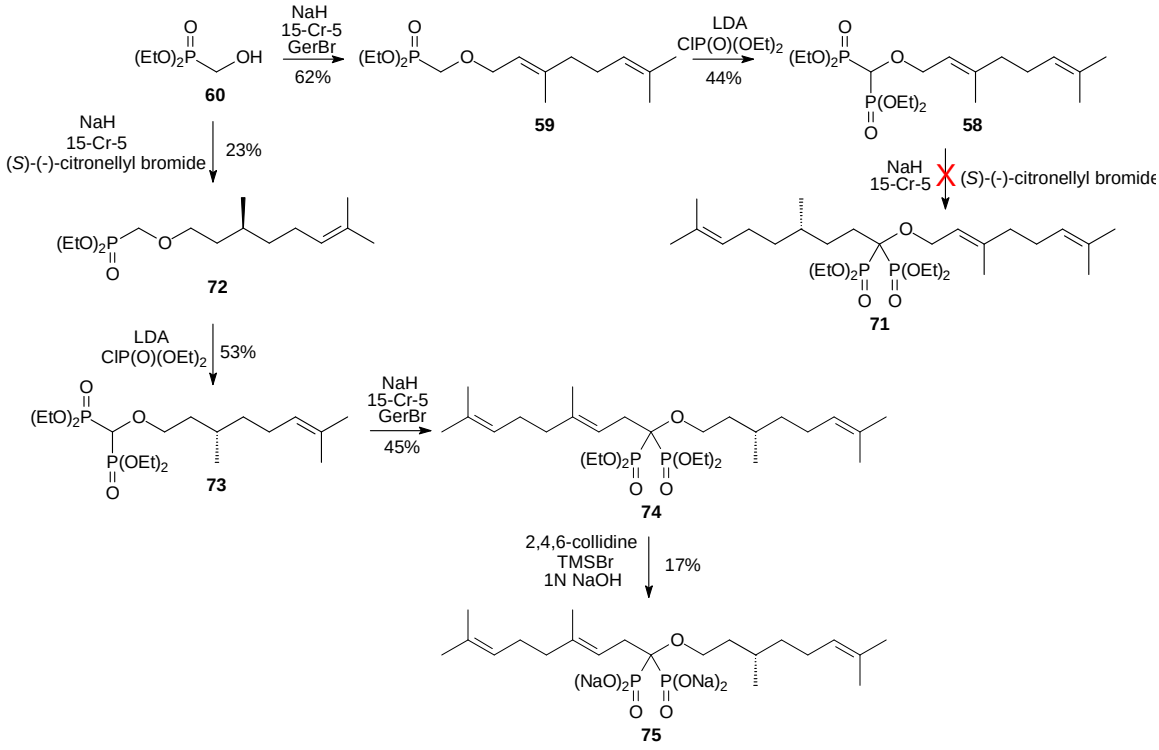

Figure 23. Synthesis of *C*-geranyl-*O*-citronellyl bisphosphonate **75**

Seven compounds have been prepared in this family (Figure 24). Along with the parent compound, DGBP, these compounds were submitted to our collaborators for biological studies and they obtained some positive results.

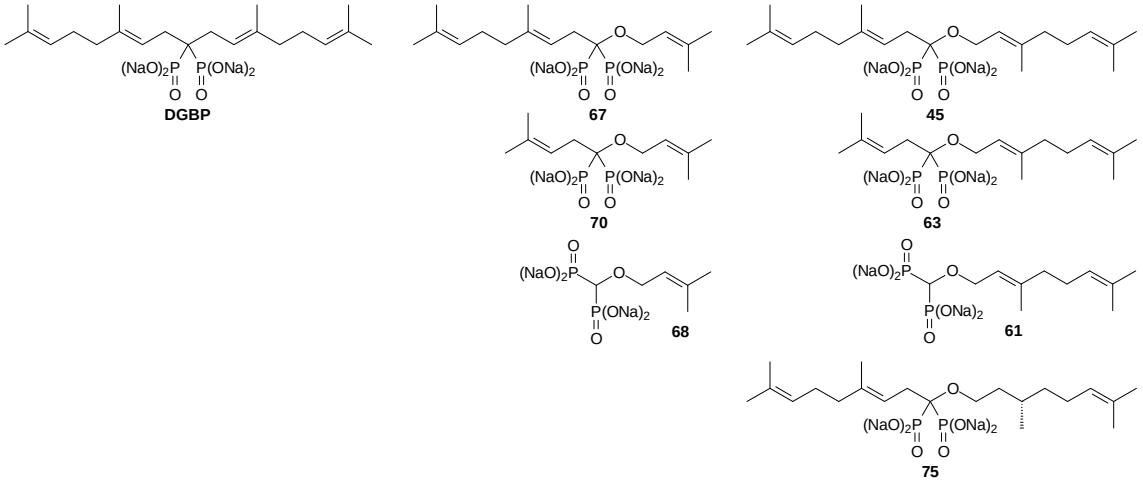

Figure 24. DGBP and its analogues

Biological results

As shown in Figure 25, in the mevalonate pathway, the substrates FPP with a fifteen carbon side chain and IPP with a five carbon side chain are joined by the enzyme GGDPS, to yield GGPP which has a twenty carbon side chain. By inhibition of GGDPS, we expect to see a decrease in intracellular GGPP concentration and less protein geranylgeranylation.[8]

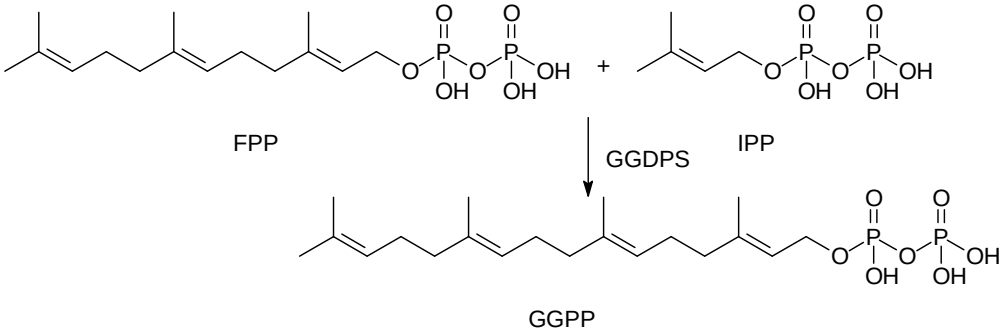

Figure 25. GGPP formation

The effects of compounds **45**, **63** and **67** on intracellular FPP and GGPP levels were examined at different concentrations. The known GGPP inhibitor DGBP and the HMG-CoA reductase inhibitor lovastatin were used as controls. The previously reported reversed phase HPLC methodology was applied to measure the intracellular FPP and GGPP levels.[76] Following incubation of K562 cells and the test compounds for 48 hours, cells were counted. Isoprenoid pyrophosphates were extracted from cell pellets with a standard extraction solvent (butanol/75mM ammonium hydroxide/ethanol 1:1.25:2.75). The FPP and GGPP in the residue were incorporated into fluorescent GGVLS and GCVLL peptides by FTase or GGTase I after drying down the extract under a stream of nitrogen gas. Reverse phase HPLC with a fluorescence detector was applied to separate and quantify the prenylated fluorescent peptides.

According to the results shown in Figure 26, all three of the dialkylated compounds (**45**, **63** and **67**), demonstrated the ability to decrease the concentration of GGPP and to raise the concentration of FPP, with compound **67**, the *C*-geranyl-*O*-prenyl bisphosphonate, being the most active. This result is consistent with the known GGDPS inhibitor DGBP and quite different from the HMG-CoA inhibitor, lovastatin, which reduced the concentration of both FPP and GGPP. In contrast, while the monoalkylated **68** has no effect on FPP/GGPP levels, compound **61** increases both FPP and GGPP levels. Because monoalkylated bisphosphonates lack the "V-shape" structure, they likely do not compete as effectively with substrates as do the dialkylated bisphosphonates. The mechanism behind compound **61**'s effects on GGPP levels remains to be determined.

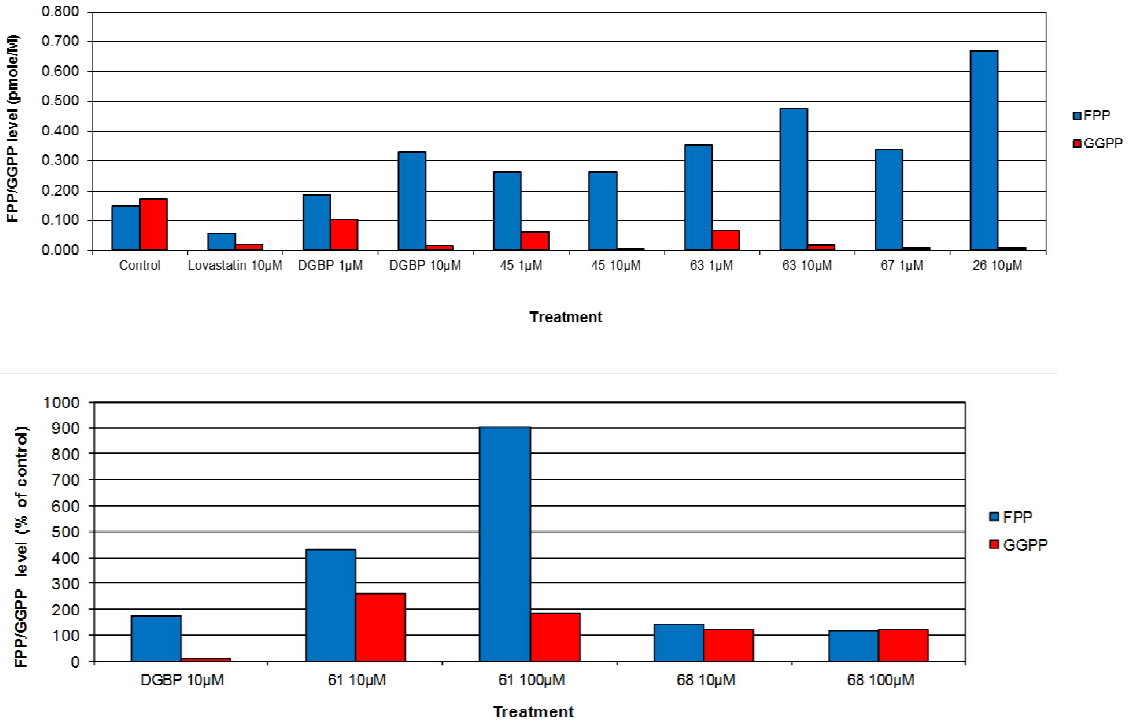

Figure 26. Effects of compounds on FPP and GGPP levels

This series of compounds also was tested against the K562 chronic leukemia cells for their abilities to induce cytotoxicity as measured by an MTT assay. Cells and potential drugs were incubated for 24-72 hours at 37 ºC and 5% CO_2. The experiment was performed following a previously reported MTT assay method.[77]

As shown in Figure 27, DGBP was used as a positive control for a comparison with compounds **45**, **61**, **68**, **63**, and **67**. Interestingly, both mono alkylated bisphosphonates **61** and **68** do not display any activity in the MTT assay. In contrast, all the dialkylated bisphosphonates compounds (**45**, **63**, and **67**) decreased MTT activity after 72 hours.

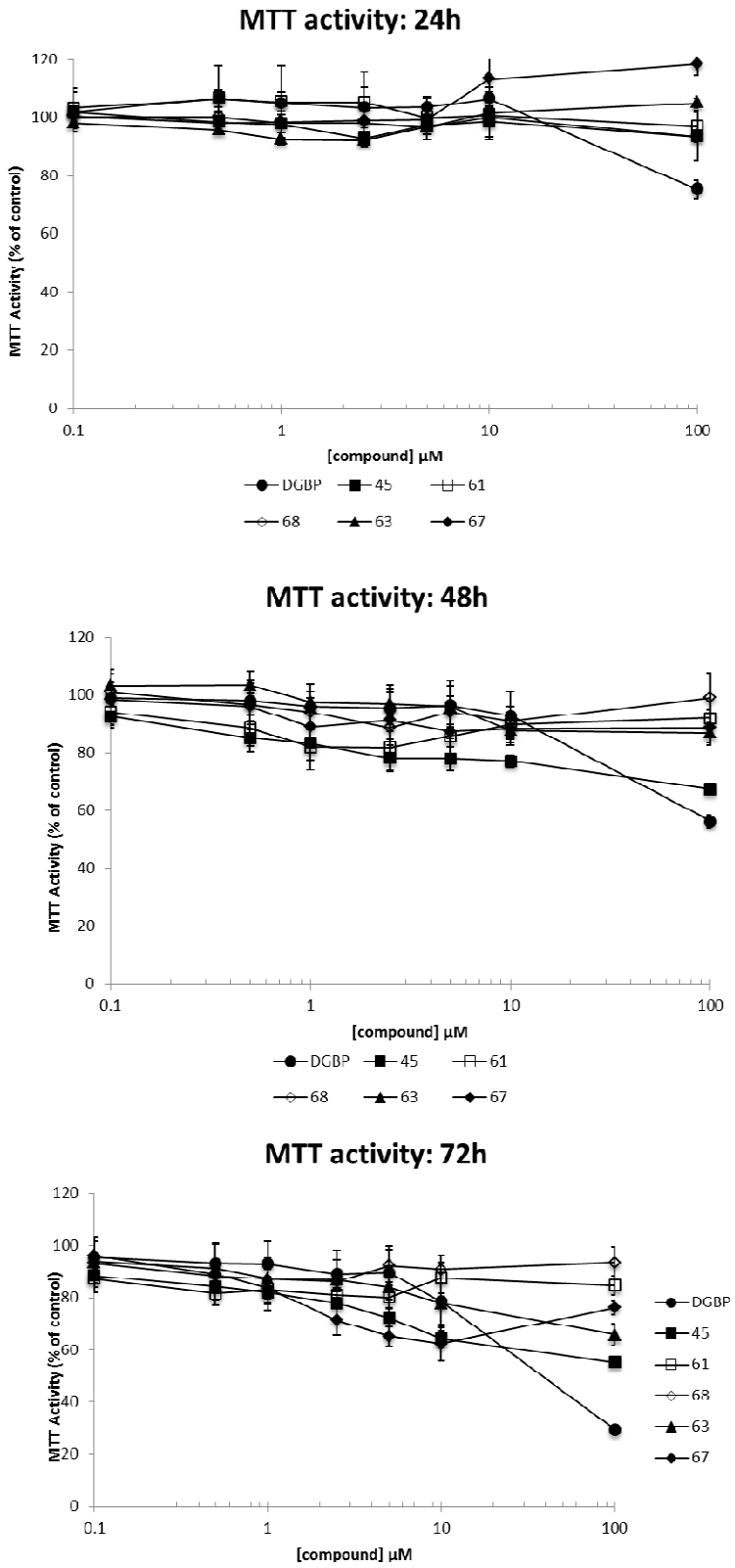

Figure 27. MTT Cytotoxicity Assay

Furthermore, these compounds have been screened in K562 cells using western blot studies to examine if they selectively inhibit protein gernylgeranylation over protein farnesylation. When the farnesylation of RAS protein is disrupted, both farnesylated RAS (lower band) and non-farnesylated RAS (upper band) can be observed on the gel. Therefore, according to the results obtained (Figure 28), none of the tested compounds inhibited FDPS.

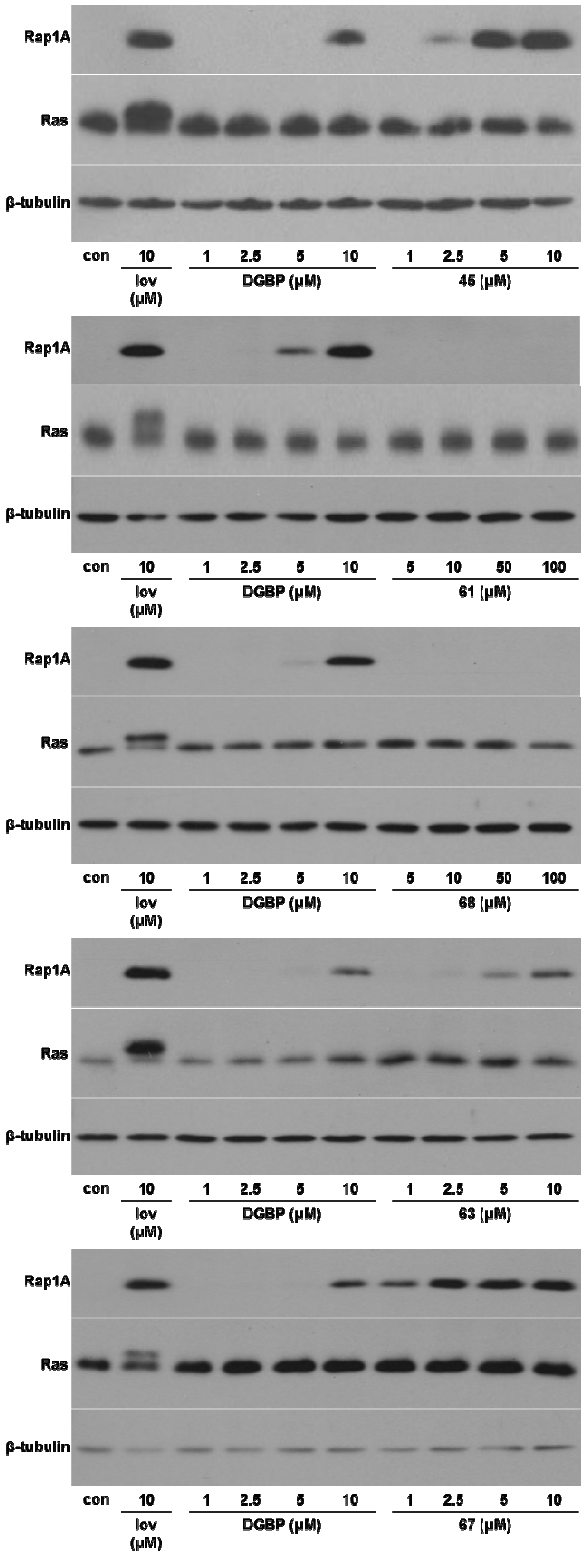

Figure 28. Effects of the novel bisphosphonates on Rap1a and Ras prenylation

To measure inhibition of GGDPS in cell culture is somewhat more complicated. GGPP is a substrate for both GGTase I and GGTase II. Rap1a is an example of a GGtase I substrate and Rab6 is a substrate for GGTase II. Inhibition of GGDPS will result in disruption of geranylgeranylation of both GGTase I and II substrates. Unlike RAS protein, only non-geranylgeranylated Rap1A protein can be detected on the gel using a commercially available antibody. As shown in Figure 28, only the dialkylated bisphosphonates **45**, **63** and **67** reveal non-modified Rap1A protein which means these compounds inhibit the geranylgeranylation of GGTase I substrates. The *C*-geranyl-*O*-prenyl bisphosphonate **67** was the most active, because the non-modified Rap1A protein can be detected at the lowest inhibitor concentration, 1 μM. To determine if the GGTase II pathway is also affected, evidence of non-modified Rab6 protein is needed. The antibody for Rab6 detects both modified and non-modified proteins but the two forms cannot be directly separated on the gel. To detect these forms separately, K562 cells were lysed with TX-114 detergent which separates cell lysate into a cytosolic (aqueous) fraction and a membrane (detergent) fraction. As a result, the geranylgeranylated protein will be in the detergent layer and the non-geranylgeranylated protein remains in the aqueous layer. Western blot analysis using the antibody directed against Rab6 can be used for both the aqueous and detergent fractions (Figure 29). The outcome of tests of the GGTase II activity is parallel to those found with GGTase I: three dialkylated bisphosphonates **45**, **63**, and **67** disrupt this route. The only chiral compound in this family, the *C*-geranyl-*O*-citronellyl bisphosphonate **75**, also was studied. Like all other dialkylated bisphosphonates, it selectively inhibits GGDPS over FDPS as well.

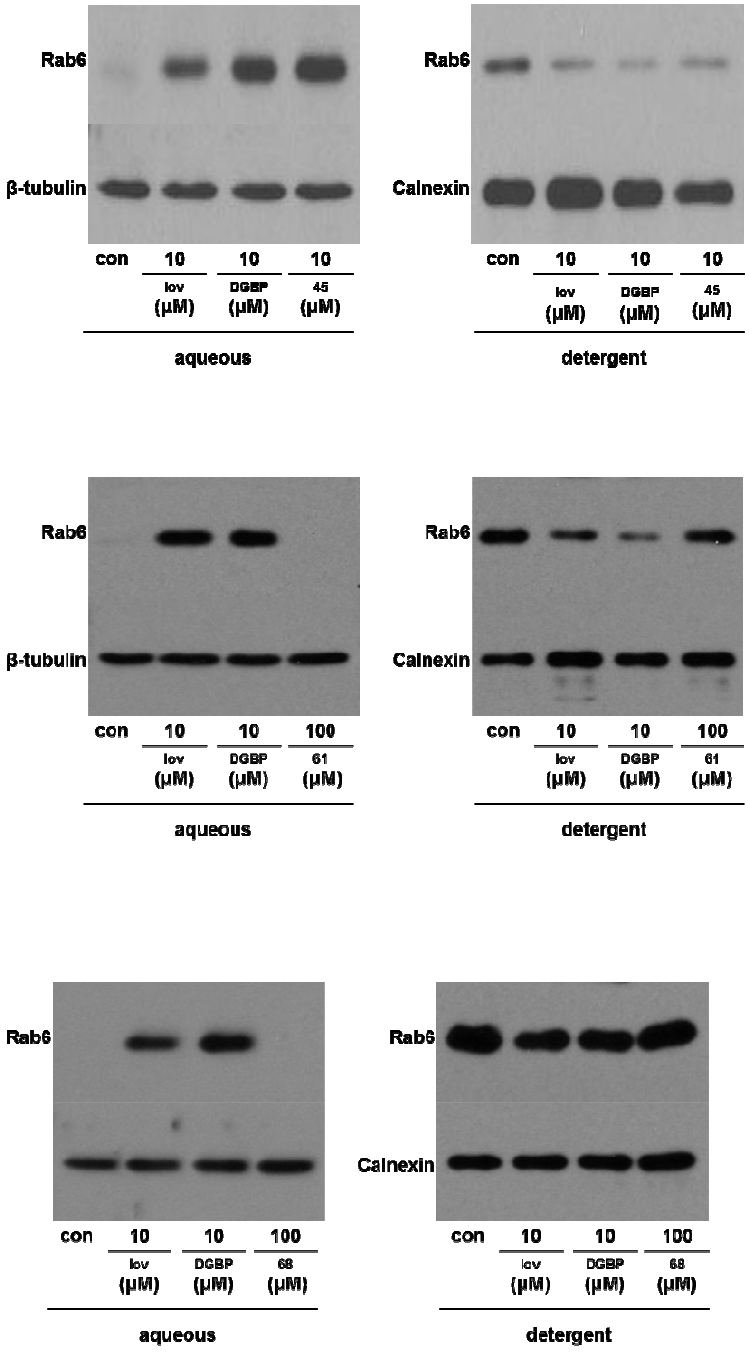

Figure 29. Effects of the novel bisphosphonates on Rab prenylation

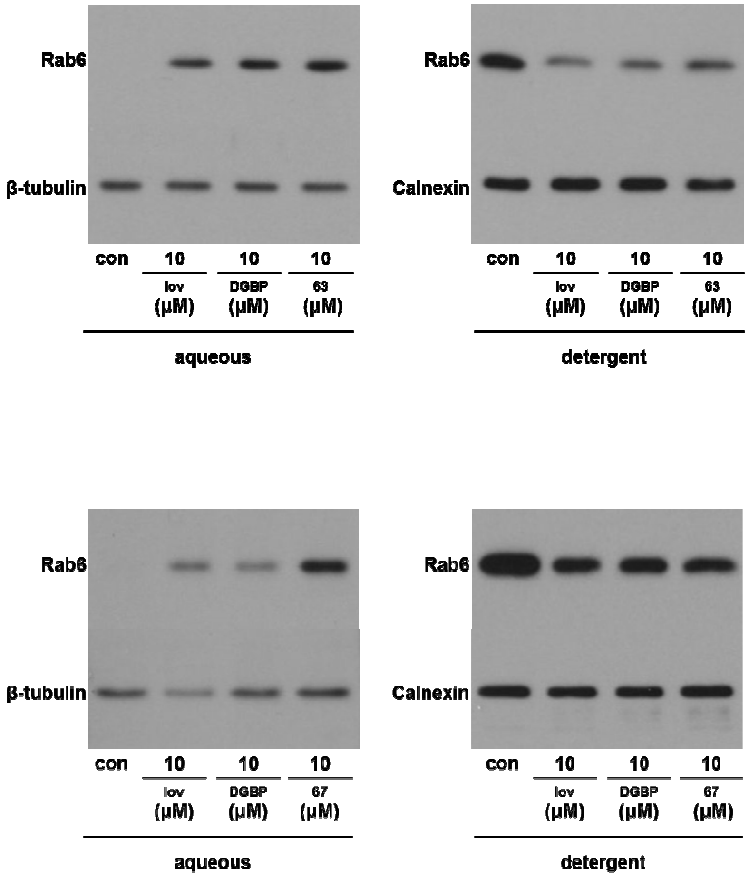

Figure 29 continued

The IC_{50} values of these compounds when they were tested against GGDPS and FDPS *in vitro* (table 1) have been evaluated as well. Not surprisingly, the *C*-prenyl-*O*-prenyl bisphosphonate **75**, which has the two shortest side chains, shows little activity in assays with both GGDPS and FDPS. In contrast to our expectations, most dialkylated bisphosphonates, including compounds **45**, **63** and **67**, did not demonstrate better potency than the parent compound, DGBP. However, the activity of the *C*-geranyl-*O*-geranyl bisphosphonate **45** is weaker than the *C*-prenyl-*O*-geranyl bisphosphonate **63** and

stronger than *C*-geranyl-*O*-prenyl bisphosphonate **67**. This data does support the hypothesis that the *C* terminal side chain and *O* terminal side chain will be orientated in a specific manner inside the enzyme. More excitingly, the *C*-geranyl-*O*-citronellyl bisphosphonate **75** shows the best potency in this class. Its IC_{50} value is 82 nM, which is about 3-fold more potent than the parent compound DGBP. This may suggest that the stereogenic center plays an important role to fit the *O*-terminal side chain in the enzyme pocket and boost the potency significantly.

Compound	GGDPS IC_{50} (nM)	FDPS IC_{50} (nM)
DGBP	262	> 10000
36 (Zoledronate)	ND	18
45	408	> 10000
63	274	> 10000
67	684	830
70	4750	5260
75	82	> 10000

Table 1. Compound activities against GGDPS and FDPS[48]

CHAPTER III

DEVELOPMENT OF INHIBITORS OF GGTASE II

As discussed in the last chapter, GGPP is used in the cell for protein prenylation of small GTPases such as Ras, Rab, Rho and Rac. There are several possible ways to disrupt the prenylation of these proteins. The most common way is to use statins to inhibit HMG-CoA reductase which catalyzes the very first step of the mevalonate pathway[78]. However, while statins diminish the generation of GGPP,[16,32,55] many other cellular processes are disrupted by these drugs as well, including protein farnesylation and cholesterol generation.[79] An effective alternative would be development of inhibitors selectively targeting either GGDPS, GGTase I, or GGTase II.[80] Unlike FTase and GGTase I, the modification of Rab protein requires one additional component, the Rab escort protein (REP), which delivers the Rab protein to GGTase II for further modification.[81] Several inhibitors of FTase and GGTase I have been reported,[82,83] but very few inhibitors have been identified to inhibit GGTase II. One of the known inhibitors is the chemical 3-PEHPC (**76**), an analogue of the clinically used bisphosphonate, risedronate (**35**, Figure 30). Although this compound has a high selectivity for GGTase II, a high concentration of this compound is necessary to generate any cellular effect with a reported IC_{50} value of about 600 μM.[84] More recently, McKenna et al, identified a carboxylic acid analogue of minodronate, (+)-3-IPEHPC, which is about 25 times more potent than 3-PEHPC.[85]

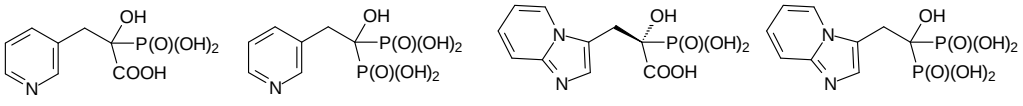

76 (3-PEHPC) **35** (risedronate) **77** ((+)-(S)-3-IPEHPC) **78** (minodronate)

Figure 30. GGTase II inhibitors and their parent compounds

To synthesize a more potent inhibitor, our initial approach was based on the analysis of the crystal structure of GGPP bound to GGTase II (Figure 31). Three different sites were identified, including the pyrophosphate recognition site which binds the polar head group of GGPP, the catalytic Zn binding site, and the terminal isoprene pocket that holds the final olefin of the C-20 chain.

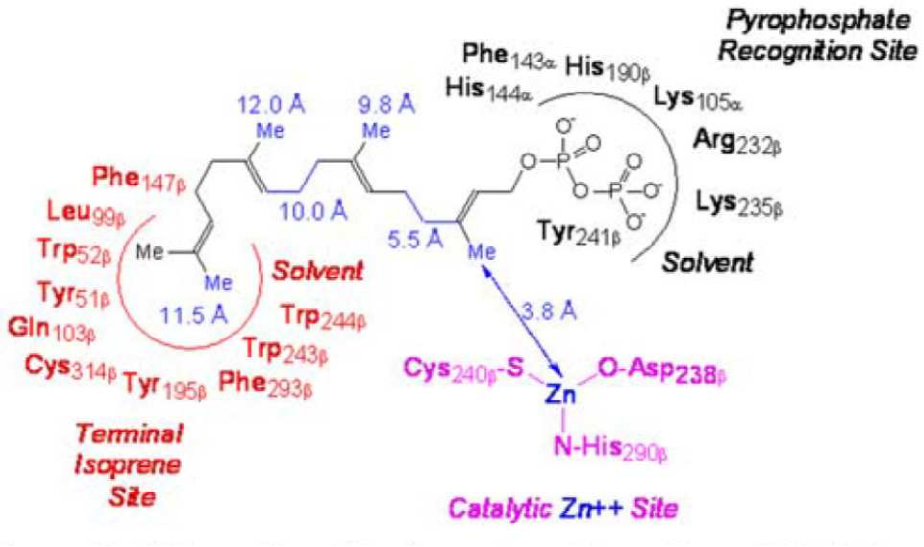

Figure 31. Schematic of the bound conformation of GGPP in GGTase II

The new generation of inhibitors we designed is shown in Figure 32. According to the previous research, the triazole group has been identified as a potential Zn binding group,[86,87] which can be assembled easily by a copper catalyzed click reaction between an alkyl azide and an acetylene in excellent yield.[88] A bisphosphonate head group was

intended to mimic the pyrophosphate head group within with the active site of the enzyme. At the same time, the terminal isoprenoid chain was designed to insert into the hydrophobic pocket. According to this design concept, a number of modifications can be done to prepare different analogues. For example, the bisphosphonate head group can be modified to an α-hydroxy phosphonate to examine different binding abilities with the enzyme active site. By changing the length of the carbon bridge which connects the head group and zinc binding group, we can insure the triazole moiety is located at the most effective position to bind to the zinc atom. Modification of different tail groups will allow the potential inhibitor to occupy the best space inside the enzyme's hydrophobic pocket.

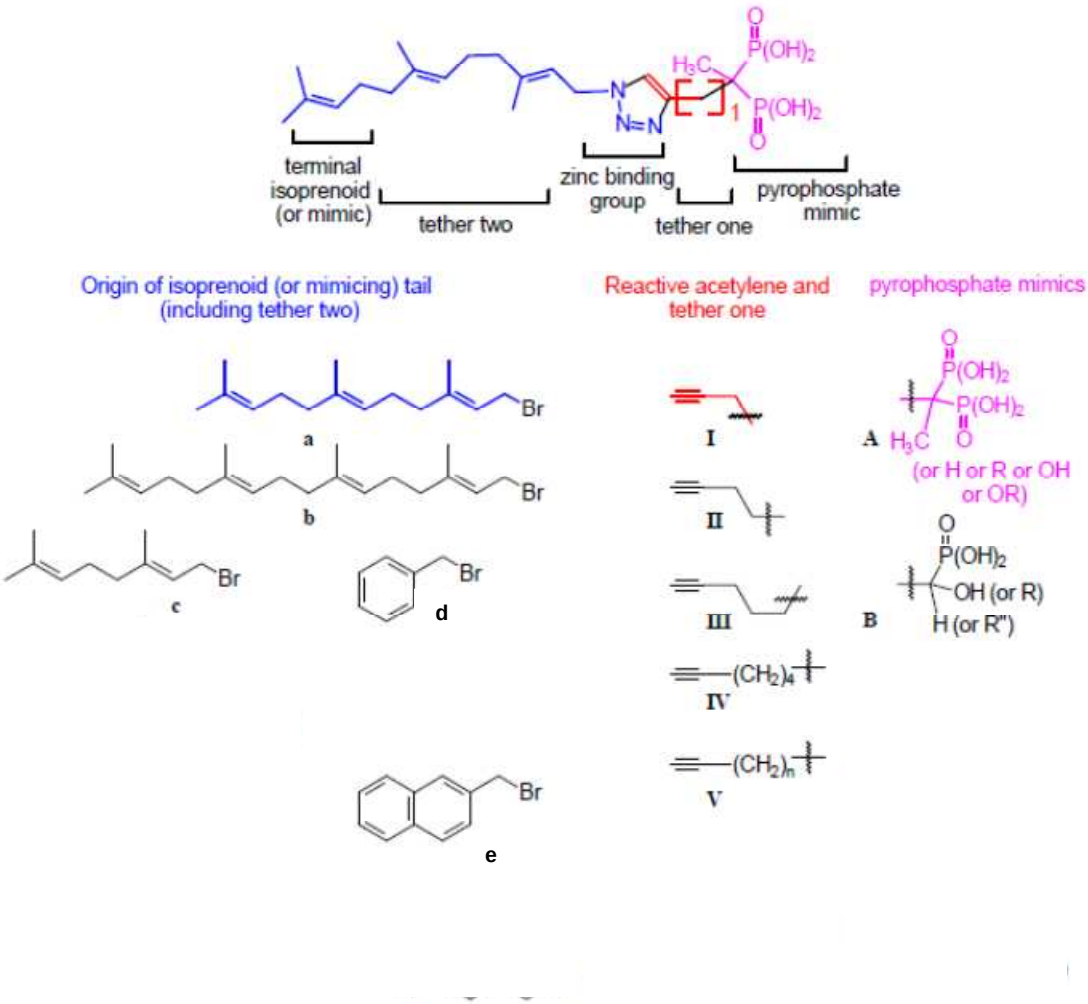

Figure 32. Prototypical GGTase II inhibitor with representative isoprenoid, reactive acetylenes, and pyrophosphate mimics

Synthesis of the first generation of triazoles

The general structure of this type of compounds can be simplified to salt **79** which is shown in Figure 33. Salt **79** would arise from the hydrolysis reaction of ethyl ester **80**, and this key triazole core structure can be assembled quickly by a coupling reaction between an acetylene **81** and an azide **82** catalyzed by a Cu (I) catalyst. This reaction is commonly known as a "click" reaction which has the following advantages: one-flask,

high regioselectivity, and high yield.[88] The acetylene **81** would be prepared from tetraethyl methylenebisphosphonate **83**.[89] Using a different starting material, such as triethyl phosphonoacetate, different head groups can be added to this family of compounds. On the other hand, azides **82** can be obtained easily from many different commercially available alcohols (**84**) which provides variety for the tail groups found in salt **79**.

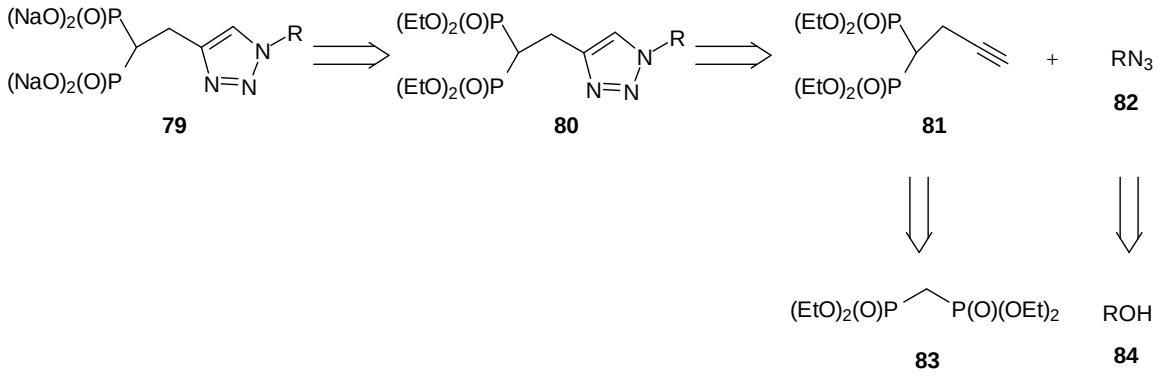

Figure 33. Retrosynthesis of triazole bisphosphonate compounds

The first analogue prepared in this family was the geranyl triazole bisphosphonate **90** (Figure 34).[47] The synthesis started with conversion of geraniol (**85)** to geranyl bromide (**86)** by treatment with PBr_3. The resulting bromide **86** was then allowed to react with a sodium azide solution to produce the corresponding allylic azide **87**. For the coupling partner, tetraethyl methylenebisphosphonate **83** was allowed to react with paraformaldehyde to form a primary alcohol intermediate, which was dehydrated upon treatment with TsOH to give the alkene **88** in 88% yield.[90] A 1,4-addition reaction condition was carried out on the intermediate **88** by addition of a slurry of sodium acetylide to produce the desired acetylene **81** which is another key intermediate for the entire synthetic approach.[89] With acetylene **81** and azide **87** in hand, the compounds

were allowed to react in a reaction catalysed by a Cu (I) catalyst to produce triazole **89** in good yield.[89,91] Ethyl ester **89** was then hydrolyzed by treatment with TMSBr and NaOH[49] to form the biologically testable salt **90**.

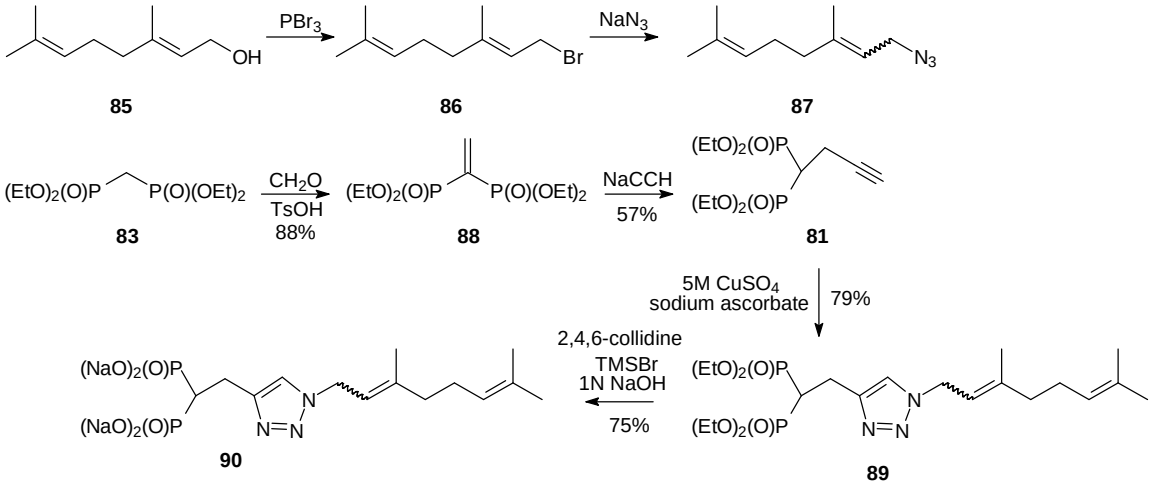

Figure 34. Synthesis of geranyl triazole bisphosphonate

A second important analogue in this family was the geranylgeranyl triazole bisphosphonate **97** (Figure 35). Because commercial geranylgeraniol is a mixture of olefin isomers, this synthesis started from farnesylacetone **91** which was treated with triethyl phosphonoacetate to generate ethyl ester **92**. Reduction by $LiAlH_4$ gave geranylgeraniol **93** in 79% yield.[92] This alcohol was then converted to the corresponding bromide **94** and then to azide **95**. Following the standard click reaction condition,

triazole **96** was obtained in 58% yield. This ester was hydrolysed to obtain salt **97**.[47]

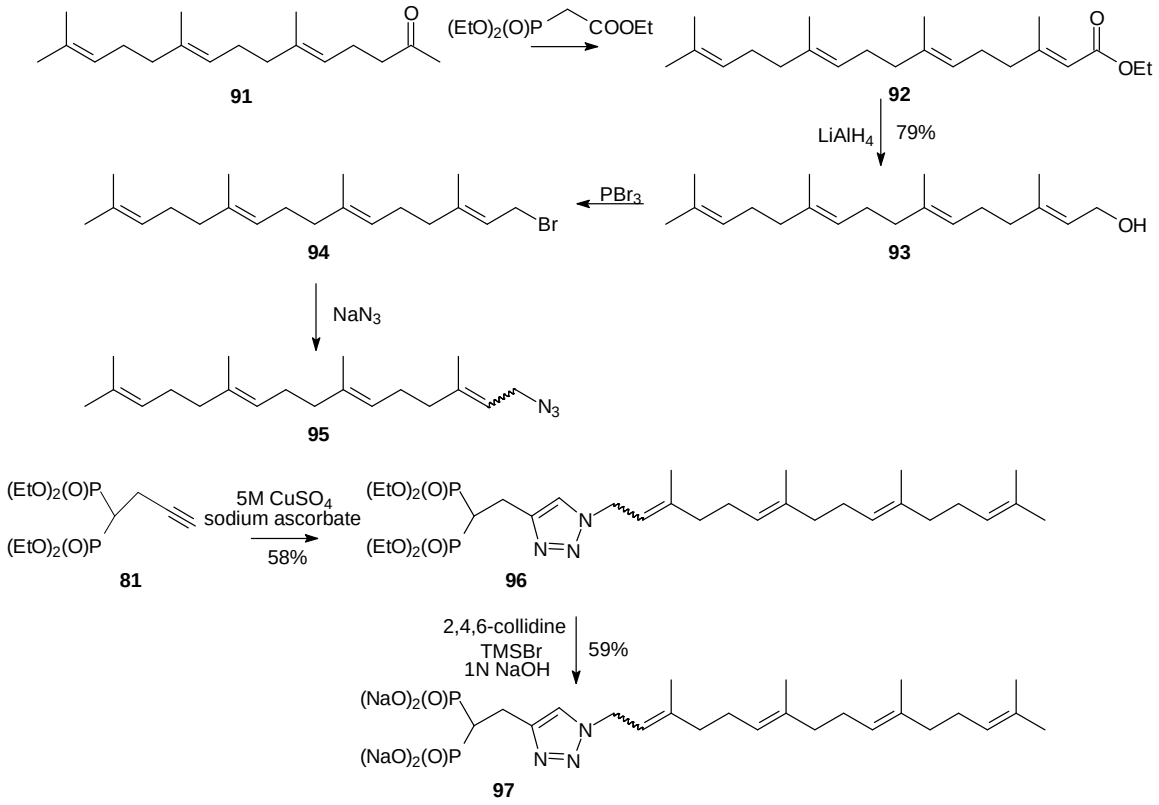

Figure 35. Preparation of geranylgeranyl triazole bisphosphonate

Following this general strategy, a number of analogues have been prepared in this family (Figure 36). Farnesyl azide was synthesized from pure *trans, trans*−farnesol. The parallel benzyl and naphthyl compounds could be easily prepared from commercially available benzyl bromide and naphthyl bromide. In contrast, the primary azide **101** is a new compound, and was synthesized for the first time here. For this target compound, diol **98** was allowed to react with 0.5 equivalents of prenyl bromide to give ether **99**.[93] A bromination reaction with CBr_4 successfully converts primary alcohol **99** to the corresponding bromide **100**[94] which was further allowed to react with NaN_3 in DMF at 100 °C to yield the desired azide **101**. The azide **101** undergoes a click reaction with

acetylene **81** to give the expected triazole **105**. Unfortunately, bisphosphonate **105** did not survive the TMSBr hydrolysis conditions, but all other bisphosphonate ethyl esters have been hydrolysed to their corresponding salts.[47]

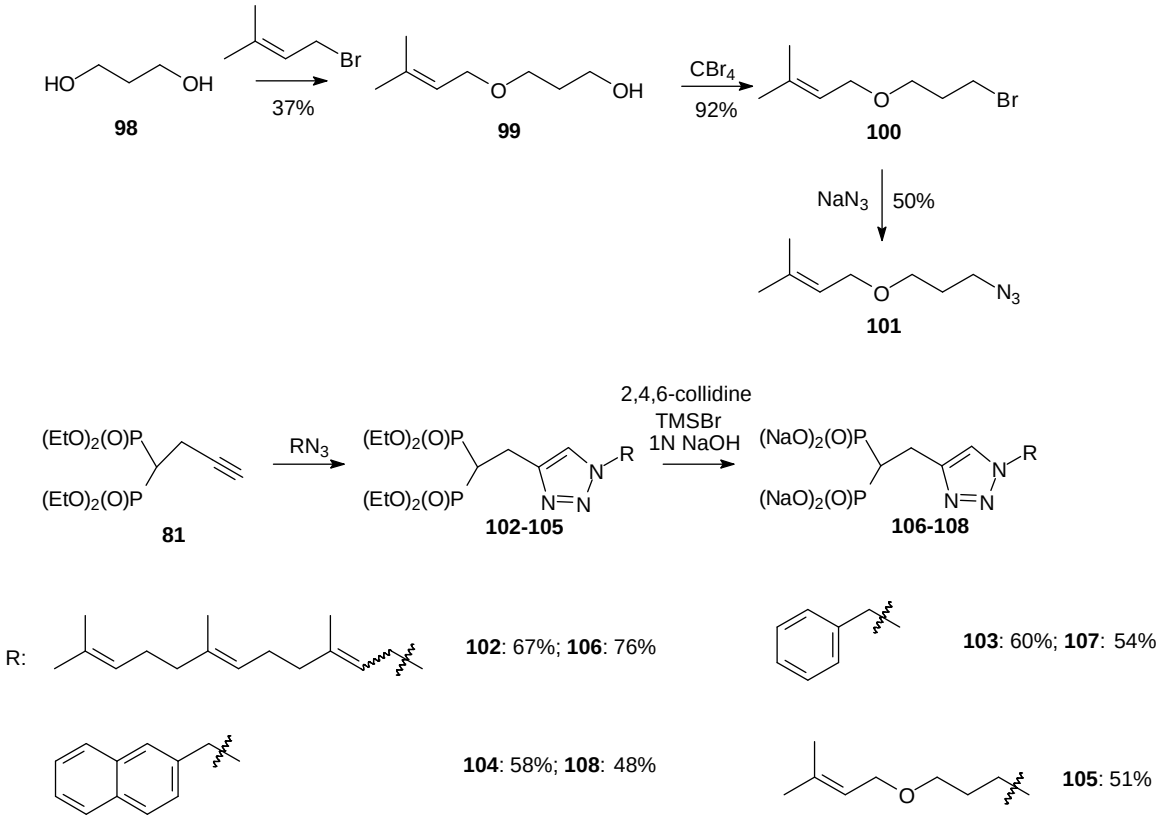

Figure 36. Additional analogues prepared

For the biological evaluation, radiolabeled GGPP, recombinant GGTase II, a Rab substrate, and REP were used to test the five new triazole bisphosphonic acids, compounds **90, 97, 106, 107,** and **108**.[95] As shown in Table 2, inhibitory activity against GGTase II was significantly affected by the length of the alkyl chain. The most active compound was geranylgeranyl triazole bisphosphonate **97**, which bears the longest side chain. In contrast, little activity against GGTase II was displayed by the geranyl length compound **90**, and the farnesyl length compound **106** displayed only modest activity.

Following a 48 h incubation, the ability to induce cytotoxicity in the human-derived myeloma cell line RPMI-8226 was also tested with these five compounds.[96] Interestingly, there was not a uniform correlation between the observed cytotoxicity and the GGTase II inhibitory activity. The most potent compound in the MTT assay was the napthyl derivative **108**. Although it is still unclear what mechanism(s) of action is (are) responsible for this compound's cytotoxic effect, cellular assays demonstrated that this compound does not affect protein farnesylation or geranylgeranylation.[47]

Compound	GGTase II IC_{50}	MTT IC_{50}
90	> 2 mM	> 1 mM
97	0.10 mM	1 mM
106	0.65 mM	0.9 mM
107	2 mM	> 1 mM
108	> 2 mM	0.2 mM

Table 2. Biological activities of triazoles **90**, **97**, **106**, **107** and **108**[47]

Although the first generation triazole bisphosphonates have been prepared as described above, a significant synthetic limitation that cannot be ignored was that some of these compounds were not obtained as single olefin isomers. When geranyl triazole bisphosphonate **90** was formed, unexpected carbon peaks were observed in the unsaturated region of the ^{13}C NMR spectrum. The same concern also was found with the farnesyl and geranylgeranyl triazole bisphosphonates **106** and **97**. The common feature of these three molecules is they all have an allylic side chain with olefin stereochemistry at the first internal olefin. Formation of olefin stereoisomers was suspected.

At least two different possibilities might cause this isomerization problem. First of all, when acetylene and alkyl azide react to form the triazole ring, two possible isomers could be generated and different regioisomers might be formed, such as compounds **109** and **110** in Figure 37. However, according to Sharpless and Fokin's research, to generate a product like **109** or **110**, either copper (I) or ruthenium catalyst is needed respectively. Furthermore, these two catalysts should afford a very clean reaction product as a single isomer.[88,97] A second possible source of the isomerization would be impurities from starting material acetylene **81** or alkyl azide **111**. Both the ^{1}H and ^{13}C NMR spectra indicated that acetylene **81** was a material with high purity. In contrast, the NMR data of azide **111** (n = 2) was very similar to what was observed with triazole **89**, especially in that in contained overabundance of olefin resonances.

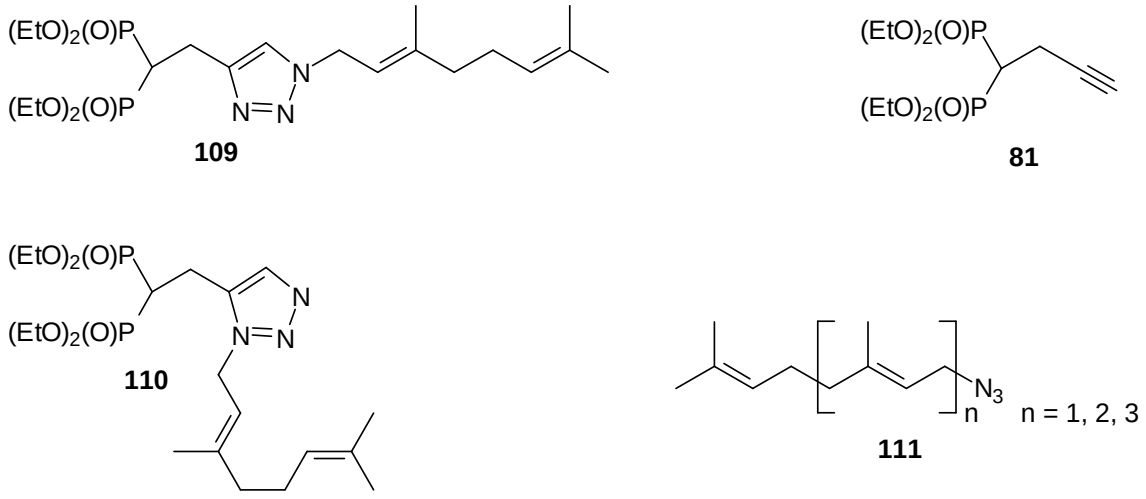

Figure 37. Possible isomerization problems

Further investigation of azides **111** reveals that there is an allylic azide rearrangement reaction as shown in Figure 38.[98] Assuming that the pure allylic azide **112** is obtained, it will undergo a sigmatropic rearrangement spontaneously to form the secondary azide **114**. This new azide also can rearrange back to a primary allylic azide form, but there is no stereocontrol for this reaction stage. Although the *trans* configuration is more favored than the *cis* one, this azide isomer mixture is composed of three different components, including the *trans* allylic azide **116**, the *cis* allylic azide **115** and the secondary azide **114**. Upon treatment under click reaction condition, a tertiary azide, such as compound **117** will not be able to cyclize with acetylene to form a triazole ring, but both *trans* and *cis* allylic azides are reactive. Once again, although the *trans* allylic azide is more reactive than the *cis* isomer, the final product will be a mixture of *trans* and *cis* compounds.[98] This phenomenon easily explains the isomerization problem with these isoprenoid azides.

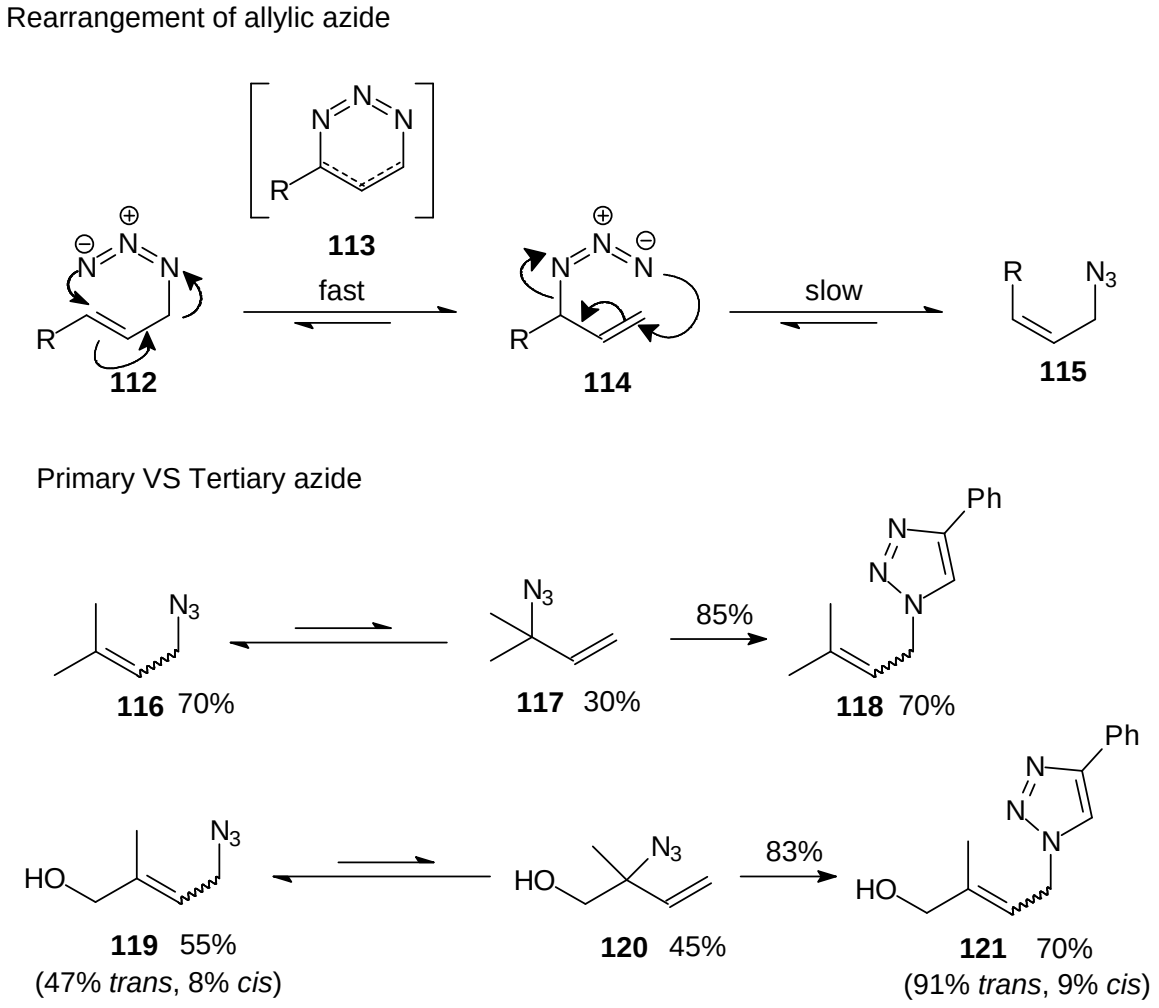

Figure 38. Sigmatropic rearrangement reactions of allylic azides[98]

After learning of this rearrangement reaction, we assumed that either the *trans* allylic alcohol geraniol, or the *cis* allylic alcohol nerol would lead to the same product mixture. To test this assumption, a new synthesis starting from nerol was carried out. As shown in Figure 39, this synthesis began with nerol (**122**). The alcohol was converted to azide **124** through bromide **123** by standard conditions as described above. With azide **124** and acetylene **81** in hand, these two intermediates were treated under click reaction condition to form the triazole **125**. The NMR data for triazole **125** was carefully

compared with compound **89**, which was the product obtained from the starting material, geraniol (**85**). The spectra of these two reaction products were almost identical and indicated that both are mixtures containing about 67% *trans* and 33% *cis* isomers, which were not readily separable.

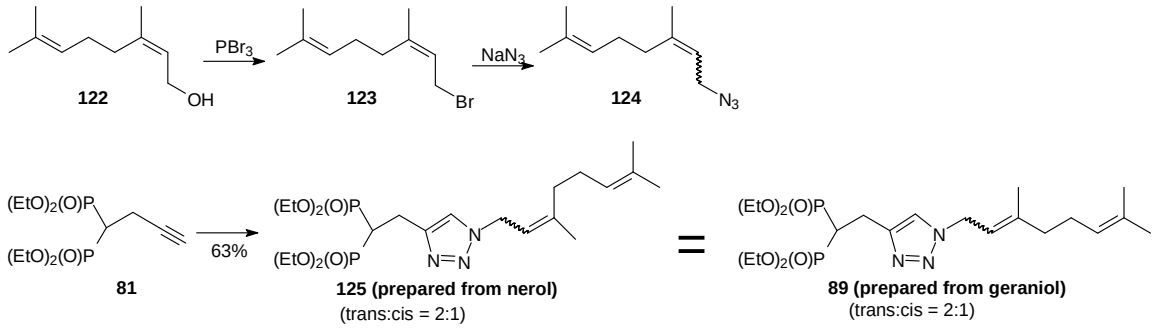

Figure 39. Study of sigmatropic rearrangement reaction

Because the first generation compounds we provided for the biological studies were isomer mixtures, and according to feedback from the preliminary results, the compound which bears the longest side chain, geranylgeranyl triazole bisphosphonate **97** was the one most active against GGTase II,[47] it was important to seek a synthetic route to prepare this compound as a single isomer. Therefore, the next research objective became determination of a strategy to address this allylic azide rearrangement. To work out this issue, there are several potential solutions. One might think that changing the allylic azide to a primary azide would avoid such a problem. One possible strategy would be to insert one additional CH_2 group between the azide and alkene functional groups to make a homoallylic azide. An alternate solution would be to add a protecting group to mask the original alkene functional group and its stereochemistry, and then regenerate the olefin with stereoselectivity after the formation of triazole ring. The advantage of this solution is that extra length is not added to the side chain, and it could keep its original

trans or *cis* configuration. I chose to investigate this option to address the stereochemical problem.

A common way to protect an alkene functional group is to allow reaction with *m*CPBA to form an epoxide ring (Figure 40). However, deoxygenation with stereocontrol is a challenge, especially with the unknown effects of the triazole ring and bisphosphonate moiety. According to Caputo's study, an epoxide can be removed by treatment with trimethylsilyl halide.[99] Halide anion will open the epoxide **128** from the back to form the intermediate **129**. Reaction with a second halide anion follows an E2 elimination mechanism to regenerate alkene **130** with its original configuration.

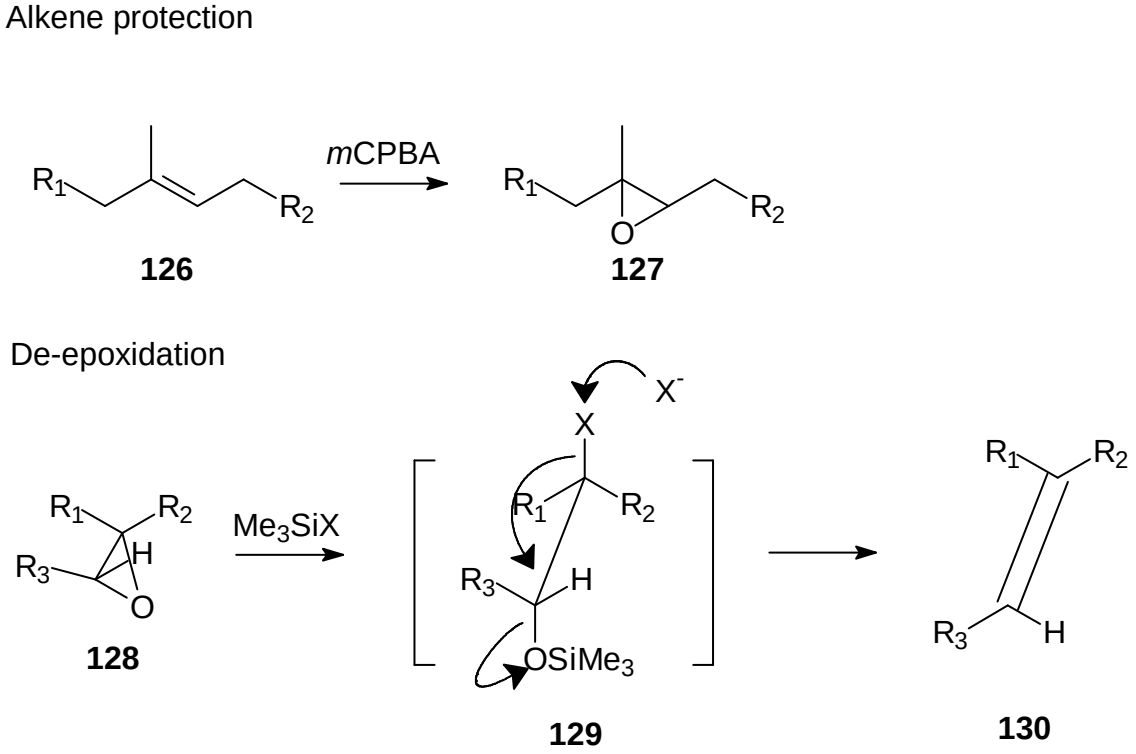

Figure 40. Alkene protection and deprotection

To apply this strategy, it was necessary to selectively protect the internal olefin of geraniol which was readily accomplished by methods of Sharpless.[100] Following his

conditions, geraniol (**85**) was allowed to react with TBHP in a reaction catalysed by vanadyl acetylacetonate[100,101] to give epoxide **131** in 71% yield. The primary alcohol **131** was converted to the mesylate first and then to bromide **132**,[102] which further reacted with sodium azide in DMF (with protection from light) to yield azide **133**.[103] With both azide **133** and acetylene **81** in hand, under the click reaction conditions the resulting cyclization product bisphosphonate **134** was generated as a single isomer.

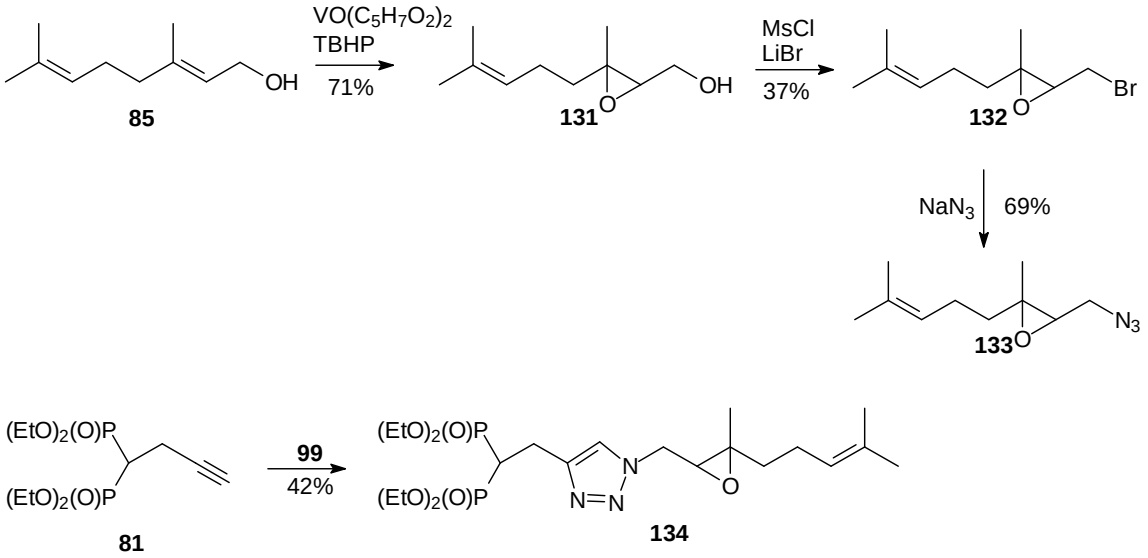

Figure 41. Alkene protection

At this stage, the key issue of the synthesis becomes reduction of the epoxide with stereocontrol. Following Caputo's procedure, NaI was treated with TMSCl first and followed by the addition of epoxide **134** to allow reaction at room temperature.[99] However, only unreacted starting material was observed by TLC without any desired product generated. One potential alternative would be Sonnet's in situ conditions.[104] Therefore, NaI and trifluoroacetic anhydride (TFAA) were allowed to react to form trifluoroacetyl iodide first, which then reduces the epoxide to the corresponding olefin.

This method successfully converted epoxide **134** to alkene **135** in 55% yield. The NMR data suggested that compound **135** was obtained as a single olefin isomer as well. This compound was then hydrolysed by treatment with TMSBr and NaOH to the corresponding sodium salt **136** under standard conditions.

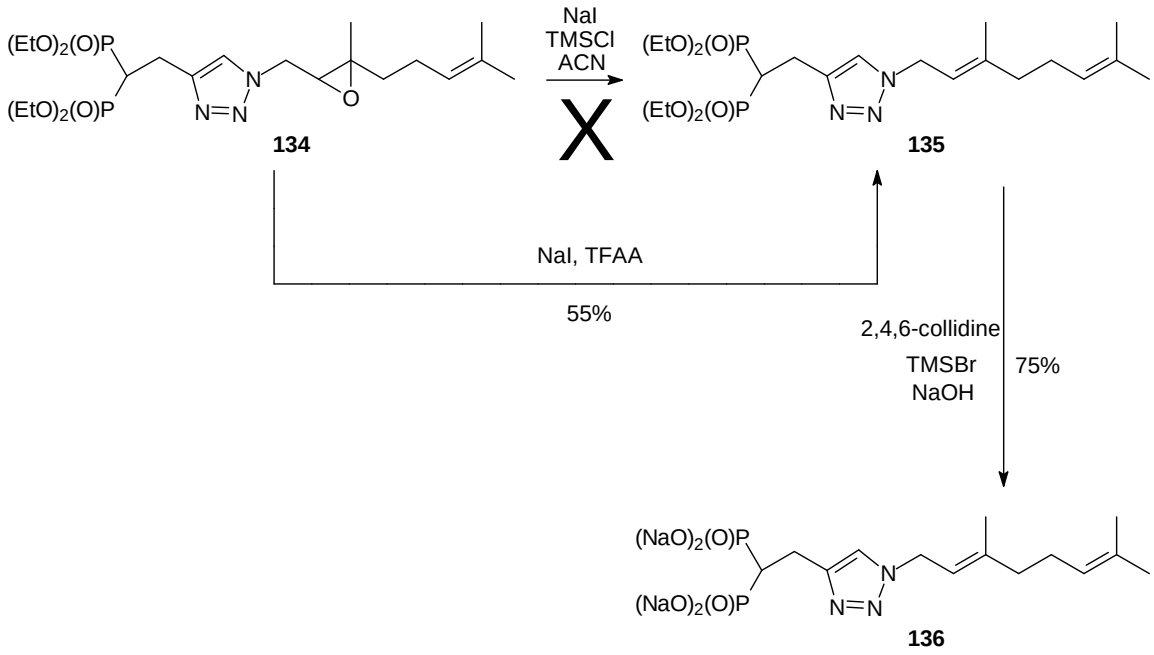

Figure 42. Epoxide reduction to olefin

The experiments described above proved that an epoxide can be used as a protecting group to avoid allylic azide rearrangements. However, it was still necessary to prove that it also holds either the original *trans* or *cis* configuration of the allylic side chain when converted back to the olefin. Therefore, it was necessary to prepare a *cis* epoxide for comparison. The parallel synthesis started from the *cis* alcohol nerol **122** (Figure 43). It was oxidized by vanadium-mediated oxidation with TBHP,[100,101] to give epoxide intermediate **137**, which was then converted to epoxide azide **139** through bromide **138**. With acetylene **81** and azide **139** in hand, they were allowed to react under

click reaction conditions to generate the triazole ring and form the bisphosphonate ethyl ester **140**.

With the same deoxygenation conditions described above, epoxide **140** was reduced by treatment with NaI and TFAA to the corresponding olefin **141** as a single isomer. The NMR spectra of olefin **141** were carefully compared with those of compound **135**. These spectra clearly indicated that these two pure isomers were different compounds. The most diagnostic carbon NMR signal was the methylene carbon adjacent to the newly formed olefin. It was observed at 39.6 ppm for compound **135** and 32.2 ppm for compound **141**. This observation is very similar to the values reported for geraniol (39.7 ppm) and nerol (32.2 ppm).[105] Tetraethyl ester **141** subsequently was hydrolysed to its corresponding sodium salt **142**. At this point, not only had we fully proved that this deoxygenation conditions restored the original olefin stereochemistry of the allylic side chain, but we also had prepared a testable compound to study the relative biological activity of these two isomers.

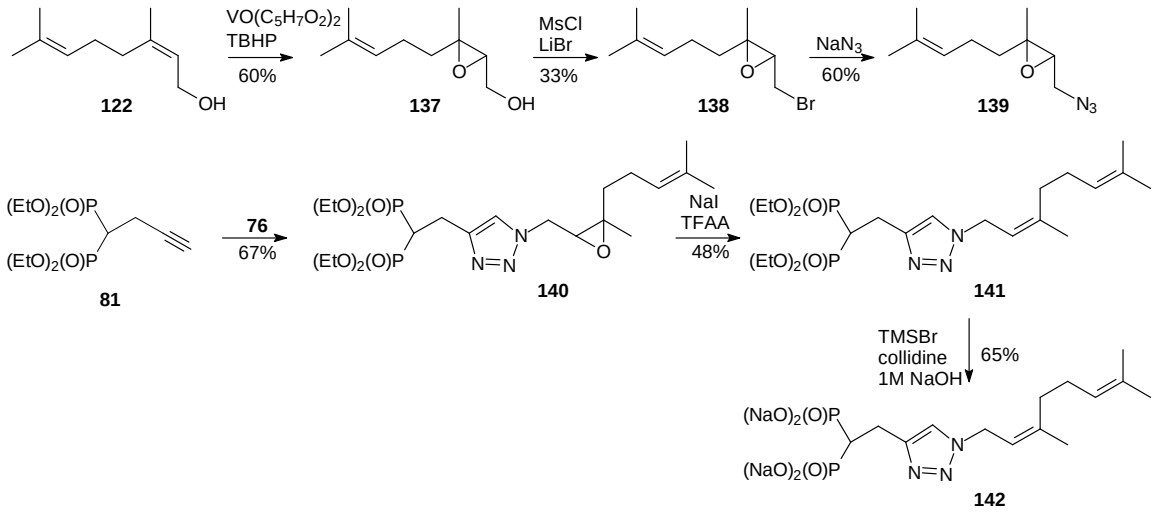

Figure 43. Synthesis of neryl triazole bisphosphonate

According to the biological results from the first generation of the triazole compounds, the analogues with longer side chain tend to have better biological potency. Therefore, the third new analogue which was prepared as a single isomer was the *trans, trans*−farnesyl triazole bisphosphonate **149** (Figure 44). With the same strategy, synthesis started from pure *trans, trans*−farnesol **143**, and the internal olefin was selectively protected as the epoxide. The resulting epoxide alcohol **144** was converted through the bromide **145** to the epoxide azide **146**, and then was allowed to cyclize with acetylene **81** to give epoxide triazole **147**. Upon treatment with NaI and TFAA, the epoxide **147** was reduced to olefin **148** which was further converted to the corresponding sodium salt **149**, the target compound.

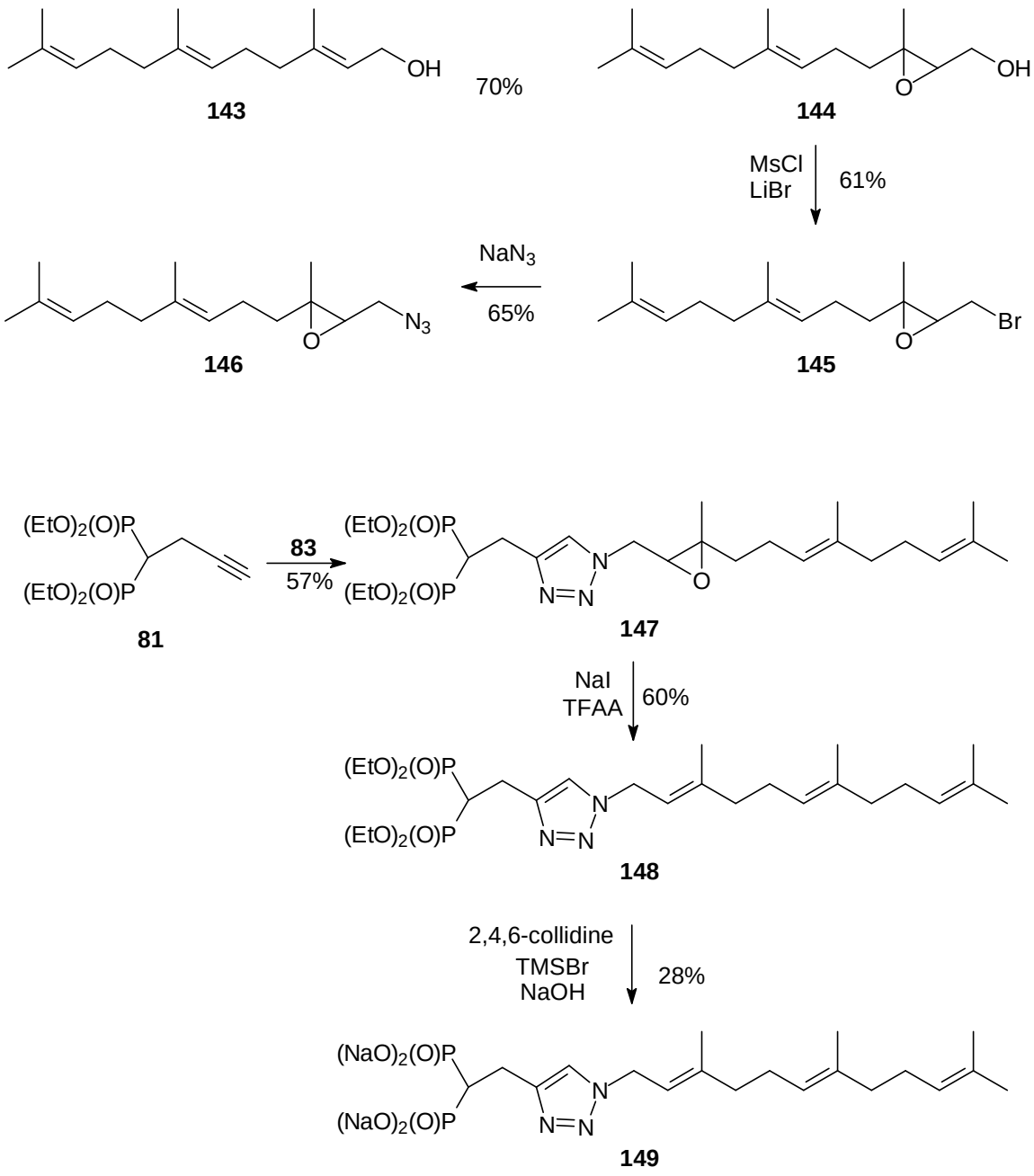

Figure 44. Synthesis of farnesyl triazole bisphosphonate

Because it would be interesting to determine if the potency would be improved with an epoxide ring on the internal olefin of the side chain, the last compounds prepared in this family were the sodium salts **150** and **152** (Figure 45). However, when ethyl ester **134** was treated under the standard hydrolysis condition, multiple phosphorus NMR

resonances were observed in the ^{31}P NMR spectrum. It is not hard to imagine that excess NaOH or a long reaction time would allow base to attack the epoxide ring and through an S_N2 reaction mechanism form diol **151**. Therefore, epoxide **134** was treated briefly with four equivalents of 1N NaOH to afford the desired product, sodium salt **150** in 46% yield. The same procedure was applied to epoxide **140** as well, to convert it to the corresponding sodium salt **152** in 76 % yield.[46]

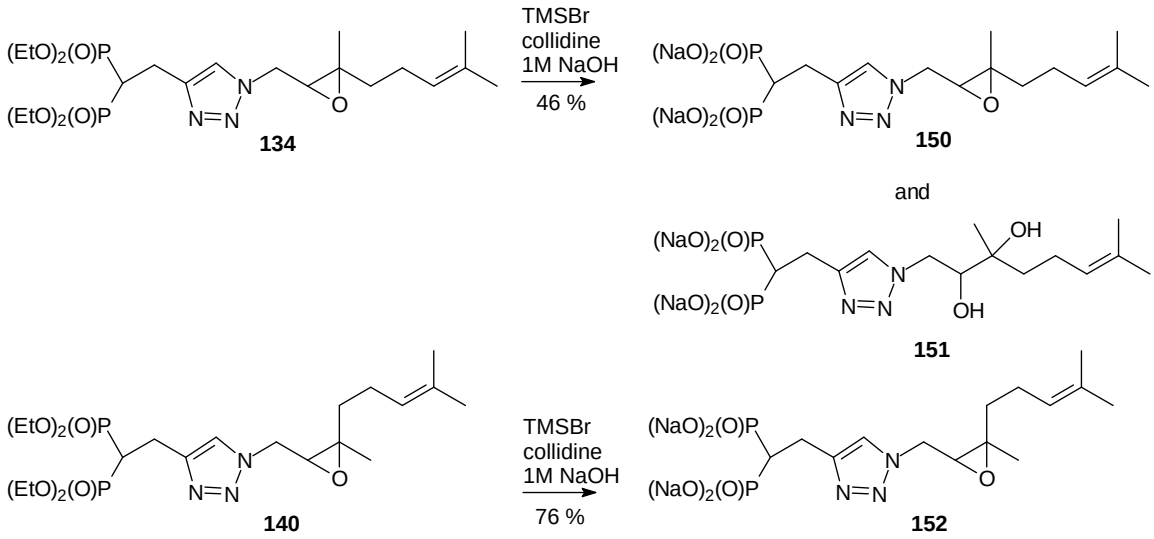

Figure 45. Synthesis of an epoxide triazole bisphosphonate

Biological results

All of the second generation triazole compounds were submitted for the biological tests as single isomers. Our preliminary studies with compound **90** revealed that it disrupts protein geranylgeranylation in intact cells. To determine whether this activity is a consequence of the geranyl and/or neryl stereochemistry, and to begin to determine the underlying mechanism of action, a series of western blot experiments was performed. Rap1a is a substrate of GGTase I while Rab6 is a substrate of GGTase II. For detection of Rap1a, whole cell lysate was prepared and an antibody that detects only unmodified

Rap1a was utilized. For Rab6, a Triton X-114 lysis was employed to generate aqueous and detergent fractions. Under control conditions, the majority of Rab6 is found in the detergent (membrane) fraction, while in the setting of an agent which disrupts Rab geranylgeranylation, Rab6 becomes localized to the aqueous (cytosolic) fraction. The known GGDPS inhibitor[31] digeranyl bisphosphonate (DGBP)[55] was used as a positive control.

As shown in Figure 46A, the positive control DGBP interrupts the geranylgeranylation of Rap1a protein, as does the *trans*, *cis* isomer mixture **90** (2 : 1 E to Z). Neryl triazole bisphosphonate **142** strongly disrupts Rap1a geranylgeranylation while geranyl triazole bisphosphonate **136** barely disrupts it (Figure 46B). In contrast, neither epoxides **150** nor **152** show any inhibition effect. Only the isoprenoid mixture **90** and the neryl **142** disprupted Rab geranylgeranylation (Figure 46A). To examine the differences of inhibition on Rap1a geranylgeranylation between *trans* compound **136** and *cis* compound **142**, the parallel experiments were carried out with a lower concentration series. Neryl triazole bisphosphonate **142** begins to show inhibition against geranylgeranylation at a 1 μM concentration while geranyl triazole bisphosphonate **136** does not have an obvious effect even at 10 μM. These experiments indicate that the *cis* compound **142** is much more potent than the *trans* compound **136** (Figure 46B).

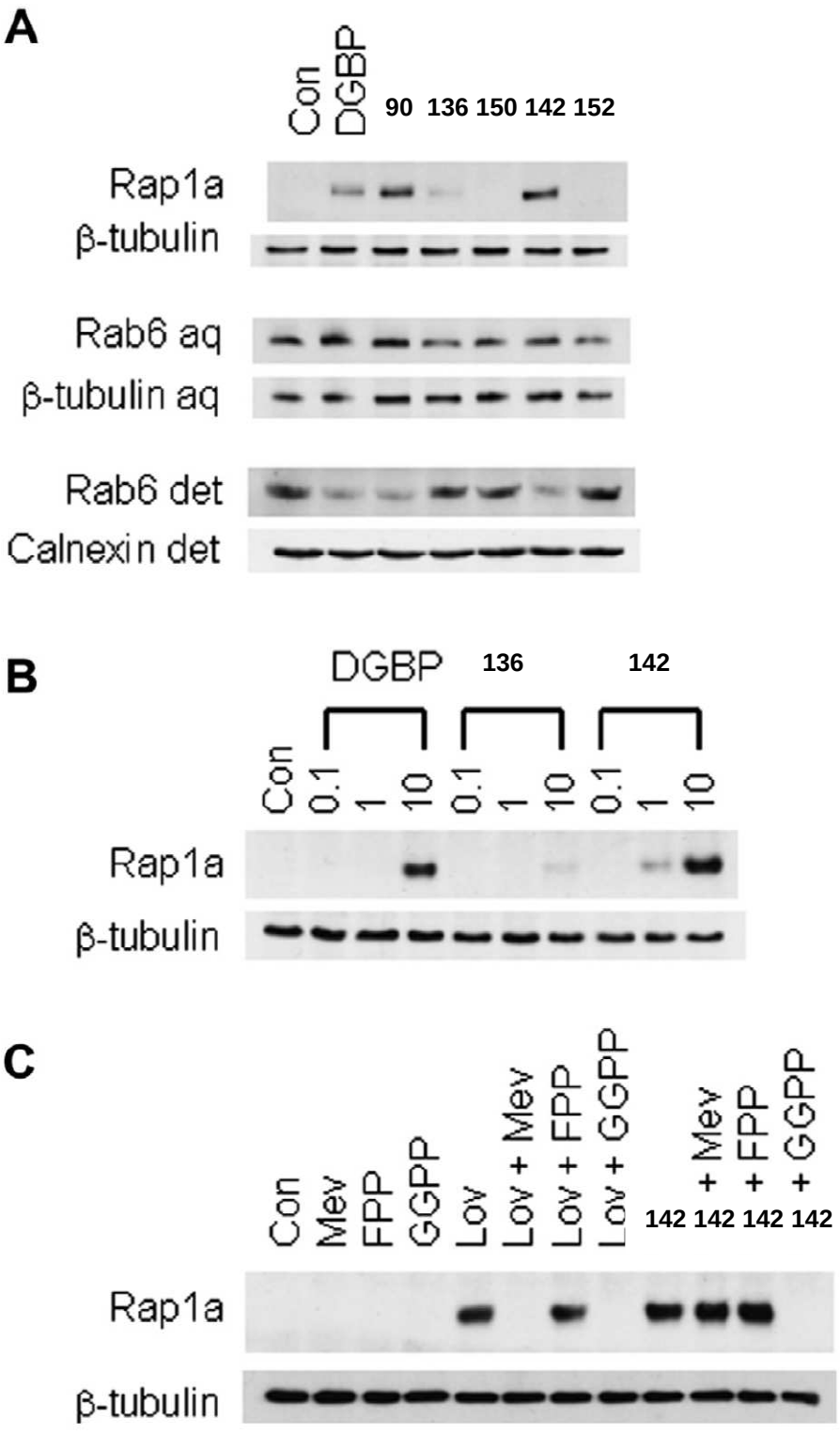

Figure 46. Neryl triazole **142** potently disrupts protein geranylgeranylation in human myeloma cells. RPMI-8226 cells were incubated for 48 hr in the presence or absence of

test compounds. Cells were lysed using RIPA buffer to generate whole cell lysate or with Triton X-114 to generate aqueous and detergent fractions. Immunoblot analysis was performed. The Rap1a antibodies detect only unmodified protein. β-Tubulin was used as a loading control for whole cell lysate and aqueous fractions while calnexin was used the loading control for the detergent fraction. The gels are representative of two independent experiments. (A) Cells were incubated in the presence or absence of 10 μM DGBP (positive control) or test compound. (B) Cells were incubated in the presence or absence of increasing concentration (0.1, 1, 10 μM) of either DGBP, **136**, **142**. (C) Addition of GGPP, but not mevalonate (Mev) or FPP, prevents the effects of compound **142** on Rap1a geranylgeranylation. Cells were incubated in the presence or absence of inhibitor (10 μM lovastatin (Lov) or 10 μM **142**) and/or isoprenoid (1 mM Mev, 10 μM FPP, or 10 μM GGPP).[46]

To confirm neryl triazole bisphosphonate **142** selectively inhibits GGDPS, an add back experiment was performed. Different isoprenoid intermediates were added separately to the cells when they were incubated with the inhibitor **142**. Lovastatin was also incubated with cells as a positive control. As shown in Figure 46, only adding back GGPP prevents inhibition of the geranylgeranylation of Rap1a. Neither mevalonate nor FPP reverse this process, which further confirms our hypothesis that this compound is a GGDPS inhibitor.

The effects of the isomer mixture **90** (2:1 E to Z), geranyl triazole **136**, and neryl triazole **142** on FPP and GGPP levels were evaluated as well (Figure 47). Because DGBP inhibits GGDPS selectively, it reduces the concentration of GGPP and causes the

accumulation of FPP. Parallel results were observed with the isomer mixture **90** and neryl triazole **142** which both significantly decrease the amount of GGPP and increase accumulation of FPP. In contrast, geranyl triazole **136** does not show a similar effect.

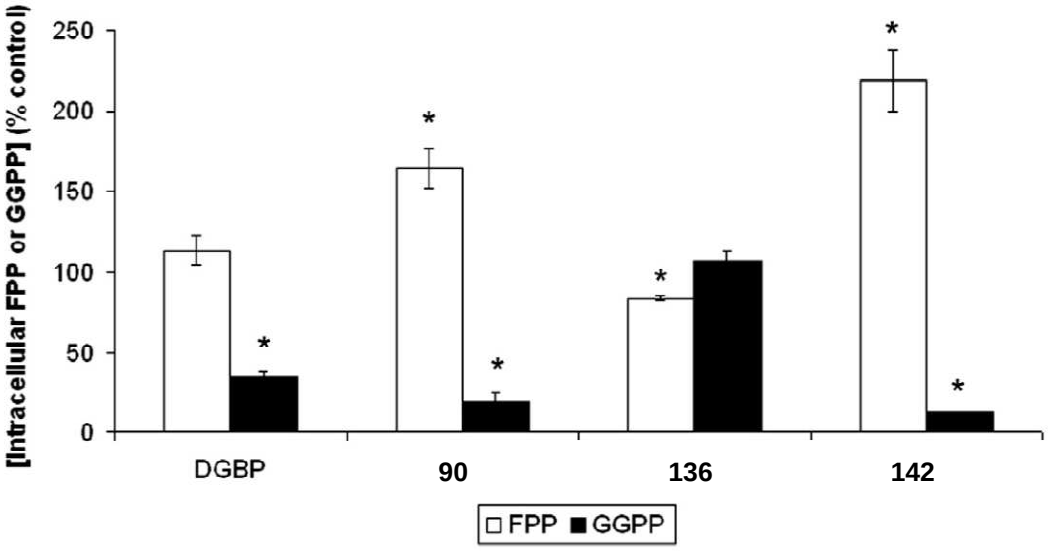

Figure 47. Neryl triazole **142** depletes cells of GGPP and increases intracellular FPP levels. RPMI-8226 cells were incubated for 24 h in the presence or absence of 1 μM test compound. DGBP was included as a positive control. Cells were counted and intracellular FPP/GGPP levels were measured. Data are expressed as a percentage of control (mean ± SD, n = 2). The * denotes $p < 0.05$ in an unpaired two-tailed t-test and compares treated cells to untreated control cells.[46]

These newly synthesized compounds also were examined for their ability to directly inhibit GGDPS and other enzymes (Table 3). The most potent compound against GGDPS is the neryl triazole bisphosphonate **142** which has an IC_{50} value of 375 nM, while the geranyl triazole bisphosphonate **136** and the two racemic epoxides are more than 45 times less potent. On the other hand, neryl triazole bisphosphonate does not

display high potency against FDPS. Similar to the finding that the isomer mixture **90** does not inhibit GGTase II, neither the *trans* compound **136** nor the *cis* compound **142** displays any activity against GGTase II, and the epoxides **150** and **152** also were inactive. At the same time, none of these five compounds shows any effective inhibition of FTase or GGTase I.

Compound	GGDPS IC_{50} (μM)	FDPS IC_{50} (μM)	FTase IC_{50} (μM)	GGTase I IC_{50} (μM)	GGTase II IC_{50} (μM)
90	2.2	84	500	200	> 1000
136	17	57	> 500	340	> 1000
142	0.38	79	400	500	> 1000
150	23	33	400	500	> 1000
152	17	47	340	300	> 1000

Table 3. Evaluation of triazole phosphonates against GGDPS and related enzymes[46]

Finally, the ability of these agents to disrupt a key cellular process in myeloma cells was examined. RPMI-8226 cells and the test compounds were incubated together and the effects on monoclonal protein trafficking were determined via lambda light chain ELISA performed on whole cell lysate. Our collaborators have previously demonstrated that agents which impair Rab geranylgeranylation disrupt monoclonal protein trafficking in myeloma cells.[106] As shown in Figure 48, the olefin mixture **90** and the positive control DGBP induce the same amount of intracellular lambda light chain accumulation. This activity must be a consequence of neryl triazole **142** given that the geranyl triazole **136** has no effect on intracellular light chain levels.

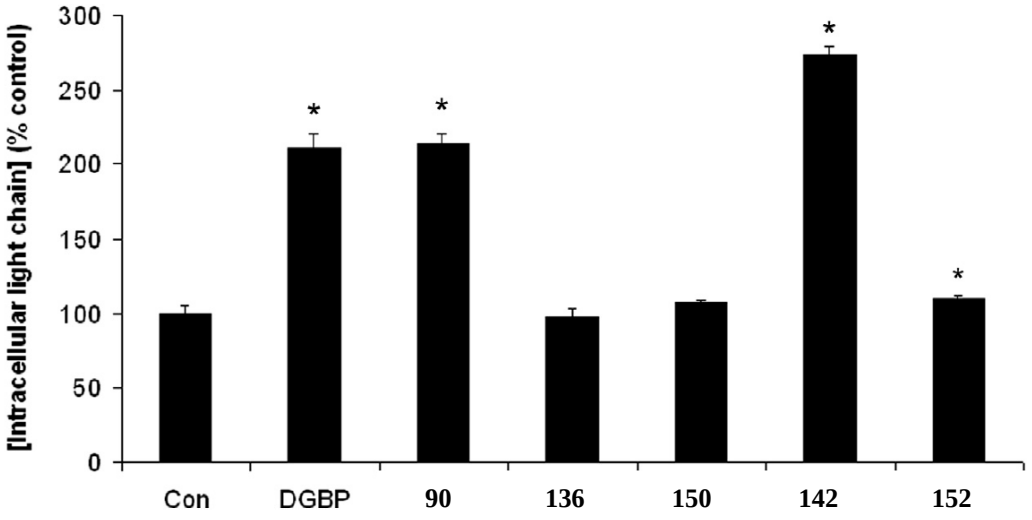

Figure 48. Neryl triazole **142** disrupts monoclonal protein trafficking in human myeloma cells. RPMI-8226 cells were incubated for 48 h in the presence or absence of 10 μM test compound or DGBP. Intracellular lambda light chain concentrations were determined via ELISA. Data are expressed as a percentage of control (mean ± SD, n = 3). The * denotes $p < 0.05$ in an unpaired two-tailed *t*-test and compares tested cells to untreated control cells. [46]

In previous studies, several GGDPS inhibitors that bear side chains of different length and olefin stereochemistry have been prepared.[32] According to our biological results, the most potent compounds as inhibitors of GGDPS are digeranyl bisphosphonate and *2E, 6E*-farnesyl bisphosphonate **153** (Figure 49), which have IC_{50} values of 0.2 μM and 0.1 μM. In contrast, dineryl bisphosphonate and neryl, geranyl bisphosphonate are 30 and 35 times less potent than digeranyl bisphosphonate while *2E, 6Z; 2Z, 6E* and *2Z, 6Z* -farnesyl bisphosphonate are about 6, 400, and 700 fold less potent than *2E*, *6E*-farnesyl bisphosphonate **153.** Furthermore, mono alkylated geranyl bisphosphonate[107] is

about 10 times more potent than the corresponding neryl bisphosphonate.[108] Based on these results, the *trans* configuration is more preferred than the *cis* configuration in the enzyme binding site. Although the C3 to C5 carbon bond length of compounds **153**/**154** is slightly different than the C3 to N5 bond length of compounds **136**/**142** due to the different bond angles in the triazole ring, if compared with these newly synthesized triazole bisphosphonate compounds, the methylene triazole functional group can be still viewed as an isopentenyl unit replacement. From this prospective, the geranyl triazole bisphosphonate **136** is a structure close to *2E*, *6E*-farnesyl bisphosphonate **153** while neryl triazole bisphosphonate **142** is a structure close to *2E*, *6Z*-farnesyl bisphosphonate **154**. From the reported biological results of farnesyl bisphosphonates **153** and **154**, one would easily predict that geranyl triazole bisphosphonate **136** should be a more potent inhibitor than neryl triazole bisphosphonate **142**. However, as discussed above, compound **142** is about 45 times more potent than compound **136**. This data suggests that the triazole functional group may play an important role in enzyme binding. By employing this special element, we may have discovered a new strategy to develop inhibitors for GGDPS. Moreover, experiments also suggest that the first olefin functional group of geranyl and neryl side chains of triazole **136** and **142** is important, because these compounds lose activity when they are protected by an epoxide gruop.

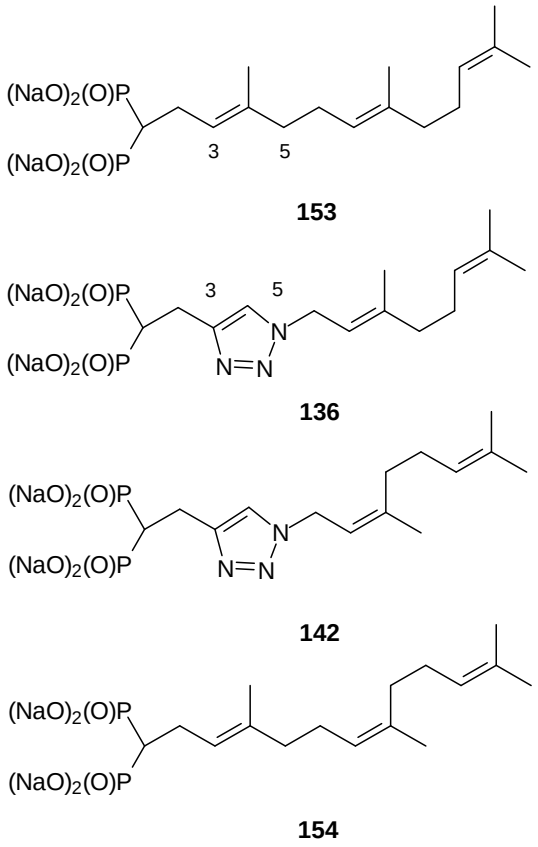

Figure 49. Comparison of farnesyl and triazole bisphosphonates[46]

Of note, the neryl triazole **142** shows better potency in inhibition of protein geranylgeranylation in cell culture studies compared with DGBP. In contrast, DGBP has a reported IC_{50} of 0.2 μM,[31] which is slightly more potent in the *in vitro* enzyme assay. This might be due to the enhanced cellular uptake of compound **142** as compared to DGBP, because it only bears one isoprenoid chain instead of two and is less hydrophobic. In the future, its effectiveness might be further enhanced through prodrug strategies,[108] although this has yet has to be examined with these triazoles. Competitive inhibition with respect to FPP as opposed to IPP has been demonstrated for DGBP,[109] but the inhibition mechanism of compound **142** remains to be determined.

CHAPTER IV

SYNTHESIS OF 3-PEHPC ANALOGUES

In the previous chapter, the development of new types of GGTase II inhibitors based on computer-assisted drug design has been discussed. By analyzing the crystal structure of GGPP bound to GGTase II (Figure 31), three different regions were identified in the substrate, including a pyrophosphate mimic, a ligand to bind to the zinc metal, and a terminal isoprene unit that inserts into the empty pocket of the enzyme to occupy that space. Based on these important substrate features, the general structure of alkyl triazole bisphosphonate inhibitors was designed (Figure 32). According to the biological results, the most potent compound against GGTase II is the geranylgeranyl triazole bisphosphonate **97** which bears the longest side chain.

As a complementary approach, we also have tried to synthesize GGTase II inhibitors based on the known inhibitor 3-PEHPC (Figure 50). Following the same concept, we tried to directly modify the structure of 3-PEHPC to incorporate three distinct motifs, a head group, a zinc binding group and an isoprenoid tail group. When viewed from this prospective the structure of 3-PEHPC has an α □ hydroxy carboxylic acid phosphonate as the head group and a pyridine ring as the potential zinc binding group. We designed compound **156** as a new analogue which has an alkyl chain on a reduced pyridine ring to occupy the hydrophobic pocket as a tail group that might achieve better potency. Preparation of the *N*-methyl compound **155** would help develop methods to synthesize such analogues, while the synthesis of *N*-geranyl compound **156** would help investigate strategies for addition of a longer hydrophobic side chain.

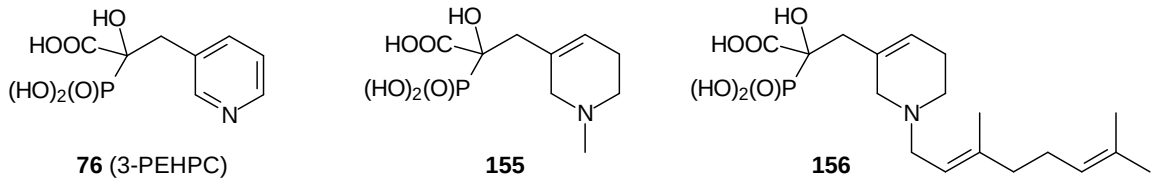

Figure 50. Structure based design of potential GGTase II inhibitors

The synthesis of 3-PEHPC is shown in Figure 51. Pyridine aldehyde **157** and the ethyl ester **158** were condensed to give the diketone **159** which is in an equilibrium with its enol form **160**. Enol **160** was then treated with diethyl phosphite to yield phosphonate **161** that was hydrolysed by treatment with aqueous HCl to generate the target molecule, acid **76**.[110]

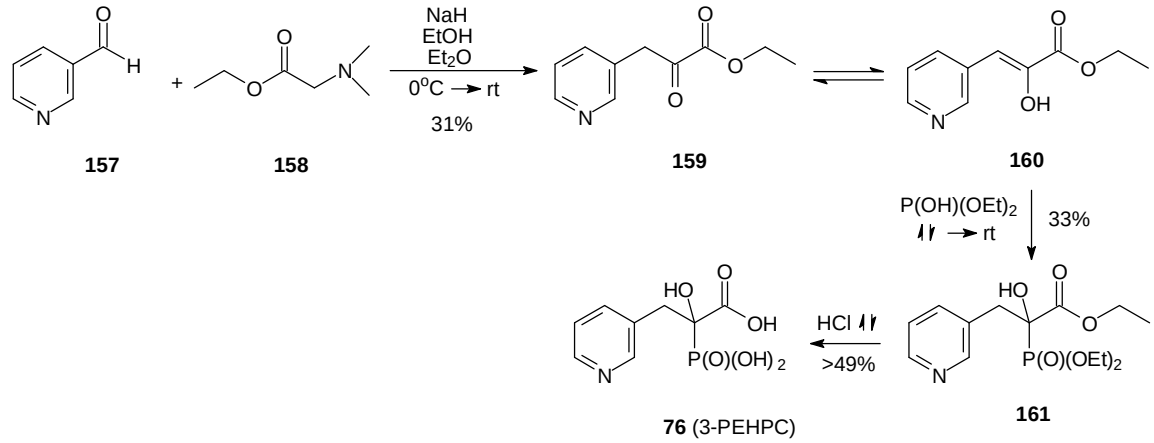

Figure 51. Synthesis of 3-PEHPC[110]

Instead of directly testing the pyridine alkylation reaction on the key intermediate **161**, methyl nicotinate **162** was used initially as a model compound. Compound **162** was treated with methyl iodide at reflux in dichloromethane overnight to generate what appeared to be the pyridinium iodide salt **163** in 100% yield. According to many reported procedures, the most common method to reduce a pyridinium is treatment with

$NaBH_4$.[111,112] Such reactions have been done under many different conditions, including $NaBH_4$ in EtOH,[113] $NaBH_4$ in EtOH /water,[112] and $NaBH_4$ in EtOH/HOAc[114] as the reaction solvent. However, none of these standard conditions reduced pyridinium salt **163** to the amine **164**. On the other hand, Okamura *et al*. developed a method to reduce *N*-methyl pyridinium iodide to *N*-methyl-1,4-dihydropyridine derivatives using $Na_2S_2O_4$.[115] Unfortunately, none of the desired product **165** was observed by ^{1}H NMR under these conditions either.

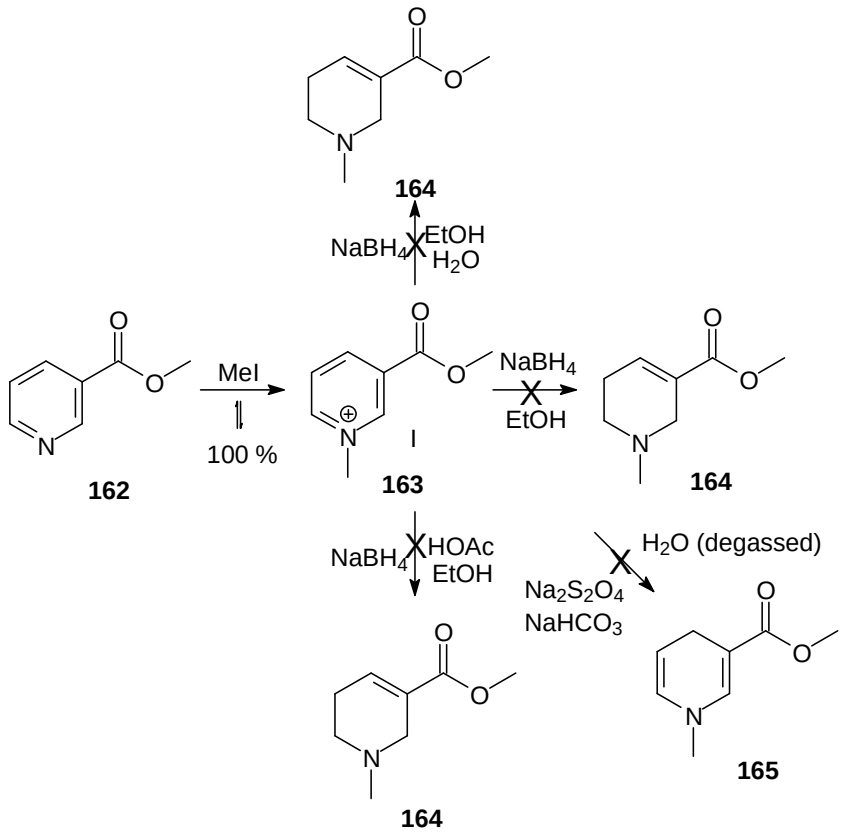

Figure 52. Reduction of pyridinium salt

Because it was difficult to reduce the pyridinium iodide **163** under variations of known conditions, the identification of this intermediate was questioned. A new synthesis allowed methyl nicotinate **162** to react with iodomethane in acetone at room

temperature instead of reflux in dichloromethane.[116] Through this new method, the pyridinium iodide **163** was generated in 71% yield. The product was further treated with $NaBH_4$ in MeOH/HOAc to give trace amounts of amine **164** as the desired product. At the same time, compound **162** was treated with geranyl bromide in acetone to give the corresponding pyridinium bromide **166**. Part of the salt **166** was treated with the $NaBH_4$/MeOH/HOAc reduction conditions described above to afford the reduced compound **167** in 6% yield. On the other hand, part of the salt **166** was allowed to react with $NaBH_4$ in MeOH to give the desired product **167** in modest yield (32%).[117]

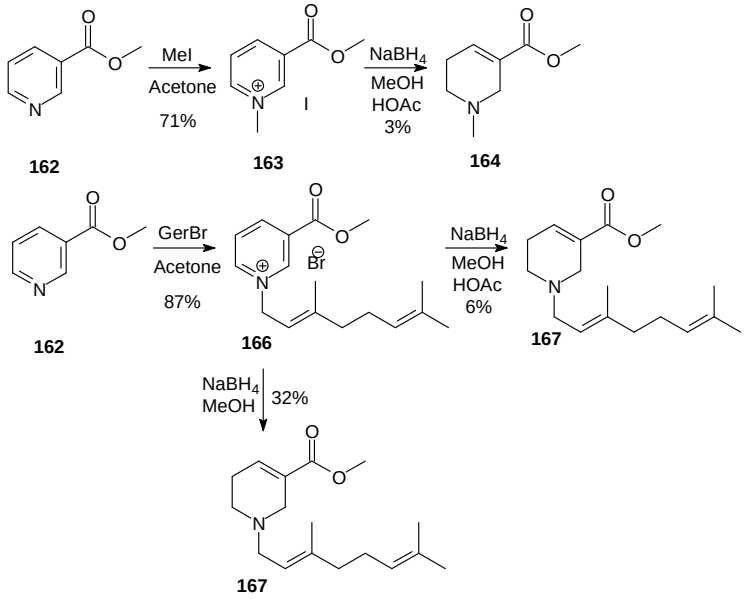

Figure 53. Study of model compound

Once the reaction method had been developed on the model compound **162**, it was applied to the 3-PEHPC precursor **161** and the rearranged compound **169** (Figure 54). Unfortunately, when compounds **161** and **169** were treated with MeI or geranyl bromide, neither reaction gave a solid from the acetone solution, with only starting material observed by TLC. Attempts to alkylate the key intermediate **161** also failed.

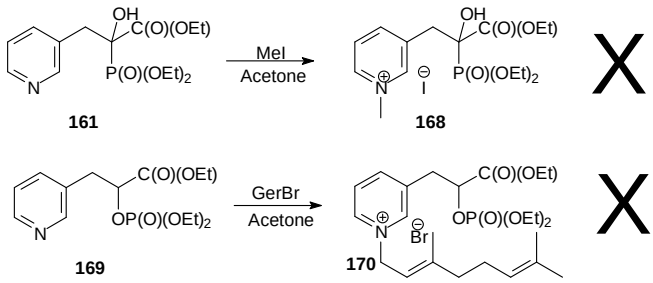

Figure 54. Attempted alkylation of 3-PEHPC precursor

Because it was difficult to alkylate the 3-PEHPC precursor **161** directly, alternate synthetic routes were evaluated. The next approach was to modify the structure of the starting aldehyde **157** (Figure 55). Therefore, it was treated under standard alkylation conditions to form the pyridinium bromide **177**, which was further allowed to react with $NaBH_4$ to give the reduced product **178**. With the alcohol **178** in hand, oxidation by MnO_2 yielded the aldehyde **179** in moderate yield, although the reaction was not optimized. Unfortunately, when aldehyde **179** was treated with *N*-*N*-dimethyl glycine ethyl ester **158** under standard condensation condition, none of the desired product **175** was generated.

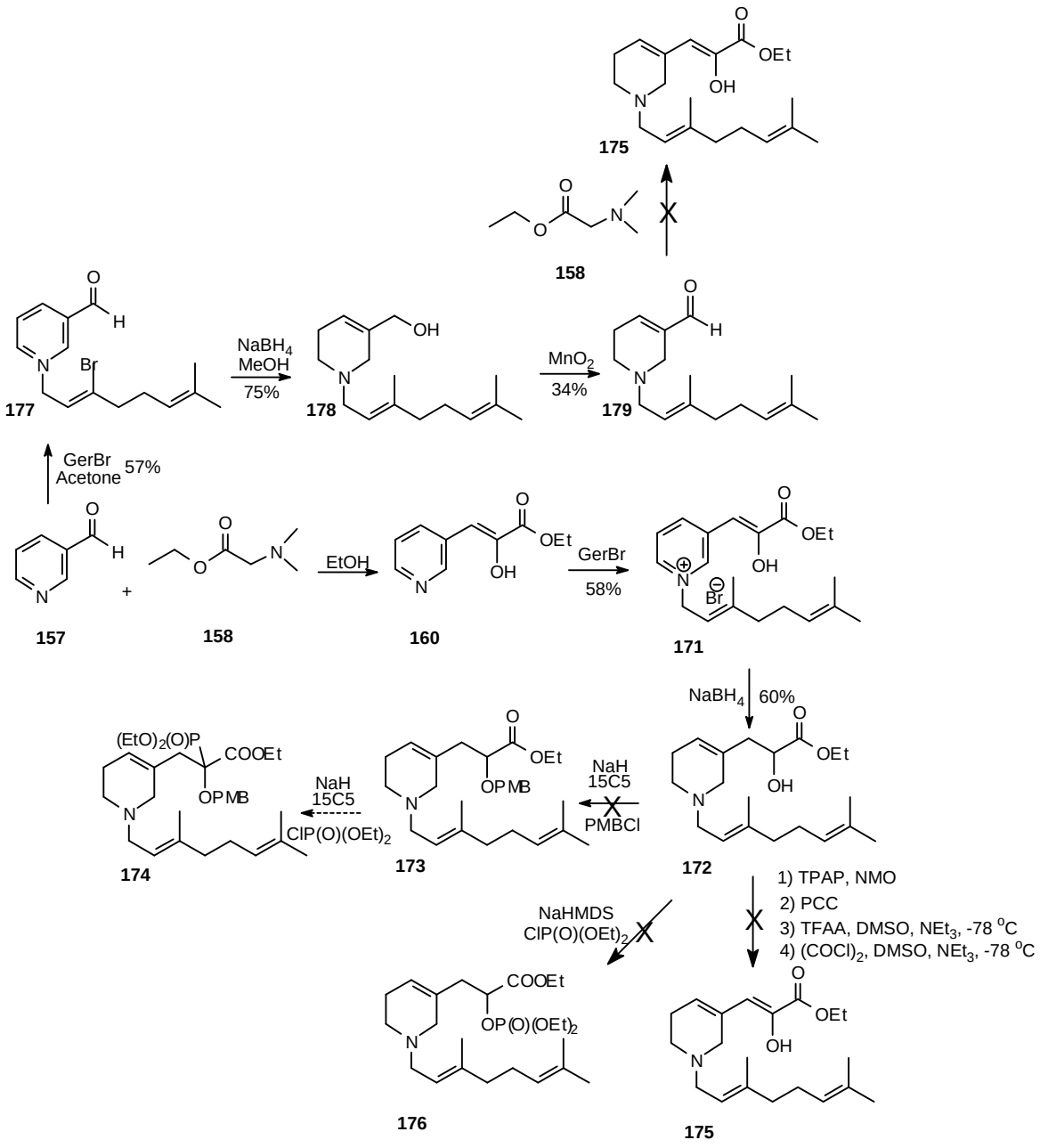

Figure 55. Evaluation of different synthetic routes

Because the original synthetic plan failed, modification was carried out on another intermediate, compound **160**. This α−keto ester was alkylated with geranyl bromide to give the pyridinium bromide **171** first, which was then reduced by treatment with $NaBH_4$

to yield alcohol **172** in 35% yield over two steps. Two advantages can be seen in alcohol **172**. In theory, it can be oxidized to produce the key intermediate **175** directly. Alternatively, it could be protected with a PMB protecting group to yield phenol ether **173** which might be further deprotonated and allowed to react with diethyl chlorophosphate to generate phosphonate **174**. However, it was difficult to establish either of these two synthetic routes. Many oxidation reaction conditions were explored with alcohol **172**, including TPAP,[42,118] Jones oxidation[119,120] and two different Swern oxidation conditions,[121,122] but none of them oxidized the alcohol to the key intermediate **175**. The attempted protection reaction of alcohol **172** also was not successful. Only the starting material PMBCl was recovered from this reaction mixture. Although a good NMR spectrum and HRMS data were obtained for alcohol **172**, to prove it was of good quality an experiment was designed. Because an O-P bond could be easily assembled between an oxygen atom and a phosphate group, alcohol **172** was deprotonated by NaHMDS first and then treated with diethyl chlorophosphate. If the desired O-P product **176** could be obtained, it would verify the quality of alcohol **172**. Based on the analysis of the ^{31}P NMR spectrum, peaks at 9.80 ppm, 9.22 ppm, 4.05 ppm, -9.20 ppm and -13.3 ppm were observed from a spectrum of unpurified material and none of these resonances was easily recognized as the phosphate **176**. This experimental result may also explain why alcohol **172** was extremely hard to oxidize or protect with different reaction conditions. Reevaluation of the assigned structure must be pursued.

Because it was difficult to synthesize the target molecule **156** via modification of the starting material **157** or intermediate **160**, different alkylation conditions were examined with the 3-PEHPC precursor **161** again. In this experiment it was heated at

reflux with geranyl bromide in dichloromethane to give the bromide salt **180** in 87% yield. Compound **180** was obtained as yellow oil which may explain why it was hard to obtain as a precipitate when the parallel reaction was run in acetone. With the bromide salt in hand, it was reduced upon treatment with $NaBH_4$ under acidic conditions to give the key intermediate **181**. In order to form this reduced pyridine ring moiety, many challenges were faced. Because an α–hydroxy group is found in the head group structure, regular $NaBH_4$ reduction condition might rearrange a phosphonate to a phosphate functional group. To avoid such rearrangement reactions, compound **180** was treated with $NaBH_4$ in HOAc. According to a ^{31}P NMR spectrum of the reaction mixture, the starting material was converted to the desired reduced compound **181** in almost quantitative yield with little rearranged product **176** generated. However, when the reaction was worked up, only trace amounts of the desired compound **181** could be isolated. It was also found that the reduced product **181** was unstable even in an anhydrous environment, presumably because the tertiary amine can induce the rearrangement. To avoid this side reaction, acidic H_2O (10% HOAc in H_2O) was added to quench the reduction reaction and the tertiary nitrogen was thus protonated to form a cationic center. The resulting compound **182**, which was relatively stable compared with compound **181**, could be isolated in a better yield.

The hydrolysis reaction of compound **182** was attempted under many different conditions, including treatments with TMSBr/2,4,6-collidine,[49] morpholine,[123] concentrated HCl,[110] and TMSBr[49] (Figure 56). When compound **182** was treated with TMSBr and 2, 4, 6-collidine, a rearrangement reaction happened, and the same rearrangement was observed when it was treated with morpholine under reflux condition.

When it was heated under reflux in concentrated HCl, decomposition was observed. In addition, isomerization of the geranyl side chain might be caused by acid to give different isomers. Furthermore, compound **182** also was treated with TMSBr in anhydrous CH_3CN in the absence of collidine. Although the ^{31}P NMR resonance shifted from 17.1 ppm to 15.2 ppm, which suggests the generation of the desired acid, several important ^{1}H NMR resonances were absent, which made it difficult to identify the product structure.

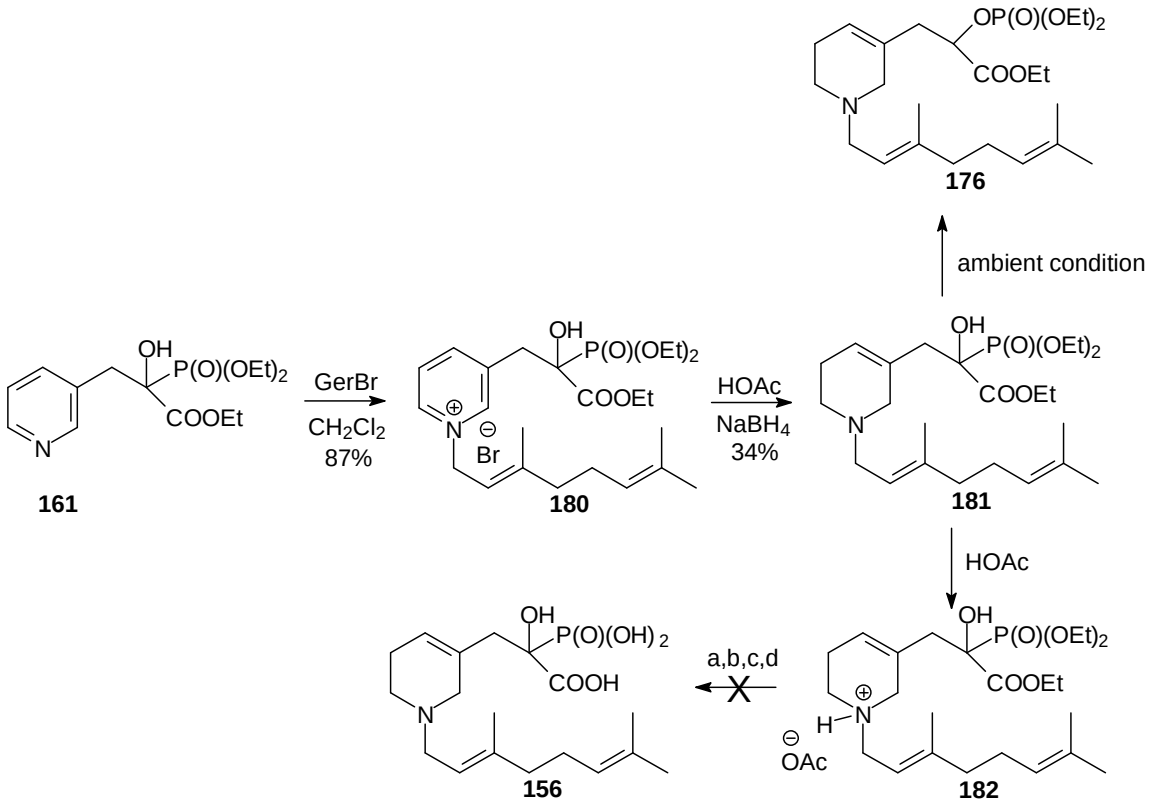

a, TMSBr, 2,4,6-collidine, H_2O; b, Morpholine, reflux; c, HCl, reflux; d, TMSBr, CH_3CN, H_2O

Figure 56. Synthesis of *N*-geranyl reduced 3-PEHPC

According to Artyushin's work,[124] TMSBr should cleave only phosphonic ethyl esters. To convert the carboxylic ester to the corresponding acid, further treatment with NaOH or LiOH is required. Because only a diethyl phosphonate group could undergo

rearrangement under basic condition, once the phosphonic acid was obtained, it should be stable under basic conditions. Therefore, this alternate strategy may yet help to solve the problem of obtaining the acid product **156**.

As discussed above, many synthetic challenges and difficulties were faced to prepare *N*-alkyl derivatives of 3-PEHPC. At the same time, we designed a second type of analogue, the *N*-oxide derivatives **183**. We are interested in whether the *N*-oxide functional group will display a better zinc binding ability when compared to the original pyridine ring. The known analogue of 3-PEHPC, 3-PEPC (**184**), has a similar potency for inhibition of Rab prenylation but because it lacks the germinal hydroxyl group it is more stable.[125] Therefore, we also decided to attempt preparation of 3-PEPC and its *N*-oxide analogue **185** as well, for comparison of their biological activity with 3-PEHPC and its analogue.

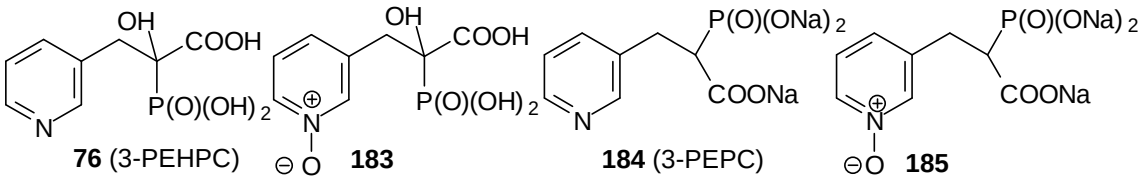

Figure 57. *N*-Oxide derivatives of 3-PEHPC and 3-PEPC

The synthesis of the two *N*-oxide analogues of 3-PEHPC is shown in Figure 58. Pyridine aldehyde **157** was condensed with carboxylic ethyl ester **158** to afford the keto ester **159**, which was further treated with diethyl phosphite to give the key intermediate **161**. With compound **161** in hand, it was allowed to react with *m*CPBA to oxidize the pyridine ring and give *N*-oxide **186**. Acid hydrolysis of *N*-oxide **186** converted it to the corresponding acid **183**. To study the biological activity of a substrate that bears a

phosphate head group, and to allow comparison with the synthetic target **183**, the rearranged *N*-oxide **188** also was synthesized through base catalysed rearrangement reaction of *N*-oxide **186** and acid catalysed hydrolysis of the ethyl esters of compound **187**.

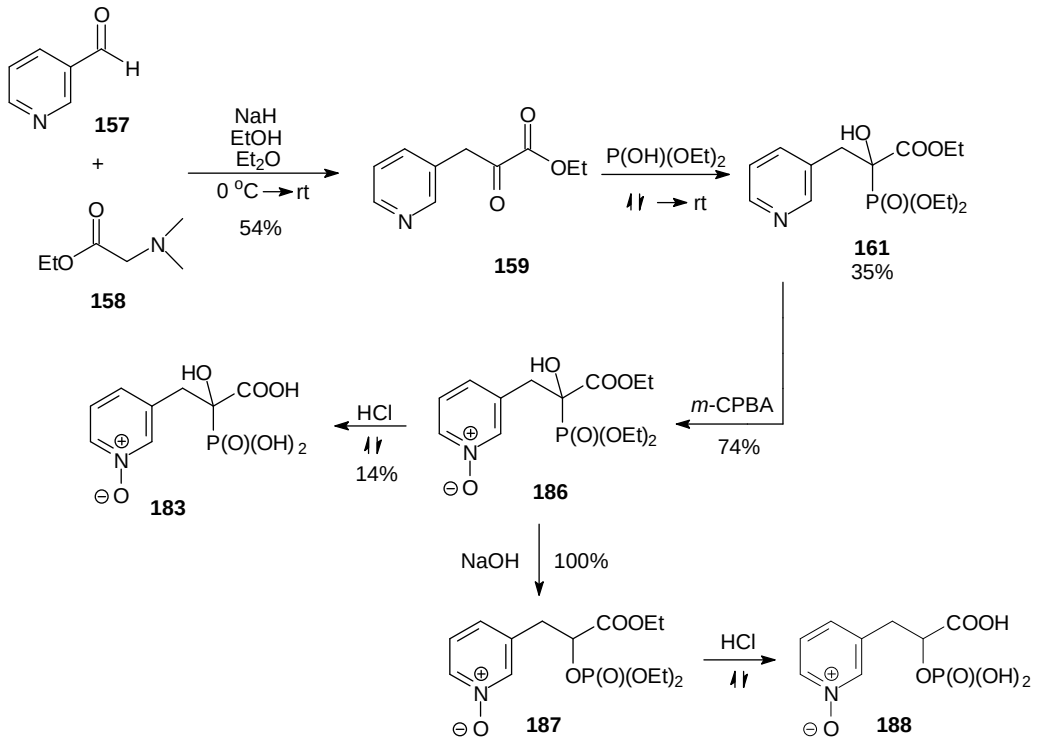

Figure 58. Synthesis of *N*-oxide analogues of 3-PEHPC

The GGTase II inhibitor 3-PEPC (**184**), which has a potency similar to 3-PEHPC, was pursued through a parallel synthesis. However, at the beginning it was hard to obtain the target molecule **184** following a literature procedure.[126] One of the major problems was poor solubility of the starting material, commercially available hydrochloride salt **190**, in organic solvents such as THF and DMF. To overcome this problem through a new synthesis, the hydrochloride salt was first neutralized by treatment with $NaHCO_3$ to give compound **190** as a free base which was then added to a solution of the triethyl

phosphonoacetate **189** anion in situ. The reaction mixture was allowed to stir overnight to form the 3-PEPC precursor **191** in 41% yield. With the key intermediate **191** in hand, part of the material was converted directly to 3-PEPC **184** by hydrolysis while the remaining material was treated with the same *m*CPBA oxidation conditions described above to generate *N*-oxide **192**. Hydrolysis of ester **192** by treatment with HCl gave the corresponding acid **185**. At this point, the known GGTase II inhibitors, 3-PEHPC, and 3-PEPC and their new *N*-oxide analogues **183**, **185** have been prepared and provided to Dr. Holstein's research group for biological evaluation.

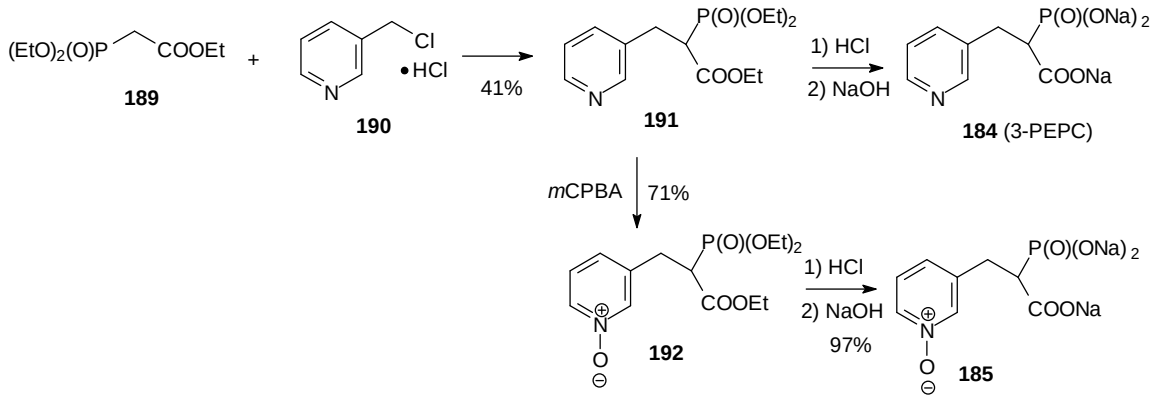

Figure 59. Synthesis of 3-PEPC and its *N*-oxide analogue

Biological results

The submitted compounds were tested in several bioassays, including an enzyme assay with GGTase II, an MTT cytotoxicity assay and an immunoblot analysis. In the GGTase II assay, recombinant GGTase II, Rab 1A, REP-1 and [^{3}H]-GGPP were incubated in the presence or absence of the test compounds for 20 minutes at 37 °C. The reaction was stopped by the addition of 10% HCl/EtOH and the radiolabeled Rab 1A was collected and counted using a scintillation counter. In the MTT cytotoxicity assay, RPMI-8226 human myeloma cells were incubated in the presence or absence of the test

compounds for 48 hours prior to the addition of the MTT salt solution. Following solubilization, absorbance was read on a microplate reader. For immunoblot analysis, RPMI-8226 cells were incubated in the presence or absence of the test compounds for 48 hours. Whole cell lysate was obtained using a RIPA buffer while aqueous and detergent fractions were obtained using a Triton X-114 lysing protocol. Protein content was determined via BCA. Equal amounts of total protein were loaded on acrylamide gels and then transferred to a PDVF membrane. Primary and secondary antibodies were added and proteins were visualized using an ECL chemiluminescence detection kit.

Although the reported IC_{50} value of 3-PEHPC against GGTase II is about 600 μM,[84] much lower activity was observed in these assays (> 1 mM). Unfortunately, none of the analogues **183**, **184** and **185** showed any improved potency. All four of these compounds could only inhibit about 20% geranylgeranylation even at a 2 mM concentration. At the same time, at concentrations higher than 1000 μM, 3-PEHPC **76** and its *N*-oxide analogue **183** displayed a slightly better potency on MTT assay than 3-PEPC and its *N*-oxide analogue **185** which barely showed any cytotoxicity.

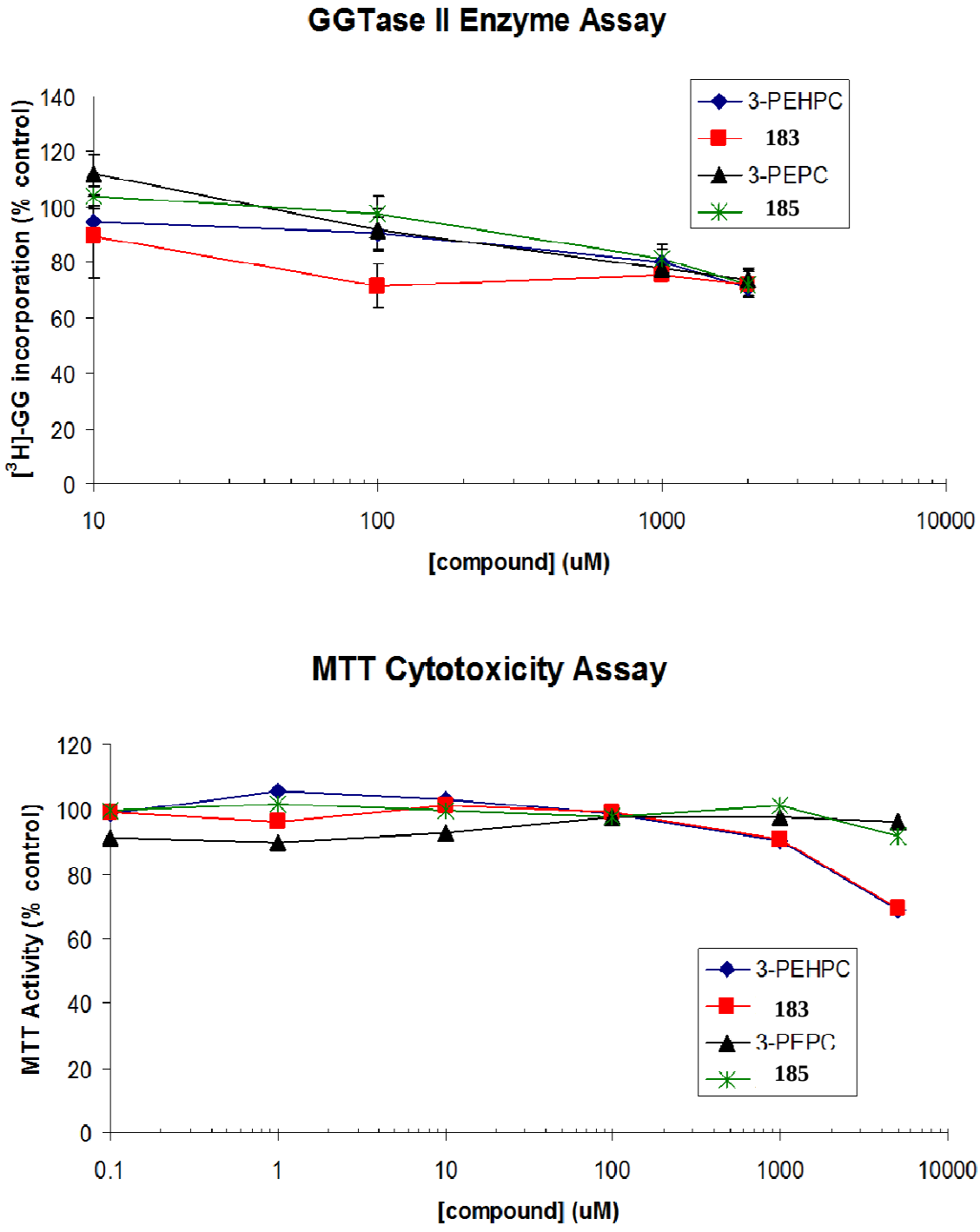

Figure 60. Effects of 3-PEHPC and derivatives on GGTase II activity and cytotoxicity (RPMI-8226 cells). Data are displayed as mean +/- SD (n=2 for GGTase II assay, n=3 for MTT assay).

These four compounds also were evaluated in RPMI-8226 human-derived myeloma cells. As shown in Figure 61, only the positive control, lovastatin, interrupts the geranylgeranylation of Rap1a protein, and none of other compounds display any inhibitory effect. Blots for Rab6 demonstrate that 3-PEHPC most effectively disrupts Rab geranylgeranylation while *N*-oxide **184** and **185** appear to have little effect. The ability of these compounds to induce apoptosis was studied as well. Three compounds, 3-PEHPC, 3-PEPC and *N*-oxide **185** all induce PARP cleavage at 5 mM concentrations.

These experiment results indicate that the *N*-oxide functional group does not enhance the compounds' binding ability with GGTase II. Analogues **183** and **185** preserve have less potency than their parent compounds, 3-PEHPC and 3-PEPC.

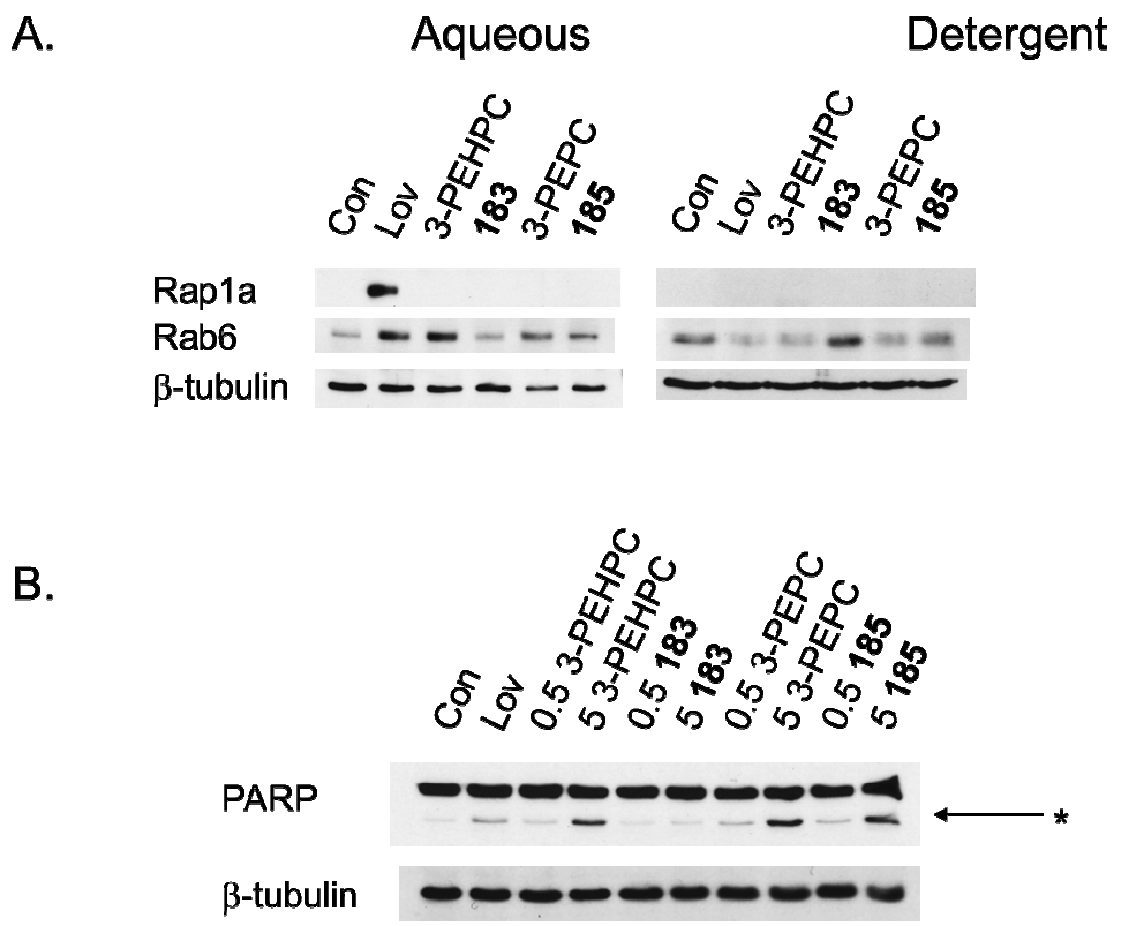

Figure 61. Effects of 3-PEHPC derivatives in RPMI-8226 human myeloma cells. A) 3-PEHPC derivatives disrupt Rab geranylgeranylation to varying degrees and do not impair Rap1a geranylgeranylation. Cells were incubated for 48 hours in the presence or absence of 10 mM lovastatin (Lov) or 5 mM of the 3-PEHPC-related compounds. Cells were then lysed using Triton X-114 and aqueous (non-membrane) and detergent (membrane) fractions were obtained. Immunoblot analysis was performed for Rap1a (antibody only recognizes unmodified Rap1a), Rab6, and b-tubulin (as a loading control). B) 3-PEHPC derivatives induce apoptosis. Cells were incubated for 48 hours in the presence or absence of 10 mM lovastatin (Lov) or 0.5 or 5 mM of the 3-PEHPC-related compounds.

Whole cell lysate was obtained and immunoblot analysis was performed for PARP (* represents cleaved PARP) and β-tubulin (loading control).

CHAPTER V

CONCLUSIONS AND FUTURE WORK

In Chapter II, a methodology to prepare the *C*-alkyl-*O*-alkyl bisphosphonates as analogues for DGBP has been presented. In the original synthesis route, the key intermediate α–hydroxy bisphosphonate undergoes a rearrangement reaction under basic condition and even without added base in some cases. To avoid such a problem, the α–oxygen was alkylated first to form an ether moiety before the bisphosphonate group was assembled. Following this strategy, a series of analogues, including dialkylated bisphosphonates and mono-alkylated bisphosphonates, has been synthesized. Dialkylated bisphosphonates **45**, **63, 67** and **75** show a similar effect to the parent compound, DGBP, selectively inhibiting GGDPS over FDPS. The *C*-geranyl-*O*-citronellyl bisphosphonate **75** displays the best potency in this family which could be related to a novel biological effect brought about by its chiral center. However, the detailed mechanism is still unclear at this point. In contrast, the mono-alkylated bisphosphonates **61**, **68**, and the *C*-prenyl-*O*-prenyl bisphosphonate **70** only weakly disrupt this biosynthetic pathway.

Because *C*-geranyl-*O*-(*S*)-citronellyl bisphosphonate **75** demonstrates the best activity against GGDPS, to determine the importance of the S chiral center, it would be interesting to synthesize the opposite enantiomer of compound **75**, the *C*-geranyl-*O*-(*R*)-citronellyl bisphosphonate **196** (Figure 62). Because *R*-citronellol is more expensive than *S*-citronellol, this starting material can be obtained by reduction reaction of a less expensive, commercially available compound, *R*-citronellal **193**.[127] With the alcohol in hand, it should undergo the same transformations used to prepare compound **75**, to afford the desired target molecule **196**.

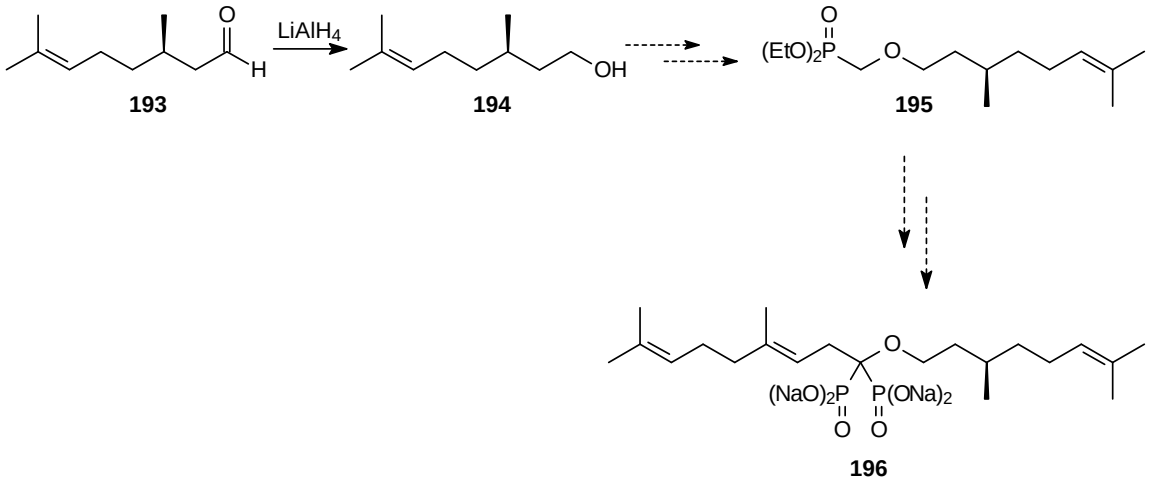

Figure 62. Synthesis of *C*-geranyl-*O*-(*R*)-citronellyl bisphosphonate

The studies described earlier have demonstrated that the activity of the *C*-prenyl-*O*-geranyl bisphosphonate **63** is about 1.7 times stronger than the *C*-geranyl-*O*-geranyl bisphosphonate **45** and 2.9 times better than the isomeric *C*-geranyl-*O*-prenyl bisphosphonate **67**. This data suggests that the *C*-terminal side chain and *O*-terminal side chain may be orientated in a certain order inside the enzyme. If that is the case, then the presence of a five carbon side chain unit on the *C*-terminal and a ten carbon side chain unit on the *O*-terminal is more preferred than other combinations. In addition, the most potent compound currently is *C*-geranyl-*O*-(*S*)-citronellyl bisphosphonate **75**. Therefore, by summarising all the information that has been discussed, the *C*-prenyl-*O*-citronellyl bisphosphonate **197** would be another interesting compound to synthesize. If our entire hypothesis is correct, compound **197** will display the best potency in this family.

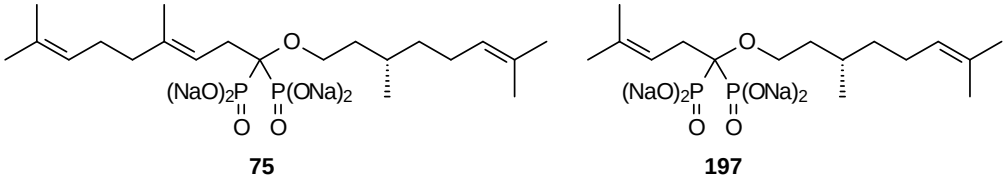

Figure 63. Citronellyl analogue

More recently, a methodology to prepare α-alkyl-1,1,1-trisphosphonate has been successfully developed in our group (Figure 64).[71,91,128] To add the third phosphonate group to a bisphosphonate, a 1-alkyl-1,1-bisphosphonate (**198**) can be treated with NaHMDS and diethyl chlorophosphite to form the C-P bond. When followed by addition of H_2O_2, the phosphonite will be oxidized to a phosphonate group in situ. This method has been tested with different substrates with yields ranging from 59% to 79%.[71,91] The synthesis, biological application and clinical study of bisphosphonates have been widely reported.[29,32,107,129,130] In contrast, trisphosphonate compounds have not been studied extensively. Therefore, it would be interesting to study the synthesis and biological effect of novel trisphosphonates.

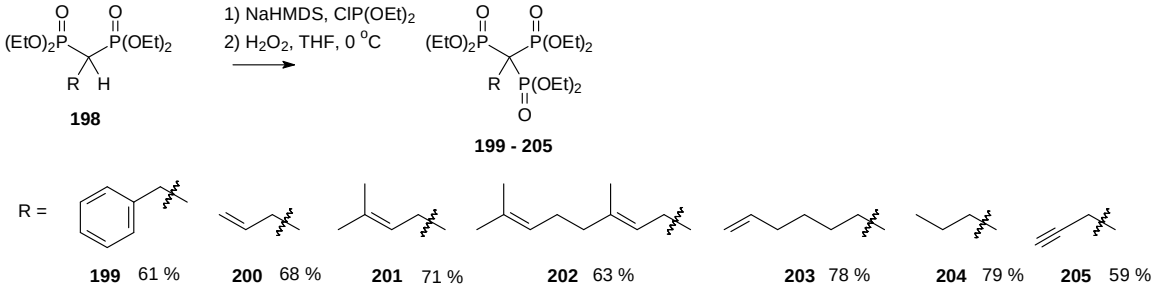

Figure 64. Synthesis of α-alkyl-1,1,1-trisphosphonate

In Chapter III, a method to synthesize the alkyl triazole bisphosphonates has been developed. With this method, the first generation of triazole compounds has been prepared. According to the biological studies, the most active compound against GGTase II is the geranylgeranyl triazole bisphosphonate **97** which has an IC_{50} value of 0.1 mM. However, with the original synthetic method, geranyl, farnesyl and geranylgeranyl triazole bisphosphonates could not be obtained as single olefin isomers due to an allylic

azide rearrangement reaction. To overcome this isomerization problem, an epoxide was used as a protecting group on the internal olefin of the starting materials geraniol and nerol, to preserve their original *trans* and *cis* configurations. After formation of the triazole, the epoxide was reduced stereoselectively to the *cis* or *trans* olefin. One of the newly synthesized compounds, neryl triazole bisphosphonate **108** has been demonstrated to be a potent inhibitor against GGDPS instead of GGTase II. This important discovery may open a new opportunity for the design of a new family of GGDPS inhibitors in the future.

Because we already have discovered that the mixture of geranylgeranyl triazole isomers is the most potent inhibitor of GGTase II, it will be important to synthesize this compound as a single isomer. As shown in Figure 65, with geranylgeraniol **93** in hand, the internal olefin can be protected by an epoxide. The alcohol **206** would then be converted to azide **207** through the bromide. Triazole **208** can be formed by click reaction between azide **207** and acetylene bisphosphonate **81**. The reduction reaction of epoxide **208** will afford olefin **209** with the original *trans* configuration. We expect the target molecule **209** to display a better activity against GGTase II compared with the isomer mixture **97**. If not, other geometric isomers could be prepared by parallel synthetic routes.

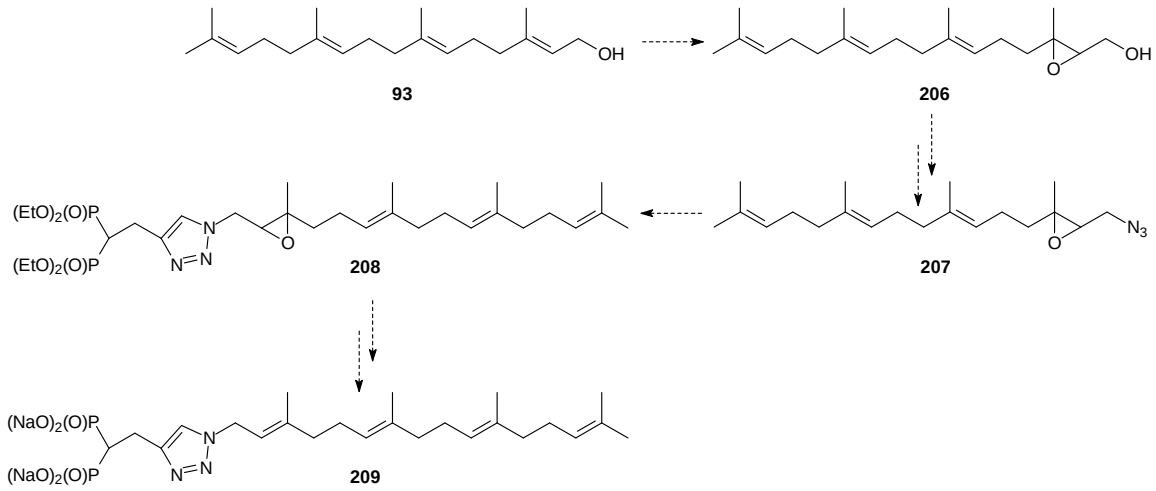

Figure 65. Synthesis of pure geranylgeranyl triazole bisphosphonate **209**

It has been discussed that the newly synthesized triazole compounds involve three different groups, including the head group, the triazole as a potential zinc binding group, and the tail group, which all take different roles in enzyme binding. While extensive research has been done on modification of the tail groups, not as much has been done yet to explore the value of different head groups. Because the parent compound, 3-PEHPC, bears a carboxylic acid and phosphonic acid head group, synthesis of triazole compounds with the same type of head group will provide an opportunity to examine the bioactivity of different head groups. To quickly evaluate if a head group will afford the same or even better potency, compound **212f** is an ideal synthetic target. However, it will be important to prepare other members in this family, **212(a-e)**, which may lead to other significant discoveries. The carboxy phosphonates **212b** and **212c** would be of special interest, because their bisphosphonate analogues **136** and **142** have demonstrated inhibition of GGDPS over GGTase II. At this point, all the identified GGDPS inhibitors carry a bisphosphonate head group, but at the same time not many compounds with different head groups have been examined. With compounds **212b** and **212c** in hand, we

can evaluate how a head group binds in the GGDPS active site. If they display better activity, it will be a significant aide in design of the next generation of GGDPS inhibitors.

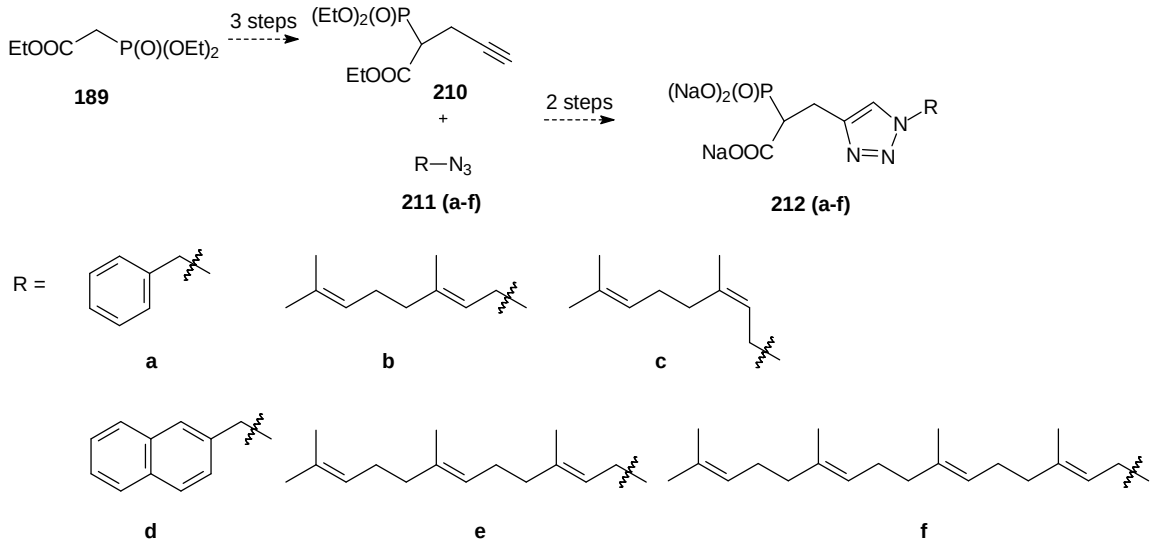

Figure 66. Synthesis of triazoles with a different head group

In Chapter IV, although the alkylation and reduction conditions of pyridine ring have been successfully studied on both model compounds and key synthetic intermediate from the PEHPC synthesis, many challenges were encountered in the synthesis of *N*-alkyl derivatives of 3-PEHPC. Further investigations of hydrolysis of the *N*-alkyl derivative **149** are critically needed to complete the study. On the other hand, to prepare a different type of analogue, *m*CPBA was found to be an efficient reagent to oxidize the pyridine ring to the corresponding *N*-oxide. With the method developed, 3-PEHPC, 3-PEPC, and their *N*-oxide derivatives have been synthesized. Unfortunately, compared with the parent compound 3-PEHPC, these three analogues do not display better potency with respect to GGTase II inhibition or cytotoxicity. Interestingly *N*-oxide **185** does induce apoptosis in myeloma cells. These findings suggest that this agent may have effects on cellular targets which are unrelated to protein prenylation.

To overcome the challenging hydrolysis of the head group of compound **182**, it might be useful to attempt a stepwise hydrolysis. As discussed earlier, the presence of 2,4,6-collidine results in rearrangement of the phosphonate to a phosphate. To avoid such a problem, the phosphonate group might be hydrolysed by treatment with TMSBr. Once the phosphonic acid group is formed, it should not undergo a rearrangement. To hydrolyse the carboxylate ethyl ester group, the intermediate could then be treated with either NaOH or LiOH to convert the ester to the sodium or lithium salt, which upon acidification with HCl should afford the corresponding acid.

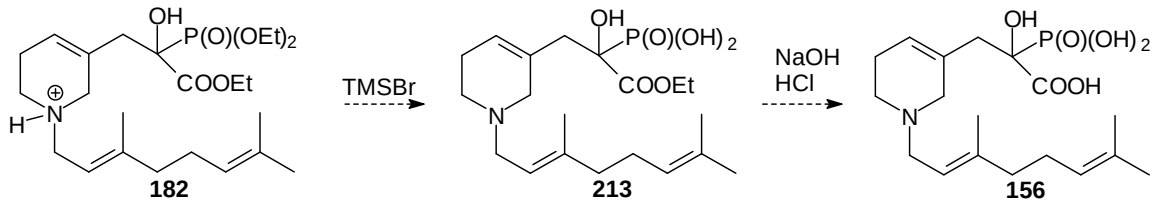

Figure 67. Hydrolysis of C-P head group

Many synthetic challenges were encountered in the synthesis of *N*-alkyl 3-PEHPC analogues, and most were due to the rearrangement of the phosphonate to the α–hydroxy group. Therefore, special conditions were required to keep the reaction environment acidic. To quickly assemble a testable compound and examine the design concept of sequential hydrolysis, it would be easier to synthesize the *N*-alkyl analogue of 3-PEPC which has a similar biological effect.[125]

The suggested synthetic route is shown in Figure 68. Following the previously described procedure, the anion of triethyl phosphonoacetate **189** can be treated with neutralized pyridine chloride **190** to afford the desired product **191**. With this intermediate in hand, the alkylation conditions employed to alkylate the 3-PEHPC

precursor **161** can be applied in this series. Upon reflux of compound **191** and geranyl bromide in DCM overnight, the bromide salt **214** should be obtained. Because there is no α–hydroxy moiety on this head group, simply treating the bromide salt **214** with $NaBH_4$ in MeOH could reduce it to amine **215**. Because it cannot undergo a rearrangement reaction, either the carboxylic ester or the phosphonate esters can be hydrolysed first, depending on how the reaction proceeds. Through this method, target molecule **217** might be obtained.

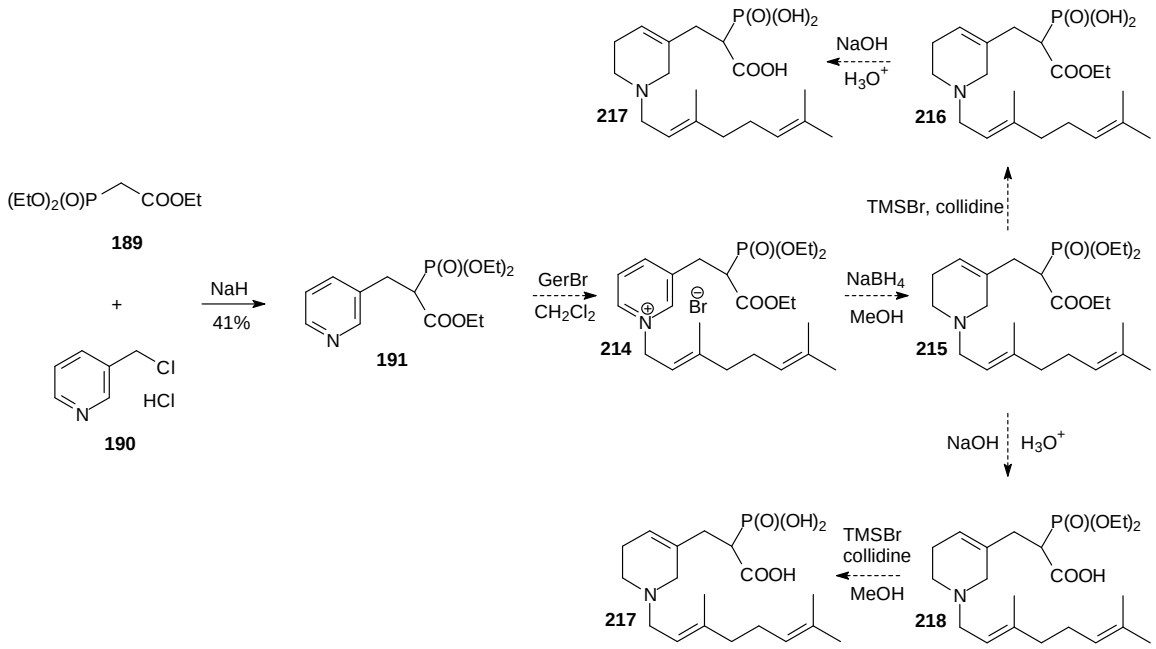

Figure 68. Synthesis of *N*-alkyl 3-PEPC analogues

While bisphosphonates were known to have biological activity before this work, these efforts have produced new compounds bearing both alkyl and alkoxy groups on the geminal carbon. Furthermore, click chemistry has been shown to be an efficient strategy for assembly of GGDPS inhibitors. Finally, derivatives of PEHPC may yet prove to be more potent inhibitors of GGTase II, and these studies have highlighted some aspects of

its reactivity. The new activity observed with these compounds strongly encourages further research into phosphonate-based inhibitors of isoprenoid biosynthesis.

CHAPTER VI

EXPERIMENTAL PROCEDURES

General experimental procedures.[48]

Tetrahydrofuran (THF) was freshly distilled from sodium/benzophenone, while methylene chloride (CH_2Cl_2) was distilled from calcium hydride prior to use. All other reagents and solvents were purchased from commercial sources and used without further purification. All reactions in nonaqueous solvents were conducted in flame-dried glassware under a positive pressure of argon and with magnetic stirring. The NMR spectra were obtained at 300, 400, or 500 MHz for ^1H, and 75, 100, or 125 MHz for ^{13}C, with internal standards of $(CH_3)_4Si$ (^1H, 0.00) or $CDCl_3$ (^1H, 7.27; ^{13}C, 77.2 ppm) for non-aqueous samples or D_2O (^1H, 4.80) and 1,4-dioxane (^{13}C, 66.7 ppm) for aqueous samples. The ^{31}P chemical shifts were reported in ppm relative to 85% H_3PO_4 (external standard). High resolution mass spectra were obtained at the University of Iowa Mass Spectrometry Facility. Silica gel (60 Å, 0.040–0.063 mm) was used for flash chromatography.

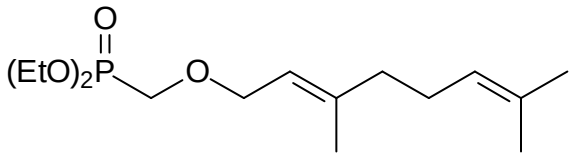

59

(*E*)-diethyl (((3,7-dimethylocta-2,6-dien-1-yl)oxy)methyl)phosphonate 59. Diethyl hydroxymethylphosphonate (**60**, 1 mL, 6.8 mmol) was added dropwise to a solution of NaH (60% dispersion in mineral oil, 300 mg, 7.5 mmol) in THF (7 mL) in an ice bath, followed by addition of 15-crown-5 (0.1 mL, 1 M in THF). After 30 minutes, geranyl bromide (1.62 g, 7.5 mmol) was added to the reaction mixture and it was allowed

to react at room temperature overnight. Once the reaction was complete based on analysis of the ^{31}P NMR spectrum, saturated NH_4Cl was added. The resulting residue was extracted with Et_2O, the organic extracts were combined, dried (Na_2SO_4), concentrated in vacuo, and purified by column chromatography (5% EtOH in hexane) to afford the desired product **59** as a colorless oil (1.27 g, 62%): ^1H NMR (300 MHz, $CDCl_3$) δ 5.31 (t, J = 6.5 Hz, 1H), 5.08 (t, J = 4.9 Hz, 1H), 4.25**–**4.09 (m, 6H), 3.74 (d, J_{HP} = 8.6 Hz, 2H), 2.17**–**1.98 (m, 4H), 1.68 (s, 6H) 1.60 (s, 3H), 1.35 (t, J = 7.3 Hz, 6H); ^{13}C NMR (75 MHz, $CDCl_3$) δ 141.7, 131.5, 123.6, 119.6, 69.0 (d, J_{CP} = 12.7 Hz), 62.9 (d, J_{CP} = 166.0 Hz), 62.1 (d, J_{CP} = 6.1 Hz, 2C), 39.4, 26.0, 25.5, 17.4, 16.3, 16.2 (2C); ^{31}P NMR (121 MHz, $CDCl_3$) δ 22.0.

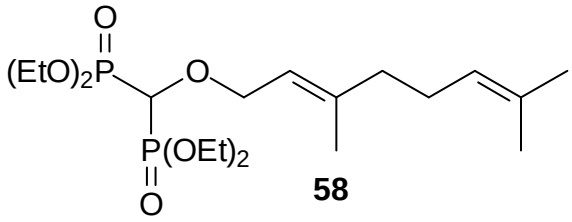

58

(*E*)-tetraethyl (((3,7-dimethylocta-2,6-dien-1-yl)oxy)methylene)bis(phosphonate) 58. Prepared according to the general procedure given for compound **65**: yield, 44%; colorless oil; ^1H NMR (300 MHz, $CDCl_3$) δ 5.26 (t, J = 7.0 Hz, 1H), 5.01 (t, J = 6.7 Hz, 1H), 4.27 (t, J = 7.5 Hz, 2H), 4.23–4.10 (m, 8H), 3.95 (t, J_{HP} = 17.6 Hz, 1H), 2.09–1.93 (m, 4H), 1.63 (s, 3H), 1.63 (s, 3H), 1.60 (s, 3H), 1.28 (t, J = 7.3 Hz, 12H); ^{13}C NMR (75 MHz, $CDCl_3$) δ 142.1, 131.0, 123.2, 119.0, 70.1 (t, J_{CP} = 157.9 Hz), 69.2 (t, J_{CP} =5.1 Hz), 62.7 (t, J_{CP} = 4.1 Hz, 2C), 62.5 (t, J_{CP} = 3.2 Hz, 2C), 39.1, 25.7, 25.0, 17.0, 15.9 (t, J_{CP} = 2.4 Hz, 2C), 15.8 (t, J_{CP} = 2.7 Hz, 2C), 15.8; ^{31}P NMR (121 MHz, $CDCl_3$) δ 16.1; HRMS (ES^+, m/z) calcd for $(M+Na)^+$ $C_{19}H_{38}O_7P_2Na$: 463.1991; found: 463.1972.

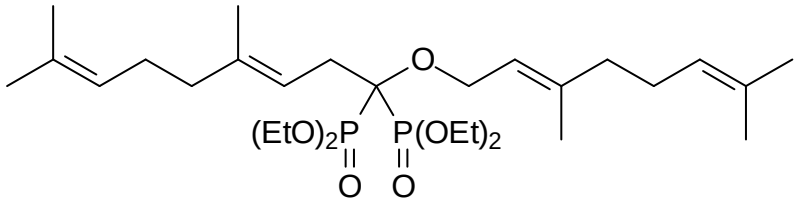

46

Tetraethyl ((*E*)-1-(((E)-3,7-dimethylocta-2,6-dien-1-yl)oxy)-4,8-dimethylnona-3,7-diene-1,1-diyl)bis(phosphonate) 46. Compound **58** (325 mg, 0.74 mmol) was added into a solution of NaH (60% dispersion in mineral oil, 50 mg, 1.25 mmol) in THF (3 mL), 15-crown-5 (0.1 mL, 1M in THF) was added, and the reaction mixture was allowed to stir for 30 minutes. Geranyl bromide (300 mg, 1.38 mmol) was then added and the reaction was allowed to stir at room temperature overnight. Reaction progress was monitored by analysis of the ^{31}P NMR spectrum. Once it was complete, water was added to quench the reaction. The resulting solution was then extracted with EtOAc and washed with brine. The organic layer was dried (Na_2SO_4) and concentrated in vacuo, and the residue was purified by column chromatography (5% EtOH in hexane) to afford compound **46** as a colorless oil (220 mg, 51%): ^{1}H NMR (300 MHz, $CDCl_3$) δ 5.50 (t, *J* = 6.7 Hz, 1H), 5.34 (t, *J* = 5.6 Hz, 1H), 5.16–5.05 (m, 2H), 4.37 (d, *J* = 6.8 Hz, 2H), 4.30–4.17 (m, 8H), 2.98–2.82 (m, 2H), 2.16–1.98 (m, 8H), 1.68 (s, 12H), 1.61 (s, 6H), 1.35 (t, *J* = 6.9 Hz, 6H), 1.35 (t, *J* = 6.9 Hz, 6H); ^{13}C NMR (75 MHz, $CDCl_3$) δ 139.6, 136.7, 131.4, 131.2, 124.3, 123.9, 120.8, 117.8 (t, J_{CP} = 7.9 Hz), 80.7 (t, J_{CP} = 151.0 Hz), 63.2 (t, J_{CP} = 3.6 Hz, 2C), 62.9 (t, J_{CP} = 3.7 Hz, 2C), 40.0, 39.5, 30.0, 26.6, 26.3, 25.6 (2C), 17.6 (2C), 16.5 (t, J_{CP} = 3.0 Hz, 2C), 16.4 (t, J_{CP} = 2.5 Hz, 2C), 16.4, 16.3; ^{31}P NMR (121 MHz, $CDCl_3$) δ 19.0; HRMS (ES^+, *m*/*z*) calcd for $(M+Na)^+$ $C_{29}H_{54}O_7NaP_2$: 599.3243; found: 599.3244.

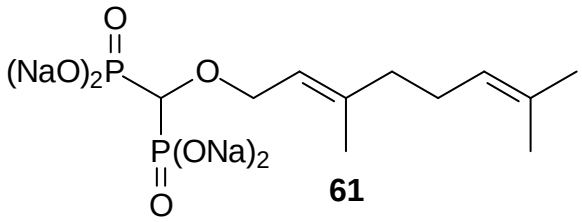

61

Sodium (*E*)-(((3,7-dimethylocta-2,6-dien-1-yl)oxy)methylene)bis(phosphonate) 61. Prepared according to the general procedure given for compound **63**: yield, 17%; white solid; ^{1}H NMR (300 MHz, D_2O) δ 5.49 (t, *J* = 6.6 Hz, 1H), 5.29–5.21 (m, 1H), 4.32 (d, *J* = 7.1 Hz, 2H), 3.67 (t, J_{HP} =15.2 Hz, 1H), 2.25–2.08 (m, 4H), 1.74 (s, 3H), 1.72 (s, 3H), 1.66 (s, 3H); ^{13}C NMR (75 MHz, D_2O) δ 142.1, 133.8, 124.3, 120.8, 75.7 (t, J_{CP} = 130.3 Hz), 69.8, 39.0, 25.8, 24.9, 17.0, 15.8; ^{31}P NMR (121 MHz, D_2O) δ 14.1; HRMS (ES^-, *m*/*z*) calcd for $(M-H)^-$ $C_{11}H_{21}O_7P_2$: 327.0763; found: 327.0748.

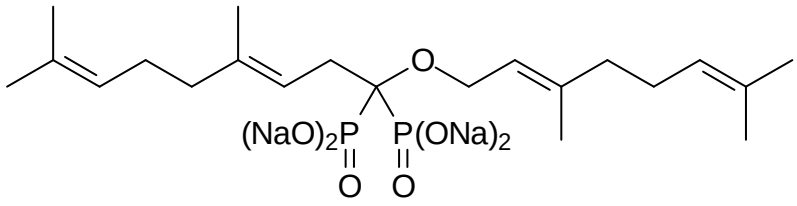

45

Sodium ((*E*)-1-(((*E*)-3,7-dimethylocta-2,6-dien-1-yl)oxy)-4,8-dimethylnona-3,7-diene-1,1-diyl)bis(phosphonate) 45. Prepared according to the general procedure given for compound **63**: yield, 20%; white solid; ^{1}H NMR (500 MHz, D_2O) δ 5.65 (t, *J* = 6.5 Hz, 1H), 5.39 (t, *J* = 6.2 Hz, 1H), 5.27–5.18 (m, 2H), 4.32 (d, *J* = 6.9 Hz, 2H), 2.88 (td, J_{HP} = 14.1 Hz, *J* = 6.5 Hz, 2H), 2.19–2.12 (m, 4H), 2.11–2.05 (m, 4H), 1.70 (s, 6H), 1.69 (s, 6H), 1.65 (s, 3H), 1.64 (s, 3H); ^{13}C NMR (125 MHz, D_2O) δ 141.2, 137.1, 133.7, 133.5, 125.2, 124.7, 121.3, 119.7 (t, J_{CP} = 7.8 Hz), 79.5 (t, J_{CP} = 131.8 Hz), 62.7 (t, J_{CP} = 6.5 Hz), 39.4, 38.9, 28.7, 26.1, 25.7, 25.0, 18.5, 17.1, 17.1, 15.9, 15.6; ^{31}P NMR (201

MHz, D_2O) 17.5; HRMS (ES^-, *m*/*z*) calcd for $(M-H)^- C_{21}H_{37}O_7P_2$: 463.2015; found: 463.2021.

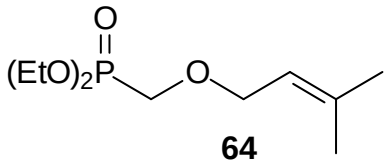

64

Diethyl (((3-methylbut-2-en-1-yl)oxy)methyl)phosphonate 64. Yield, 77%; colorless oil; ^{1}H NMR (300 MHz, $CDCl_3$) δ 5.36–5.28 (m, 1H), 4.23–4.11 (m, 4H), 4.10 (d, J = 7.1 Hz, 2H), 3.74 (d, J_{HP} = 8.4 Hz, 2H), 1.76 (s, 3H), 1.70 (s, 3H), 1.35 (t, J = 7.0 Hz, 6H); ^{13}C NMR (75 MHz, $CDCl_3$) δ 137.8, 119.6, 68.6 (d, J_{CP} = 12.0 Hz), 62.7 (d, J_{CP} = 166.8 Hz), 61.7 (d, J_{CP} = 6.1 Hz, 2C), 25.2, 17.4, 15.9 (d, J_{CP} = 5.1 Hz, 2C); ^{31}P NMR (121 MHz, $CDCl_3$) δ 21.7.

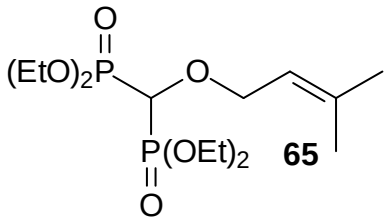

65

Tetraethyl (((3-methylbut-2-en-1-yl)oxy)methylene)bis(phosphonate) 65.[75] A solution of *n*-butyllithium in hexanes (8.8 mL, 21.2 mmol) was added to a solution of diisopropylamine (2.75 mL, 19.5 mmol) in THF (16 mL) at **–**78 °C and the reaction was allowed to stir for 30 minutes. Ether **64** (2 g, 8.5 mmol) was then added to the reaction mixture dropwise (over 90 minutes), allowed to react for one additional hour, and then followed by the careful addition of diethyl chlorophosphate (2.9 mL, 19.5 mmol). After it was allowed to warm to room temperature slowly and to stir overnight, the reaction was quenched by addition of water. The aqueous layer was extracted with EtOAc, and the combined organic layers were dried (Na_2SO_4) and concentrated in vacuo. The resulting

residue was purified by column chromatography (5% EtOH in hexane) to afford the desired product **65** as a colorless oil (1.39 g, 44%): ^{1}H NMR (300 MHz, $CDCl_3$) δ 5.34 (t, J = 7.2 Hz, 1H), 4.36–4.08 (m, 8H), 4.32 (d, J = 7.1 Hz, 2H), 4.03 (t, J_{HP} = 17.5 Hz, 1H), 1.77 (s, 3H), 1.72 (s, 3H), 1.37 (t, J = 7.3 Hz, 12H); ^{13}C NMR (75 MHz, $CDCl_3$) δ 139.1, 119.3, 70.1 (t, J_{CP} = 156.9 Hz), 69.4 (t, J_{CP} = 5.2 Hz), 62.9 (t, J_{CP} = 2.6 Hz, 2C), 62.7 (t, J_{CP} = 3.2 Hz, 2C), 25.4, 17.6, 16.1 (t, J_{CP} = 2.9 Hz, 2C), 16.0 (t, J_{CP} = 3.6 Hz, 2C); ^{31}P NMR (121 MHz, $CDCl_3$) δ 16.2; HRMS (ES^+, m/z) calcd for $(M+Na)^+$ $C_{14}H_{30}O_7NaP_2$: 395.1365; found: 395.1395.

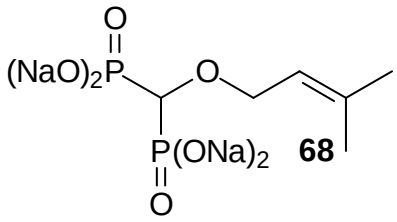

68

Sodium (((3-methylbut-2-en-1-yl)oxy)methylene)bis(phosphonate) 68. Yield, 73%; white solid; ^{1}H NMR (300 MHz, D_2O) δ 5.38 (t, J = 6.7 Hz, 1H), 4.25 (d, J = 7.2 Hz, 2H), 3.67 (t, J_{HP} = 16.2 Hz, 1H), 1.74 (s, 3H), 1.68 (s, 3H); ^{13}C NMR (100 MHz, D_2O) δ 140.2, 119.9, 74.1 (t, J_{CP} = 140.6 Hz), 69.8, 25.1, 17.5; ^{31}P NMR (121 MHz, D_2O) δ 13.9; HRMS (ES^-, m/z) calcd for $(M-H)^-$ $C_6H_{13}O_7P_2$: 259.0137; found: 259.0145.

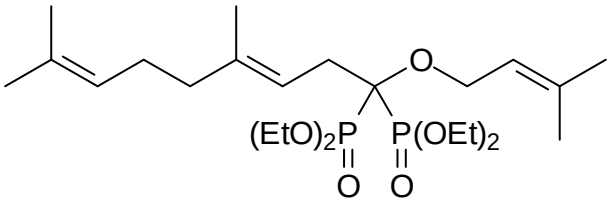

66

(*E*)-tetraethyl (4,8-dimethyl-1-((3-methylbut-2-en-1-yl)oxy)nona-3,7-diene-1,1-diyl)bis(phosphonate) 66. Yield, 37%; colorless oil; ^{1}H NMR (300 MHz, $CDCl_3$) δ 5.48 (t, J = 6.2 Hz, 1H), 5.31 (t, J = 6.7 Hz, 1H), 5.16–5.04 (m, 1H), 4.33 (d, J = 6.8 Hz,

2H), 4.30–4.10 (m, 8H), 2.89 (td, J_{HP} = 14.5 Hz, J = 6.4 Hz, 2H), 2.15–1.96 (m, 4H), 1.72 (s, 3H), 1.68 (s, 3H), 1.67 (s, 3H), 1.65 (s, 3H), 1.60 (s, 3H), 1.34 (t, J = 7.0 Hz, 6H), 1.34 (t, J = 6.8 Hz, 6H); ^{13}C NMR (100 MHz, $CDCl_3$) δ 136.8, 136.5, 131.4, 124.4, 121.2, 117.9 (t, J_{CP} = 8.1 Hz), 80.8 (t, J_{CP} = 150.6 Hz), 63.4 (t, J_{CP} =3.2 Hz), 63.4 (t, J_{CP} =4.5 Hz, 2C), 63.0 (t, J_{CP} = 3.6 Hz, 2C), 40.1, 30.2, 26.7, 25.8, 25.8, 18.2, 17.7, 16.6 (t, J_{CP} = 2.4 Hz, 2C), 16.6 (t, J_{CP} = 3.0 Hz, 2C), 16.5; ^{31}P NMR (121 MHz, $CDCl_3$) δ 19.1; HRMS (ES^+, *m*/*z*) calcd for $(M+H)^+$ $C_{24}H_{47}O_7P_2$: 509.2797; found: 509.2803.

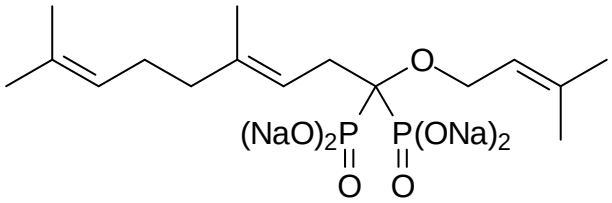

67

Sodium (*E*)-(4,8-dimethyl-1-((3-methylbut-2-en-1-yl)oxy)nona-3,7-diene-1,1-diyl)bis(phosphonate) 67. Yield, 33%; white solid; ^{1}H NMR (500 MHz, D_2O) δ 5.65 (t, J = 6.3 Hz, 1H), 5.39 (t, J = 6.6 Hz, 1H), 5.25 (t, J = 6.0 Hz, 1H), 4.31 (d, J = 7.0 Hz, 2H), 2.87 (td, J_{HP} = 13.3 Hz, J = 6.4 Hz, 2H), 2.20–2.12 (m, 2H), 2.11-2.05 (m, 2H), 1.75 (s, 3H), 1.70 (s, 6H), 1.69 (s, 3H), 1.65 (s, 3H); ^{13}C NMR (125 MHz, D_2O) δ 138.7, 137.1, 133.6, 124.7, 121.1, 119.7 (t, J_{CP} = 7.8 Hz), 79.5 (t, J_{CP} = 131.7 Hz), 62.7 (t, J_{CP} = 6.0 Hz), 39.3, 28.9, 26.0, 25.0, 24.9, 17.5, 17.1, 15.5; ^{31}P NMR (201 MHz, D_2O) δ 17.5; HRMS (ES^-, *m*/*z*) calcd for $(M-H)^-$ $C_{16}H_{29}O_7P_2$: 395.1389; found: 395.1400.

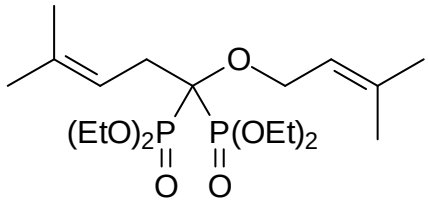

69

Tetraethyl (4-methyl-1-((3-methylbut-2-en-1-yl)oxy)pent-3-ene-1,1-diyl)bis(phosphonate) 69. Yield, 29%; colorless oil; ^{1}H NMR (500 MHz, $CDCl_3$) δ 5.45 (t, *J* = 6.5 Hz, 1H), 5.31 (tt, *J* = 6.9 HZ, J_{HP} = 1.4 Hz, 1H), 4.33 (d, *J* = 6.7 Hz, 2H), 4.28–4.18 (m, 8H), 2.87 (td, J_{HP} = 14.7 Hz, *J* = 6.8 Hz, 2H), 1.73 (s, 6H), 1.67 (s, 3H), 1.65 (s, 3H), 1.34 (t, *J* = 7.6 Hz, 6H), 1.34 (t, *J* = 7.2 Hz, 6H); ^{13}C NMR (125 MHz, $CDCl_3$) δ 136.6, 133.3, 121.2, 118.1 (t, J_{CP} = 7.8 Hz), 80.8 (t, J_{CP} = 150.5 Hz), 63.5 (t, J_{CP} = 5.2 Hz), 63.3 (t, J_{CP} = 3.2 Hz, 2C), 63.1 (t, J_{CP} = 3.7 Hz, 2C), 30.4, 26.1, 25.8, 18.2, 18.1, 16.6 (t, J_{CP} = 2.6 Hz, 4C); ^{31}P NMR (201 MHz, $CDCl_3$) δ 19.0; HRMS (ES^+, *m*/*z*) calcd for $(M+Na)^+$ $C_{19}H_{38}O_7NaP_2$: 463.1991; found: 463.1989.

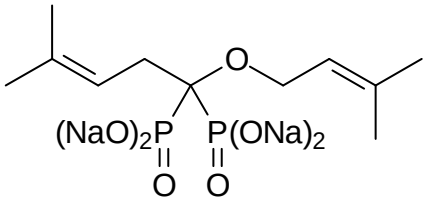

70

Sodium (4-methyl-1-((3-methylbut-2-en-1-yl)oxy)pent-3-ene-1,1-diyl)bis(phosphonate) 70. Yield, 87%; white solid; ^{1}H NMR (500 MHz, D_2O) δ 5.70 (s, 1H), 5.39 (t, *J* = 5.9 HZ, 1H), 4.30 (d, *J* = 6.7 Hz, 2H), 2.82 (td, J_{HP} = 12.4 Hz, *J* = 5.7 Hz, 2H), 1.75 (s, 3H) 1.74 (s, 3H), 1.69 (s, 3H), 1.68 (s, 3H); ^{13}C NMR (125 MHz, D_2O) δ 137.9, 132.7, 121.7, 121.5 (t, J_{CP} = 7.7 Hz), 80.4 (t, J_{CP} = 127.1 Hz), 62.4 (t, J_{CP} =5.5 Hz), 30.3, 25.3, 25.1, 17.5, 17.4; ^{31}P NMR (201 MHz, D_2O) δ 17.7; HRMS (ES^-, *m*/*z*) calcd for $(M-H)^-$ $C_{11}H_{21}O_7P_2$: 327.0763; found: 327.0780.

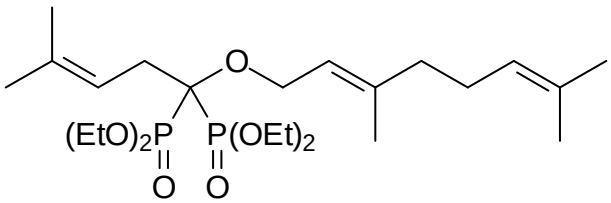

62

(*E*)-tetraethyl (1-((3,7-dimethylocta-2,6-dien-1-yl)oxy)-4-methylpent-3-ene-1,1-diyl)bis(phosphonate) 62. Yield, 30%; colorless oil; ^{1}H NMR (300 MHz, $CDCl_3$) δ 5.45 (t, *J* = 6.9 Hz, 1H), 5.33 (t, *J* = 6.5 Hz, 1H), 5.13–5.04 (m, 1H), 4.37 (d, *J* = 6.5 Hz, 2H), 4.30–4.16 (m, 8H), 2.88 (td, J_{HP} = 14.2 Hz, *J* = 6.5 Hz, 2H), 2.15–1.97 (m, 4H), 1.73 (s, 3H), 1.68 (s, 3H), 1.66 (s, 6H), 1.61 (s, 3H), 1.35 (t, *J* = 6.9 Hz, 6H), 1.34 (t, *J* = 7.3 Hz, 6H); ^{13}C NMR (75 MHz, $CDCl_3$) δ 139.7, 133.2, 131.6, 124.0, 120.8, 118.0 (t, J_{CP} = 7.5 Hz), 80.7 (t, J_{CP} = 150.9 Hz), 63.3 (t, J_{CP} = 5.9 Hz), 63.3 (t, J_{CP} = 3.2 Hz, 2C), 63.0 (t, J_{CP} = 3.0 Hz, 2C), 39.5, 30.2, 26.4, 26.0, 25.7, 18.1, 17.7, 16.5 (t, J_{CP} = 3.2 Hz, 4C), 16.5; ^{31}P NMR (121 MHz, $CDCl_3$) δ 19.0; HRMS (ES^+, *m*/*z*) calcd for $(M+Na)^+$ $C_{24}H_{46}O_7P_2Na$: 531.2617; found: 531.2619.

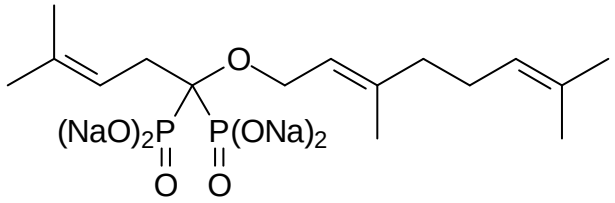

63

Sodium (*E*)-(1-((3,7-dimethylocta-2,6-dien-1-yl)oxy)-4-methylpent-3-ene-1,1-diyl)bis(phosphonate) 63. 2,4,6-Collidine (0.22 mL, 1.67 mmol) was added to an ice cold solution of bisphosphonate **62** (85 mg, 0.17 mmol) in CH_2Cl_2 (5 mL) followed by the addition of excess TMSBr (0.27 mL, 2.00 mmol). The reaction was allowed to warm slowly to rt and allowed to stir overnight. Once the reaction was complete based on analysis of the ^{31}P NMR spectrum, the volatile materials were removed in vacuo. The resulting residue was washed with toluene and concentrated repeatedly to remove any remaining TMSBr. It was treated with NaOH (0.27 mL 5M NaOH, 2 mL H_2O) for 10 minutes and then the water was removed on a lyophilizer to obtain the crude salt. This material was precipitated from water by addition of acetone to obtain the desired product,

the salt **63** as a white solid (77 mg, 94%): ^{1}H NMR (500 MHz, D_2O) δ 5.84 (s, 1H), 5.39 (t, *J* = 6.8 Hz, 1H), 5.22–5.17 (m, 1H), 4.17 (d, *J* = 7.0 Hz, 2H), 2.89–2.79 (m, 2H), 2.16–2.03 (m, 4H), 1.72 (s, 3H), 1.69 (s, 3H), 1.68 (s, 3H), 1.65 (s, 3H), 1.62 (s, 3H); ^{13}C NMR (125 MHz, D_2O) δ 140.6, 133.7, 131.4, 124.2, 123.1 (t, J_{CP} = 6.4 Hz), 122.4, 82.4 (t, J_{CP} = 134.7 Hz), 61.1 (t, J_{CP} = 6.2 Hz), 39.1, 29.7, 25.9, 25.4, 25.0, 17.4, 17.1, 15.6; ^{31}P NMR (201 MHz, D_2O) δ 17.8; HRMS (ES^-, *m*/*z*) calcd for $(M-H)^-$ $C_{16}H_{29}O_7P_2$: 395.1389; found: 395.1388.

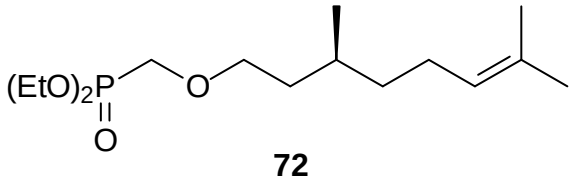

72

(*S*)-diethyl (((3,7-dimethyloct-6-en-1-yl)oxy)methyl)phosphonate 72. Yield, 34%; colorless oil; ^{1}H NMR (500 MHz, $CDCl_3$) δ 5.10–5.05 (m, 1H), 4.20–4.12 (m, 4H), 3.75 (dd, J_{HP} = 8.7 Hz, *J* = 1.9 Hz, 2H), 3.63–3.57 (m, 2H), 2.05–1.89 (m, 2H), 1.70–1.53 (m, 2H), 1.66 (s, 3H), 1.59 (s, 3H), 1.43–1.28 (m, 2H), 1.34 (t, *J* = 7.4 Hz, 6H), 1.23–1.12 (m, 1H), 0.90 (d, *J* = 6.7 Hz, 3H); ^{13}C NMR (125 MHz, $CDCl_3$) δ 130.1, 124.0, 71.2 (d, J_{CP} = 11.5 Hz), 64.3 (d, J_{CP} = 165.6 Hz), 61.4 (d, J_{CP} = 5.7 Hz, 2C), 36.4, 35.7, 28.6, 24.9, 24.7, 18.7, 16.8, 15.7 (d, J_{CP} = 5.4 Hz, 2C); ^{31}P NMR (201 MHz, $CDCl_3$) δ 21.0; HRMS (ES^+, *m*/*z*) calcd for $(M+H)^+$ $C_{15}H_{32}O_4P$: 307.2038; found: 307.2044.

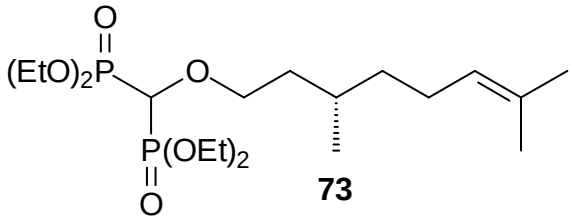

73

(*S*)-tetraethyl (((3,7-dimethyloct-6-en-1-yl)oxy)methylene)bis(phosphonate) 73. Yield, 53%; colorless oil; ^{1}H NMR (400 MHz, $CDCl_3$) δ 5.12–5.05 (m, 1H), 4.30–4.20 (m, 8H), 3.91 (t, J_{HP} = 17.6 Hz, 1H), 3.85–3.75 (m, 2H), 2.06–1.88 (m, 2H), 1.73–1.49 (m, 2H), 1.67 (s, 3H), 1.60 (s, 3H), 1.47–1.25 (m, 2H), 1.36 (t, *J* = 7.0 Hz, 12H), 1.23–1.12 (m, 1H), 0.91 (d, *J* = 6.7 Hz, 3H); ^{13}C NMR (100 MHz, $CDCl_3$) δ 130.5, 124.3, 73.2 (t, J_{CP} = 157.0 Hz), 73.0 (t, J_{CP} =4.6 Hz), 62.9 (t, J_{CP} = 3.1 Hz), 62.8 (t, J_{CP} = 3.3 Hz), 62.7 (t, J_{CP} = 3.5 Hz), 62.7 (t, J_{CP} = 3.2 Hz), 36.7, 36.4, 28.8, 25.2, 25.0, 19.0, 17.2, 16.1 (t, J_{CP} = 3.6 Hz, 2C), 16.0 (t, J_{CP} = 3.1 Hz, 2C); ^{31}P NMR (121 MHz, $CDCl_3$) δ 15.8; HRMS (ES^+, *m*/*z*) calcd for $(M+H)^+$ $C_{19}H_{41}O_7P_2$: 443.2328; found: 443.2325.

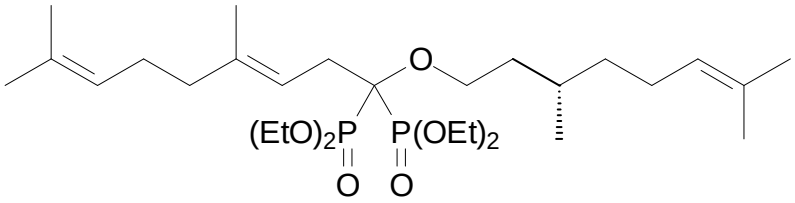

74

(S,*E*)-tetraethyl (1-((3,7-dimethyloct-6-en-1-yl)oxy)-4,8-dimethylnona-3,7-diene-1,1-diyl)bis(phosphonate) 74. Yield, 45%; colorless oil; ^{1}H NMR (400 MHz, $CDCl_3$) δ 5.46 (t, *J* = 6.3 Hz, 1H), 5.15–5.05 (m, 2H), 4.29–4.16 (m, 8H), 3.87–3.78 (m, 2H), 2.79 (td, J_{HP} = 14.8 Hz, *J* = 6.6 Hz, 2H), 2.14–1.90 (m, 6H), 1.76–1.52 (m, 4H), 1.68 (s, 3H), 1.65 (s, 3H), 1.60 (s, 3H), 1.60 (s, 3H), 1.40–1.30 (m, 15H), 1.22–1.12 (m, 1H), 0.89 (d, *J* = 6.5 Hz, 3H); ^{13}C NMR (100 MHz, $CDCl_3$) δ 136.8, 131.3, 131.1, 124.9, 124.4, 117.8 (t, J_{CP} = 7.9 Hz), 81.0 (t, J_{CP} = 150.4 Hz), 84.7 (t, J_{CP} =5.5 Hz), 63.3 (t, J_{CP} = 2.9 Hz), 63.3 (t, J_{CP} = 3.6 Hz), 62.9 (t, J_{CP} = 3.2 Hz), 62.9 (t, J_{CP} = 4.3 Hz), 40.0, 37.4 (2C), 29.9, 29.4, 26.7, 25.7 (2C), 25.5, 19.6, 17.7, 17.6, 16.6 (t, J_{CP} = 3.3 Hz, 2C), 16.5 (t, J_{CP} = 3.3 Hz, 2C), 16.4; ^{31}P NMR (121 MHz, $CDCl_3$) δ 19.2; HRMS (ES^+, *m*/*z*) calcd for $(M+H)^+$ $C_{29}H_{57}O_7P_2$: 579.3580; found: 579.3573.

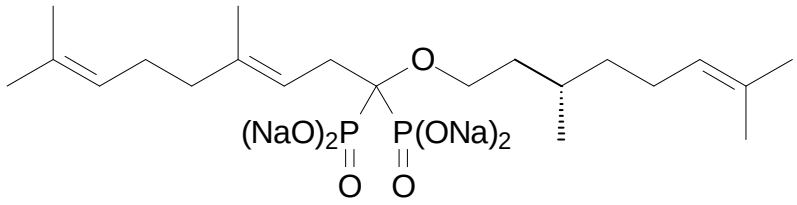

75

Sodium (S,*E*)-(1-((3,7-dimethyloct-6-en-1-yl)oxy)-4,8-dimethylnona-3,7-diene-1,1-diyl)bis(phosphonate) 75. Yield, 17%; white solid; ^{1}H NMR (500 MHz, D_2O) δ 5.73 (t, *J* = 5.5 Hz, 1H), 5.28–5.22 (m, 2H), 3.85–3.73 (m, 2H), 2.87–2.75 (m, 2H), 2.20–1.95 (m, 6H), 1.71 (s, 3H), 1.70 (s, 3H), 1.67 (s, 3H), 1.65 (s, 3H), 1.64 (s, 3H), 1.61–1.45 (m, 2H), 1.44–1.31 (m, 2H), 1.22–1.12 (m, 1H), 0.89 (d, *J* = 6.4 H, 3H); ^{13}C NMR (125 MHz, D_2O) δ 136.0, 133.5, 133.1, 125.5, 124.9, 121.6, 80.0 (t, J_{CP} = 126.5 Hz), 64.9, 39.5, 37.3, 36.9, 29.4, 26.2, 25.0 (3C), 24.9, 19.2, 17.1, 17.0, 15.5; ^{31}P NMR (201 MHz, D_2O) δ 17.7; HRMS (ES^-, *m*/*z*) calcd for $(M-H)^-$ $C_{21}H_{39}O_7P_2$: 465.2171; found: 465.2168.

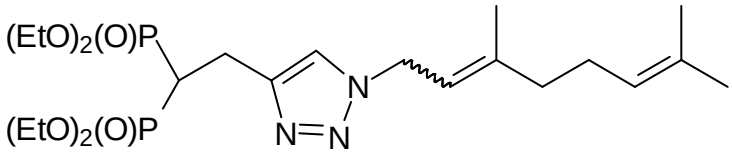

89

Representative procedure for the cycloaddition. Preparation of 1-Geranyl-4-[2,2]-bis(diethyoxyphosphinyl)ethyl-1H-1,2,3-triazole (89). Geranyl bromide (455 mg, 2.10 mmol) was dissolved in DMF (5 mL) and NaN_3 (133 mg, 2.10 mmol) was added to the solution. The mixture was allowed to stir for 15 min after which a solution of *t*-BuOH/H_2O (5 mL) was added along with tetraethyl-(3-butyn-1-ylidene)-1,1-bisphosphonate (**83**, 228 mg, 0.72 mmol). The solution was allowed to stir while $CuSO_4$ (5 M, 0.10 mL) and sodium ascorbate (8.3 mg, 0.43 mmol) were added. The mixture was

allowed to stir overnight, and then EDTA and 1M NH_4OH were added. The resulting solution was placed in a continuous liquid-liquid extractor and extracted for 24 h with EtOAc, or extracted with EtOAc in a separatory funnel. The organic portion was concentrated *in vacuo* and the resulting oil was purified via flash chromatography (silica gel, 10% EtOH in hexanes) to provide the desired triazole **89** (79%).

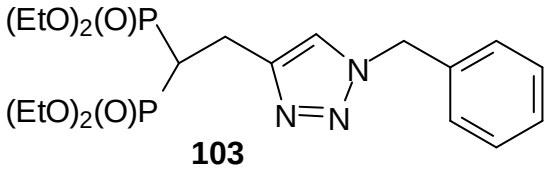

103

Tetraethyl (2-(1-benzyl-1H-1,2,3-triazol-4-yl)ethane-1,1-diyl)bis(phosphonate) 103. Yield, 60%; colorless oil; the ^{1}H and ^{31}P NMR data agreed with that previously reported; the ^{13}C data was very similar: δ 145.4 (t, J_{CP} = 8.9 Hz), 134.8, 128.9 (2C), 128.5, 128.0 (2C), 122.1, 62.7 (d, J_{CP} = 6.5 Hz, 2C), 62.3 (d, J_{CP} = 6.7 Hz, 2C), 53.9, 36.5 (t, J_{CP} = 132.7 Hz), 22.1 (t, J_{CP} = 4.6 Hz, 2C), 16.2 (d, J_{CP} = 5.8 Hz, 2C), 16.1 (d, J_{CP} = 6 Hz, 2C).[89]

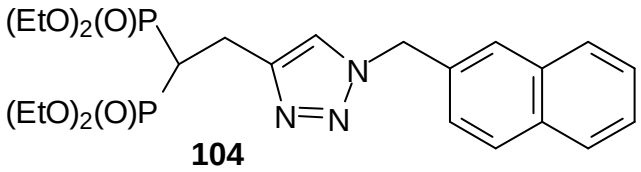

104

Tetraethyl (2-(1-(naphthalen-2-ylmethyl)-1H-1,2,3-triazol-4-yl)ethane-1,1-diyl)bis(phosphonate) 104. Yield, 58%; colorless oil; ^{1}H NMR: δ 7.84–7.80 (m, 3H), 7.76 (s, 1H), 7.52–7.49 (m, 3H), 7.40–7.36 (m, 1H), 5.64 (s, 2H), 4.21–4.00 (m, 8H), 3.34 (td, J_{HP} = 16.3 Hz, J = 6.8 Hz, 2H), 2.99 (tt, J_{HP} = 23.6 Hz, J = 6.0 Hz, 1H), 1.24 (t, J = 7.2 Hz, 6H), 1.21 (t, J = 7.1 Hz, 6H); ^{13}C NMR: δ 145.4 (t, J_{CP} = 8.4 Hz), 133.1, 133.0, 132.2, 128.9, 127.8, 127.6, 127.2, 126.6, 126.5, 125.3, 122.2, 62.6 (d, J_{CP} = 6.8 Hz, 2C), 62.3 (d, J_{CP} = 6.7 Hz, 2C), 54.1, 36.5 (t, J_{CP} = 132.9 Hz), 22.1 (t, J_{CP} = 5.2 Hz),

16.2 (d, J_{CP} = 6.1 Hz, 2C), 16.1 (d, J_{CP} = 6.0 Hz, 2C); ^{31}P NMR: δ 22.3 ppm; HRMS (ES^+, *m*/*z*) calcd for $(M+H)^+$ $C_{23}H_{34}N_3O_6P_2$: 510.1923; found: 510.1931.

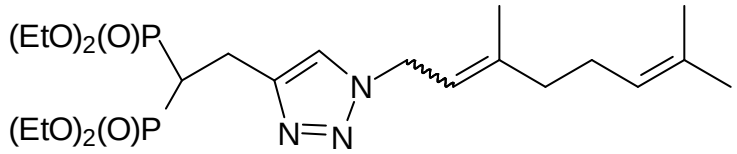

89

1-Geranyl-4-[2,2]-bis(diethyoxyphosphinyl)ethyl-1H-1,2,3-triazole 89. Yield 79%, colorless oil. ^{1}H NMR δ 7.42 (s, 1H), 5.40 (t, *J* = 7.5 Hz, 1H), 5.09–5.05 (m, 1H), 4.94–4.89 (m, 2H), 4.26–4.06 (m, 8H), 3.39–3.25 (td, J_{HP} = 16.2 Hz, *J* = 6.9 Hz, 2H), 3.01–2.91 (m, 1H), 2.19–2.00 (m, 4H), 1.78 (s, 3H), 1.69 (s, 3H), 1.60 (s, 3H), 1.38–1.24 (m, 12H); ^{13}C NMR δ 145.0, 142.8, 123.4, 121.5, 118.0, 117.1, 62.6 (dd, J_{CP} = 24.7 Hz, *J* = 6.5 Hz, 4C), 47.8, 39.4, 36.6 (t, J_{CP} = 129.5 Hz), 32.1, 22.1 (t, *J* = 4.8 Hz), 17.6, 16.4 (2C), 16.3–16.2 (m, 4C); ^{31}P NMR: δ 22.5 ppm; HRMS calculated for $C_{22}H_{42}N_3O_6P_2$ $(M+H)^+$, 506.2549; found 506.2568.

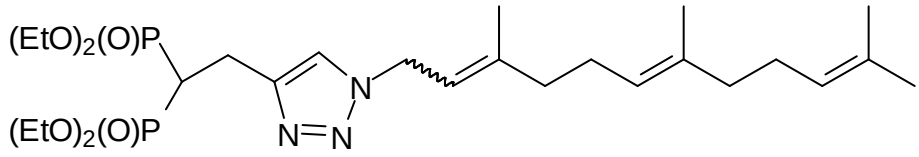

102

Tetraethyl (2-(1-((6*E*)-3,7,11-trimethyldodeca-2,6,10-trien-1-yl)-1H-1,2,3-triazol-4-yl)ethane-1,1-diyl)bis(phosphonate) 102. Yield, 67%; colorless oil; ^{1}H NMR: δ 7.38 (s, 1H), 5.39–5.30 (m, 1H), 5.10–4.98 (m, 2H), 4.90–4.82 (m, 2H), 4.19–4.01 (m, 8H), 3.26 (td, J_{HP} = 16.1 Hz, *J* = 6.3 Hz, 2H), 3.11–2.83 (m, 1H), 2.16–1.87 (m, 8H), 1.77 (s, 3H), 1.64–1.52 (m, 9H), 1.24 (t, *J* = 7.1 Hz, 6H), 1.22 (t, *J* = 7.1 Hz, 6H); ^{31}P NMR: δ 22.5 ppm; HRMS (ES^+, *m*/*z*) calcd for $C_{27}H_{50}N_3O_6P_2$ $(M+H)^+$ 574.3175; found 574.3192.

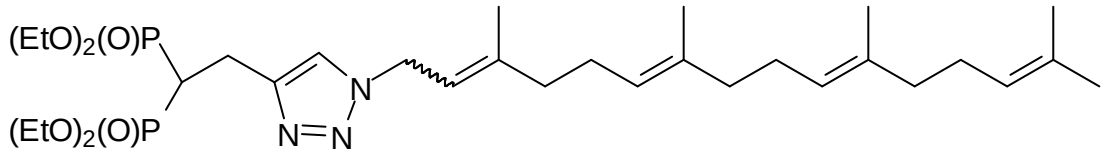

96

Tetraethyl (2-(1-((6*E*,10*E*)-3,7,11,15-tetramethylhexadeca-2,6,10,14-tetraen-1-yl)-1H-1,2,3-triazol-4-yl)ethane-1,1-diyl)bis(phosphonate) 96. Yield 58%, colorless oil; ^{1}H NMR: δ 7.43 (s, 1H), 5.41 (t, J = 6.4 Hz, 1H), 5.18–5.05 (m, 3H), 4.94–4.90 (m, 2H), 4.25–4.05 (m, 8H), 3.33 (td, J_{HP} = 16.1 Hz, J = 6.4 Hz, 2H), 3.09–2.89 (m, 1H), 2.19–1.95 (m, 12H), 1.79 (s, 3H), 1.71-1.55 (m, 12H), 1.31 (t, J = 6.9 Hz, 6H), 1.28 (t, J = 7.1 Hz, 6H); ^{31}P NMR: δ 22.5; HRMS (ES^{+}, m/z) calcd for $C_{32}H_{57}N_3O_6P_2Na$ $(M+Na)^{+}$ 664.3620; found 664.3627.

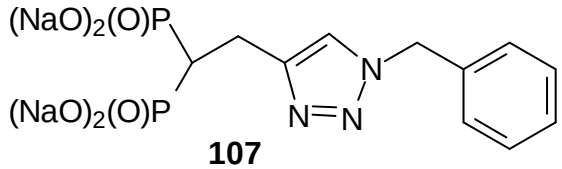

107

Representative procedure for ester hydrolysis. Preparation of sodium (2-(1-benzyl-1H-1,2,3-triazol-4-yl)ethane-1,1-diyl)bis(phosphonate) 107. TMSBr (0.35 mL, 2.6 mmol) was added to an ice cold solution of collidine (0.29 mL, 2.2 mmol) in CH_2Cl_2 (5 mL). After the solution was stirred for 30 minutes, a solution of compound **103** (100 mg, 0.22 mmol) in a small amount of CH_2Cl_2 was added and the reaction was allowed to stir overnight. Once the reaction was complete, based on analysis of the ^{31}P NMR spectrum of the reaction mixture, it was diluted with toluene. After the solvent was removed in vacuo, the residue was washed with toluene twice and dried to remove any remaining TMSBr. It was then treated with 8 equiv NaOH in water (1.8 mL) overnight. The reaction mixture was then dried on a lyophilizer to obtain a crude salt, which was

then dissolved in a small amount of water, precipitated by addition of acetone, isolated by filtration, and dried. It was then dissolved in water and lyophilized to produce the pure white salt.

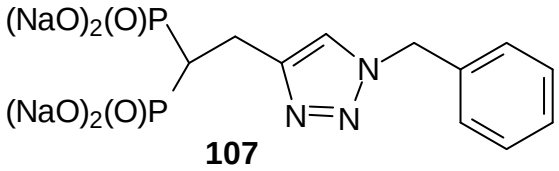

107

Sodium (2-(1-benzyl-1H-1,2,3-triazol-4-yl)ethane-1,1-diyl)bis(phosphonate) 107. Yield, 54%; white powder; ^{1}H NMR (D_2O): δ 7.92 (s, 1H), 7.58–7.32 (m, 5H), 5.60 (br, 2H), 3.24 (br, 2H), 2.70–2.21 (m, 1H); ^{13}C NMR (D_2O): δ 147.4, 135.2, 129.2 (2C), 128.7, 128.1 (2C), 124.3, 53.8, 39.5 (t, J_{CP} = 125.2 Hz), 21.8; ^{31}P NMR (D_2O): δ 18.8 ppm; HRMS (ES$^-$, *m*/*z*) calcd for $(M-H)^-$ $C_{11}H_{14}N_3O_6P_2$: 346.0358; found: 346.0354.

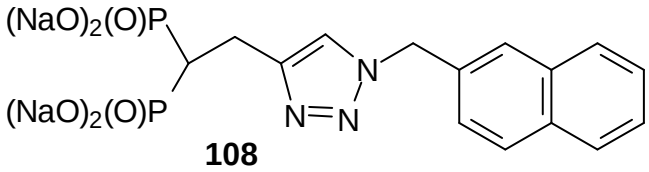

108

Sodium (2-(1-(naphthalen-2-ylmethyl)-1H-1,2,3-triazol-4-yl)ethane-1,1-diyl)bis(phosphonate) 108. Yield, 48%; white powder; ^{1}H NMR (D_2O): δ 7.94–7.66 (m, 5H), 7.56–7.46 (m, 2H), 7.32 (d, *J* = 8.0 Hz, 1H), 5.62 (s, 2H), 3.24 (br, 2H), 2.44 (t, J_{HP} = 20.7 Hz, 1H); ^{13}C NMR (D_2O): δ 133.0, 132.8, 132.6, 128.9, 128.0, 127.8, 127.1, 126.8 (2C), 125.5, 124.4, 53.9, 39.5 (t, J_{CP} = 114.4 Hz, 1C), 21.9; ^{31}P NMR (D_2O): δ 18.8 ppm; HRMS (ES$^-$, *m*/*z*) calcd for $(M-H)^-$ $C_{15}H_{16}N_3O_6P_2$: 396.0514; found: 396.0504.

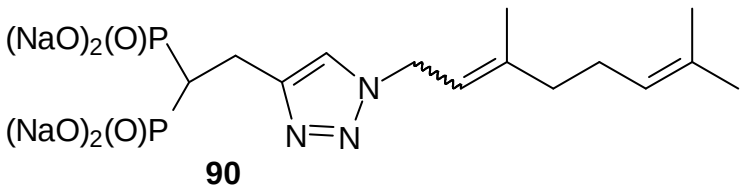

90

Sodium (2-(1-(3,7-dimethylocta-2,6-dien-1-yl)-1H-1,2,3-triazol-4-yl)ethane-1,1-diyl)bis(phosphonate) 90. Yield, 75%; white powder; ^{1}H NMR (D_2O): δ 7.86 (s, 1H), 5.58–5.48 (m, 1H), 5.18 (s, 1H), 5.01–4.97 (m, 2H), 3.20 (td, J_{HP} = 14.5 Hz, J = 7.0 Hz, 2H), 2.30–2.16 (m, 5H), 1.82 (s, 3H), 1.68–1.60 (m, 6H); ^{31}P NMR (D_2O): δ 18.9 ppm; HRMS (ES^-, *m*/*z*) calcd for $(M-H)^-$ $C_{14}H_{24}N_3O_6P_2$: 392.1140; found: 392.1148.

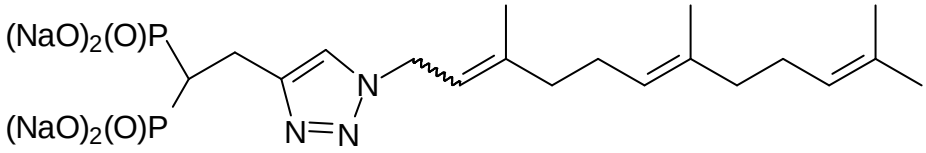

106

Sodium (2-(1-((6*E*)-3,7,11-trimethyldodeca-2,6,10-trien-1-yl)-1H-1,2,3-triazol-4-yl)ethane-1,1-diyl)bis(phosphonate) 106. Yield, 76%; white powder; ^{1}H NMR (D_2O): δ 7.84–7.70 (m, 1H), 5.45–5.30 (m, 1H), 5.10–4.96 (m, 2H), 4.89–4.84 (m, 2H), 3.21 (s, 2H), 2.55–2.35 (m, 1H), 2.12–1.88 (m, 8H), 1.75–1.67 (m, 3H), 1.56–1.49 (m, 9H); ^{31}P NMR (D_2O): δ 19.0 ppm.

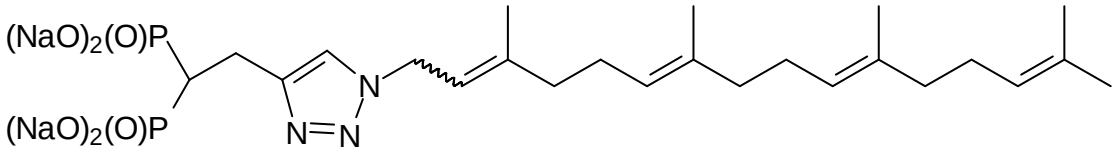

97

Sodium (2-(1-((6*E*,10*E*)-3,7,11,15-tetramethylhexadeca-2,6,10,14-tetraen-1-yl)-1H-1,2,3-triazol-4-yl)ethane-1,1-diyl)bis(phosphonate) 97. Yield, 59%; white powder; ^{1}H NMR (D_2O): δ 7.87–7.68 (m, 1H), 5.48–5.32 (m, 1H), 5.06 (br, 3H), 4.92 (br, 2H), 3.23 (br, 2H), 2.65–2.40 (m, 1H), 2.20–1.85 (m, 12H), 1.84–1.67 (m, 3H), 1.61(s, 6H), 1.53 (s, 6H); ^{31}P NMR (D_2O): δ 19.2 ppm.

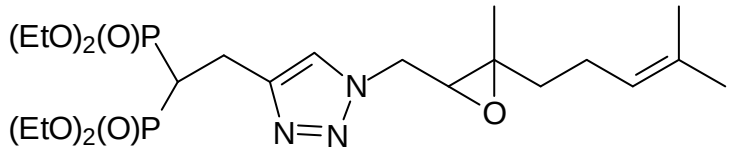

134

Tetraethyl (*E*)-(2-(1-((3-methyl-3-(4-methylpent-3-en-1-yl)oxiran-2-yl)methyl)-1H-1,2,3-triazol-4-yl)ethane-1,1-diyl)bis(phosphonate) (134). Solid NaN_3 (180 mg, 2.79 mmol) was added to a solution of bromide **132**[101,102] (434 mg, 1.86 mmol) in DMF (3 mL) and the reaction was allowed to stir overnight at rt while protected from light in a flask wrapped with aluminum foil.[103] Once the reaction was complete, it was diluted with EtOAc and the solid was removed by filtration. After the filtrate was washed with water (five times) and then with brine to remove any remaining DMF, the organic layer was dried (Na_2SO_4) and concentrated in vacuo to obtain the azide as a colorless oil (250 mg, 69%). (^{1}H NMR (300 MHz, $CDCl_3$) δ 5.08 (t, *J* = 7.1 Hz, 1H), 3.47–3.41 (m, 2H), 2.98 (t, *J* = 6.0 Hz, 1H), 2.15–2.05 (m, 2H), 1.76–1.42 (m, 2H), 1.70 (s, 3H), 1.62 (s, 3H), 1.32 (s, 3H)). Without further purification, the azide **133** (250 mg, 1.29 mmol) and tetraethyl-(3-butyn-1-ylidene)-1,1-bisphosphonate[89] (**81**, 200 mg, 0.6 mmol) were dissolved in a solution of water in *t*-BuOH (1:4, 3 mL), followed by addition of $CuSO_4$ (5 M, 0.01 mL) and sodium ascorbate (40 mg, 0.20 mmol) in sequence. After the reaction was allowed to stir overnight at rt, the solvent was removed under vacuum. The resulting residue was dissolved in brine and extracted with EtOAc. The combined organic layer was washed with 5% NH_4OH, dried (Na_2SO_4), and concentrated in vacuo. The resulting oil was purified via flash chromatography (10% EtOH in hexanes) to provide the desired triazole **134** as a colorless oil (130 mg, 42%): ^{1}H NMR (400 MHz, $CDCl_3$) δ 7.63 (s, 1H), 5.04 (t, *J* = 7.1 Hz, 1H), 4.69 (dd, *J* = 14.4, 4.1 Hz, 1H), 4.26 (dd,

J = 14.8, 7.2 Hz, 1H), 4.22–4.09 (m, 8H), 3.35 (td, J_{HP} = 16.0 Hz, *J* = 6.2 Hz, 2H), 3.10 (dd, *J* = 7.6 Hz, 4.4 Hz, 1H), 2.98 (tt, J_{HP} = 23.5 Hz, *J* = 6.4 Hz, 1H), 2.07 (td, *J* = 8.2 Hz, 7.6 Hz, 2H), 1.73–1.63 (m, 1H), 1.67 (s, 3H), 1.60 (s, 3H), 1.54–1.45 (m, 1H), 1.42 (s, 3H), 1.33–1.27 (m, 12H); ^{13}C NMR (75 MHz, $CDCl_3$) δ 145.5 (t, J_{CP} = 7.8 Hz), 132.5, 122.9, 122.7, 62.8 (d, J_{CP} = 6.5 Hz, 2C), 62.6 (d, J_{CP} = 6.6 Hz, 2C), 61.4, 60.4, 49.9, 38.1, 36.6 (t, J_{CP} = 132.5 Hz), 25.7, 23.5, 22.1 (t, J_{CP} = 4.0 Hz), 17.7, 17.0, 16.4 (d, J_{CP} = 3.1 Hz, 2C), 16.3 (d, J_{CP} = 2.3 Hz, 2C); ^{31}P NMR (121 MHz, $CDCl_3$) δ 22.3; HRMS (ES^-, *m*/*z*) calcd for $(M-H)^-$ $C_{14}H_{24}N_3O_7P_2$: 408.1090; found: 408.1114.

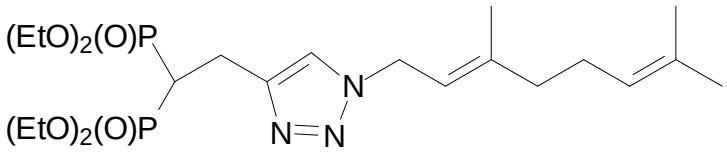

135

Tetraethyl (*E*)-(2-(1-(3,7-dimethylocta-2,6-dien-1-yl)-1H-1,2,3-triazol-4-yl)ethane-1,1-diyl)bis(phosphonate) (135). Sodium iodide (60 mg, 0.4 mmol) was weighed in a round bottom flask and dried in an oven overnight. After the salt was dissolved in acetonitrile/THF (1:1, 1 mL), trifluoroacetic anhydride (0.014 mL, 0.1 mmol) was added. After 5 minutes, when the solution had turned to a deep yellow color, it was cooled in an ice bath. The starting material **134** (50 mg, 0.1 mmol) was then added to the reaction vessel as a neat oil. After an additional 5 minutes, the ice bath was removed and the reaction mixture was allowed to stir overnight at rt. Once the reaction was complete based on TLC analysis (5% MeOH/EtO_2), it was diluted with saturated $NaHSO_3$. The aqueous layer was extracted with Et_2O, the organic extracts were combined, dried (Na_2SO_4), and concentrated in vacuo. Final purification by column chromatography (10% MeOH/Et_2O) afforded the desired product **135** as a colorless oil

(28 mg, 55%): ^{1}H NMR (500 MHz, $CDCl_3$) δ 7.44 (s, 1H), 5.40 (tq, *J* = 7.1 Hz, 1.0 Hz, 1H), 5.06 (t, *J* = 5.7 Hz, 1H), 4.92 (d, *J* = 6.9 Hz, 2H), 4.22–4.07 (m, 8H), 3.32 (td, J_{HP} = 15.6 Hz, *J* = 6.3 Hz, 2H), 3.03 (tt, J_{HP} = 23.6 Hz, *J* = 6.3 Hz, 1H), 2.14–2.04 (m, 4H), 1.78 (s, 3H), 1.68 (s, 3H), 1.60 (s, 3H), 1.28 (t, *J* = 7.0 Hz, 6H), 1.28 (t, *J* = 7.1 Hz, 6H); ^{13}C NMR (125 MHz, $CDCl_3$) δ 145.2 (t, J_{CP} = 7.8 Hz), 143.1, 132.3, 123.6, 121.7, 117.3, 63.1, 63.0, 62.7, 62.7, 48.0, 39.6, 36.7 (t, J_{CP} = 132.6 Hz), 30.5, 26.3, 25.9, 22.3 (t, J_{CP} = 4.4 Hz), 17.9, 16.5, 16.4, 16.4, 16.4; ^{31}P NMR (202 MHz, $CDCl_3$) δ 22.5; HRMS (ES^+, *m*/*z*) calcd for $(M+H)^+$ $C_{22}H_{42}N_3O_6P_2$: 506.2549; found: 506.2547.

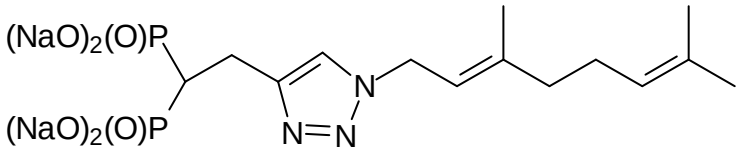

136

Sodium (*E*)-(2-(1-(3,7-dimethylocta-2,6-dien-1-yl)-1H-1,2,3-triazol-4-yl)ethane-1,1-diyl)bis(phosphonate) (136). Collidine (0.21 mL, 1.57 mmol) was added into an ice cold solution of compound **135** (79 mg, 0.16 mmol) in CH_2Cl_2 (3.5 mL) followed by addition of TMSBr (0.25 mL, 1.88 mmol) and the reaction was allowed to stir overnight at rt. Once the reaction was complete, based on analysis of the ^{31}P NMR spectrum of the reaction mixture, it was diluted with toluene. After the solvent was removed in vacuo, the residue was washed with toluene five more times and dried to remove any remaining TMSBr. It was then treated with 1N NaOH (1.0 mL, 1 mmol) overnight. The reaction mixture was then dried on a lyophilizer to obtain the salt, which was then dissolved in a small amount of water, precipitated by addition of acetone, isolated by filtration, and dried. This material was further dissolved in water and lyophilized to produce the pure white salt **136** (59 mg, 75%): ^{1}H NMR (500 MHz, D_2O) δ

7.81 (s, 1H), 5.45 (t, J = 6.6 Hz, 1H), 5.12 (s, 1H), 4.97 (d, J = 7.4 Hz, 2H), 3.22 (td, J_{HP} = 14.7 Hz, J = 6.2 Hz, 2H), 2.42 (tt, J_{CP} = 21.2 Hz, J = 6.4 Hz, 1H), 2.17–2.05 (m, 4H), 1.78 (s, 3H), 1.64 (s, 3H), 1.56 (s, 3H), ^{13}C NMR (125 MHz, D_2O) δ 147.0 (t, J_{CP} = 3.7 Hz), 143.7, 133.5, 123.9, 123.6, 117.1, 47.9, 39.6 (t, J_{CP} = 118.6 Hz), 38.7, 25.6, 25.0, 21.8 (t, J_{CP} = 3.4 Hz), 17.1, 15.7; ^{31}P NMR (202 MHz, D_2O) δ 18.8; HRMS (ES^+, m/z) calcd for $(M+H)^+$ $C_{14}H_{22}N_3O_6P_2Na_4$: 482.0575; found: 482.0570.

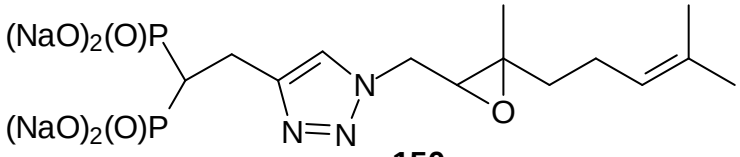

150

Sodium (*E*)-(2-(1-((3-methyl-3-(4-methylpent-3-en-1-yl)oxiran-2-yl)methyl)-1H-1,2,3-triazol-4-yl)ethane-1,1-diyl)bis(phosphonate) (150). An ice cold solution of epoxide **134** (58 mg, 0.11 mmol) in dichloromethane (3 mL) was treated with 2,4,6-collidine (0.15 mL, 1.1 mmol) and TMSBr (0.18 mL, 1.33 mmol) in sequence. After it was allowed to react overnight at rt, and the reaction was complete based on analysis of the ^{31}P NMR spectrum, the reaction solvent was removed in vacuo. The resulting residue was then dissolved in toluene and dried under vacuo, and this process was repeated five times. The white solid that formed was allowed to stir with 1N NaOH (0.55 mL, 0.55 mmol) for 2 minutes at rt followed by removal of water on a lyophilizer to obtain the initial salt. This material was further precipitated from acetone to produce the desired product **150** as a white solid (30 mg, 46%): ^{1}H NMR (500 MHz, D_2O) δ 7.92 (s, 1H), 5.16–5.08 (s, 1H), 4.76–4.73 (m, 1H), 4.58–4.50 (dd, J = 15.0 Hz, 7.2 Hz, 1H), 3.45–3.39 (dd, J = 6.4 Hz, 5.4 Hz, 1H), 3.25 (td, J_{HP} = 15.2 Hz, J = 6.4 Hz, 2H), 2.41 (tt, J_{HP} = 21.2 Hz, J = 6.6 Hz, 1H), 2.11–2.18 (m, 2H), 1.84–1.46 (m, 2H), 1.66 (s, 3H), 1.62(s, 3H),

1.49 (s, 3H); ^{13}C NMR (125 MHz, D_2O) δ 147.4, 134.0, 124.3, 123.1, 64.2, 62.0, 49.4, 39.5 (t, J_{CP} = 16.2 Hz), 37.3, 24.9, 23.2, 21.8, 16.9, 15.6; ^{31}P NMR (202 MHz, D_2O) δ 18.7; HRMS (ES^-, *m*/*z*) calcd for $(M-H)^-$ $C_{14}H_{24}N_3O_7P_2$: 408.1090; found: 408.1101.

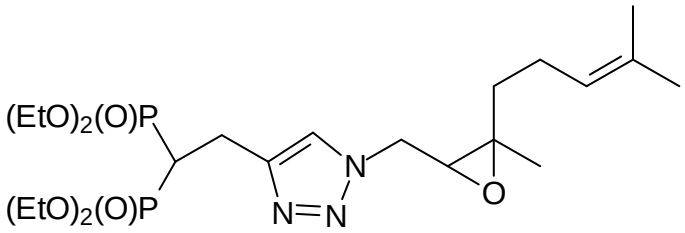

140

Tetraethyl (*Z*)-(2-(1-((3-methyl-3-(4-methylpent-3-en-1-yl)oxiran-2-yl)methyl)-1H-1,2,3-triazol-4-yl)ethane-1,1-diyl)bis(phosphonate) (140). According to the procedure described for preparation of compound **134**, bromide **138**[102] (400 mg, 1.7 mmol) was treated with NaN_3 (170 mg, 2.6 mmol). The resulting intermediate organic azide (**139**, 260 mg, 1.33 mmol) was then isolated and treated with bisphosphonate **81** (330 mg, 1.02 mmol) to afford the desired triazole **140** (354 mg, 67%) as a colorless oil after purification by flash chromatography (10% EtOH in hexanes): ^{1}H NMR (300 MHz, $CDCl_3$) δ 7.68 (s, 1H), 5.14 (t, *J* = 7.6 Hz, 1H), 4.76 (dd, *J* = 14.1 Hz, 3.3 Hz, 1H), 4.28–4.05 (m, 9H), 3.34 (td, J_{HP} = 16.5 Hz, *J* = 6.3 Hz, 2H), 3.10 (dd, *J* = 7.4 Hz, 3.7 Hz, 1H), 3.00 (tt, J_{CP} = 23.4 Hz, *J* = 6.3 Hz, 1H), 2.25–2.13 (m, 2H), 1.82–1.56 (m, 2H), 1.71 (s, 3H), 1.65 (s, 3H), 1.36 (s, 3H), 1.30 (t, *J* = 7.1 Hz, 12H); ^{13}C NMR (75 MHz, $CDCl_3$) δ 145.0 (t, J_{CP} = 7.6 Hz), 132.2, 122.6, 122.3, 62.4, 62.3, 62.1, 62.0, 61.3, 61.2, 49.4, 36.2 (t, J_{CP} = 132.6 Hz), 32.7, 25.3, 23.6, 21.7 (t, J_{CP} = 3.8 Hz), 21.5, 17.3, 16.0, 15.9, 15.9, 15.8; ^{31}P NMR (121 MHz, $CDCl_3$) δ 22.2; HRMS (ES^+, *m*/*z*) calcd for $(M+H)^+$ $C_{22}H_{42}N_3O_7P_2$: 522.2498; found: 522.2507.

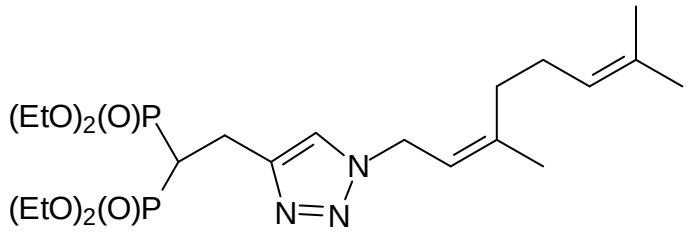

141

Tetraethyl (*Z*)-(2-(1-(3,7-dimethylocta-2,6-dien-1-yl)-1H-1,2,3-triazol-4-yl)ethane-1,1-diyl)bis(phosphonate) (141). According to the procedure employed for preparation of compound **135**, epoxide **140** (150 mg, 0.29 mmol) was treated with NaI (170 mg, 1.15 mmol) and trifluoroacetic anhydride (0.04 mL, 0.29 mmol). A parallel work-up and final purification by column chromatography gave the desired product **141** (69 mg, 48%) as a colorless oil: ^{1}H NMR (400 MHz, $CDCl_3$) δ 7.45 (s, 1H), 5.40 (t, J = 7.5 Hz, 1H), 5.13–5.06 (m, 1H), 4.90 (d, J = 7.5 Hz, 2H), 4.21–4.06 (m, 8H), 3.34 (td, J_{HP} = 16.2 Hz, J = 6.5 Hz, 2H), 3.04 (tt, J_{HP} = 23.6 Hz, J = 6.2 Hz, 1H), 2.22–2.09 (m, 4H), 1.79 (s, 3H), 1.69 (s, 3H), 1.62 (s, 3H), 1.28 (t, J = 6.9 Hz, 12H); ^{13}C NMR (100 MHz, $CDCl_3$) δ 145.0 (t, J_{CP} = 11.5 Hz), 142.8, 132.7, 123.3, 121.7, 118.1, 63.0, 62.9, 62.7, 62.6, 41.7, 36.6 (t, J_{CP} = 132.6 Hz), 32.2, 26.4, 25.8, 23.5, 22.2 (t, J_{CP} = 4.0 Hz), 17.8, 16.4, 16.4, 16.3, 16.3; ^{31}P NMR (121 MHz, $CDCl_3$) δ 22.5; HRMS (ES^+, m/z) calcd for $(M+H)^+$ $C_{22}H_{42}N_3O_6P_2$: 506.2549; found: 506.2553.

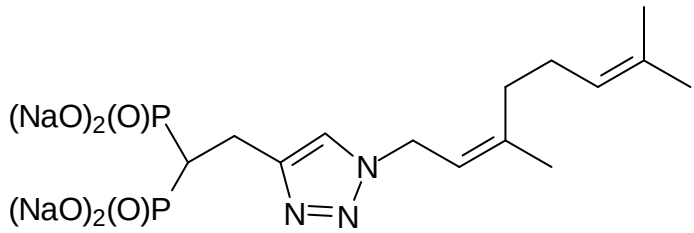

142

Sodium (*Z*)-(2-(1-(3,7-dimethylocta-2,6-dien-1-yl)-1H-1,2,3-triazol-4-yl)ethane-1,1-diyl)bis(phosphonate) (142). According to the procedure employed for

preparation of compound **136**, bisphosphonate **141** (66 mg, 0.13 mmol) was treated with collidine (0.17 mL, 1.31 mmol), TMSBr (0.21 mL, 1.57 mmol) and then 1N NaOH (0.75 mL, 0.75 mmol). A parallel work-up and final purification by precipitation gave the desired product **142** (40 mg, 64%): white solid; ^{1}H NMR (500 MHz, D_2O) δ 7.81 (s, 1H), 5.52 (t, *J* = 7.0 Hz, 1H), 5.19 (t, *J* = 7.1, 1H), 4.95 (d, *J* = 7.4 Hz, 2H), 3.14 (td, J_{HP} = 14.9 Hz, *J* = 5.5 Hz, 2H), 2.29–2.13 (m, 4H), 2.05 (tt, J_{CP} = 21.7 Hz, *J* = 5.6 Hz, 1H), 1.80 (s, 3H), 1.67 (s, 3H), 1.62 (s, 3H), ^{13}C NMR (125 MHz, D_2O) δ 150.7, 143.7, 134.2, 123.7, 123.5, 117.8, 47.8, 41.5 (t, J_{CP} = 118.0 Hz), 31.4, 25.8, 25.0, 24.4, 22.6, 17.0; ^{31}P NMR (202 MHz, D_2O) δ 19.8; HRMS (ES^-, *m*/*z*) calcd for $(M-H)^-$ $C_{14}H_{24}N_3O_6P_2$: 392.1140; found: 392.1135.

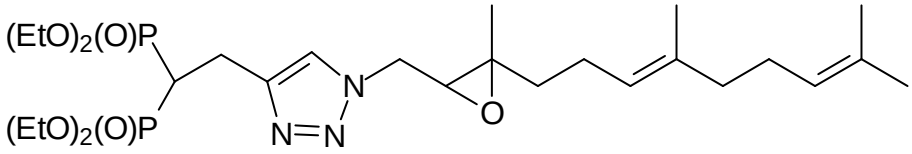

147

(*E*)-Tetraethyl (2-(1-((3-(4,8-dimethylnona-3,7-dien-1-yl)-3-methyloxiran-2-yl)methyl)-1H-1,2,3-triazol-4-yl)ethane-1,1-diyl)bis(phosphonate) 147. According to the procedure described for preparation of compound **134**, bromide **145** (500 mg, 1.7 mmol) was treated with NaN_3 (160 mg, 2.5 mmol). The resulting intermediate organic azide (**146**, 285 mg, 1.08 mmol) was then isolated and treated with bisphosphonate **81** (270 mg, 0.83 mmol) to afford the desired triazole **147** (279 mg, 57%) as a colorless oil after purification by flash chromatography (10% EtOH in hexanes): ^{1}H NMR (500 MHz, $CDCl_3$) δ 7.64 (s, 1H), 5.09–5.04 (m, 2H), 4.71 (dd, *J* = 14.2, 3.9 Hz, 1H), 4.27 (dd, *J* = 14.4, 7.4 Hz, 1H), 4.22–4.08 (m, 8H), 3.35 (td, J_{HP} = 16.2 Hz, *J* = 6.4 Hz, 2H), 3.10 (dd, *J* = 7.6 Hz, 4.2 Hz, 1H), 2.99 (tt, J_{HP} = 23.3 Hz, *J* = 6.4 Hz, 1H), 2.13–2.02 (m, 4H),

2.00–1.94 (m, 2H), 1.72–1.64 (m, 1H), 1.67 (s, 3H), 1.59 (s, 6H), 1.55–1.48 (m, 1H), 1.43 (s, 3H), 1.34–1.27 (m, 12H); ^{13}C NMR (125 MHz, $CDCl_3$) δ 145.3 (t, J_{CP} = 8.3 Hz), 135.9, 131.2, 124.0, 122.8, 122.5, 62.7 (dd, J_{CP} = 6.5, 1.0 Hz, 2C), 62.4 (dd, J_{CP} = 6.6, 1.0 Hz, 2C), 61.3, 60.2, 49.7, 39.5, 38.0, 36.5 (t, J_{CP} = 133.0 Hz), 26.5, 25.5, 23.3, 22.0 (t, J_{CP} = 4.2 Hz), 17.5, 16.8, 16.2-16.1 (m, 4C), 15.8; ^{31}P NMR (202 MHz, $CDCl_3$) δ 22.3; HRMS (ES^+, *m*/*z*) calcd for $(M+H)^+$ $C_{27}H_{50}N_3O_7P_2$: 590.3124; found: 590.3124.

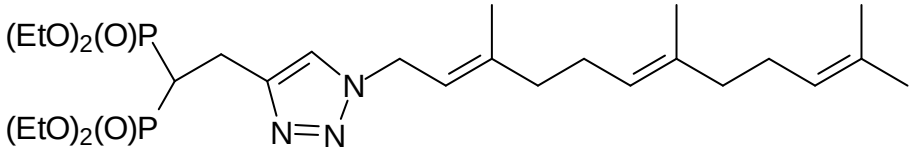

148

Tetraethyl (2-(1-((2*E*,6*E*)-3,7,11-trimethyldodeca-2,6,10-trien-1-yl)-1H-1,2,3-triazol-4-yl)ethane-1,1-diyl)bis(phosphonate) 148. According to the procedure employed for preparation of compound **135**, epoxide **147** (120 mg, 0.20 mmol) was treated with NaI (120 mg, 0.82 mmol) and trifluoroacetic anhydride (0.03 mL, 0.20 mmol). A parallel work-up and final purification by column chromatography (5% MeOH/CH_2Cl_2) gave the desired product **148** (69 mg, 60%) as a colorless oil: ^{1}H NMR (500 MHz, $CDCl_3$) δ 7.44 (s, 1H), 5.40 (t, *J* = 7.2 Hz, 1H), 5.11–5.05 (m, 2H), 4.92 (d, *J* = 7.1 Hz, 2H), 4.20–4.07 (m, 8H), 3.34 (td, J_{HP} = 16.1 Hz, *J* = 6.2 Hz, 2H), 3.02 (tt, J_{HP} = 23.4 Hz, *J* = 6.5 Hz, 1H), 2.15–1.95 (m, 8H), 1.78 (s, 3H), 1.68 (s, 3H), 1.60 (s, 3H), 1.59 (s, 3H), 1.29 (t, *J* = 7.0 Hz, 6H), 1.28 (t, *J* = 7.1 Hz, 6H); ^{13}C NMR (125 MHz, $CDCl_3$) δ 145.2, 143.2, 136.0, 131.6, 124.4, 123.5, 121.8, 117.3, 63.1, 63.0, 62.8, 62.7, 48.0, 39.9, 39.6, 36.7 (t, J_{CP} = 131.9 Hz), 26.9, 26.4, 25.9, 22.3 (t, J_{CP} = 5.0 Hz), 17.9, 16.7, 16.5, 16.5, 16.5, 16.4, 16.2; ^{31}P NMR (202 MHz, $CDCl_3$) δ 22.5; HRMS (ES^+, *m*/*z*) calcd for $(M+H)^+$ $C_{27}H_{50}N_3O_6P_2$: 574.3175; found: 574.3183.

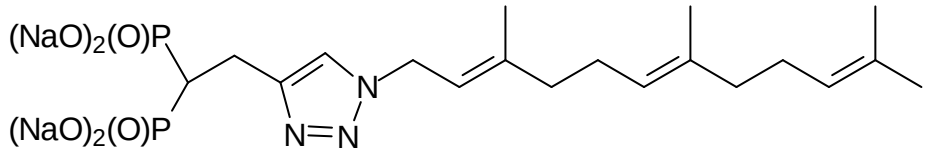

149

Sodium (2-(1-((2*E*,6*E*)-3,7,11-trimethyldodeca-2,6,10-trien-1-yl)-1H-1,2,3-triazol-4-yl)ethane-1,1-diyl)bis(phosphonate) 149. According to the procedure employed for preparation of compound **136**, bisphosphonate **148** (68 mg, 0.12 mmol) was treated with collidine (0.16 mL, 1.19 mmol) and TMSBr (0.19 mL, 1.42 mmol), and then 1N NaOH (0.95 mL, 0.95 mmol). A parallel work-up and final purification by precipitation from acetone gave the desired product **149** (18 mg, 28%): white solid; ^{1}H NMR (500 MHz, D_2O) δ 7.80 (s, 1H), 5.43 (s, 1H), 5.13–5.03 (m, 2H), 4.96 (d, J = 6.9 Hz, 2H), 3.27–3.14 (m, 2H), 2.49–2.32 (m, 1H), 2.16–1.91 (m, 8H), 1.78 (s, 3H), 1.63 (s, 3H), 1.56 (s, 6H); ^{13}C NMR (125 MHz, D_2O) δ 149.2, 143.3, 136.1, 132.4, 124.5, 123.9, 123.6, 117.3, 47.9, 39.7 (t, J_{CP} = 119.2 Hz), 39.1, 39.0, 26.1, 25.7, 25.1, 21.9 (t, J_{CP} = 2.7 Hz), 17.2, 15.8, 15.5; ^{31}P NMR (202 MHz, D_2O) δ 18.8; HRMS (ES^-, m/z) calcd for $(M-H)^-$ $C_{19}H_{32}N_3O_6P_2$: 460.1766; found: 460.1758.

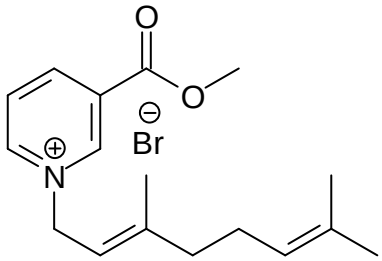

166

(*E*)-1-(3,7-Dimethylocta-2,6-dien-1-yl)-3-(methoxycarbonyl)pyridin-1-ium bromide 166. Methyl nicotinate **162** (0.765 g, 5.50 mmol) was dissolved in acetone (20.0 mL) followed by dropwise addition of geranyl bromide (3.00 g, 13.8mmol). The reaction mixture was allowed to stir overnight at rt. The resulting solid was isolated by

filtration and dried to afford a white salt in 87% yield (1.70 g): ^{1}H NMR (DMSO) δ 9.55 (d, J = 0.7 Hz, 1H), 9.22 (dd, *J* = 6.1 Hz, 1.4 Hz, 1H), 9.02–8.97 (m, 1H), 8.34–8.27 (m, 1H), 5.54 (t, *J* = 7.4 Hz, 1H), 5.41 (d, *J* = 6.9 Hz, 2H), 5.09–5.00 (m, 1H), 3.99 (d, *J* = 1.7 Hz, 3H), 2.08 (s, 4H), 1.84 (s, 3H), 1.61 (s, 3H), 1.55 (s, 3H); ^{13}C NMR (D_2O) δ 163.4, 149.2, 147.0, 145.7, 145.3, 133.8, 130.6, 128.5, 123.7, 115.1, 59.6, 53.9, 38.8, 25.4, 24.9, 17.1, 16.0.

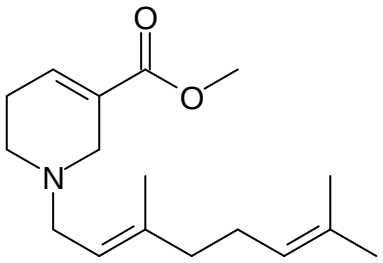

167

(*E*)-Methyl 1-(3,7-dimethylocta-2,6-dien-1-yl)-1,2,5,6-tetrahydropyridine-3-carboxylate. $NaBH_4$ (0.107 g, 2.82 mmol) was carefully added to a solution of the geranylated salt **166** (0.500 g, 1.41 mmol) in MeOH (1.6 mL)/ HOAc (0.86 mL) and allowed to react overnight. The reaction was quenched by addition of 10 mL H_2O followed by removal of MeOH under reduced pressure. The aqueous layer was washed with Et_2O twice and then treated with 5M NaOH until the pH > 10. It was then extracted with CH_2Cl_2 three times. The combined organic layer was dried (Na_2SO_4), concentrated, and purified by column chromatography (10% MeOH in CH_2Cl_2) to afford a yellow oil (23 mg, 6%): ^{1}H NMR ($CDCl_3$) δ 7.04–6.98 (m, 1H), 5.34–5.26 (m, 1H), 5.13–5.05 (m, 1H), 3.74 (s, 3H), 3.23–3.19 (m, 2H), 3.12 (d, *J* = 7.0 Hz, 2H), 2.54 (t, *J* = 5.9 Hz, 2H), 2.40–2.32 (m, 2H), 2.17–2.00 (m, 4H), 1.68 (s, 3H), 1.67 (s, 3H), 1.60 (s, 3H); ^{13}C NMR ($CDCl_3$) δ 166.6, 139.3, 138.3, 131.8, 129.2, 124.2, 120.8, 55.6, 51.8, 51.6, 48.5, 40.0, 26.8, 26.5, 25.9, 17.9, 16.6.

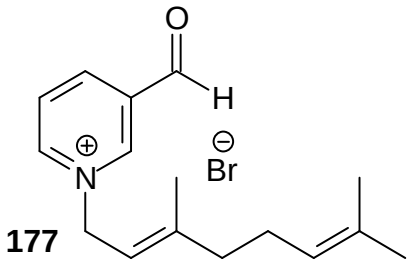

177

(*E*)-1-(3,7-Dimethylocta-2,6-dien-1-yl)-3-formylpyridin-1-ium 177. This compound was prepared from 3-pyridine carboxaldehyde (0.300 mL, 3.13 mmol) according to the general procedure given for compound **166**: yield, 57% (579 mg); yellow solid; ^{1}H NMR (D_2O) δ 8.91 (s, 1H), 8.79 (d, *J* = 6.3 Hz, 1H), 8.75 (d, *J* = 8.1 Hz, 1H), 8.10 (t, *J* = 6.9 Hz, 1H), 6.30 (s, 1H), 5.58 (t, *J* = 7.7 Hz, 1H), 5.28 (d, *J* = 7.6 Hz, 2H), 5.17 (s, 1H), 2.24 (s, 4H), 1.87 (s, 3H), 1.67 (s, 3H), 1.61 (s, 3H).

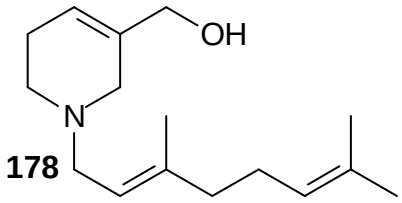

178

(*E*)-(1-(3,7-Dimethylocta-2,6-dien-1-yl)-1,2,5,6-tetrahydropyridin-3-yl)methanol 178. This compound was prepared from aldehyde **177** (2.14 g, 6.61 mmol) according to the general procedure given for compound **167**: yield, 75% (1.23 g); colorless oil; ^{1}H NMR ($CDCl_3$) δ 5.72–5.66 (m, 1H), 5.35–5.27 (m, 1H), 5.13–5.05 (m, 1H), 3.97 (s, 2H), 3.08 (d, *J* = 6.9 Hz, 2H), 2.99 (d, *J* = 1.8 Hz, 2H), 2.53 (t, *J* = 5.8 Hz, 2H), 2.25–2.15 (m, 2H), 2.15–2.00 (m, 4H), 1.67 (s, 3H), 1.65 (s, 3H), 1.60 (s, 3H); ^{13}C NMR ($CDCl_3$) δ 139.1, 137.0, 131.6, 124.3, 121.1, 120.7, 65.4, 55.8, 53.0, 49.6, 40.0, 26.7, 25.8, 25.8, 17.8, 16.6; HRMS (ES^+, *m*/*z*) calcd for $(M+H)^+$ $C_{16}H_{28}NO$: 250.2171; found: 250.2175.

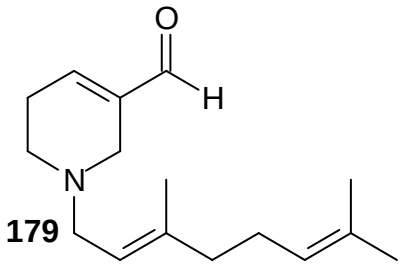

179

(*E*)-1-(3,7-Dimethylocta-2,6-dien-1-yl)-1,2,5,6-tetrahydropyridine-3-carbaldehyde 179. MnO_2 (430 mg, 4.40 mmol) was added to a solution of alcohol **178** (110 mg, 0.440 mmol) in CH_2Cl_2 (4.00 mL) and the mixture was allowed to stir overnight at rt. It was then filtered through celite which was washed extensively with CH_2Cl_2 (500 mL). The resulting organic layer was dried under reduced pressure and the residue was purified by column chromatography (10% MeOH in CH_2Cl_2) to afford a yellow oil (37 mg, 34%): ^{1}H NMR ($CDCl_3$) δ 9.43 (s, 1H), 6.88–6.84 (m, 1H), 5.33–5.25 (m, 1H), 5.13–5.04 (m, 1H), 3.20–3.16 (m, 2H), 3.13 (d, *J* = 6.8 Hz, 2H), 2.61 (t, *J* = 5.1 Hz, 2H), 2.55–2.46 (m, 2H), 2.16–2.00 (m, 4H), 1.68 (s, 3H), 1.67 (s, 3H), 1.60 (s, 3H); ^{13}C NMR ($CDCl_3$) δ 192.8, 149.1, 140.8, 139.8, 132.1, 124.5, 120.8, 55.9, 49.5, 49.4, 40.2, 27.9, 26.8, 26.2, 18.1, 16.9; HRMS (ES^+, *m*/*z*) calcd for $(M+H)^+$ $C_{16}H_{26}NO$: 248.2014; found: 248.2034.

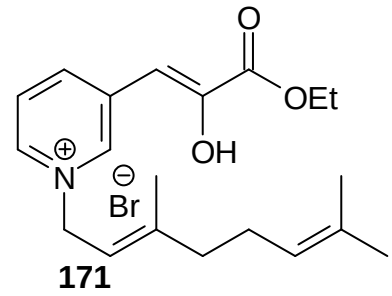

171

1-((*E*)-3,7-Dimethylocta-2,6-dien-1-yl)-3-((*Z*)-3-ethoxy-2-hydroxy-3-oxoprop-1-en-1-yl)pyridin-1-ium bromide 171. Geranyl bromide (440 mg, 2.03 mmol) was

added to a solution of pyridine **160** (157 mg, 0.81 mmol) in acetone (3 mL) and the reaction mixture was allowed to stir at rt overnight. The resulting precipitate was isolated by filtration and washed with acetone. The salt **171** was obtained in 58% yield (193 mg) as a white powder: ^{1}H NMR (DMSO-ds) δ 11.14 (s, 1H), 9.25 (s, 1H), 8.89–8.80 (m, 2H), 8.15–8.08 (m, 1H), 6.59 (s, 1H), 5.52 (t, *J* = 7.1 Hz, 1H), 5.25 (d, *J* = 7.7 Hz, 2H), 5.08–5.00 (m, 1H), 4.32 (q, *J* = 6.7 Hz, 2H), 2.13–2.06 (m, 4H), 1.84 (s, 3H), 1.59 (s, 3H), 1.54 (s, 3H), 1.31 (t, *J* = 6.9 Hz, 3H); ^{13}C NMR (DMSO-ds) δ 163.4, 146.7, 145.8, 143.5, 141.7, 141.4, 135.3, 131.4, 127.9, 123.6, 116.9, 102.8, 62.2, 58.4, 25.6, 25.5, 17.7 (2C), 16.6, 14.1.

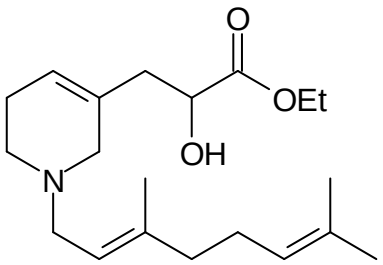

172

(*E*)-Ethyl 3-(1-(3,7-dimethylocta-2,6-dien-1-yl)-1,2,5,6-tetrahydropyridin-3-yl)-2-hydroxypropanoate 172. Salt **171** (180 mg, 0.44 mol) was dissolved in MeOH (3 mL) in a salt-ice bath followed by slow addition of $NaBH_4$ (50 mg, 1.3 mmol). After it was allowed to react overnight, water was added to quench the reaction. The MeOH was removed *in vacuo* and the remaining aqueous layer was extracted with CH_2Cl_2 three times. The combined organic layer was then dried over Na_2SO_4 and concentrated *in vacuo*. The resulting residue was purified by column chromatography (10% MeOH in CH_2Cl_2) to afford the desired product as a yellow oil (89 mg, 60%): ^{1}H NMR ($CDCl_3$) δ 5.60 (s, 1H), 5.30 (t, *J* = 6.8 Hz, 1H), 5.12–5.02 (m, 1H), 4.29–4.17 (m, 3H), 3.09 (d, *J* = 6.7 Hz, 2H), 2.98 (s, 2H), 2.55 (t, *J* = 5.6 Hz, 2H), 2.52–2.24 (m, 2H), 2.19 (s, 2H), 2.14–

2.06 (m, 4H), 1.67 (s, 3H), 1.65 (s, 3H), 1.60 (s, 3H), 1.30 (t, J = 6.6 Hz, 3H); ^{13}C NMR ($CDCl_3$) δ 174.6, 139.3, 131.7, 131.6, 124.1, 123.3, 120.4, 69.6, 61.5, 55.5 (2C), 49.0, 40.7, 39.9, 26.5, 25.9, 25.8, 17.8, 16.5, 14.3; HRMS (ES^+, m/z) calcd for $(M+H)^+$ $C_{20}H_{34}NO_3$: 336.2539; found: 336.2530.

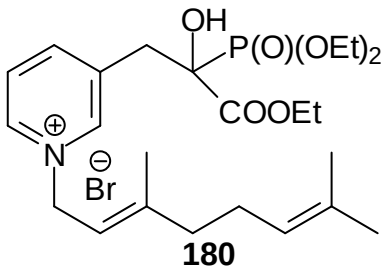

180

(*E*)-3-(2-(Diethoxyphosphoryl)-3-ethoxy-2-hydroxy-3-oxopropyl)-1-(3,7-dimethylocta-2,6-dien-1-yl)pyridin-1-ium bromide 180. Geranyl bromide (0.500 g, 2.26 mmol) was added to a solution of compound **161** (300 mg, 0.9 mmol) in CH_2Cl_2 (5 mL) and the reaction mixture was gently heated to reflux and stirred overnight. Then the volatile materials were removed in *vacuo* to give the desired product as a yellow oil in 87% yield (0.429 g): ^{1}H NMR ($CDCl_3$) δ 9.33 (d, J = 5.7 Hz, 1H), 9.18 (s, 1H), 8.45 (d, J = 8.0 Hz, 1H), 8.12 (t, J = 6.1 Hz, 1H), 5.51–5.43 (m, 3H), 5.05 (s, 1H), 4.33–3.14 (m, 6H), 3.75–3.53 (m, 2H), 2.16–2.10 (m, 4H), 1.92 (s, 3H), 1.67 (s, 3H), 1.59 (s, 3H), 1.38–1.25 (m, 9H); ^{13}C NMR ($CDCl_3$) δ 169.5 (d, J_{CP} = 2.6 Hz), 148.1, 147.0, 145.2, 142.8, 136.5 (d, J_{CP} = 12.6 Hz), 132.1, 127.5, 122.9, 115.4, 77.1 (d, J_{CP} = 159.9 Hz), 64.3 (d, J_{CP} = 2.3 Hz), 64.2 (d, J_{CP} = 1.4 Hz), 63.0, 53.5, 39.3, 36.7, 25.8, 25.5, 17.5, 17.1, 16.3 (d, J_{CP} = 5.4 Hz), 16.3 (d, J_{CP} = 5.6 Hz), 14.0; ^{31}P NMR ($CDCl_3$) δ 15.6; HRMS (ES^+, m/z) calcd for $(M-Br)^+$ $C_{24}H_{39}NO_6P$: 468.2515; found: 468.2530.

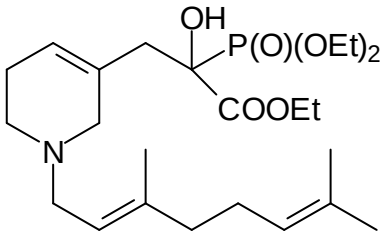

181

(*E*)-Ethyl 2-(diethoxyphosphoryl)-3-(1-(3,7-dimethylocta-2,6-dien-1-yl)-1,2,5,6-tetrahydropyridin-3-yl)-2-hydroxypropanoate 181. $NaBH_4$ (110 mg, 3 mmol) was carefully added to a solution of bromide salt **180** (110 mg, 0.2 mmol) in MeOH (3 mL)/ HOAc (0.3 mL) and the solution was allowed to react overnight. The reaction was quenched by addition of 10 mL 1% HOAc solution followed by extraction with EtOAc three times. The combined organic layer was dried (Na_2SO_4), concentrated, and purified by column chromatography (10% MeOH in CH_2Cl_2) to afford reduced pyridine **181** as a yellow oil (51 mg, 34%); ^{1}H NMR ($CDCl_3$) δ 5.31 (s, 1H), 5.01 (t, *J* = 6.7 Hz, 1H), 4.80 (t, *J* = 6.9 Hz, 1H), 4.10–3.85 (m, 6H), 2.82–2.06 (m, 8H), 2.00–1.66 (m, 6H), 1.39 (s, 3H), 1.36 (s, 3H), 1.32 (s, 3H), 1.10–1.02 (m, 9H); ^{31}P NMR ($CDCl_3$) δ 17.1.

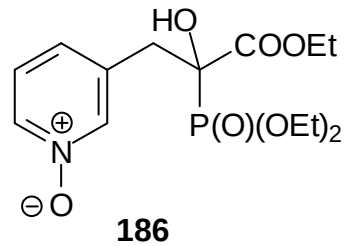

186

3-(2-(Diethoxyphosphoryl)-3-ethoxy-2-hydroxy-3-oxopropyl)pyridine 1-oxide 186. Solid *m*CPBA (210 mg, 0.930 mmol) was added to a solution of the 3-PEHPC ester **161** (206 mg, 0.620 mmol) in CH_2Cl_2 (3 mL) and the solution was allowed to react at room temperature overnight. The reaction solvent was then removed under vacuum and the resulting residue was purified by column chromatography (15% EtOH in CH_2Cl_2) to

afford the desired product as a light yellow oil (215 mg, 74%): ^{1}H NMR ($CDCl_3$) δ 8.22 (s, 1H), 8.14 (d, J = 6.4 Hz, 1H), 7.29–7.16 (m, 2H), 4.93 (s, 1H), 4.33–4.18 (m, 6H), 3.38–3.16 (m, 2H), 1.41–1.24 (m, 9H); ^{13}C NMR ($CDCl_3$) δ 170.2 (d, J_{CP} = 3.7 Hz), 140.6, 137.8, 134.3, 128.7, 125.1, 77.3 (d, J_{CP} = 160.1 Hz), 64.2 (d, J_{CP} = 7.4 Hz), 64.1 (d, J_{CP} = 7.3 Hz), 63.1, 36.7 (d, J_{CP} = 2.3 Hz), 16.4 (d, J_{CP} = 6.3 Hz), 16.4 (d, J_{CP} = 5.9 Hz), 14.1; ^{31}P NMR ($CDCl_3$) δ 16.3; HRMS (ES^+, m/z) calcd for $(M+H)^+$ $C_{14}H_{23}NO_7P_2$: 348.1212; found: 348.1214.

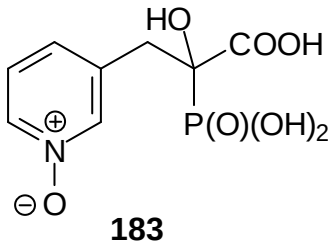

183

3-(2-Carboxy-2-hydroxy-2-phosphonoethyl)pyridine 1-oxide 183. The *N*-oxide **186** (160 mg, 0.460 mmol) was dissolved in concentrated HCl (1.60 mL) and the solution was heated at reflux overnight. After concentration under a stream of air, the resulting residue was dissolved in a minimum amount of hot water followed by the addition of acetone. This solution turned cloudy and a white solid was formed. After standing at -4 °C overnight, the resulting solid was isolated by filtration and dissolved in hot water. A white solid salt was formed upon removal of water with a lyophilizer (121 mg, 14%): ^{1}H NMR (D_2O): δ 8.39 (s, 1H), 8.36 (d, J = 6.6 Hz, 1H), 7.85 (d, J = 7.8 Hz, 1H), 7.65 (dd, J = 7.9 Hz, 6.7 Hz, 1H), 3.57 (dd, J = 14.0 Hz, J_{HP} = 4.3 Hz, 1H), 3.26 (dd, J = 13.7 Hz, J_{HP} = 7.4 Hz, 1H); ^{13}C NMR (D_2O) δ 174.2, 139.7, 137.5, 136.5, 136.3, 126.7, 77.5 (d, J_{CP} = 149.5 Hz), 37.0; ^{31}P NMR (D_2O) δ 13.3; HRMS (ES^-, m/z) calcd for $(M-H)^-$ $C_8H_9NO_7P$: 262.0117; found: 262.0112.

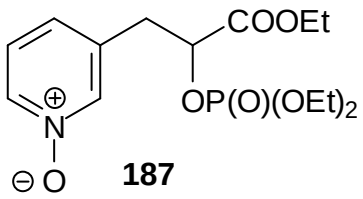

187

3-(2-((Diethoxyphosphoryl)oxy)-3-ethoxy-3-oxopropyl)pyridine 1-oxide 187. A solution of the *N*-oxide **186** (13.8 mg, 0.0396 mmol) in EtOAc was washed with saturated Na_2CO_3 and the aqueous layer was extracted with EtOAc three times. The combined organic layer was dried and concentrated to obtain the desired product as a colorless oil (13.8 mg, 100%); ^{1}H NMR (D_2O) δ 8.16–8.10 (m, 2H), 7.24–7.20 (m, 2H), 5.07–4.98 (m, 1H), 4.24 (q, J = 7.0 Hz, 2H), 4.21–3.96 (m, 4H), 3.25–3.04 (m, 2H), 1.36–1.25 (m, 9H); ^{13}C NMR (D_2O) δ 168.8 (d, J_{CP} = 3.7 Hz), 140.3, 138.2, 135.2, 127.3, 125.8, 74.6 (d, J_{CP} = 5.6 Hz), 64.7 (d, J_{CP} = 6.1 Hz), 64.5 (d, J_{CP} = 5.9 Hz), 62.3, 36.2 (d, J_{CP} = 6.0 Hz), 16.3 (d, J_{CP} = 1.7 Hz), 16.2 (d, J_{CP} = 2.4 Hz), 14.3; ^{31}P NMR (D_2O) δ -1.9.

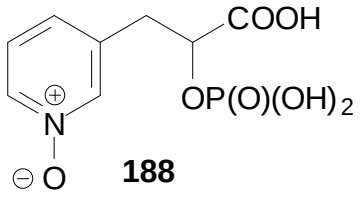

188

3-(2-Carboxy-2-(phosphonooxy)ethyl)pyridine 1-oxide 188. This compound was prepared according to the general procedure given for compound **183**: ^{31}P NMR (D_2O) δ 0.35.

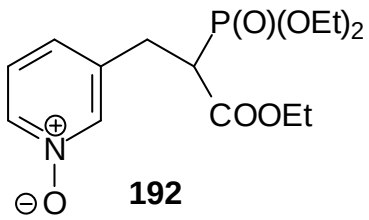

192

3-(2-(Diethoxyphosphoryl)-3-ethoxy-3-oxopropyl)pyridine 1-oxide 192. Solid *m*CPBA (0.21 g, 0.95 mmol) was added to a solution of compound **191** (200 mg, 0.63 mmol) in CH_2Cl_2 (3.0 mL) and the resulting solution was allowed to stir overnight at room temperature. Once the reaction was complete based on TLC analysis, the solvent was removed under vacuum. The resulting residue was purified by column chromatography (15% EtOH in CH_2Cl_2) to afford the desired product as a yellow oil in 71% yield (150 mg): ^{1}H NMR ($CDCl_3$) δ 7.97–7.89 (m, 2H), 7.08–6.96 (m, 2H), 4.06–3.89 (m, 6H), 3.12–2.88 (m, 3H), 1.16 (t, J = 7 Hz, 3H), 1.15 (t, J = 6.6 Hz, 3H), 1.02 (t, J = 7.5 Hz, 3H); ^{13}C NMR ($CDCl_3$) δ 167.4 (d, J_{CP} = 5.0 Hz), 139.2, 137.9 (d, J_{CP} = 15.5 Hz), 137.5, 126.4, 125.6, 63.0 (d, J_{CP} = 6.8 Hz), 62.9 (d, J_{CP} = 6.4 Hz), 61.6, 46.3 (d, J_{CP} = 129.7 Hz), 29.5 (d, J_{CP} = 3.8 Hz), 16.2 (d, J_{CP} = 1.4 Hz), 16.1 (d, J_{CP} = 2.3 Hz), 13.8; ^{31}P NMR ($CDCl_3$) δ 20.1 ppm; HRMS (ES^+, *m*/*z*) calcd for $(M+H)^+$ $C_{14}H_{23}NO_6P$: 332.1263; found: 332.1269.

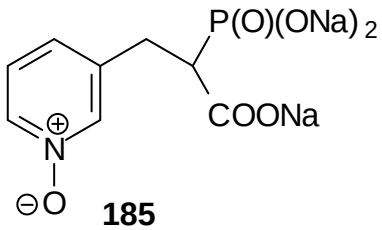

185

Sodium 3-(1-oxidopyridin-3-yl)-2-phosphonatopropanoate 185. The ethyl ester **192** (100 mg, 3.02 mmol) was heated at reflux with concentrated HCl (1 mL) overnight. Once the reaction was complete based on analysis of the ^{31}P NMR spectrum of the reaction mixture, the volatiles were removed under a stream of air. The resulting residue was dissolved in a minimum amount of NaOH (0.36 g, 9.06 mmol), acetone was added and the cloudy solution was cooled in a freezer overnight. The precipitate was then isolated by filtration, the solid was dissolved in water, treated with charcoal and the

charcoal was further removed by filtration. The resulting clear solution was dried on a lyophilizer to afford the desire product as a white solid in 97% yield (90 mg): ^{1}H NMR (D_2O) δ 8.23 (s, 1H), 8.15 (d, *J* = 6.2 Hz, 1H), 7.67 (d, *J* = 7.9 Hz, 1H), 7.51 (dd, *J* = 7.8, 6.7 Hz, 1H), 3.18–3.02 (m, 2H), 2.89–2.73 (m, 1H); ^{13}C NMR (D_2O) δ 179.8, 142.9 (d, J_{CP} = 17.1 Hz), 138.5, 136.5, 132.9, 126.7, 53.3 (d, J_{CP} = 112.4 Hz), 32.4 (d, J_{CP} = 3.1 Hz); ^{31}P NMR (D_2O) δ 15.1 ppm; HRMS (ES^-, *m*/*z*) calcd for $(M-H)^-$ $C_8H_9NO_6P$: 246.0168; found: 246.0170.

APPENDIX
SELECTED NMR SPECTRA

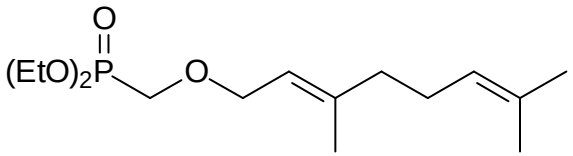

59

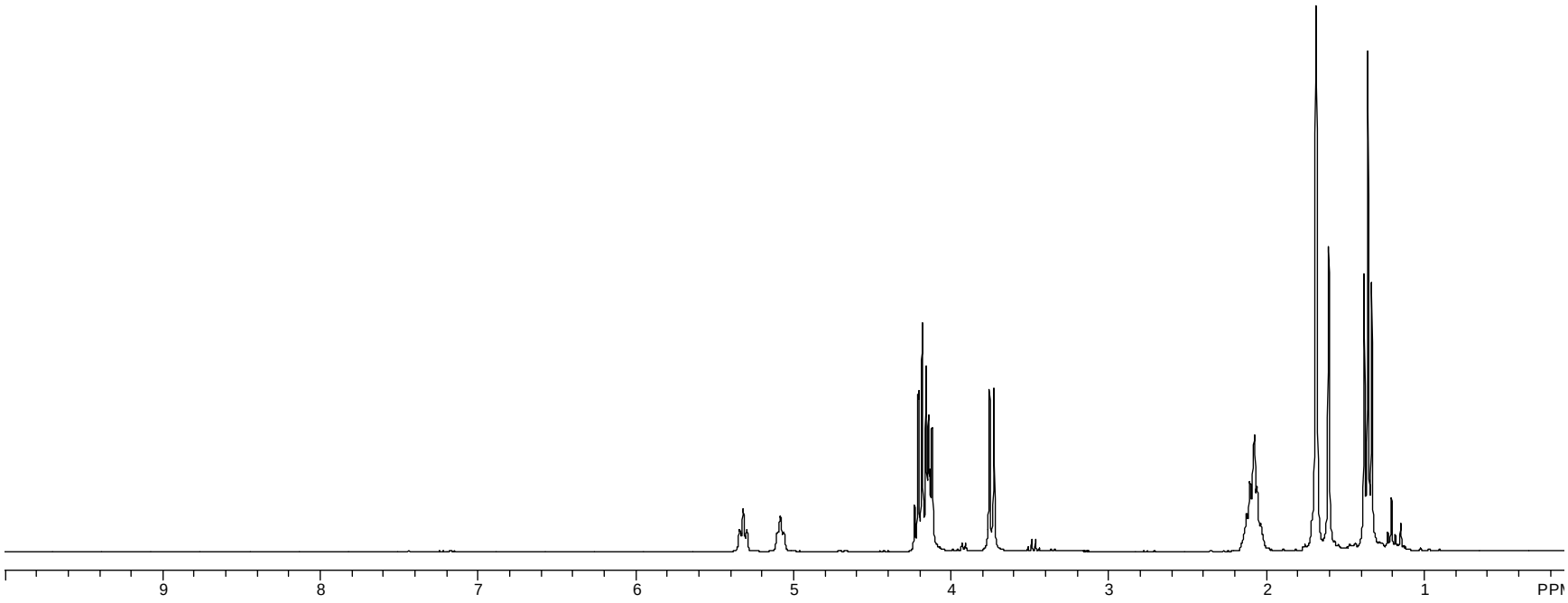

Figure A1. 300 MHz ^{1}H NMR Spectrum of Compound **59**.

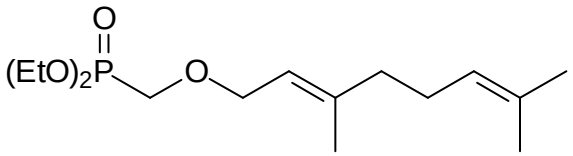

59

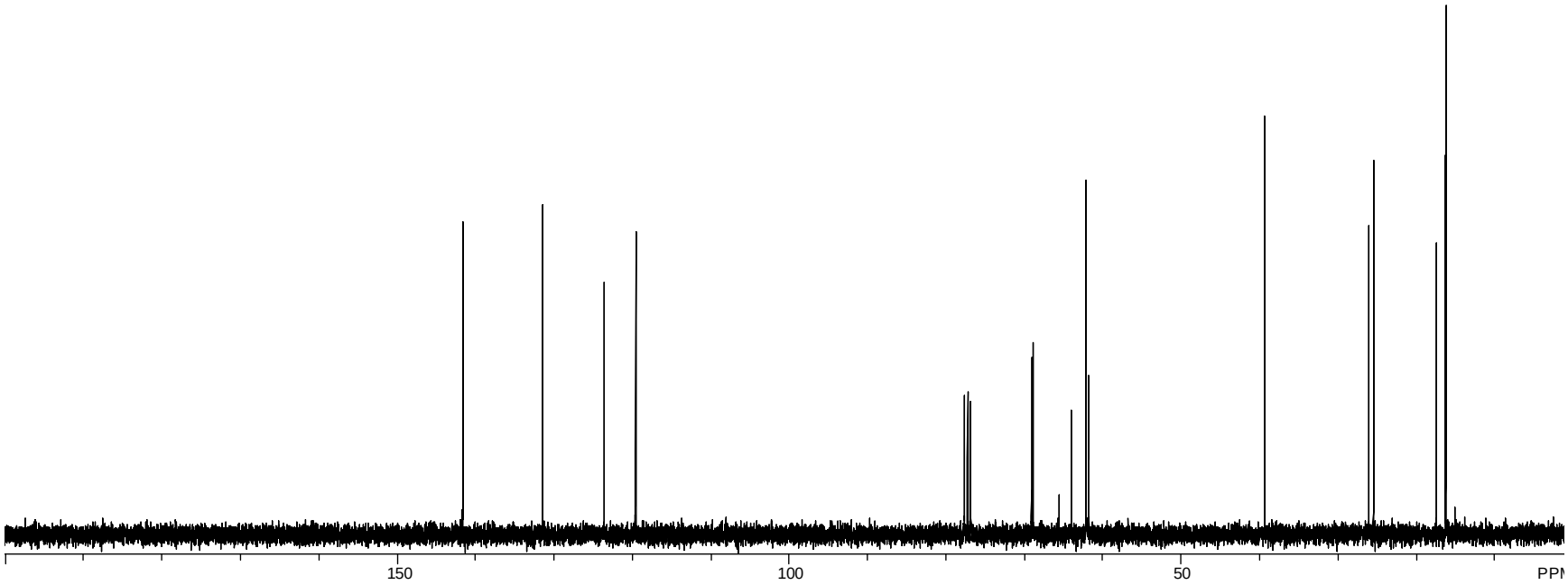

Figure A2. 75 MHz ^{13}C NMR Spectrum of Compound **59**.

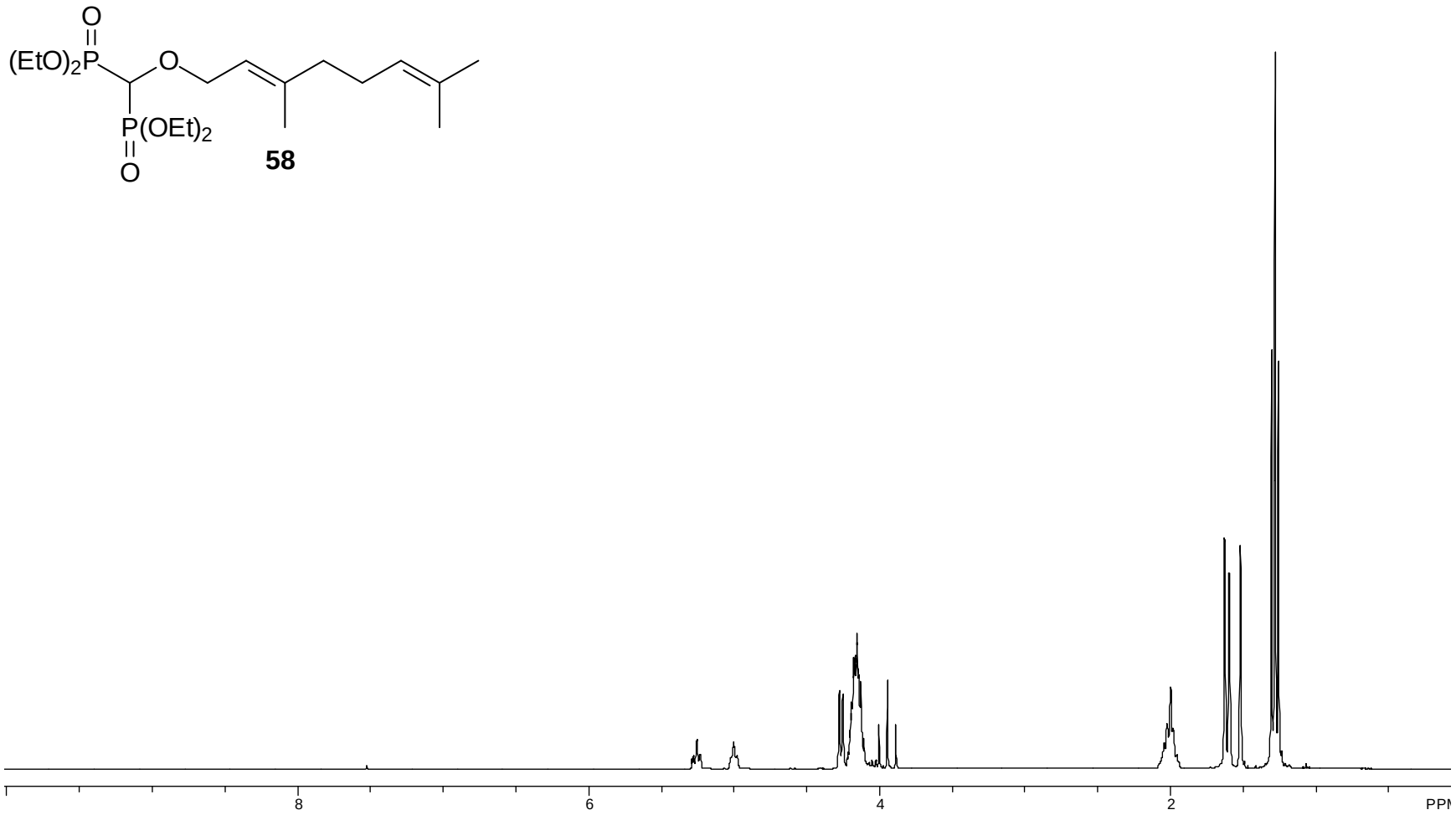

Figure A3. 300 MHz ^{1}H NMR Spectrum of Compound **58**.

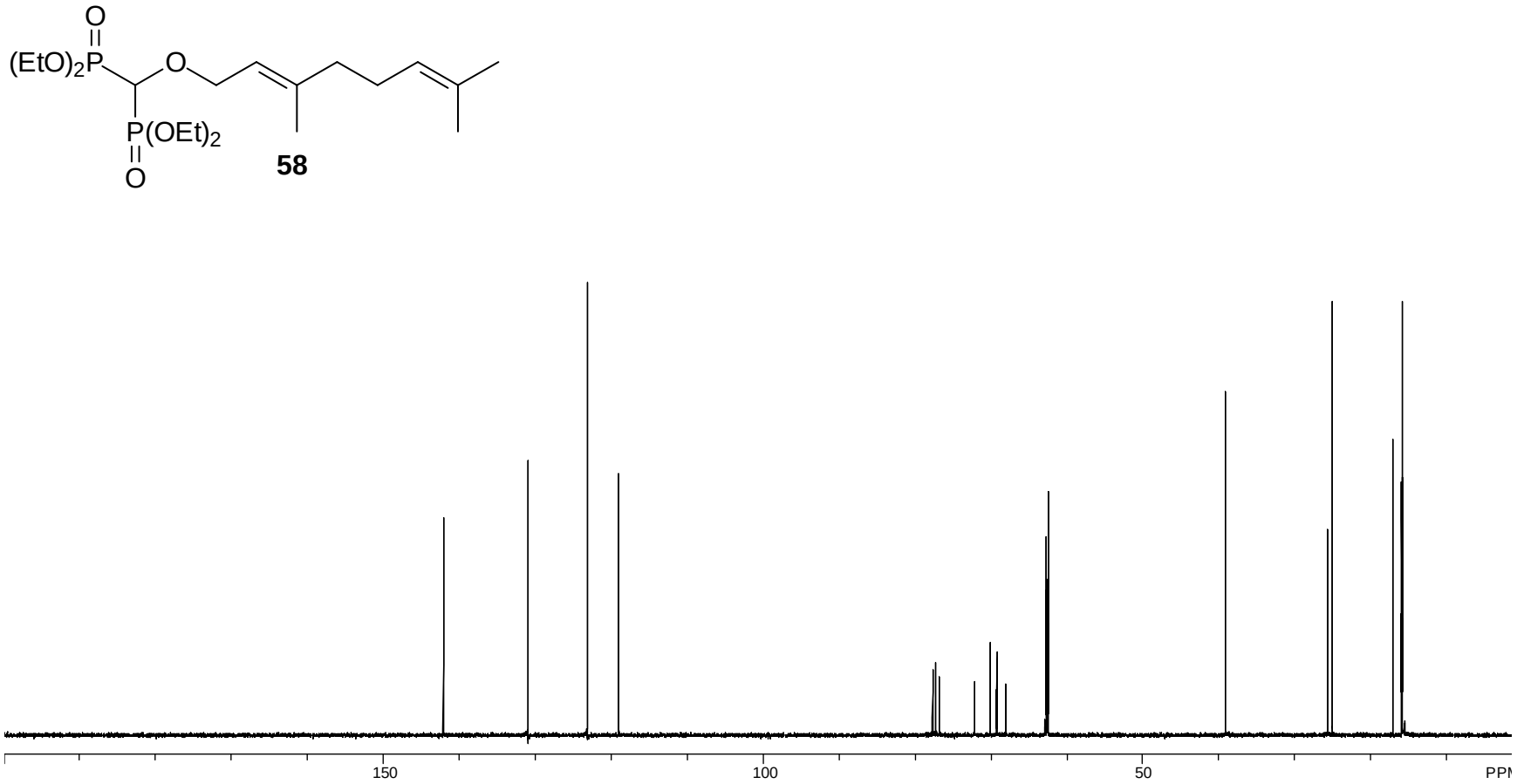

Figure A4. 75 MHz ^{13}C NMR Spectrum of Compound **58**.

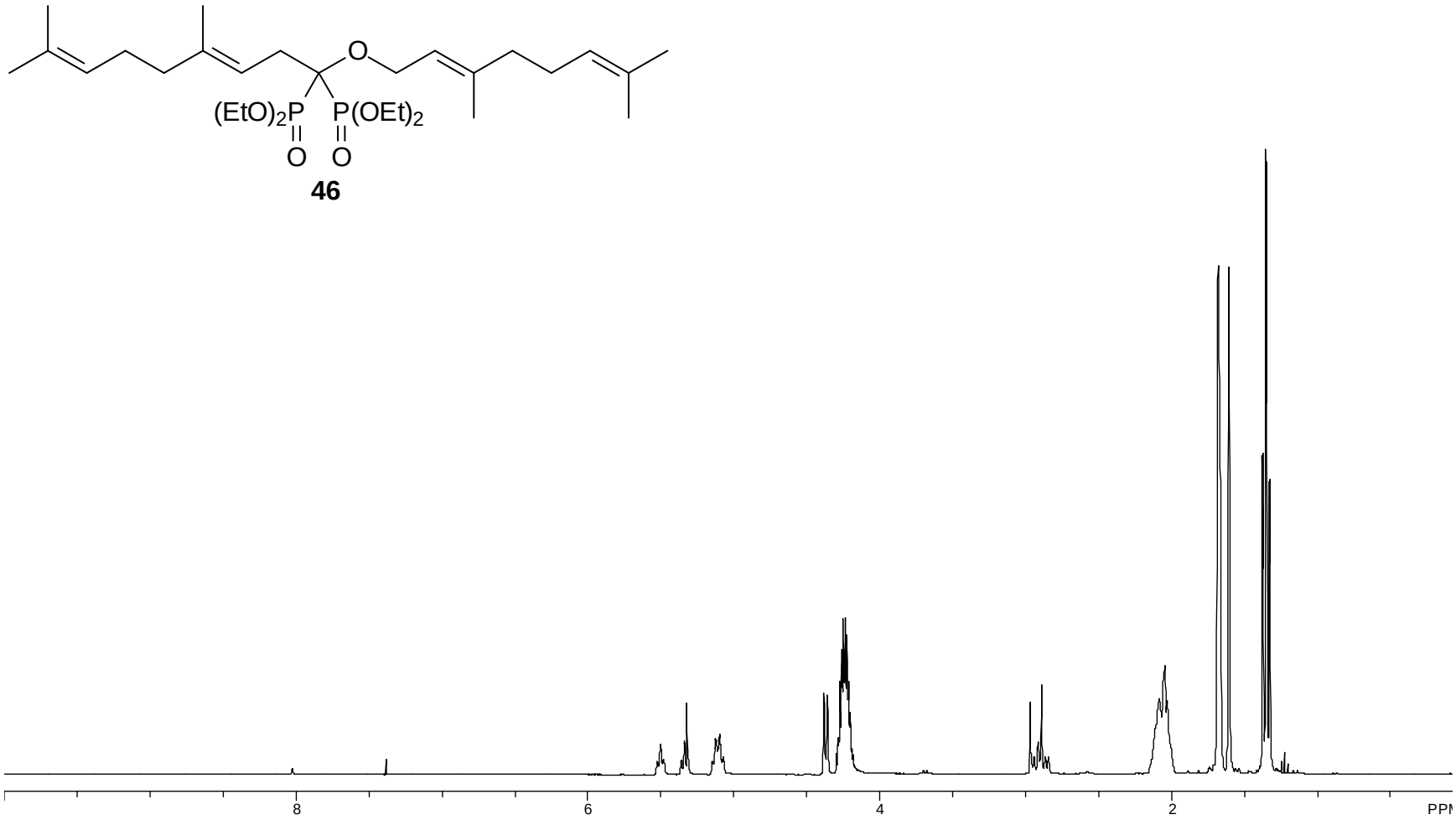

Figure A5. 300 MHz ^{1}H NMR Spectrum of Compound **46**.

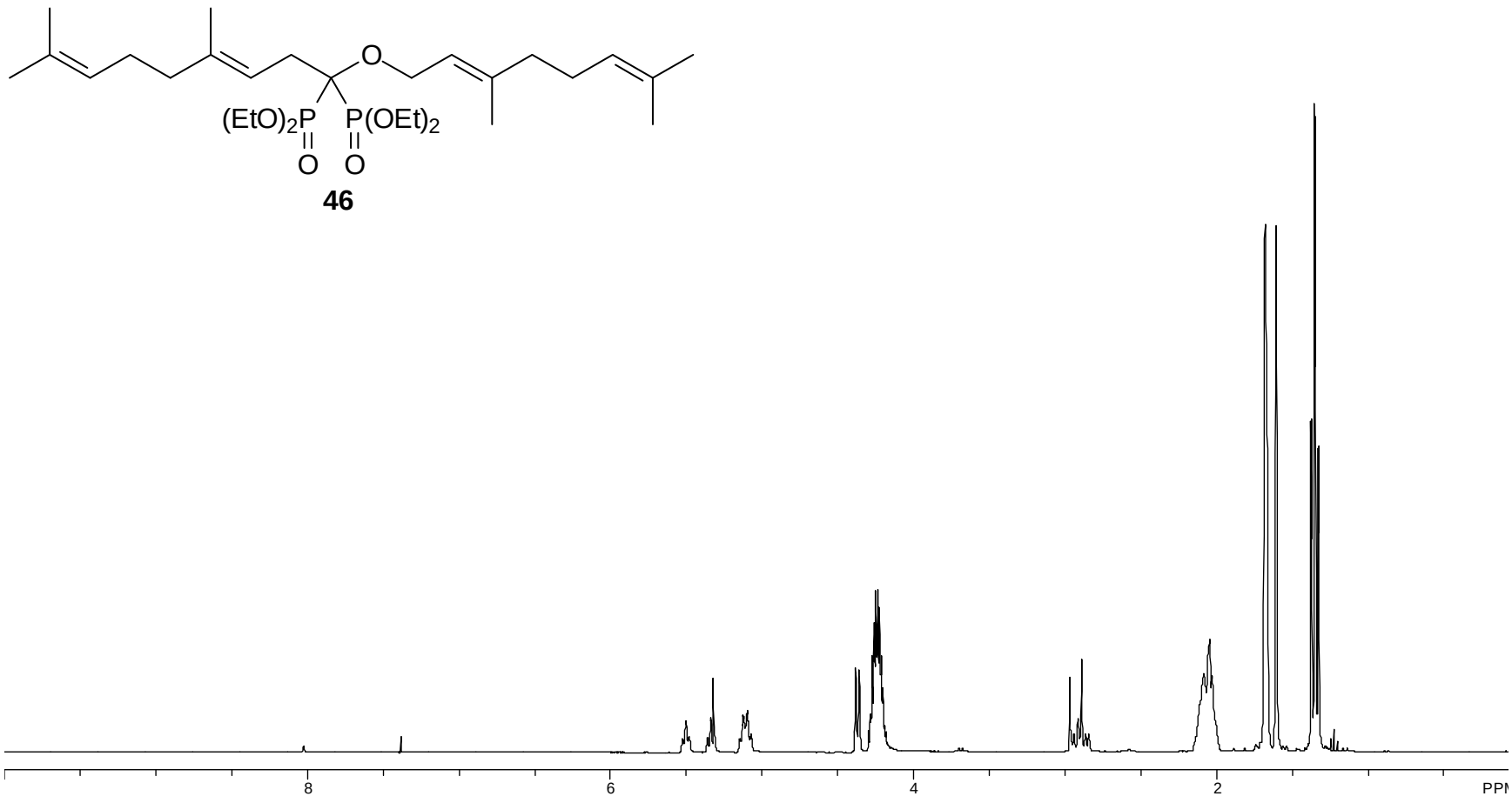

46

Figure A6. 300 MHz ^{1}H NMR Spectrum of Compound **46**.

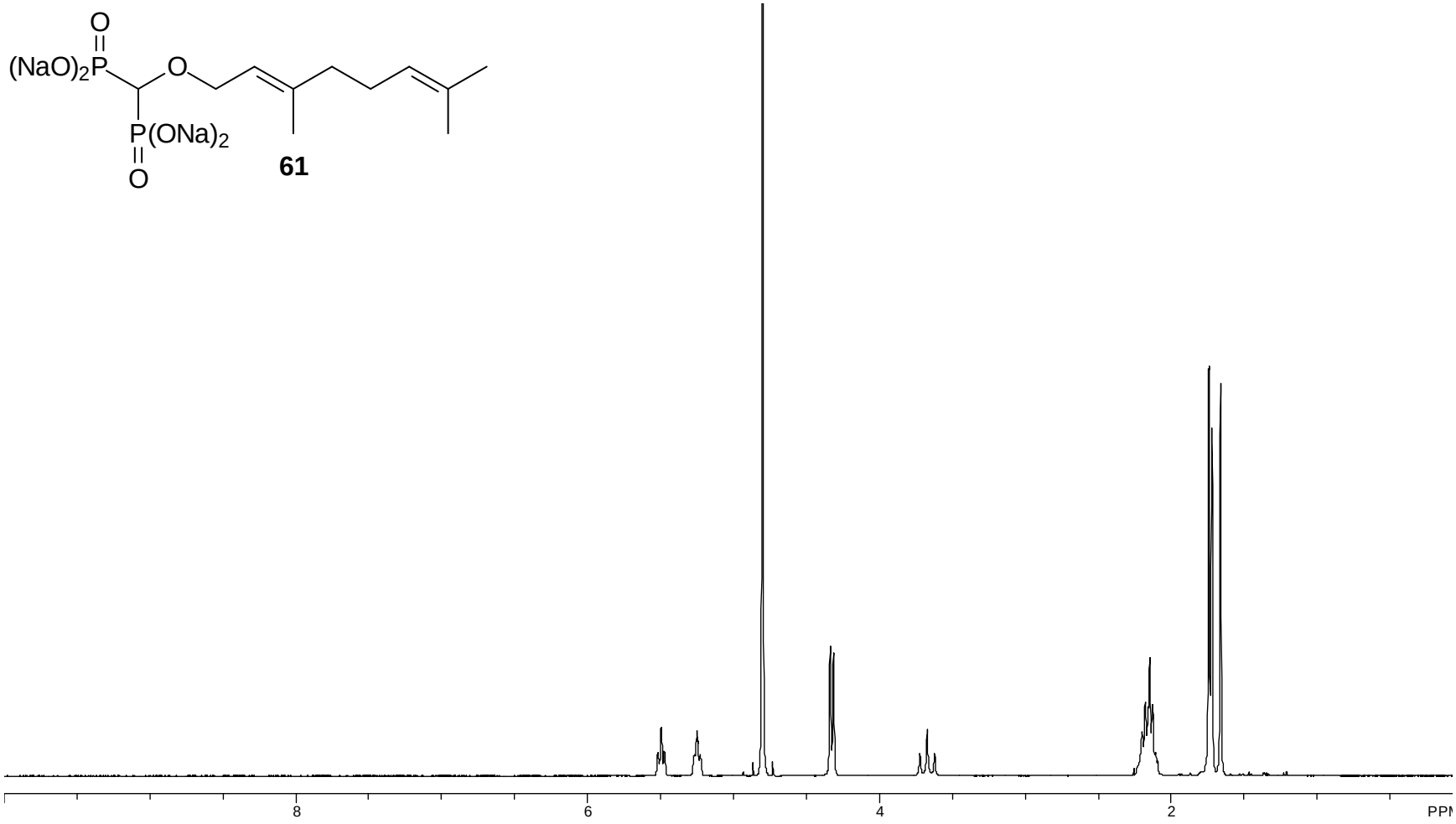

Figure A7. 300 MHz ^{1}H NMR Spectrum of Compound **61**.

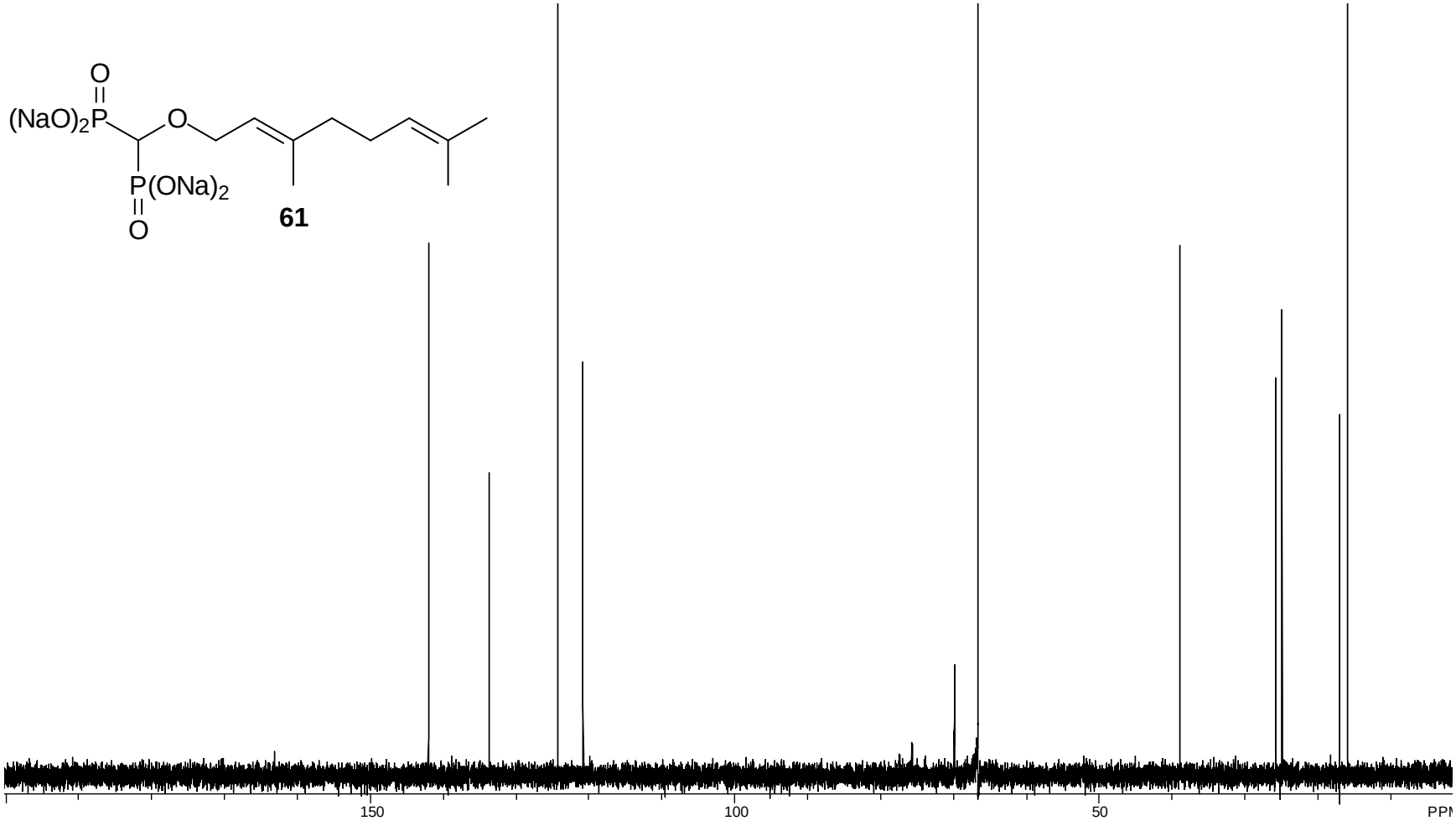

Figure A8. 75 MHz ^{1}H NMR Spectrum of Compound **61**.

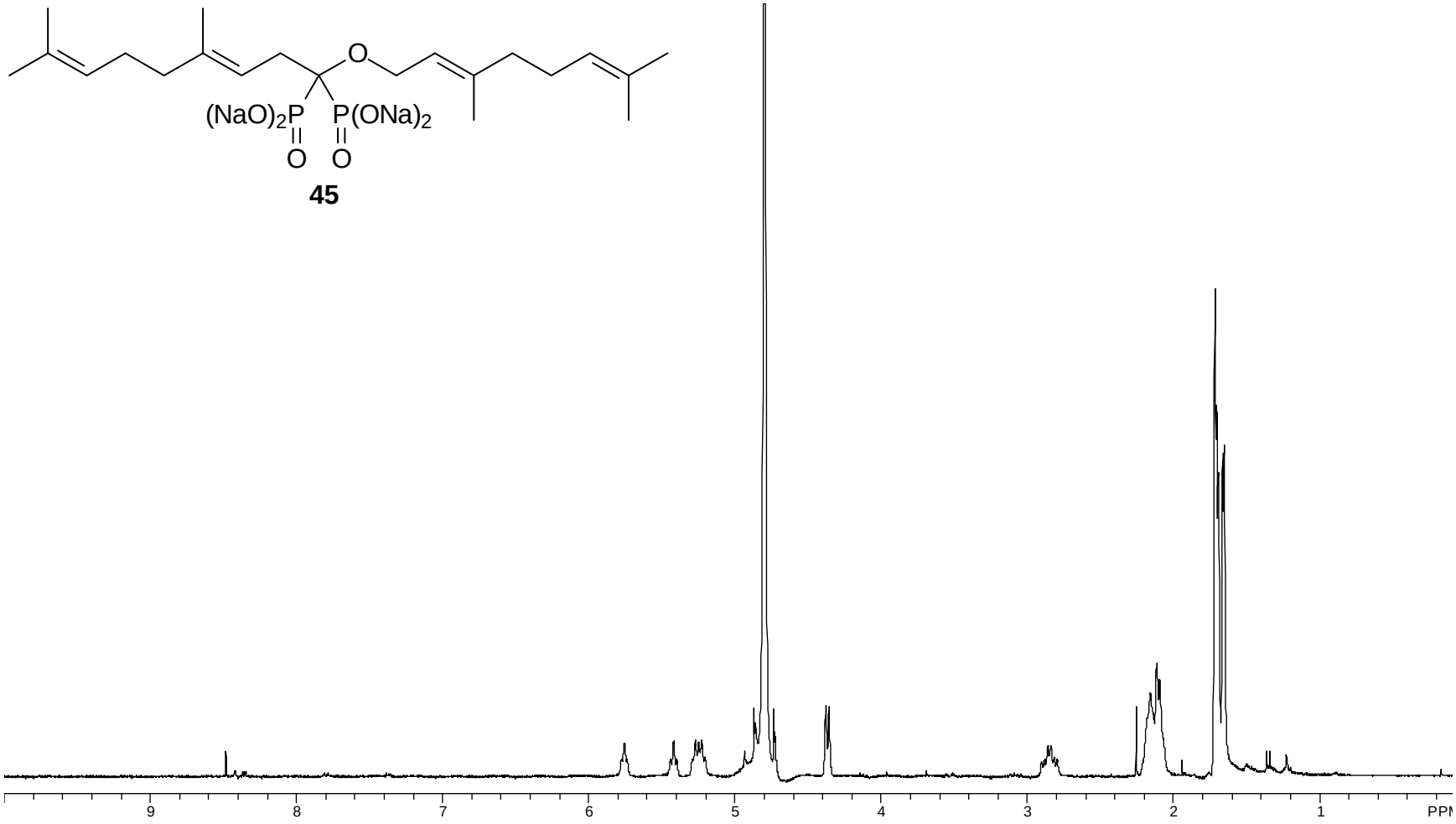

Figure A9. 300 MHz ^{1}H NMR Spectrum of Compound **45**.

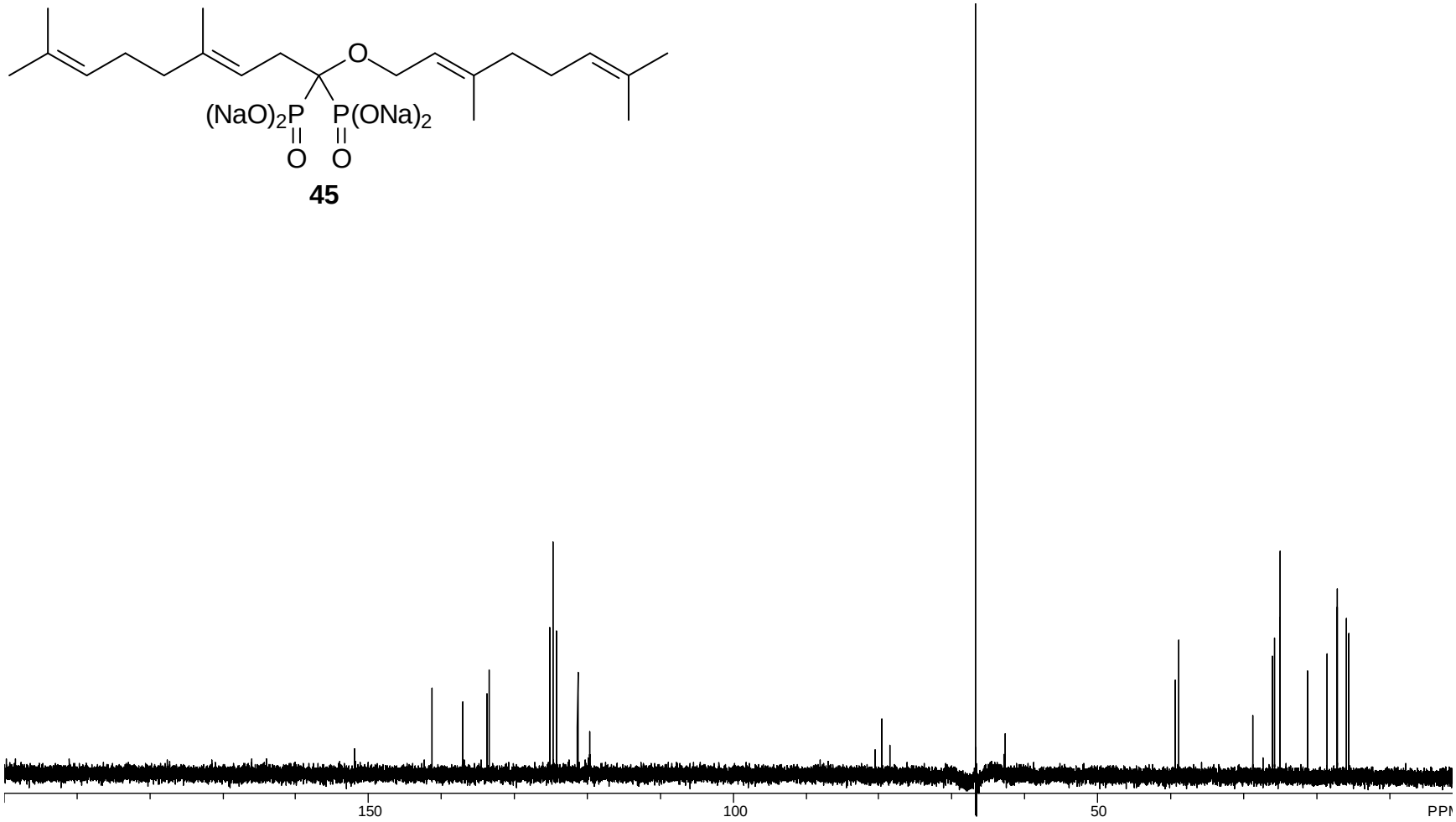

Figure A10. 125 MHz ^{13}C NMR Spectrum of Compound **45**.

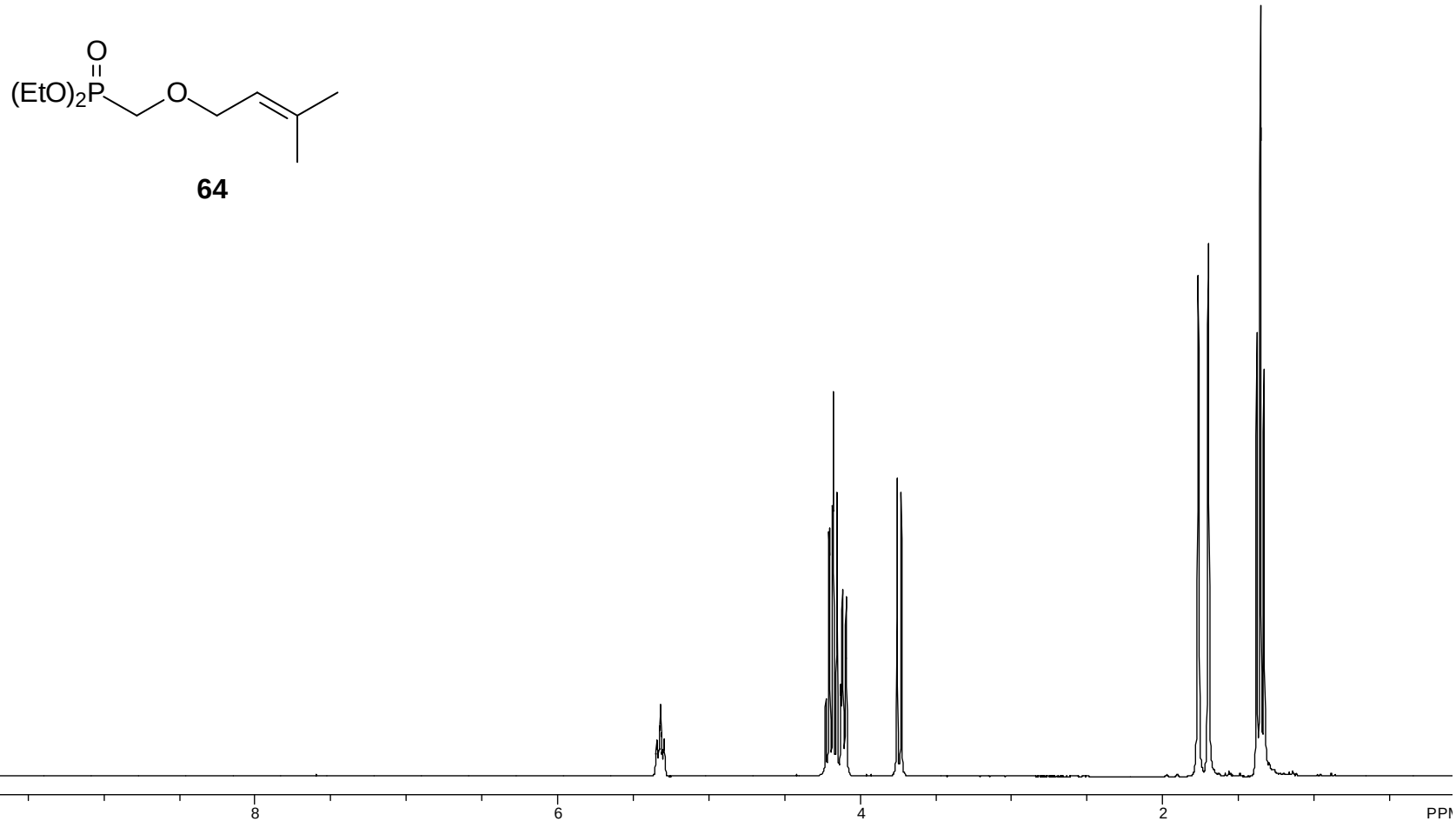

Figure A11. 300 MHz ^{1}H NMR Spectrum of Compound **64**.

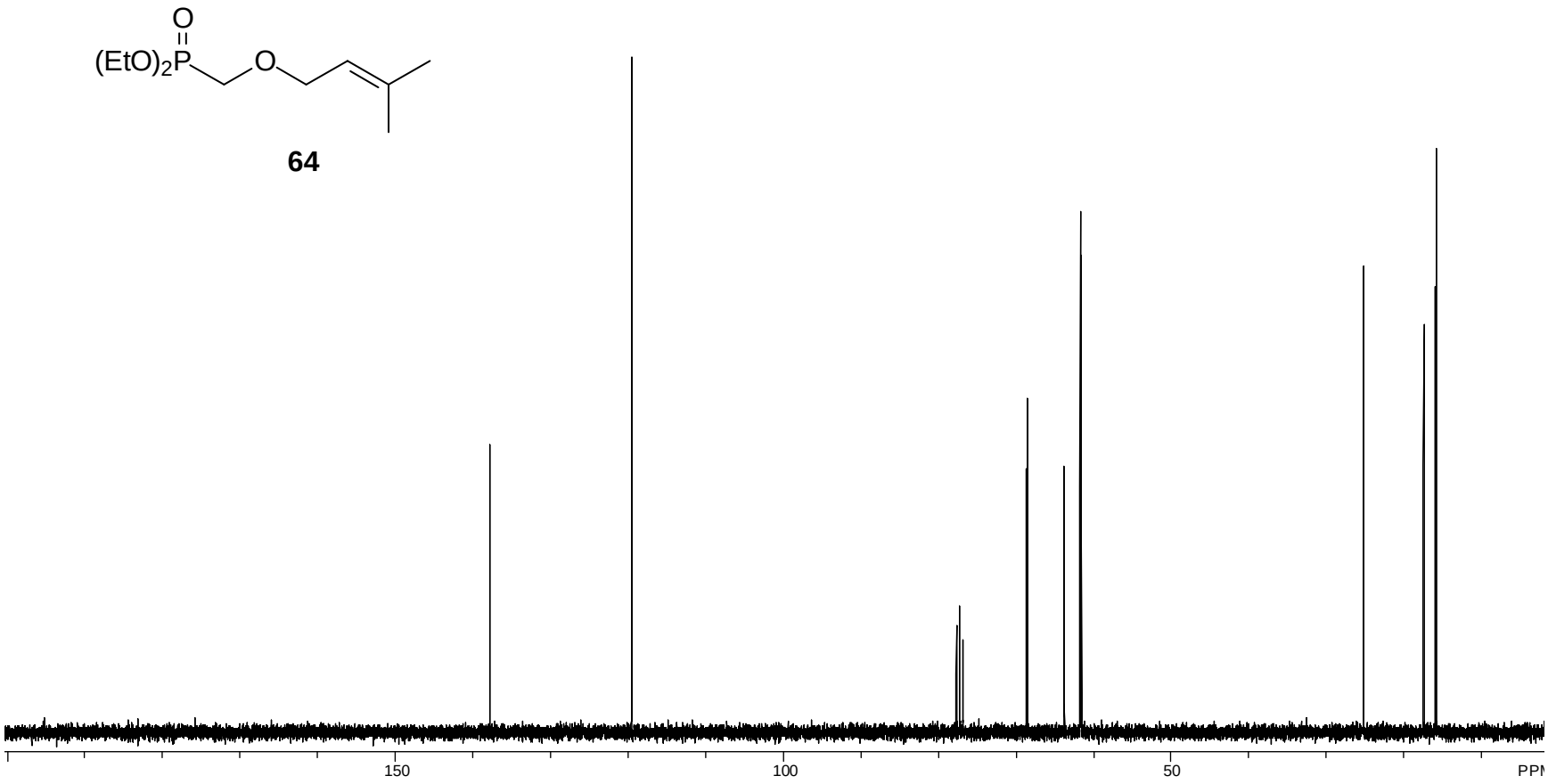

Figure A12. 75 MHz ^{13}C NMR Spectrum of Compound **64**.

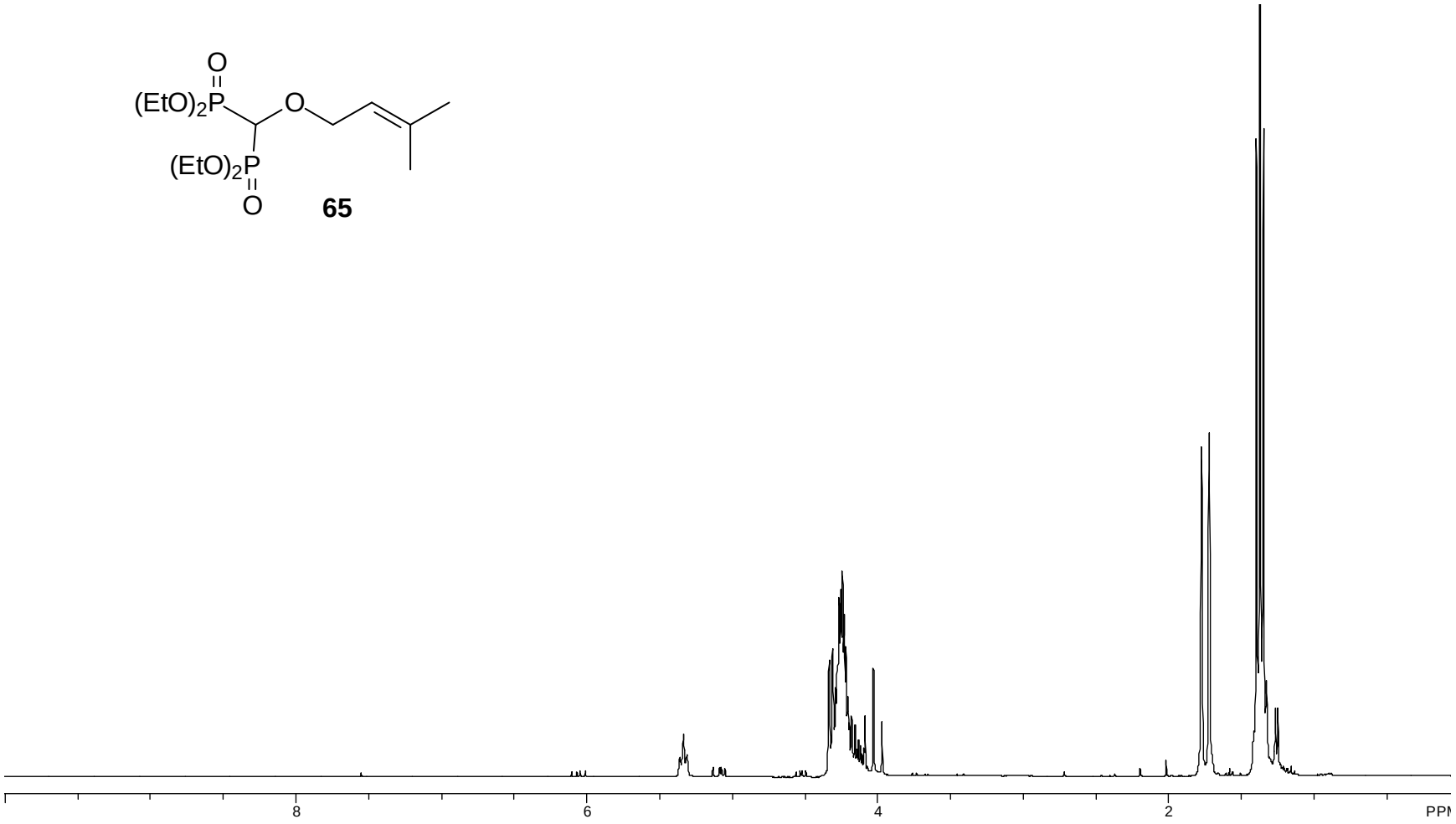

Figure A13. 300 MHz ^{1}H NMR Spectrum of Compound **35**.

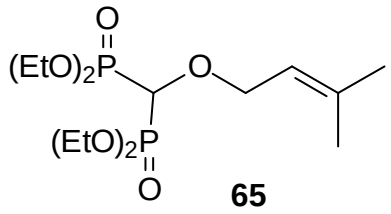

65

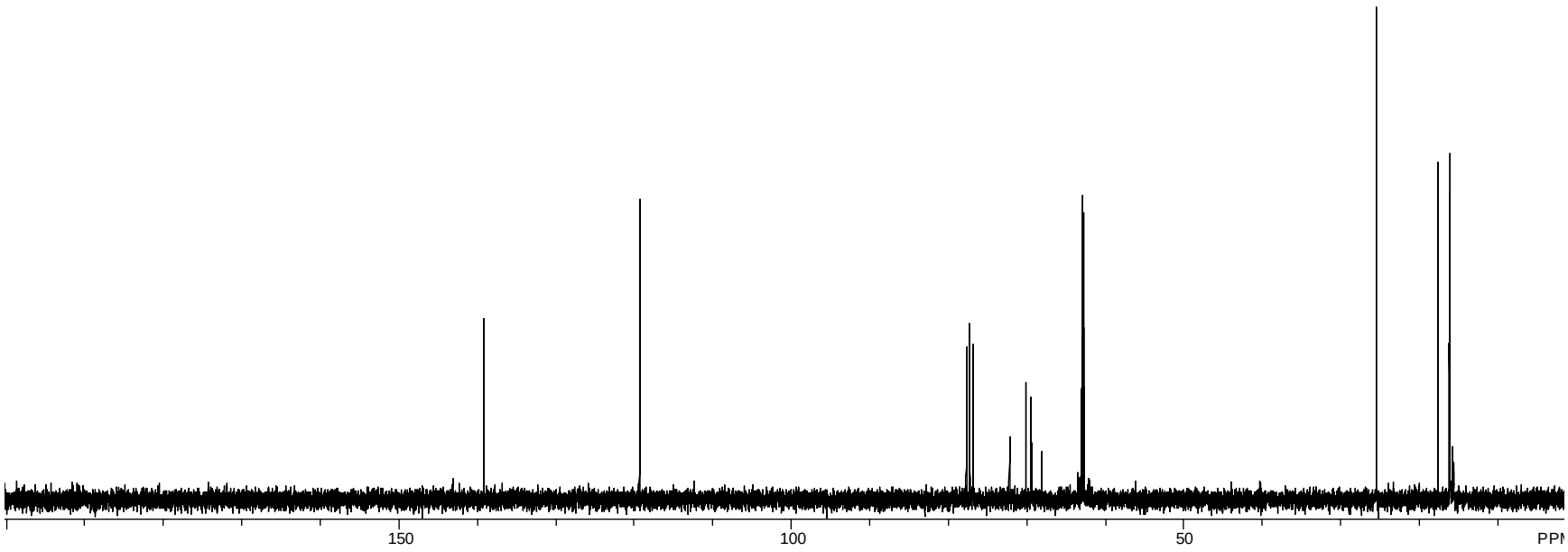

Figure A14. 75 MHz ^{13}C NMR Spectrum of Compound **65**.

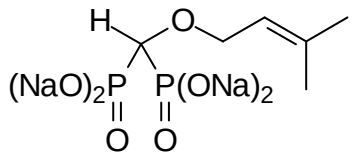

68

Figure A15. 300 MHz ^{1}H NMR Spectrum of Compound **68**.

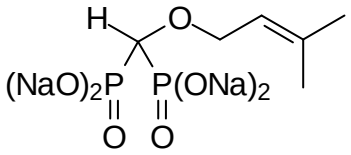

68

Figure A16. 100 MHz ^{13}C NMR Spectrum of Compound **68**.

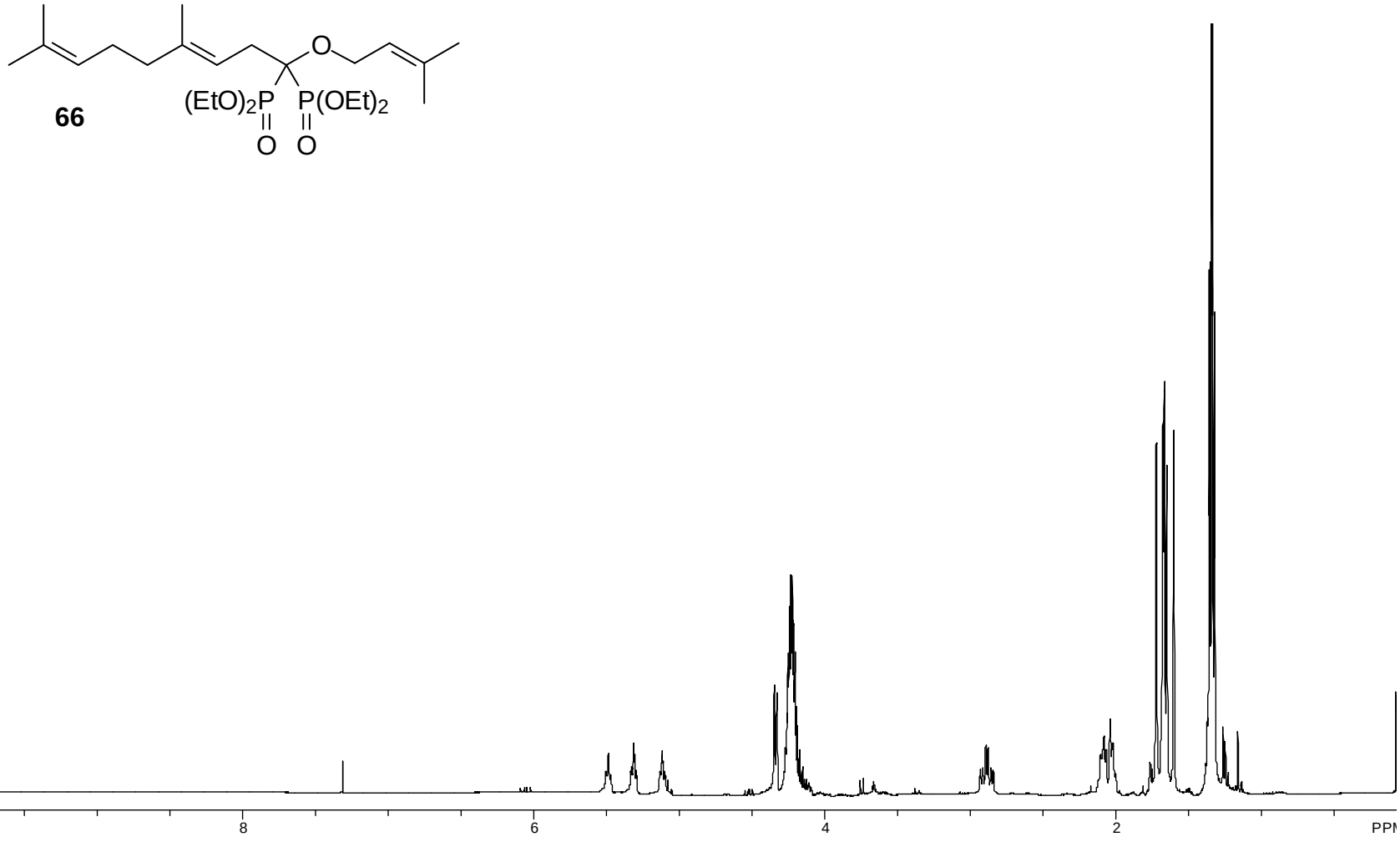

Figure A17. 400 MHz ^{1}H NMR Spectrum of Compound **66**.

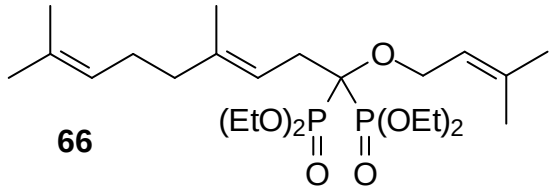

66

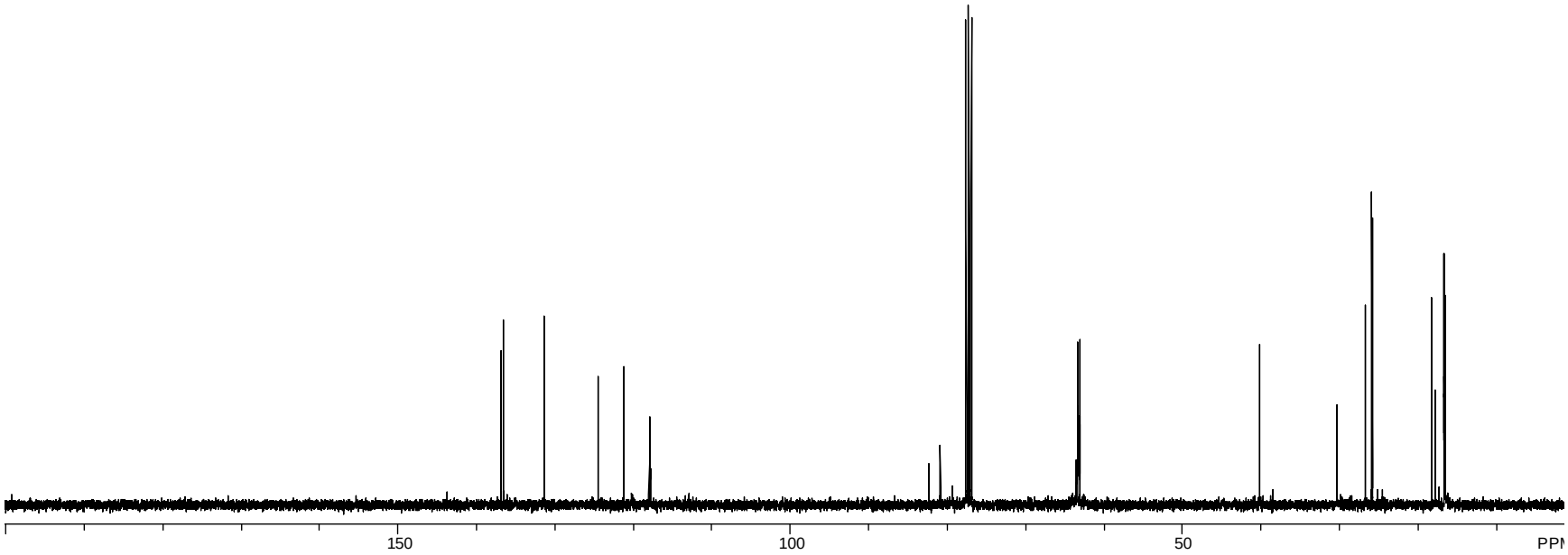

Figure A18. 100 MHz ^{13}C NMR Spectrum of Compound **66**.

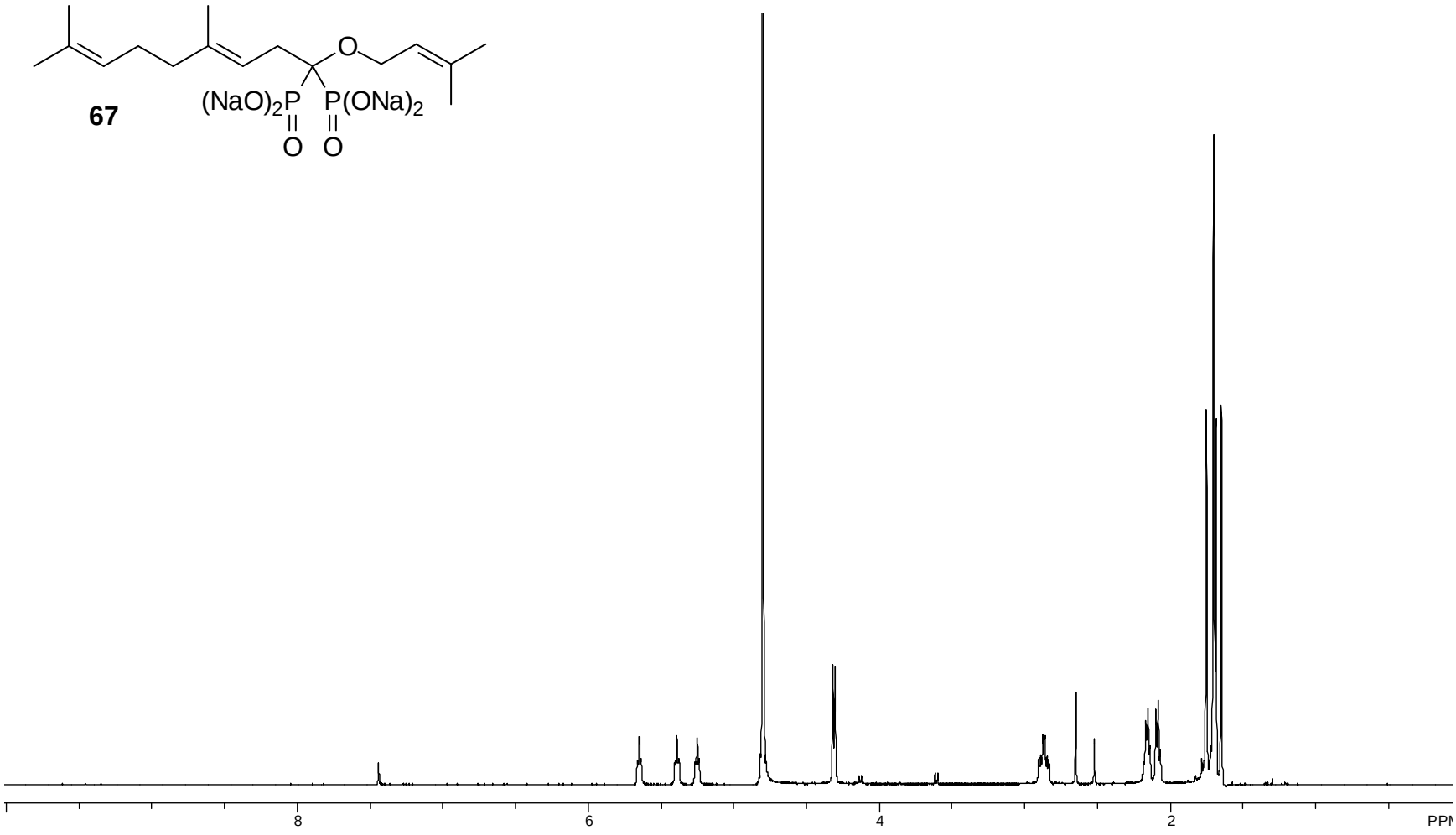

Figure A19. 500 MHz ^{1}H NMR Spectrum of Compound **67**.

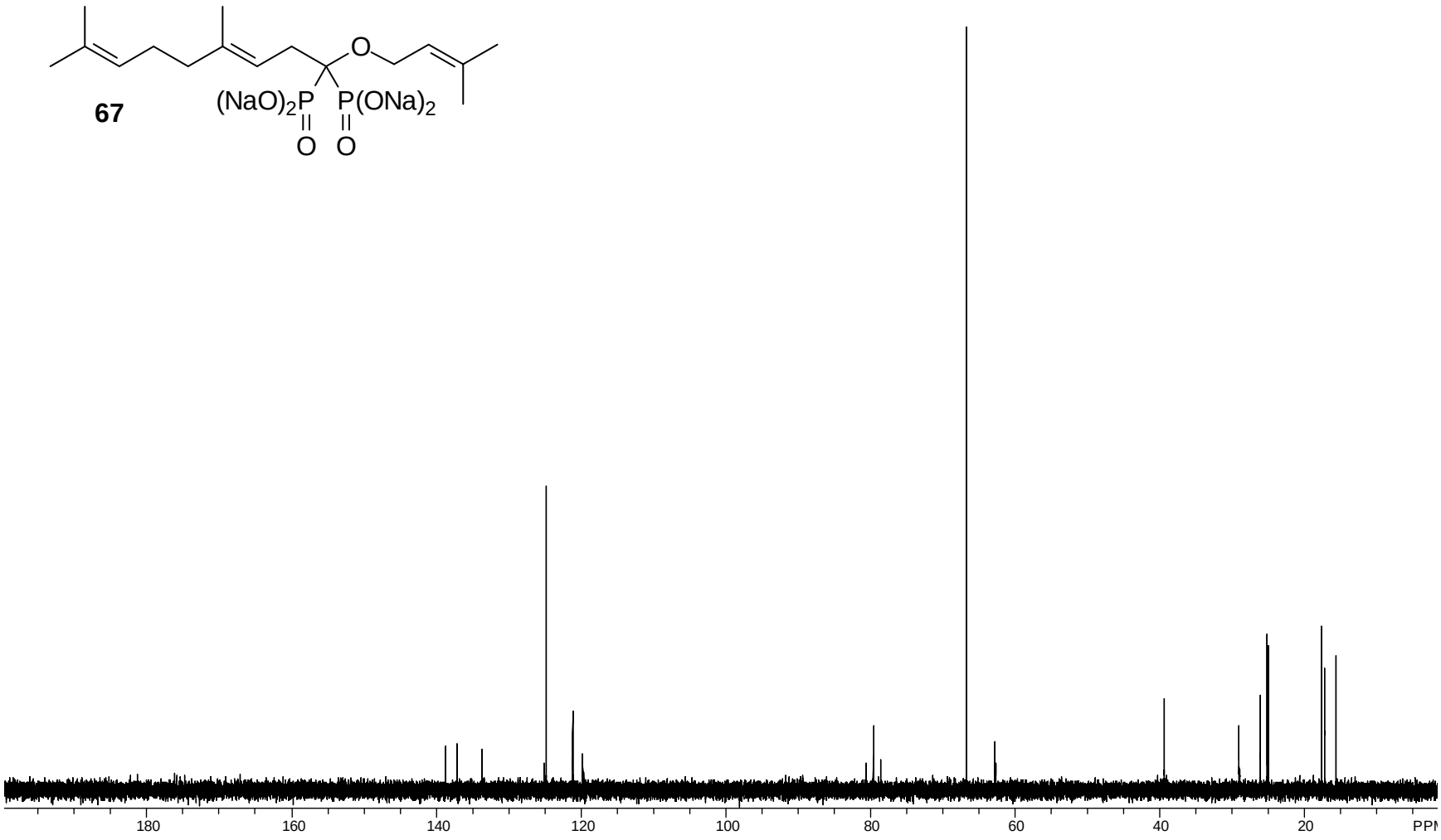

Figure A20. 125 MHz ^{13}C NMR Spectrum of Compound **67**.

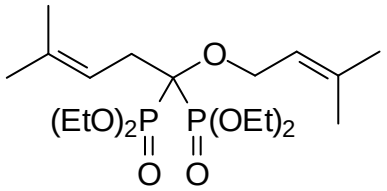

69

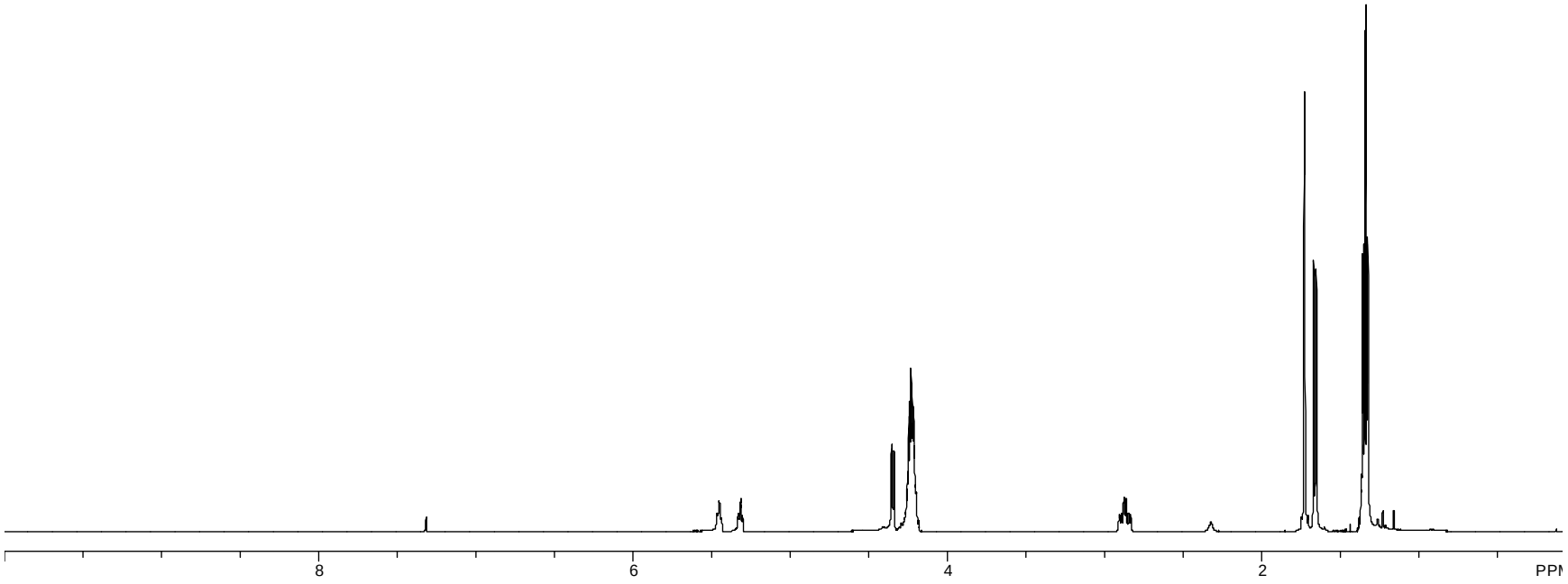

Figure A21. 500 MHz ^{1}H NMR Spectrum of Compound **69**.

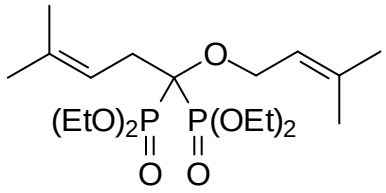

69

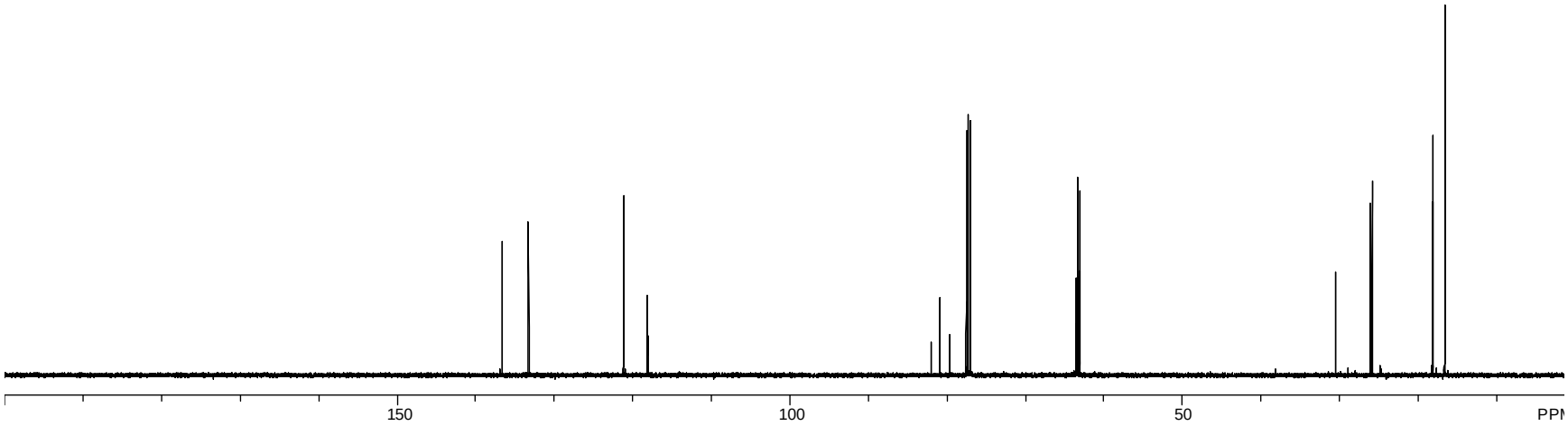

Figure A22. 125 MHz ^{13}C NMR Spectrum of Compound **69**.

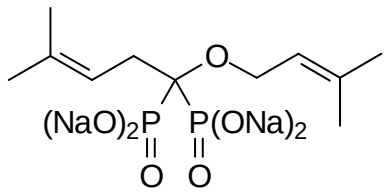

70

Figure A23. 500 MHz ^{1}H NMR Spectrum of Compound **70**.

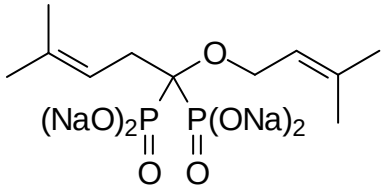

70

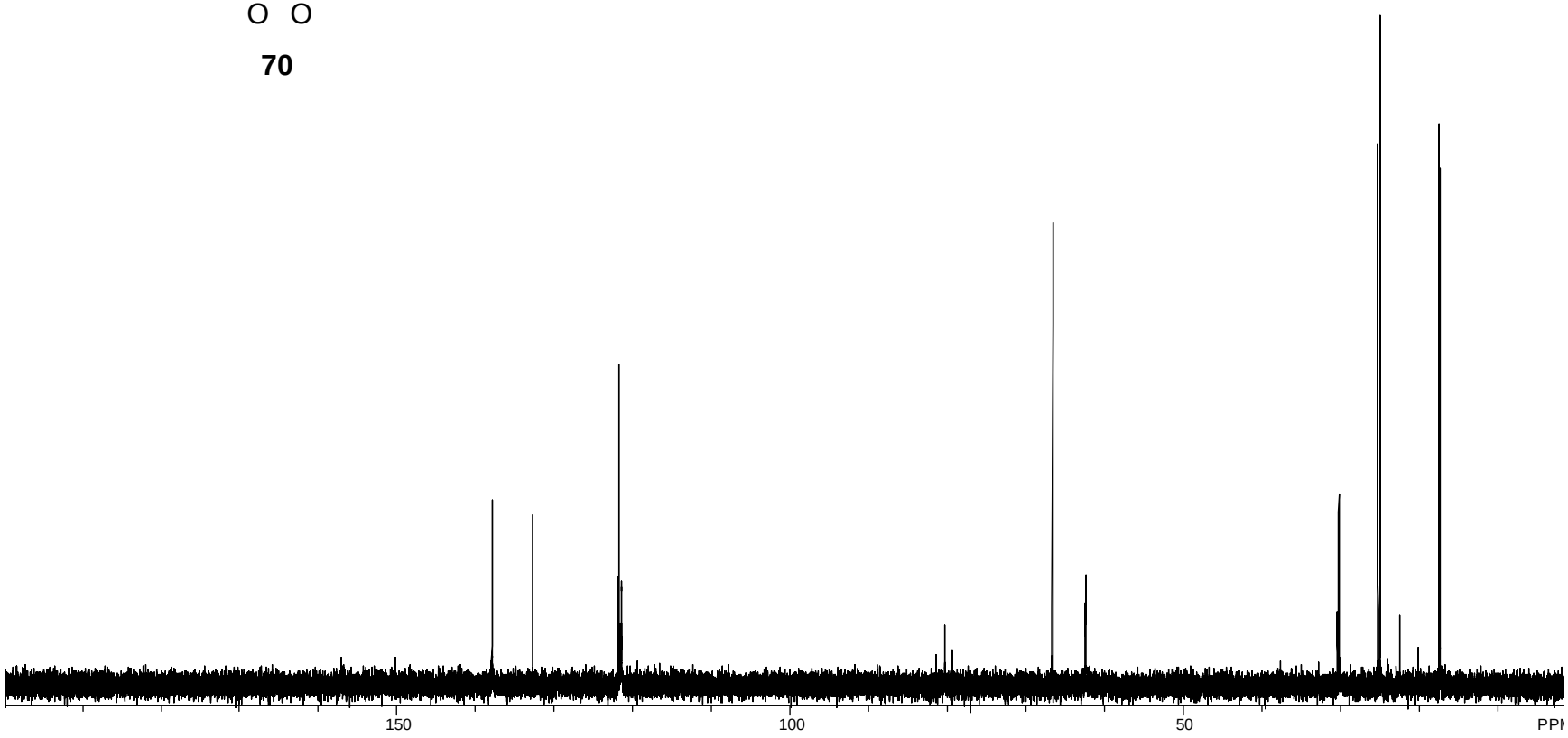

Figure A24. 125 MHz ^{13}C NMR Spectrum of Compound **70**.

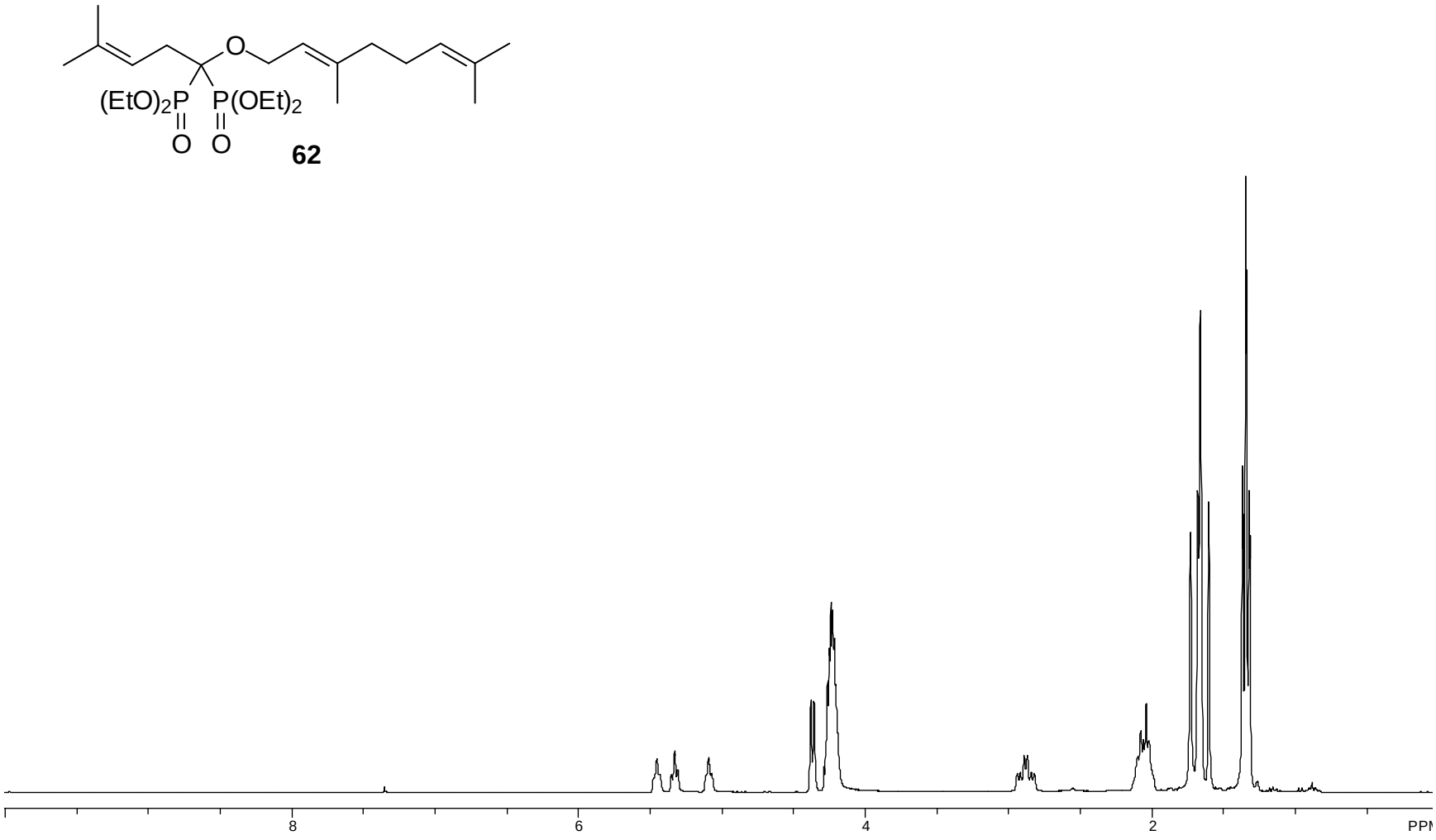

Figure A25. 300 MHz ^{1}H NMR Spectrum of Compound **62**.

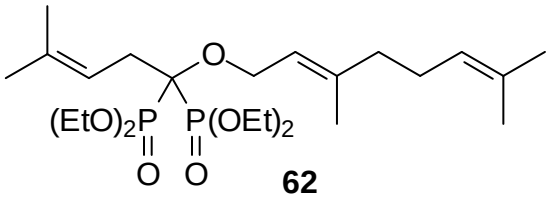

62

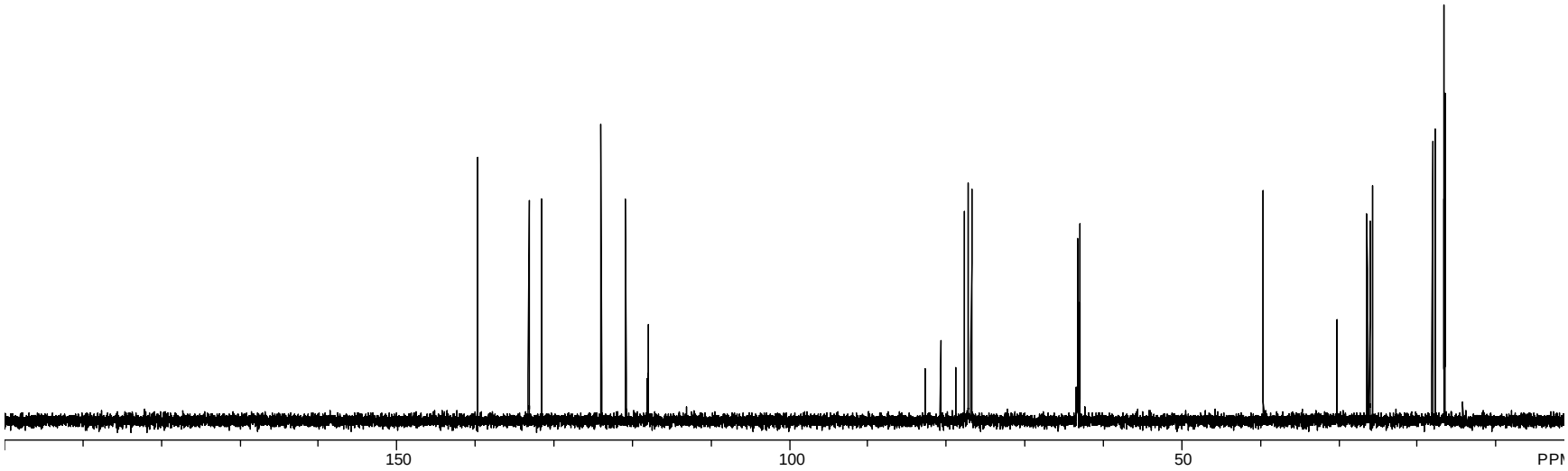

Figure A26. 75 MHz ^{13}C NMR Spectrum of Compound **62**.

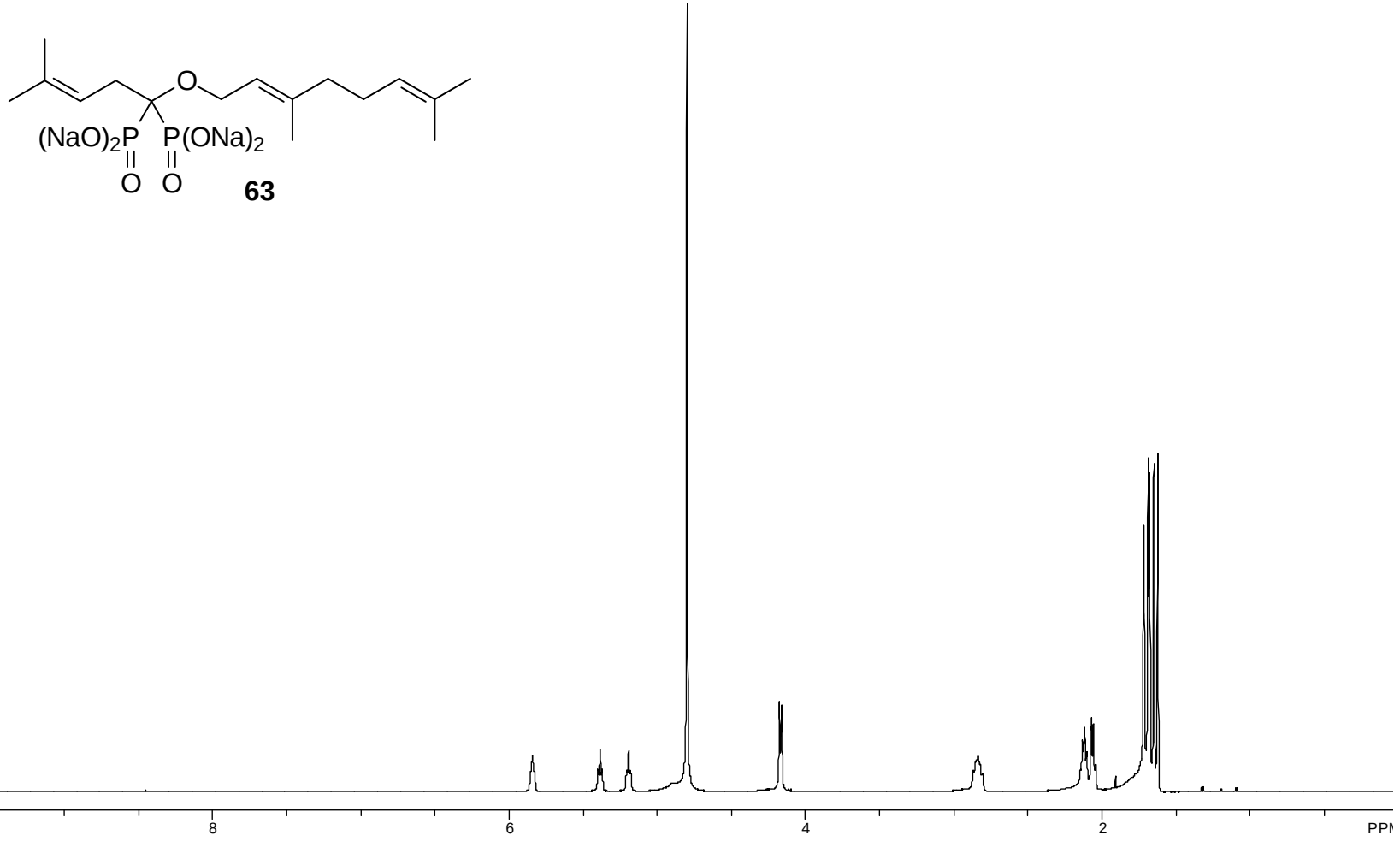

Figure A27. 500 MHz ^{1}H NMR Spectrum of Compound **63**.

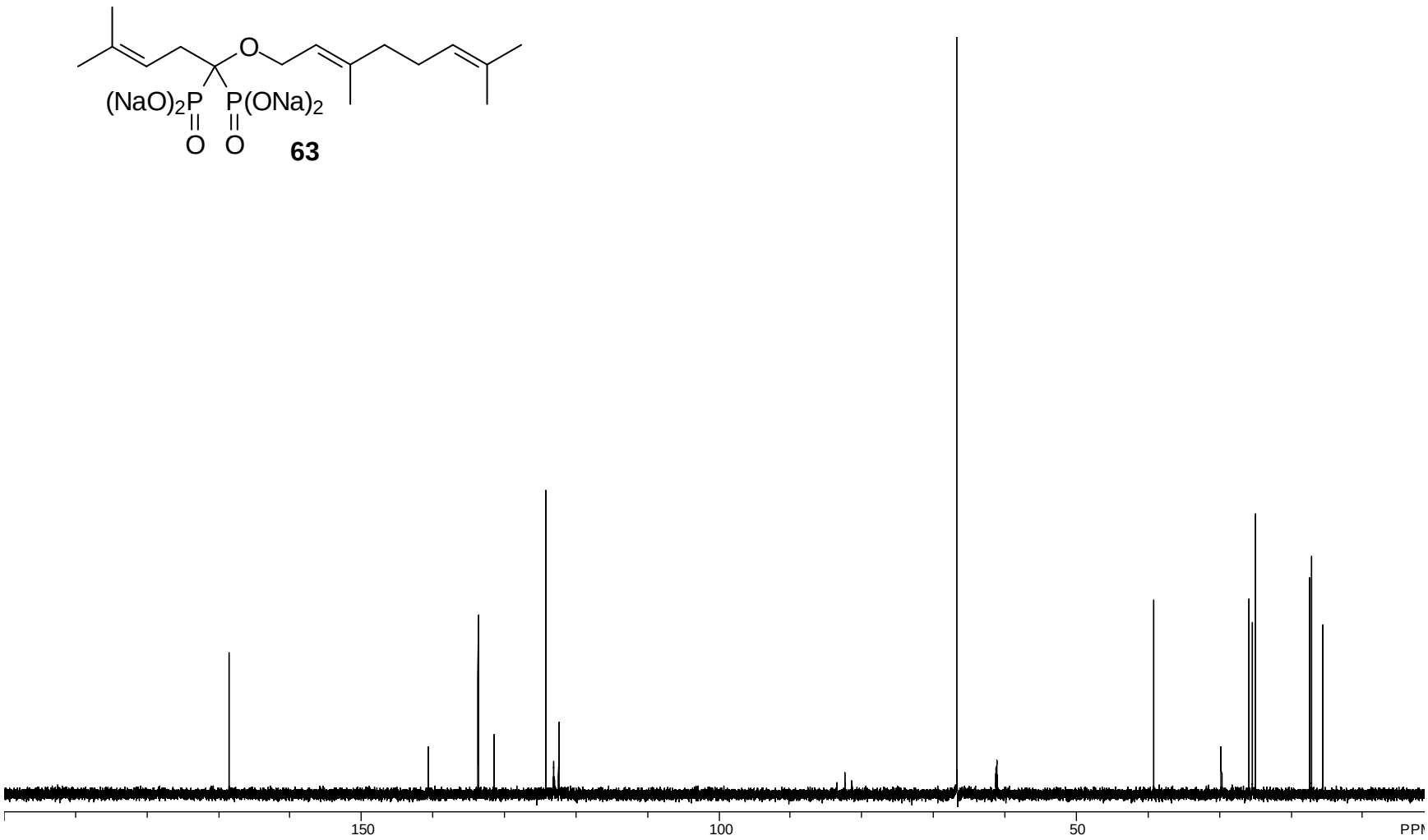

Figure A28. 125 MHz ^{13}C NMR Spectrum of Compound **63**.

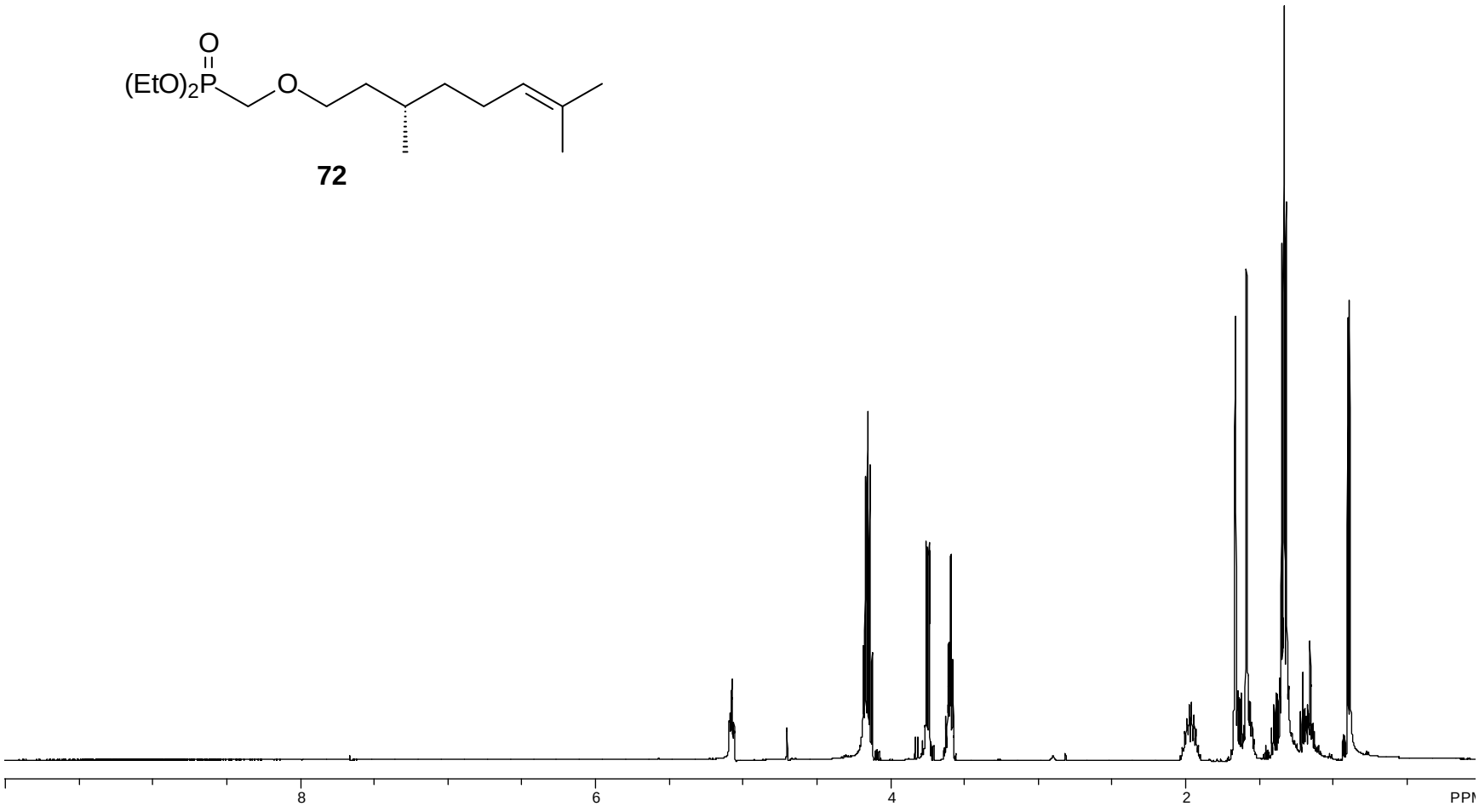

Figure A29. 500 MHz ^{1}H NMR Spectrum of Compound **72**.

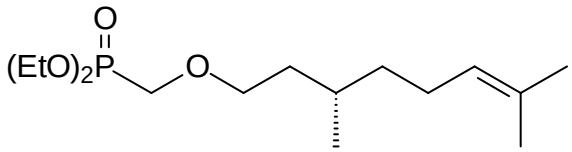

72

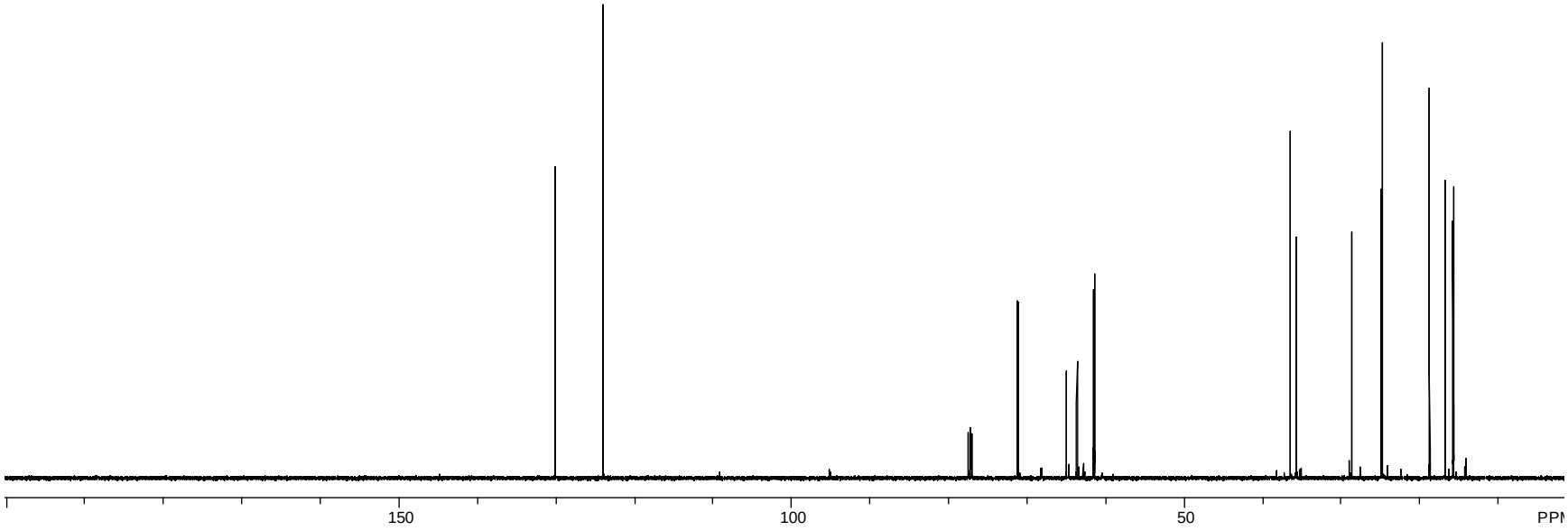

Figure A30. 125 MHz ^{13}C NMR Spectrum of Compound **72**.

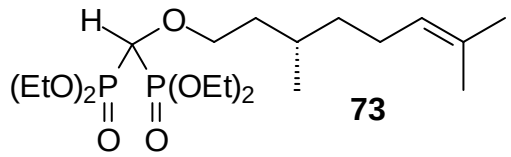

73

Figure A31. 400 MHz ^{1}H NMR Spectrum of Compound **73**.

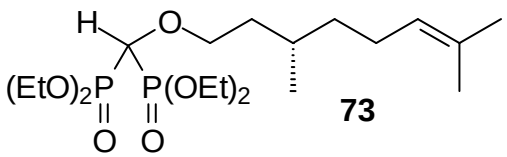

73

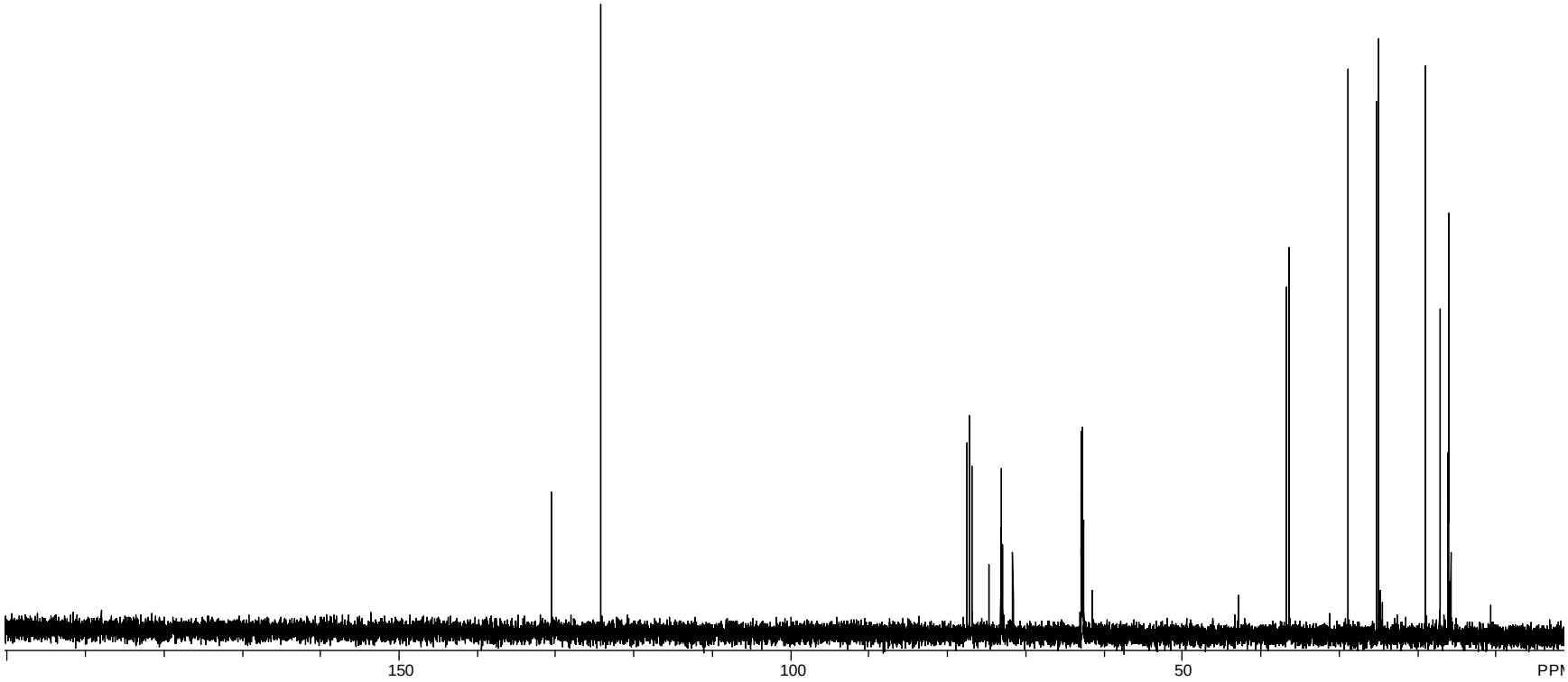

Figure A32. 100 MHz ^{1}H NMR Spectrum of Compound **73**.

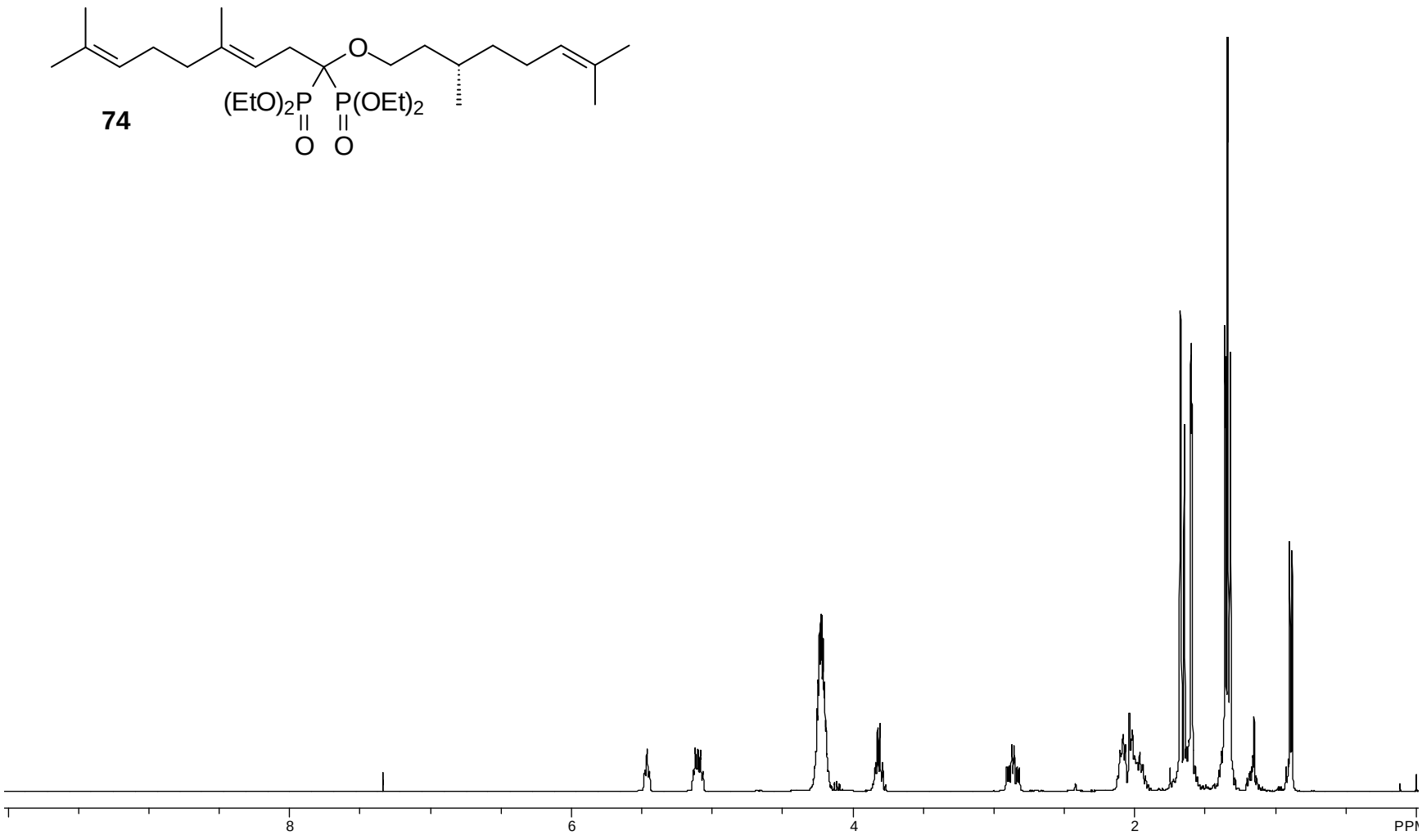

Figure A33. 400 MHz ^{1}H NMR Spectrum of Compound **74**.

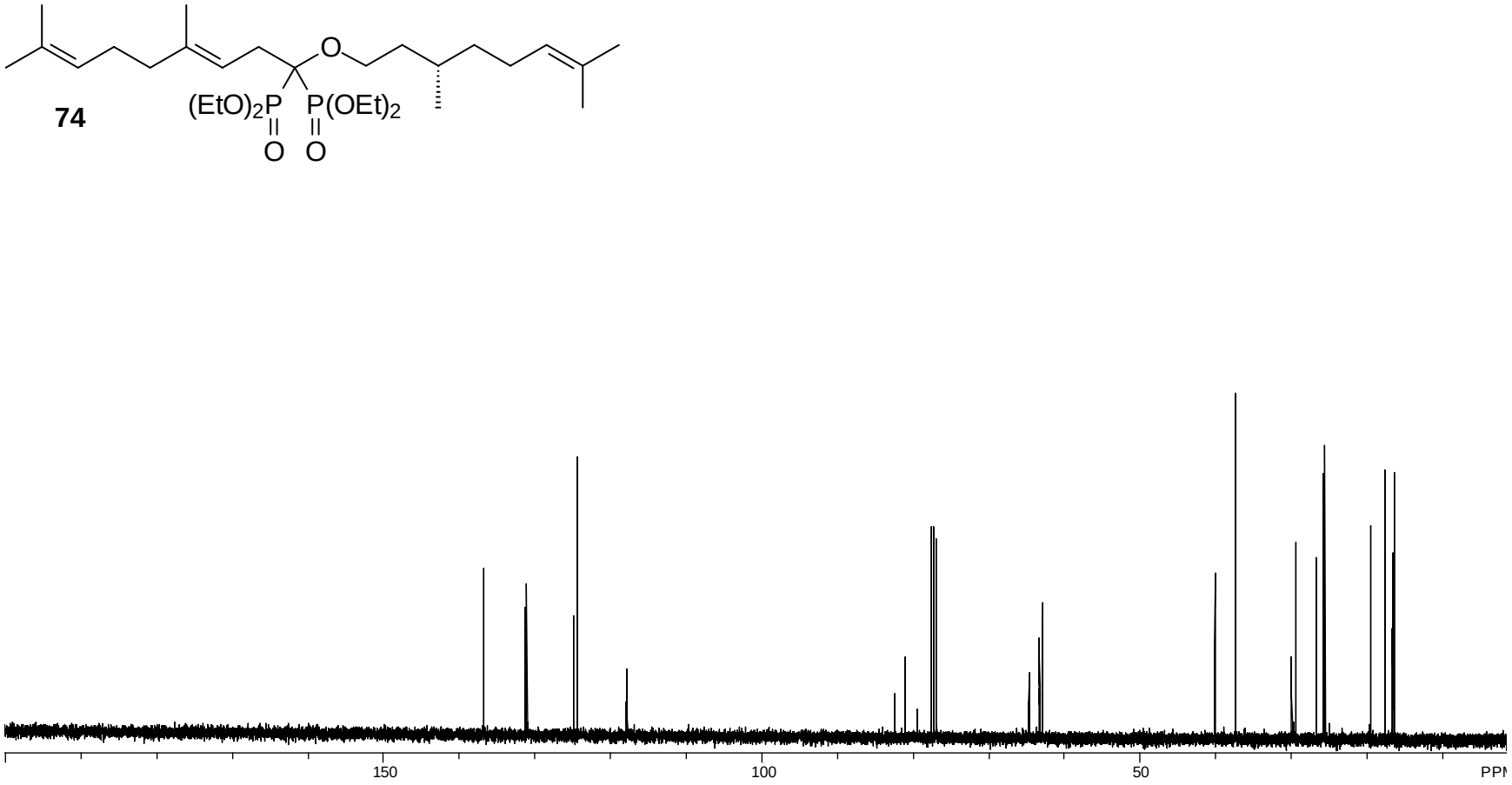

Figure A34. 100 MHz ^{13}C NMR Spectrum of Compound **74**.

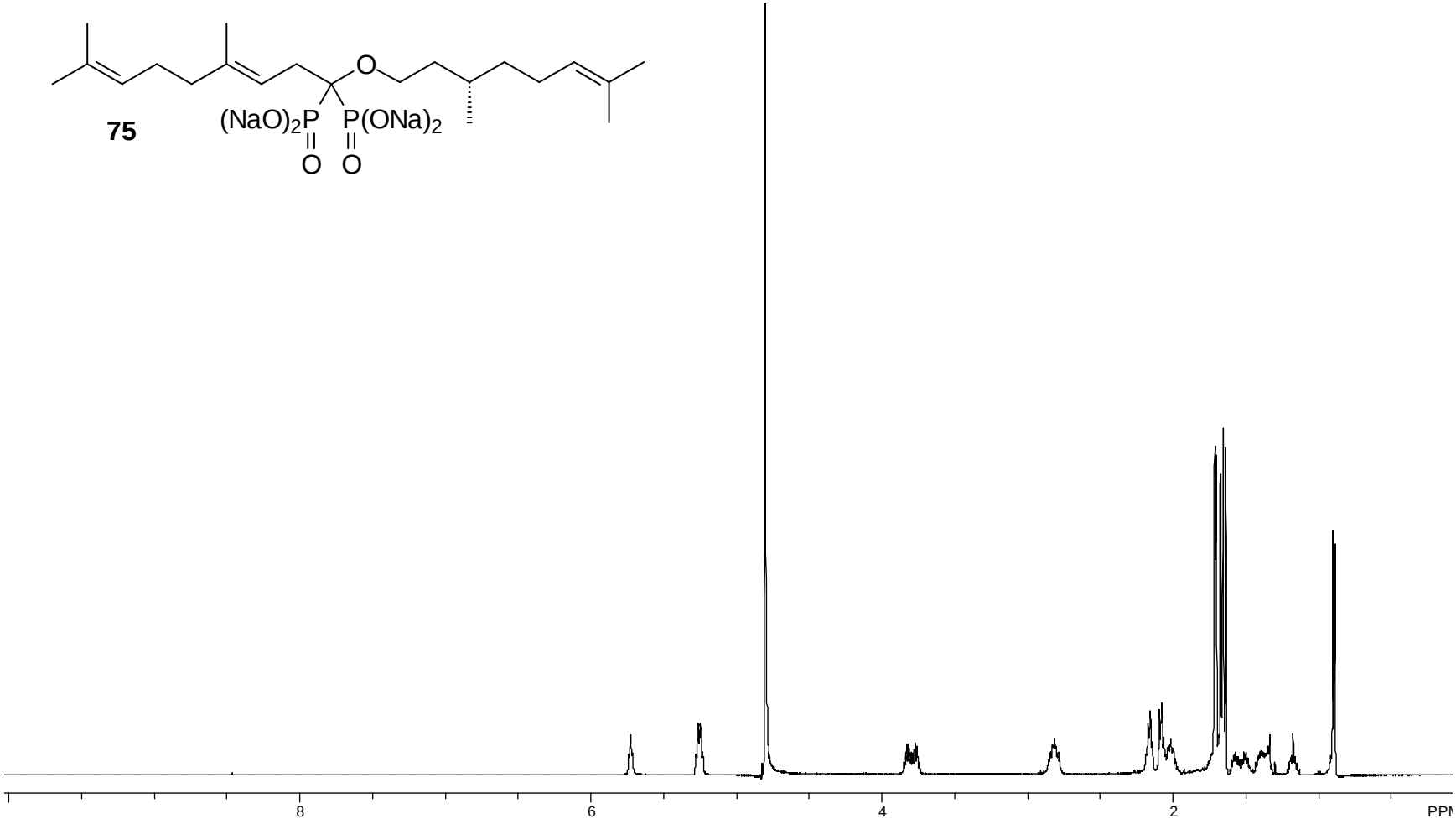

Figure A35. 500 MHz ^{1}H NMR Spectrum of Compound **75**.

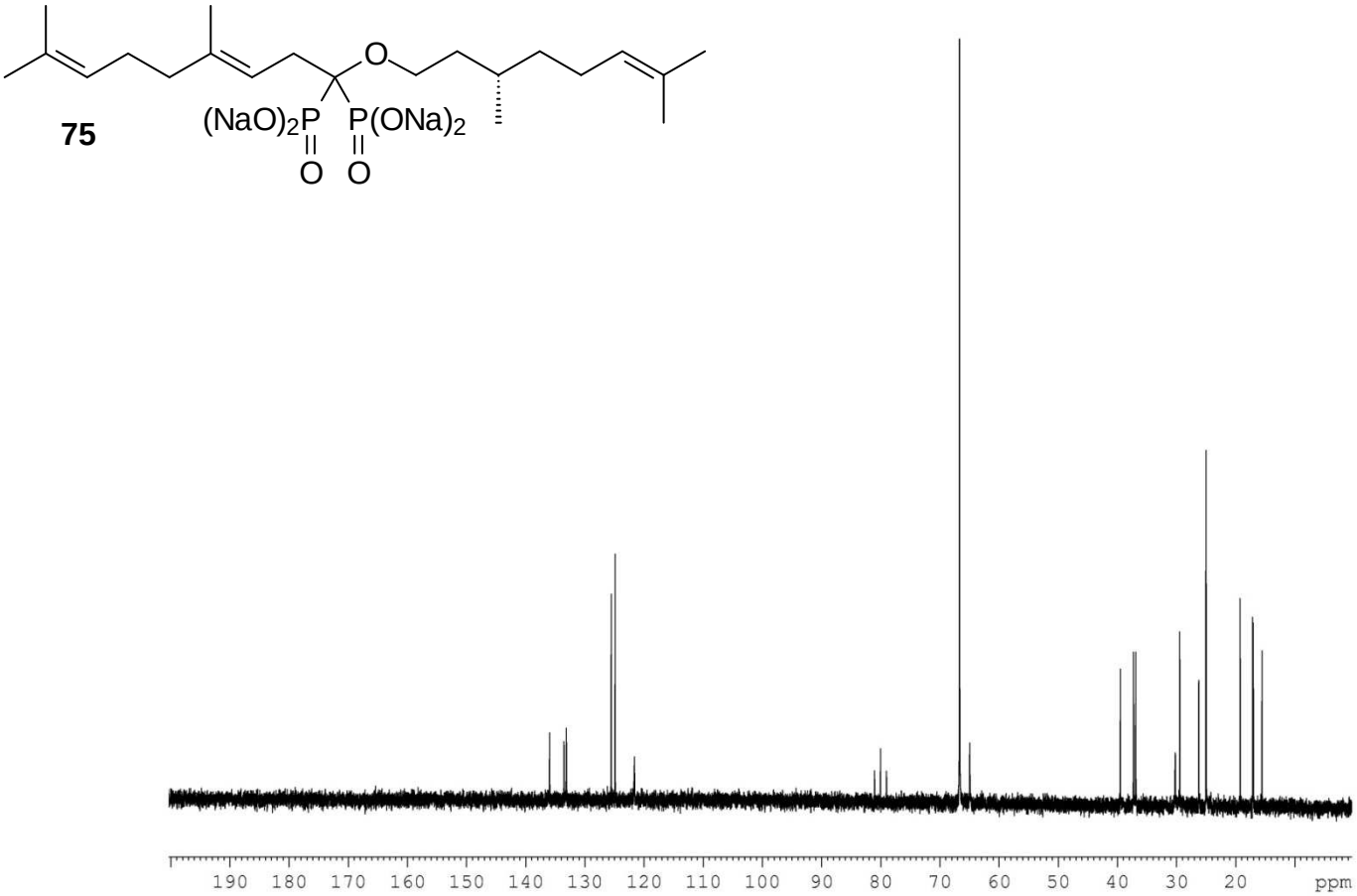

Figure A36. 125 MHz ^{13}C NMR Spectrum of Compound **75**.

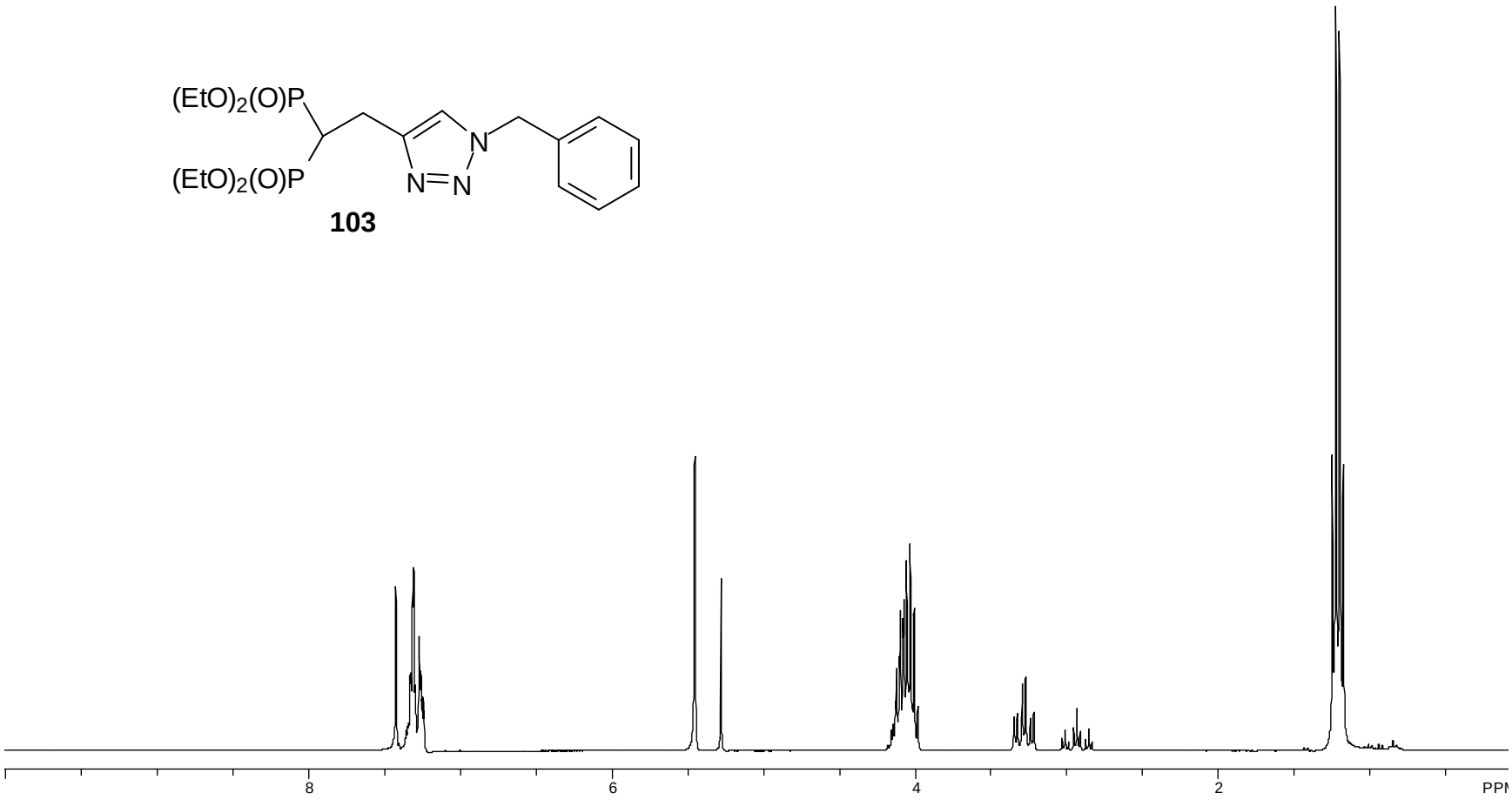

Figure A37. 300 MHz ^{1}H NMR Spectrum of Compound **103**.

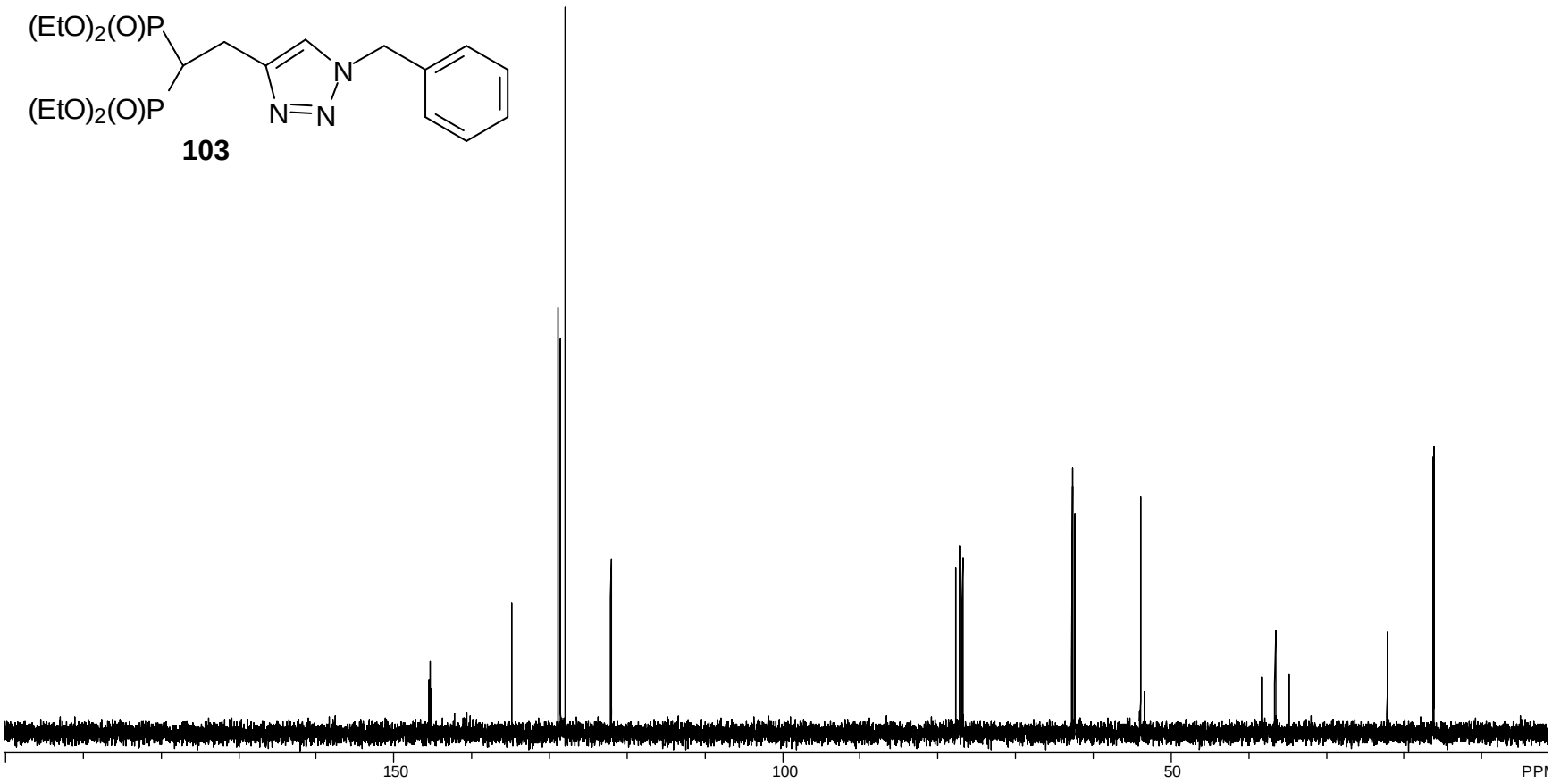

Figure A38. 75 MHz ^{13}C NMR Spectrum of Compound **103**.

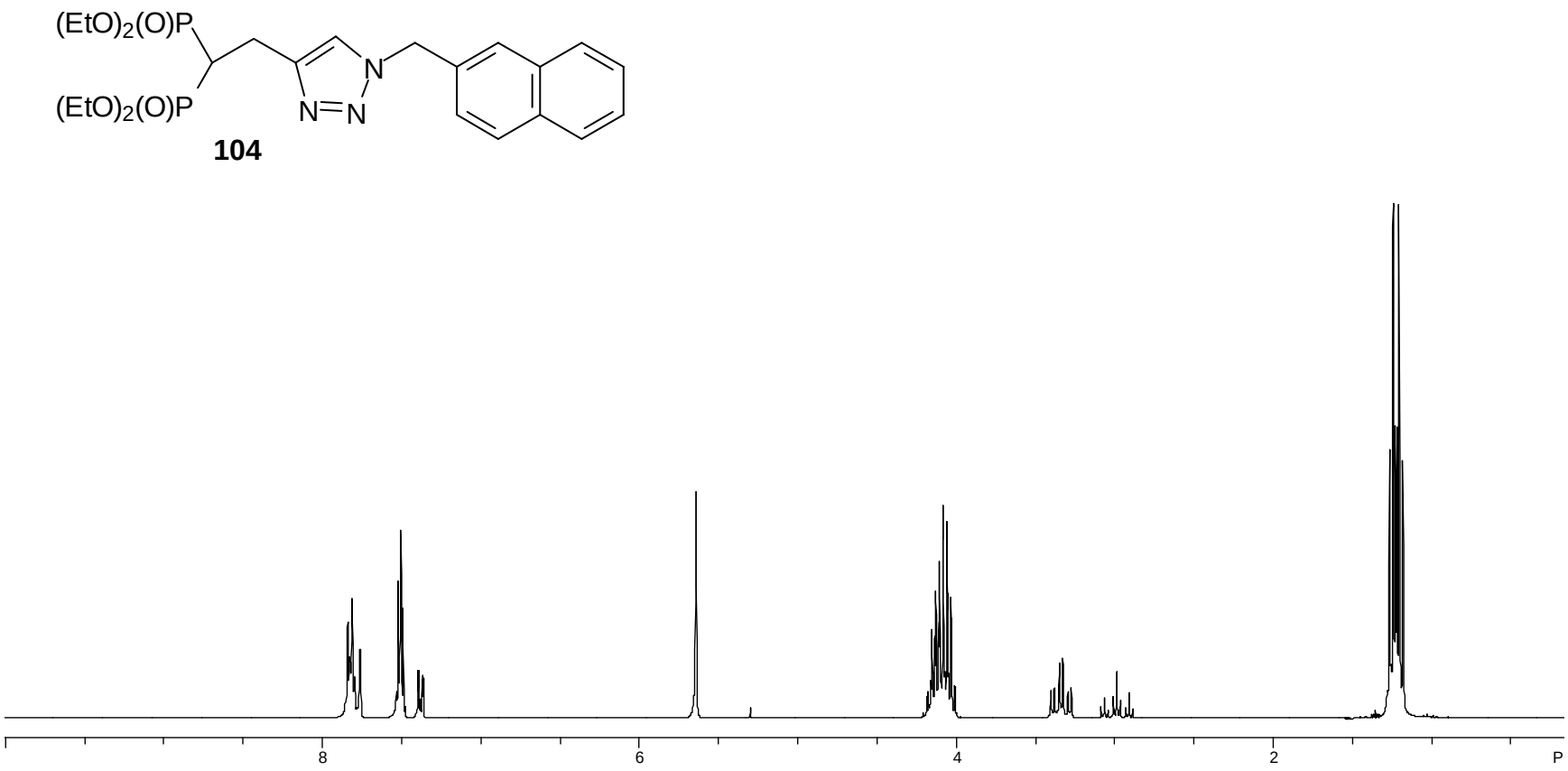

Figure A39. 300 MHz ^{1}H NMR Spectrum of Compound **104**.

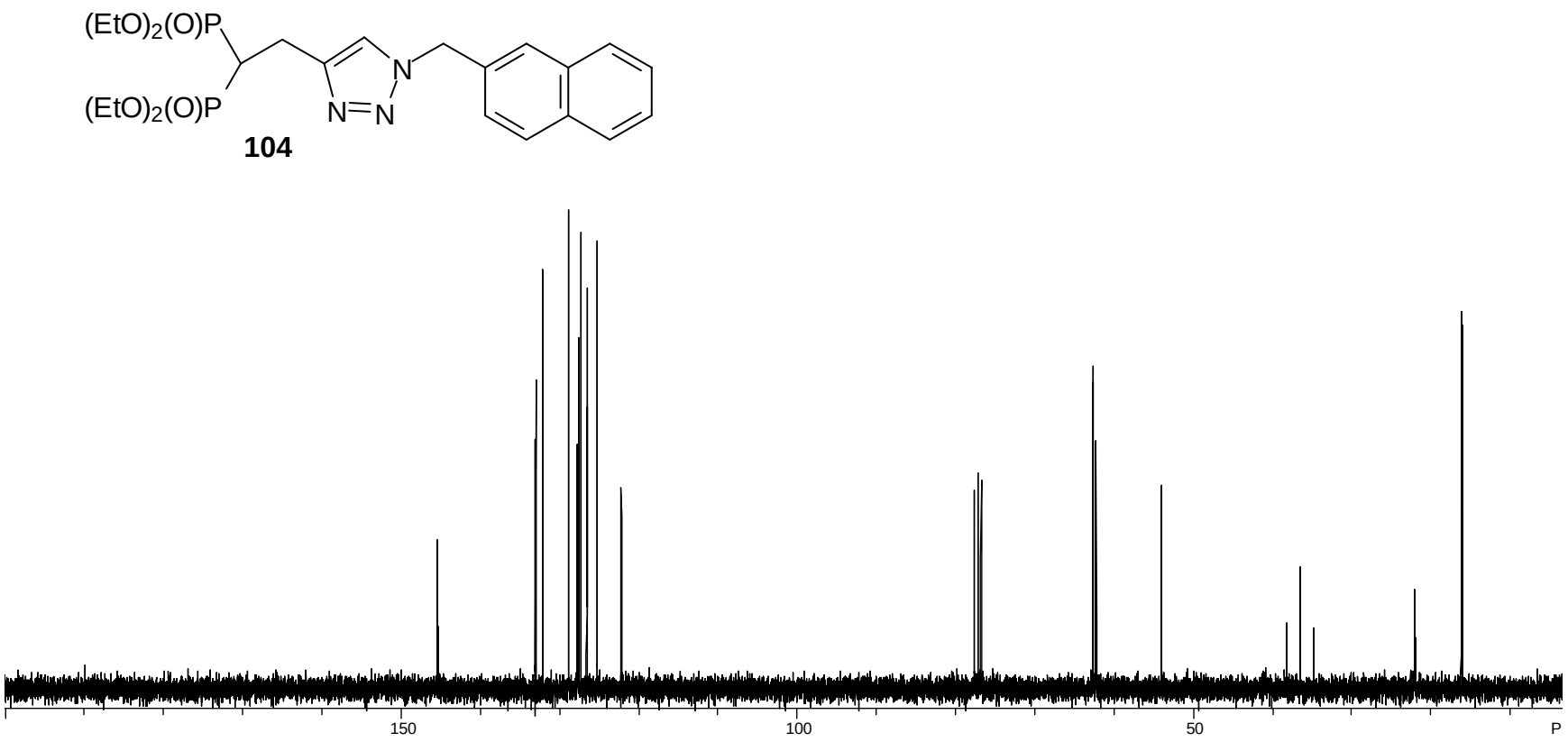

Figure A40. 75 MHz ^{13}C NMR Spectrum of Compound **104.**

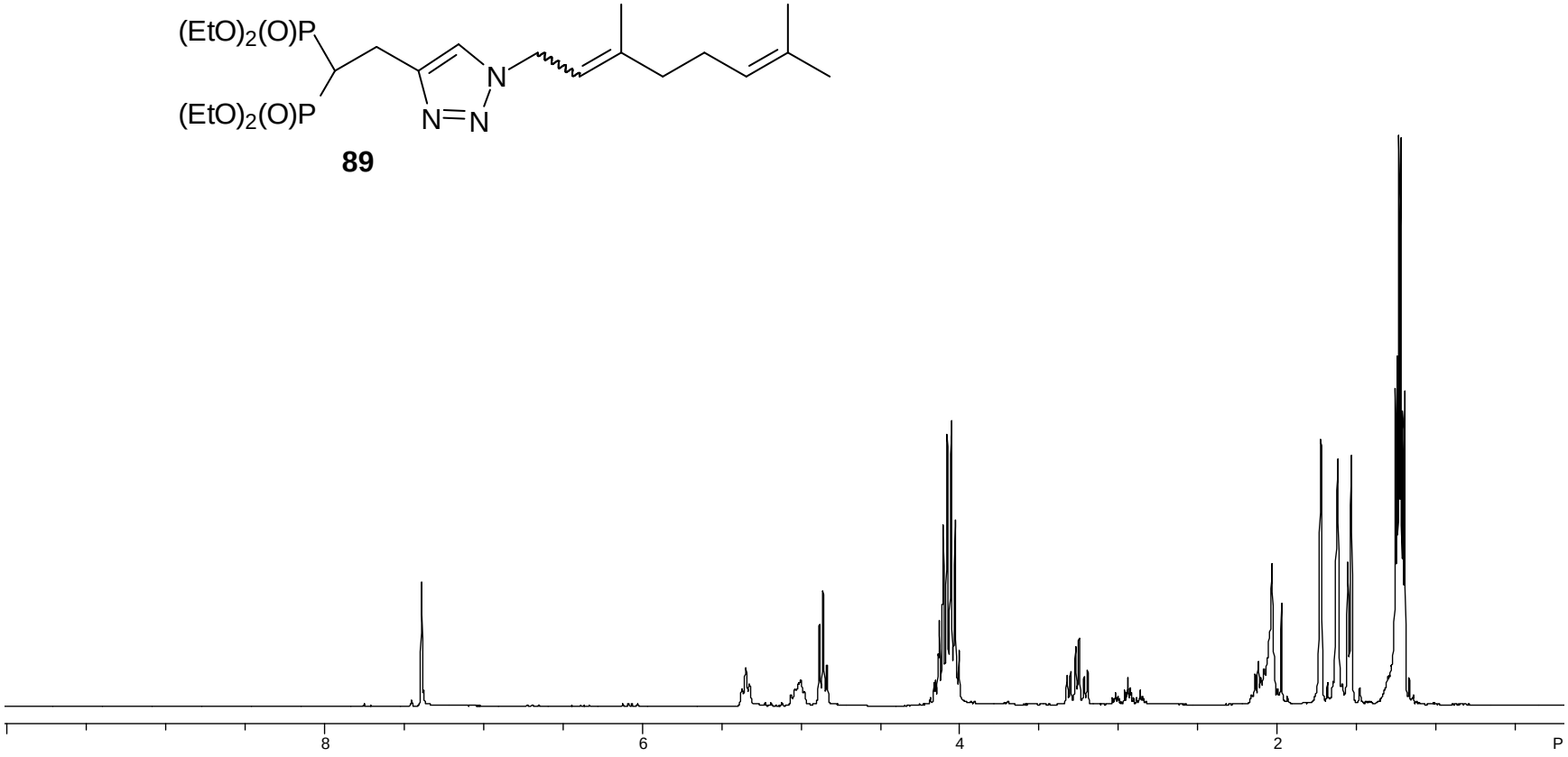

Figure A41. 300 MHz ^{1}H NMR Spectrum of Compound **89**.

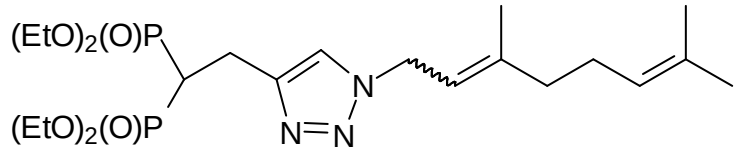

89

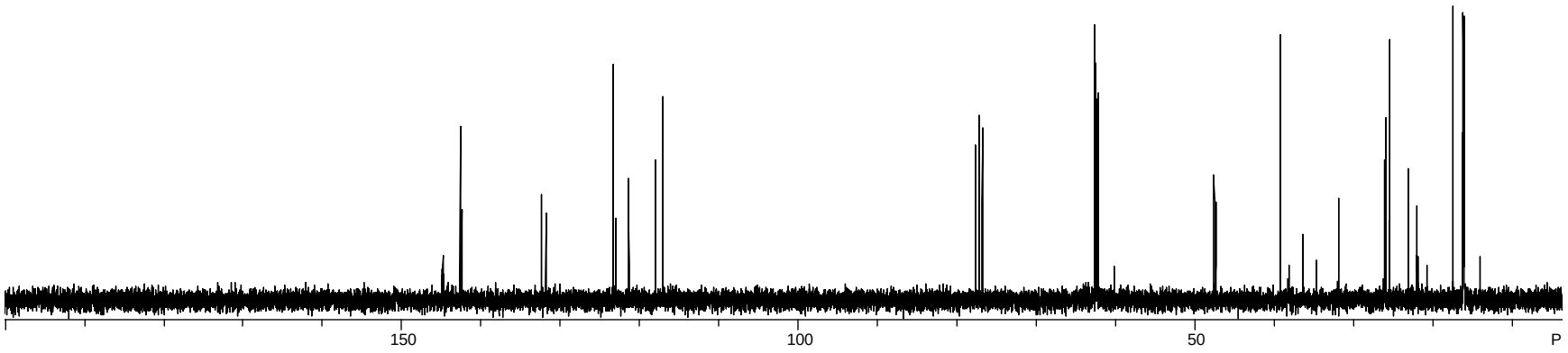

Figure A42. 75 MHz ^{13}C NMR Spectrum of Compound **89**.

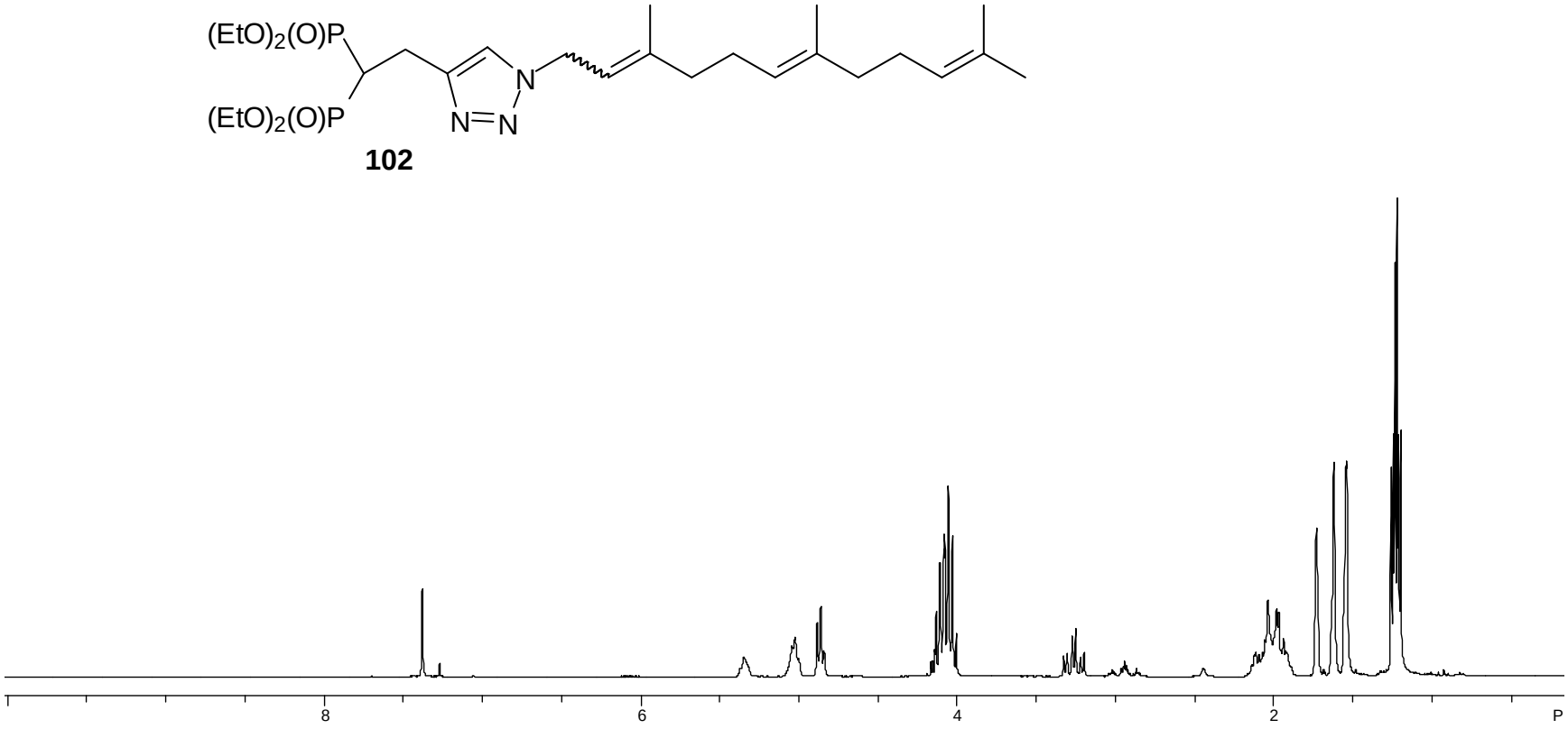

102

Figure A43. 300 MHz ^{1}H NMR Spectrum of Compound **102**.

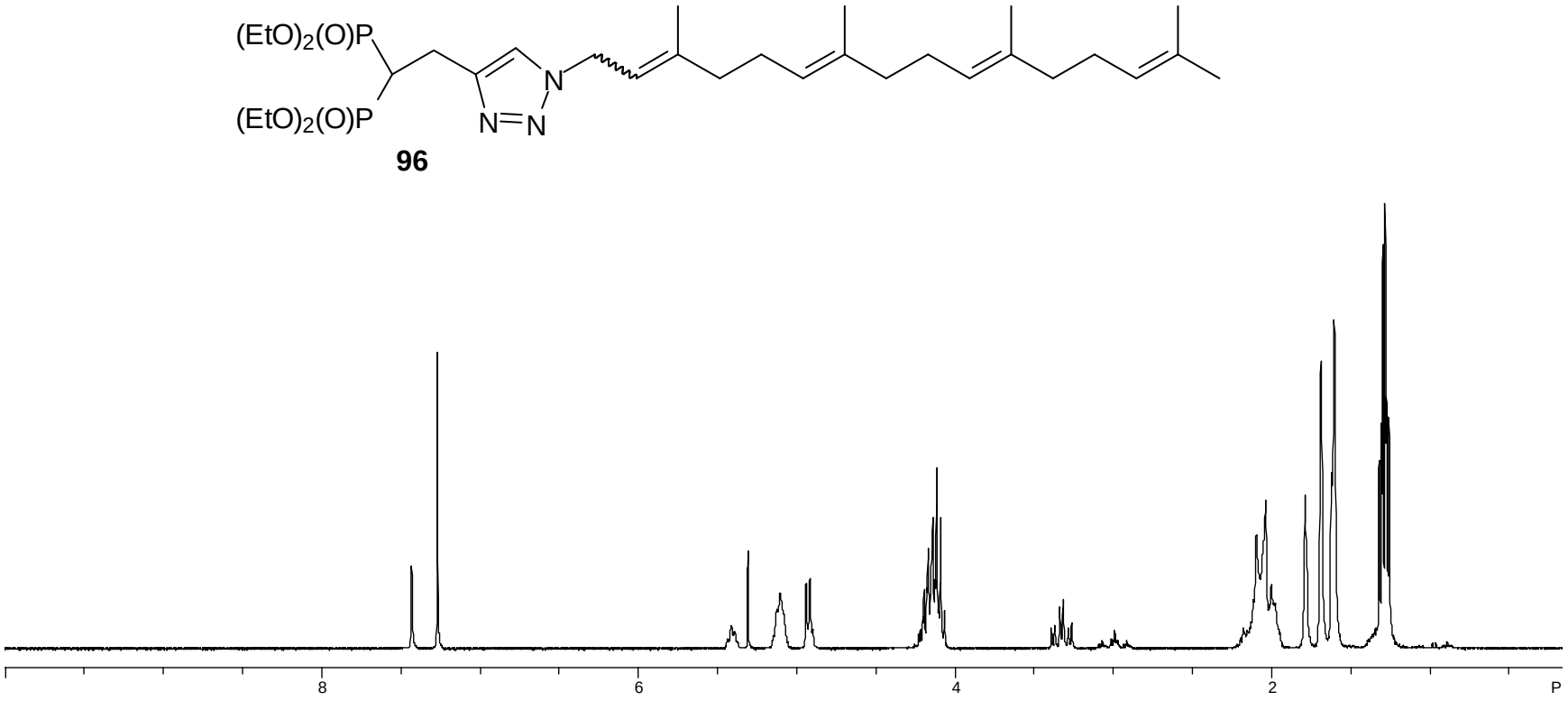

Figure A44. 300 MHz ^{1}H NMR Spectrum of Compound **96**.

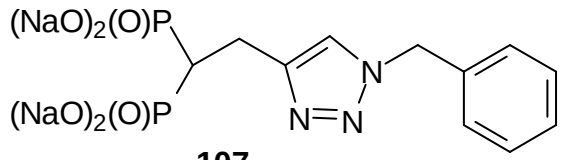

107

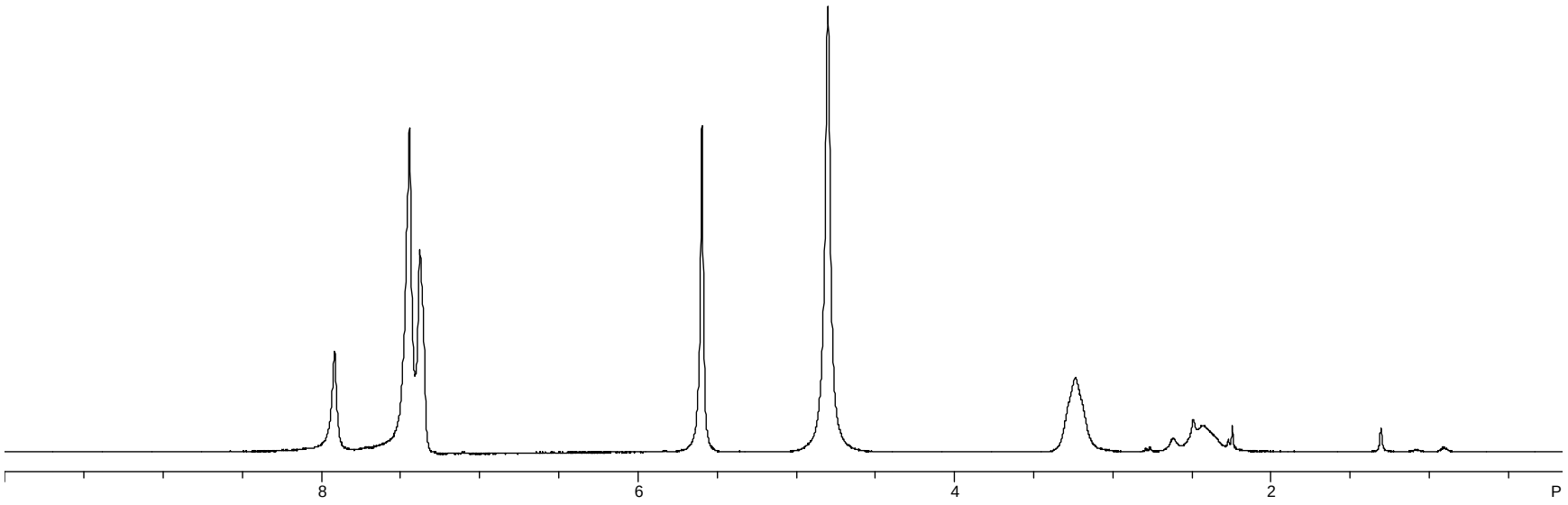

Figure A45. 300 MHz ^{1}H NMR Spectrum of Compound **107**.

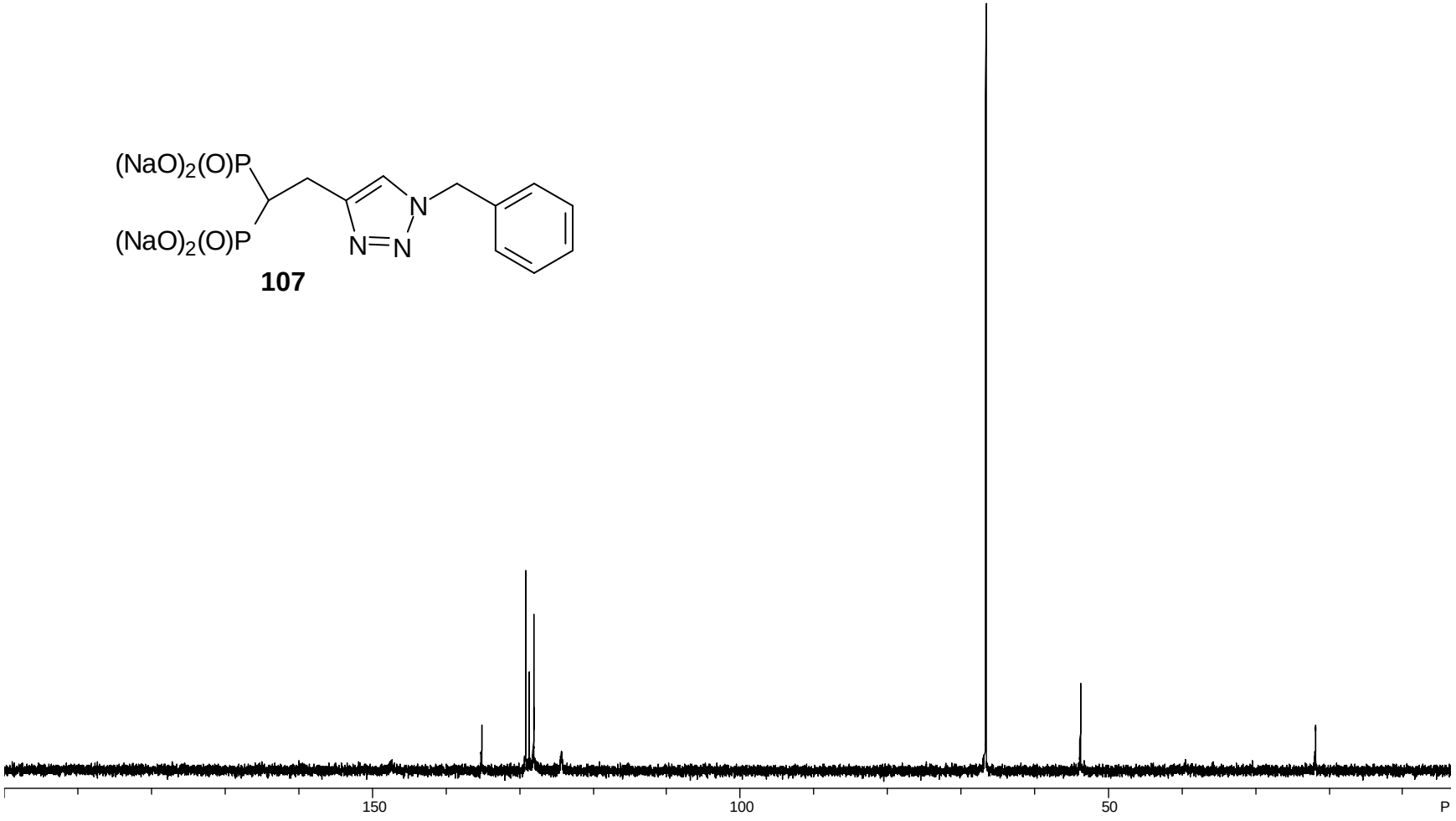

Figure A46. 125 MHz ^{13}C NMR Spectrum of Compound **107**.

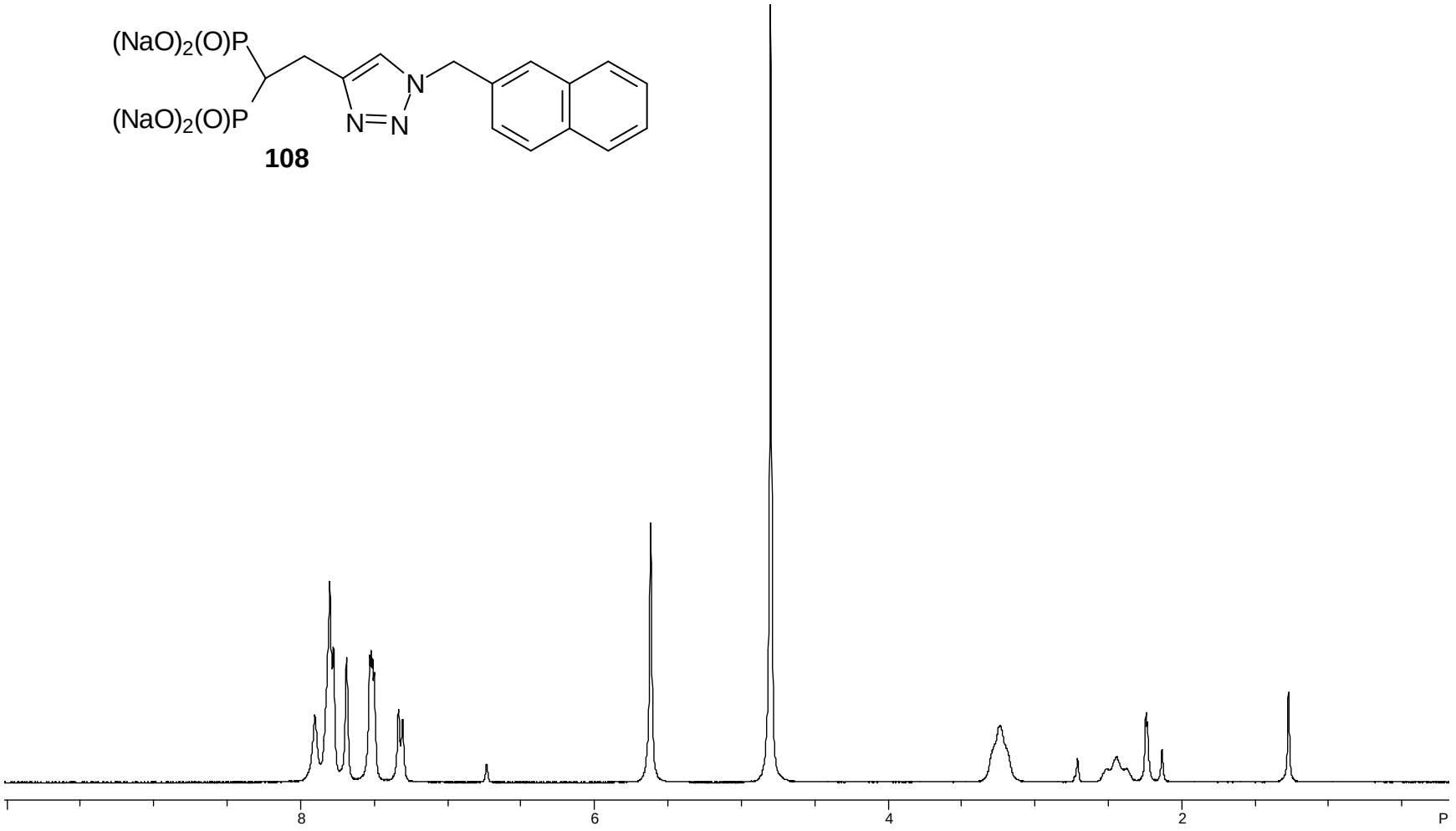

Figure A47. 300 MHz ^{1}H NMR Spectrum of Compound **108**.

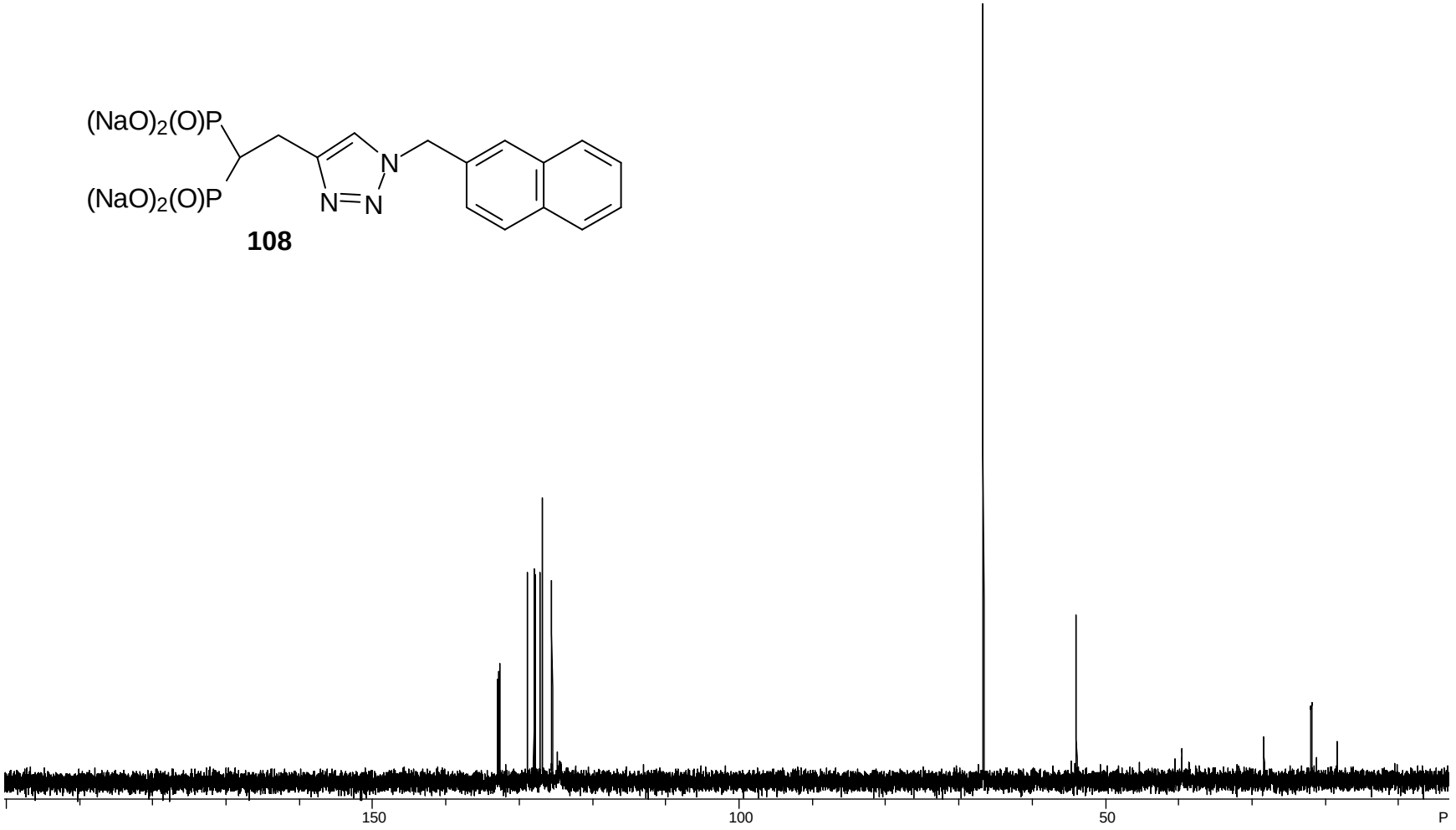

Figure A48. 125 MHz ^{13}C NMR Spectrum of Compound **108**.

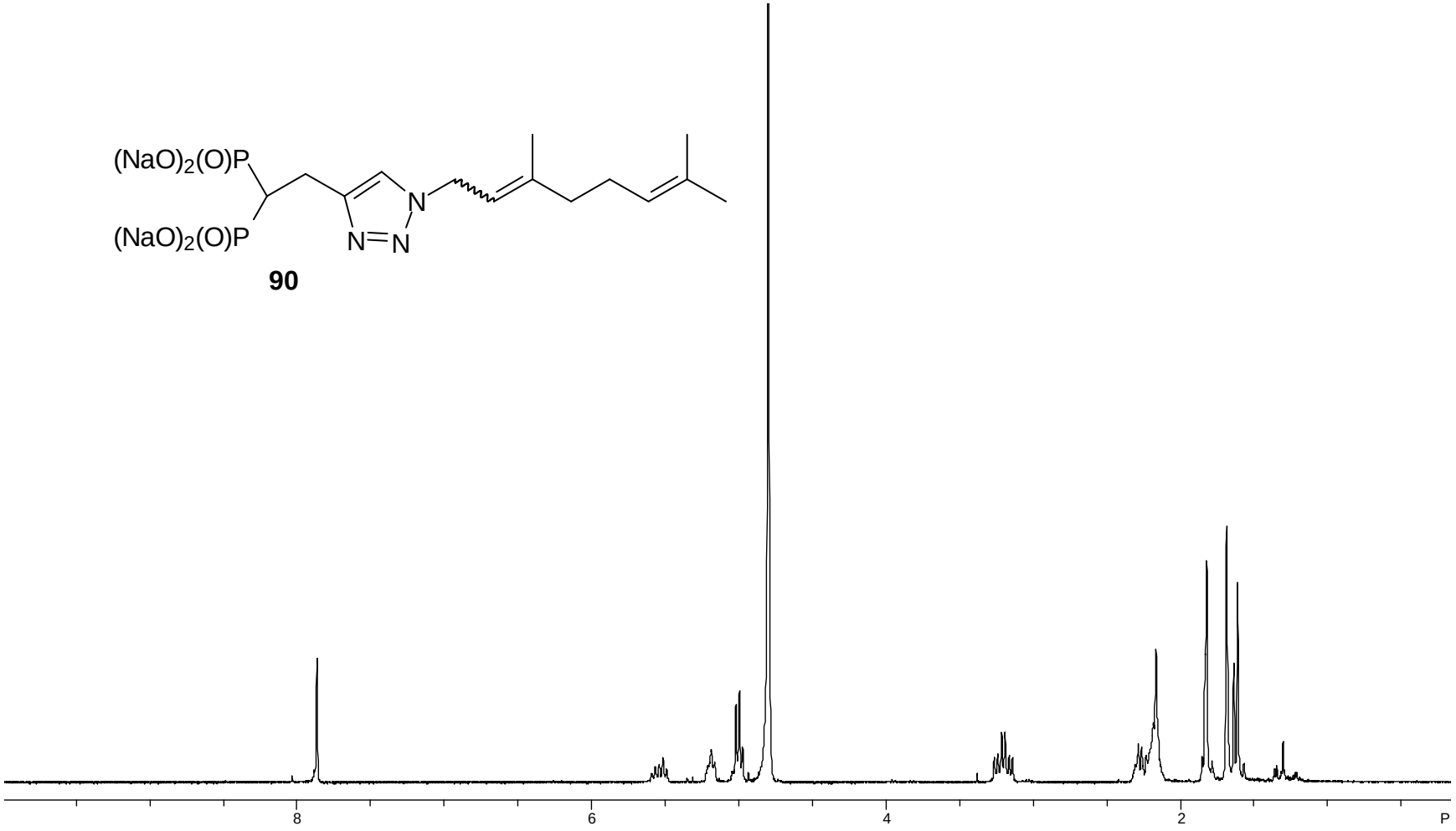

Figure A49. 300 MHz ^{1}H NMR Spectrum of Compound **90**.

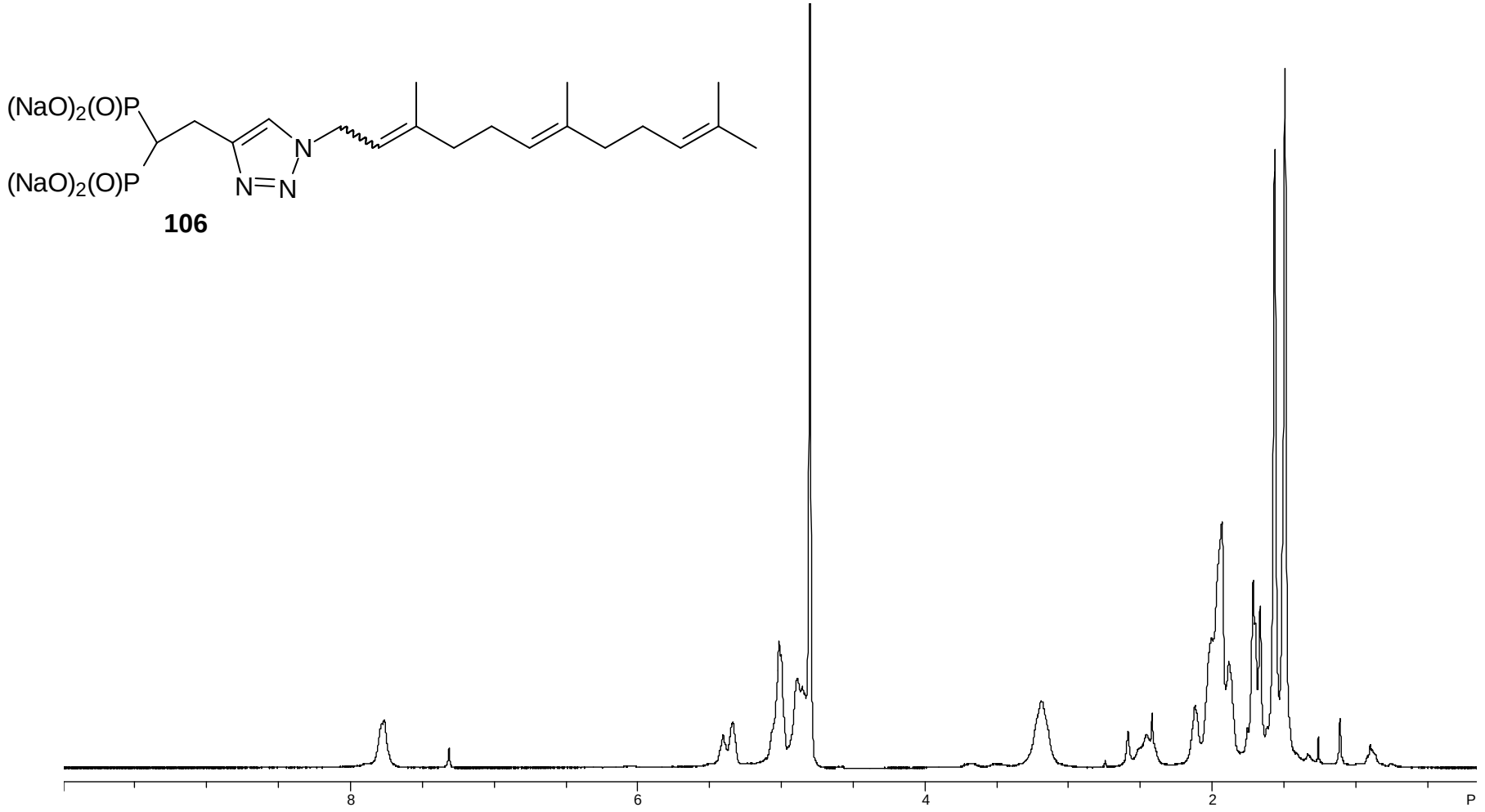

Figure A50. 400 MHz ^{1}H NMR Spectrum of Compound **106**.

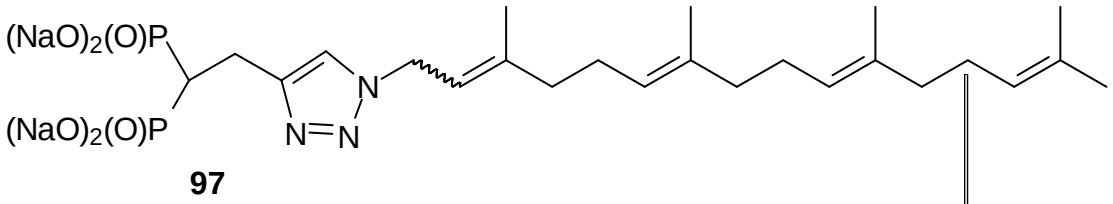

97

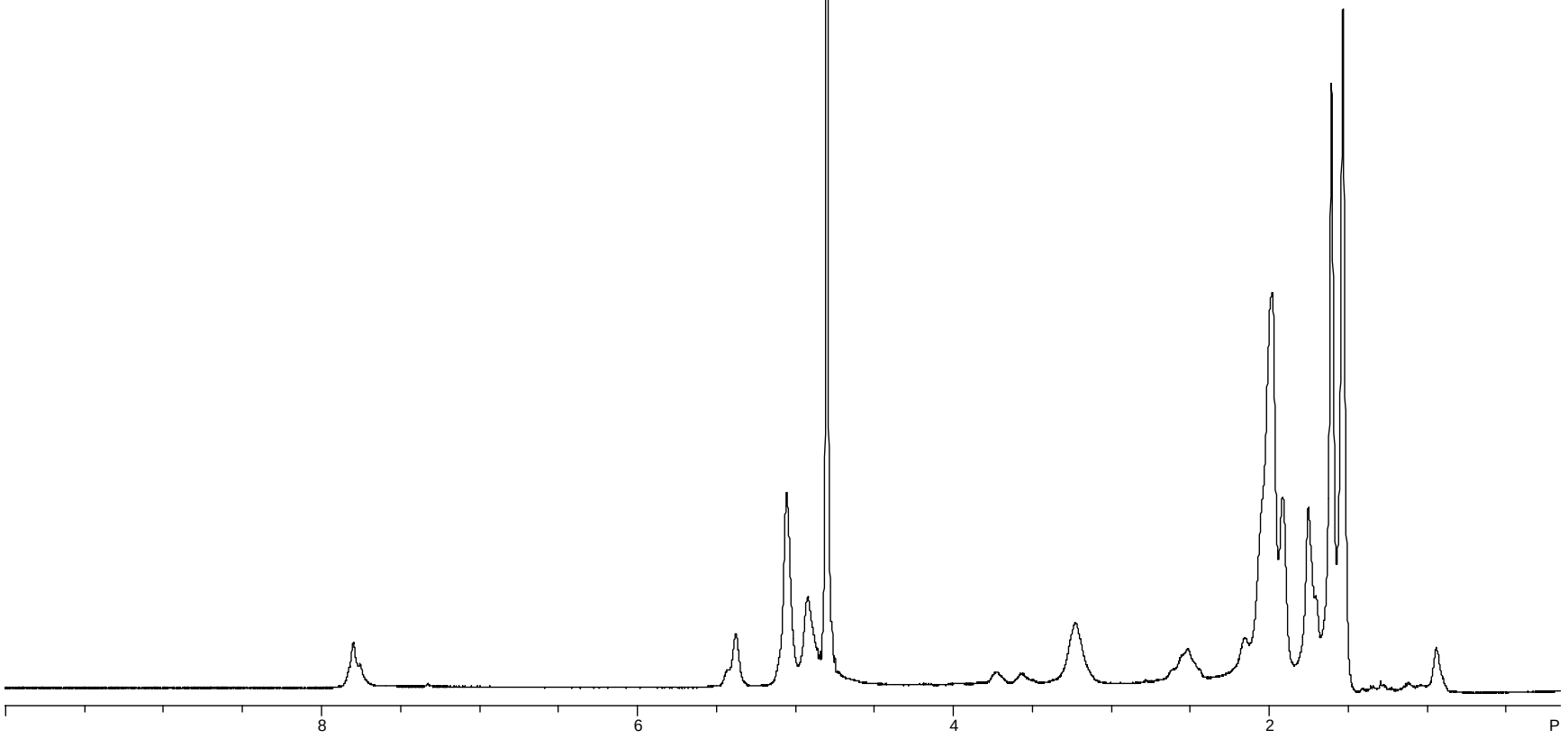

Figure A51. 500 MHz ^{1}H NMR Spectrum of Compound **97**.

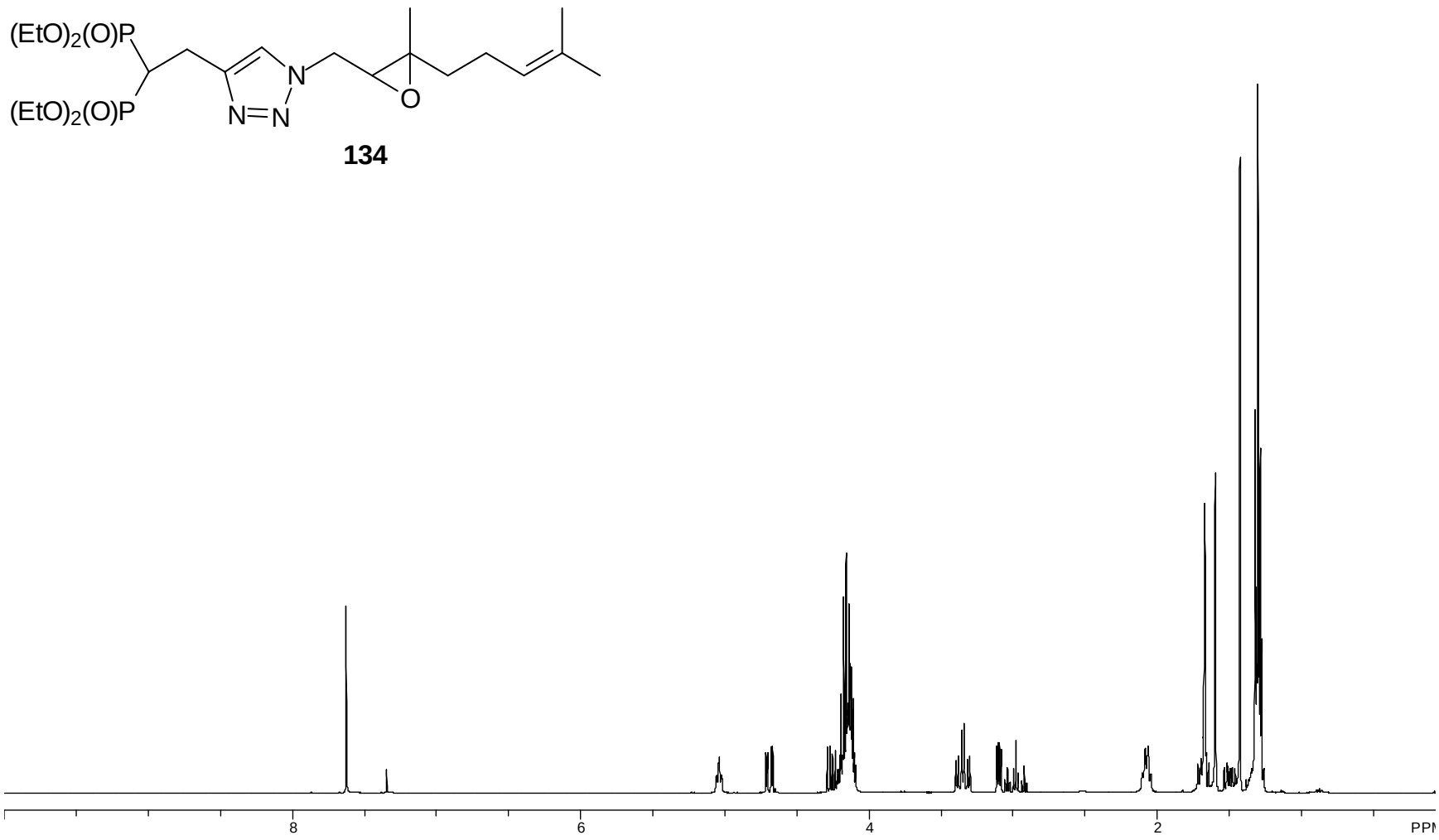

134

Figure A52. 400 MHz ^{1}H NMR Spectrum of Compound **134**.

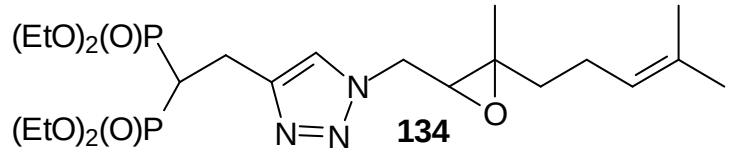

134

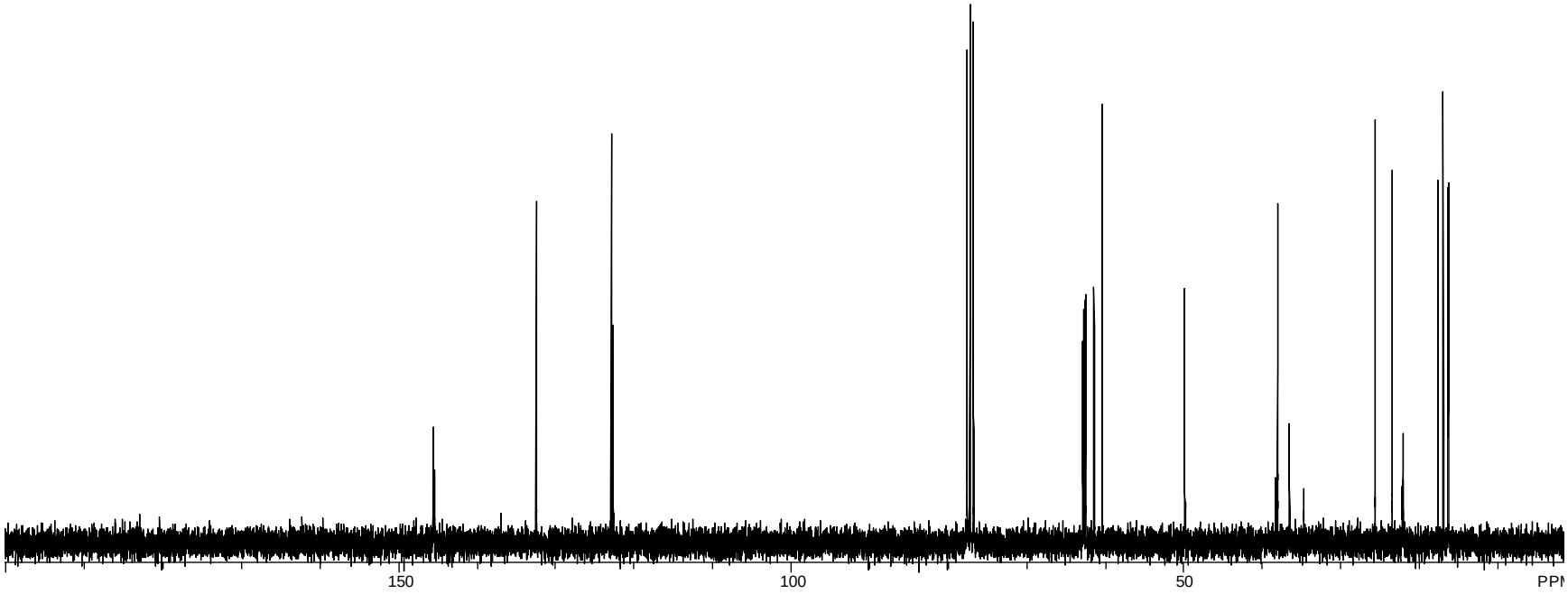

Figure A53. 75 MHz ^{13}C NMR Spectrum of Compound **134**.

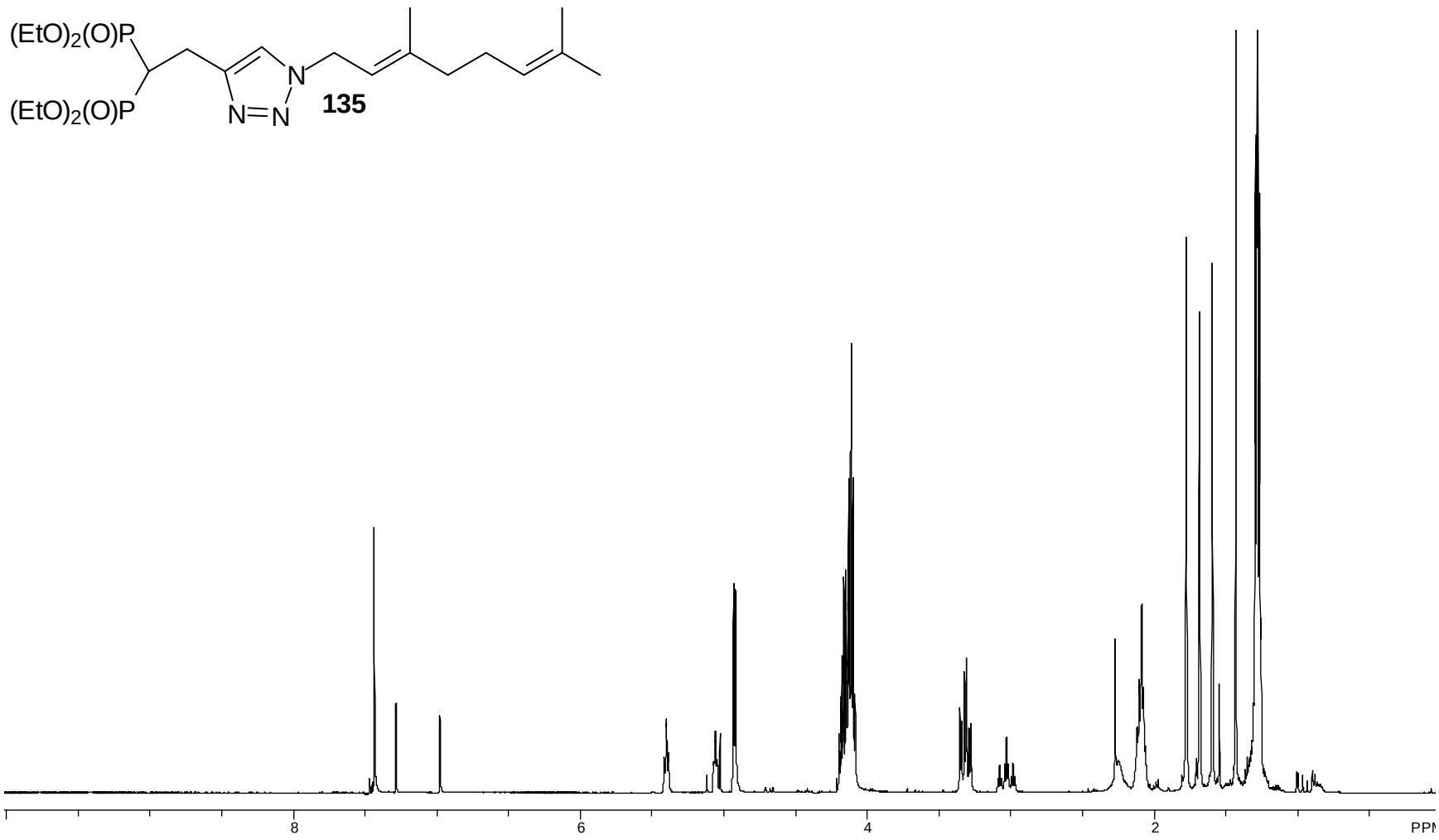

Figure A54. 500 MHz ^{1}H NMR Spectrum of Compound **135**.

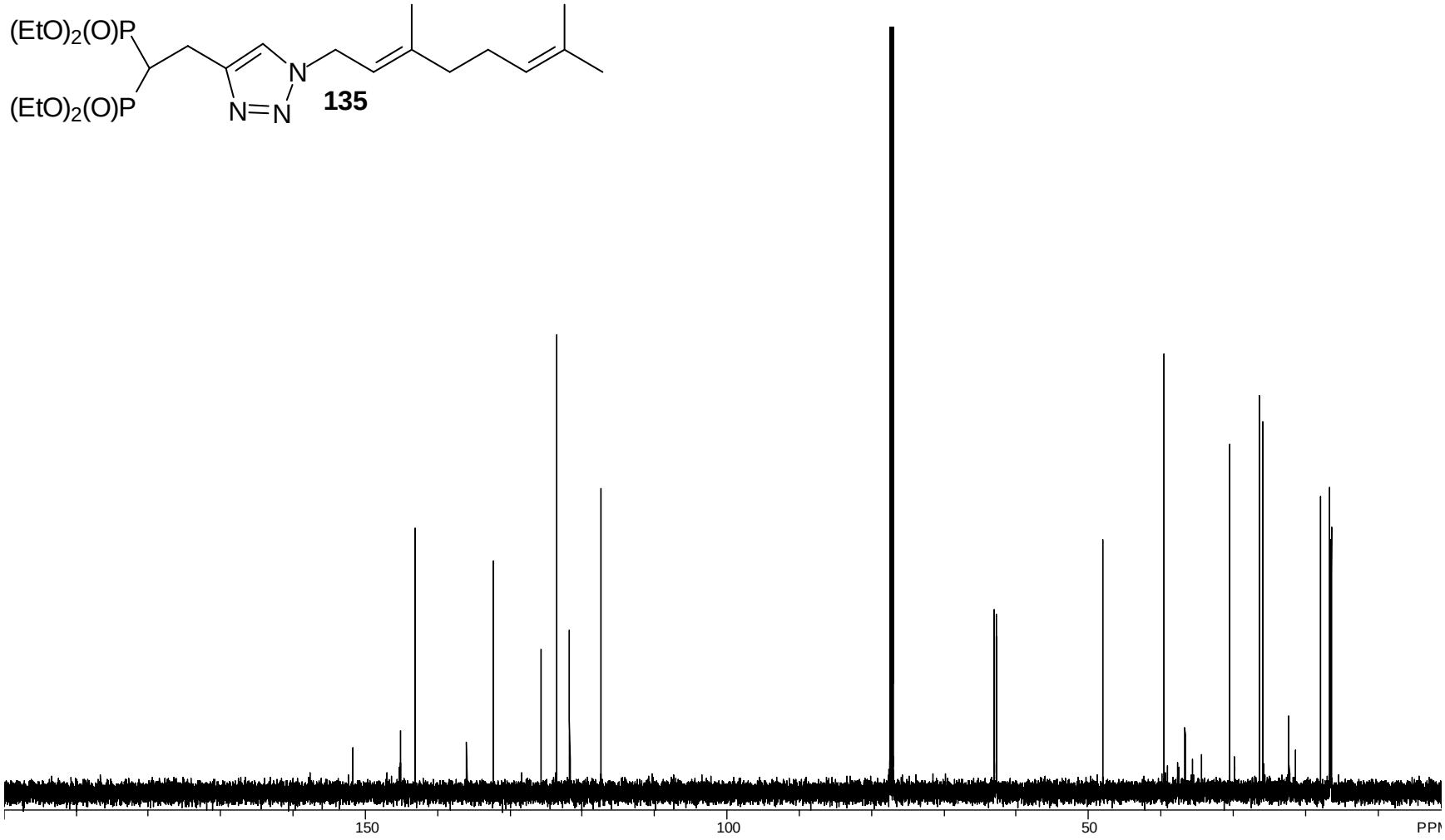

Figure A55. 125 MHz ^{13}C NMR Spectrum of Compound **135**.

Figure A56. 500 MHz ^{1}H NMR Spectrum of Compound **136**.

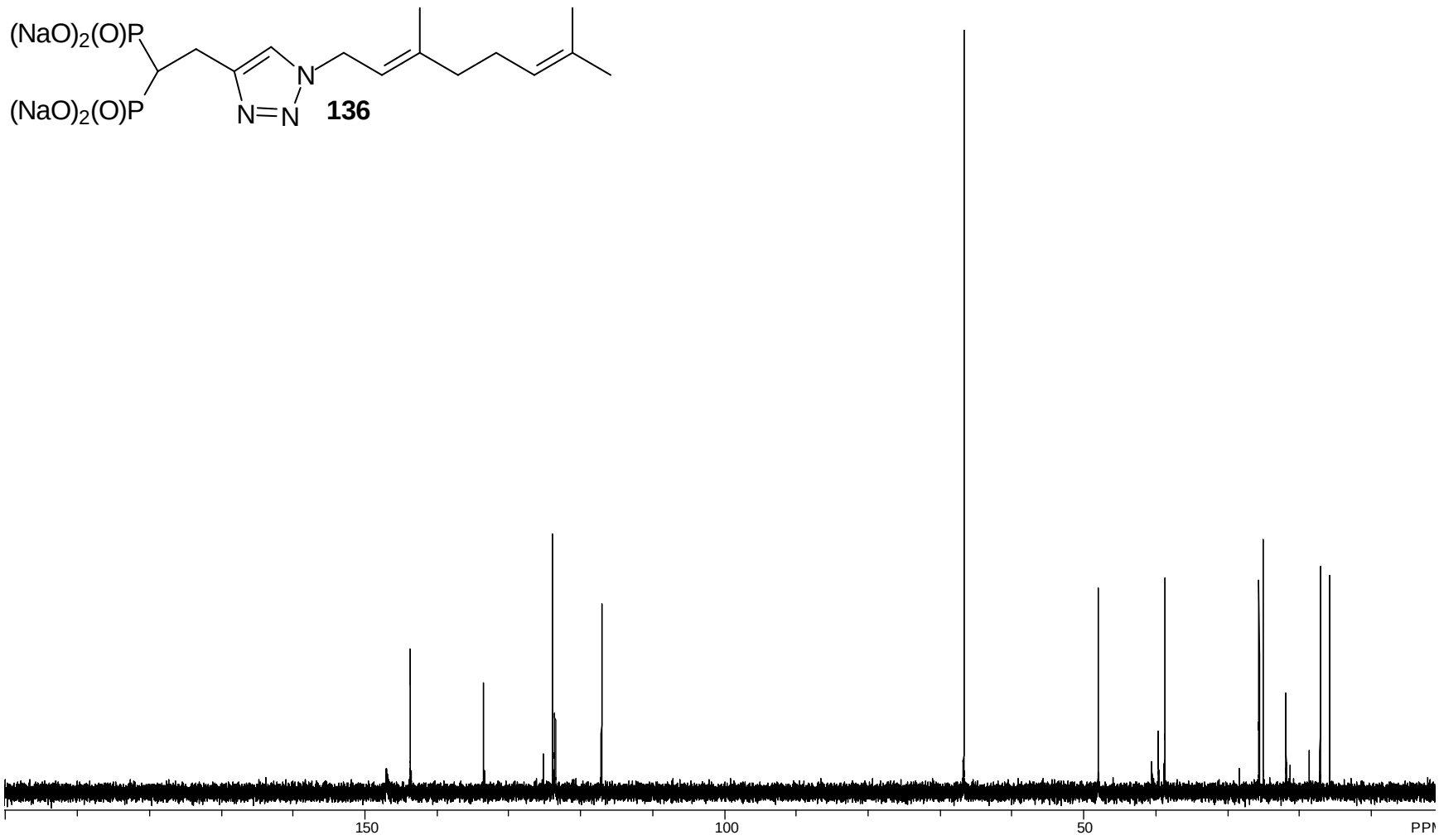

Figure A57. 125 MHz ^{13}C NMR Spectrum of Compound **136.**

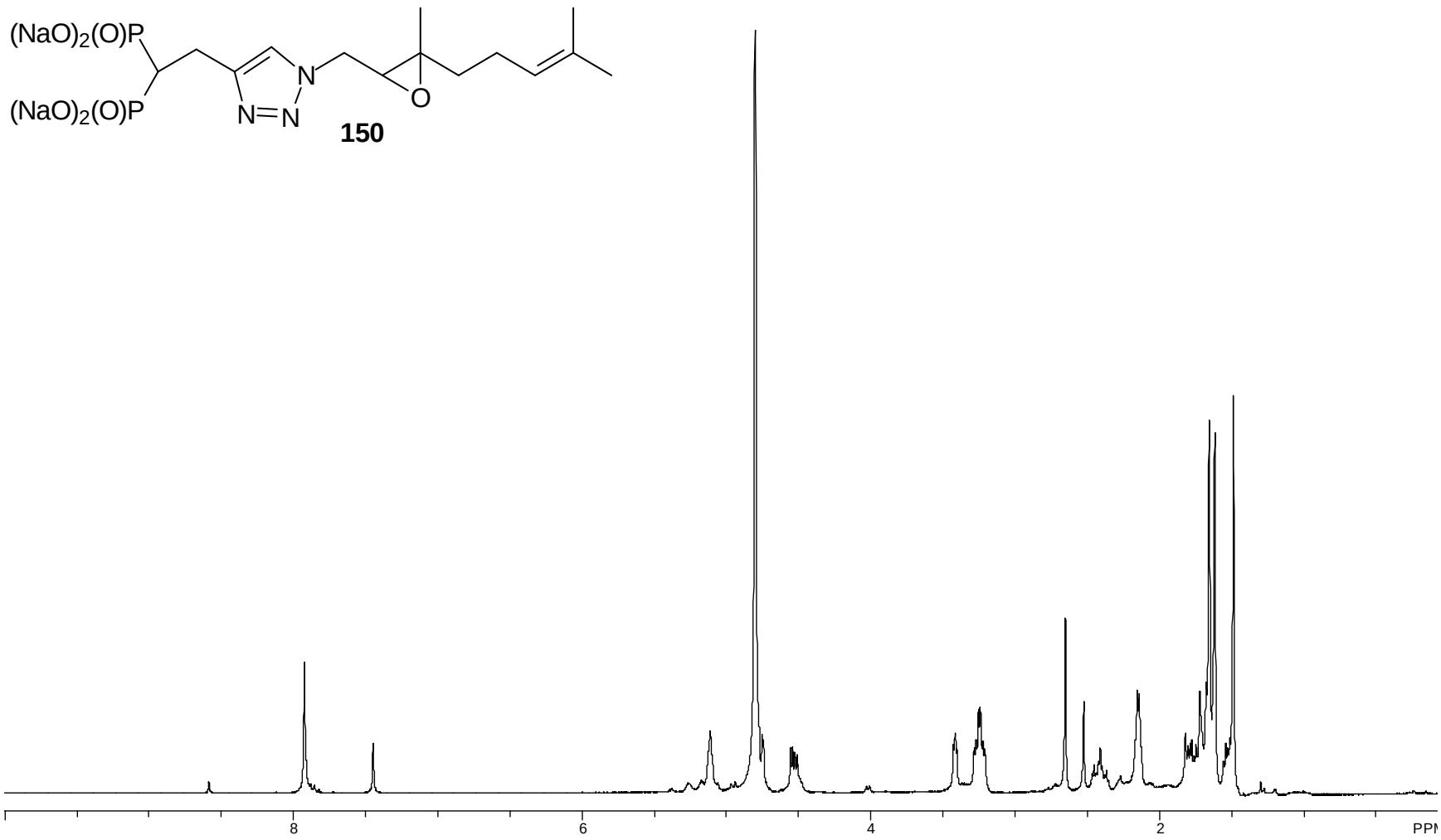

Figure A58. 500 MHz ^{1}H NMR Spectrum of Compound **150**.

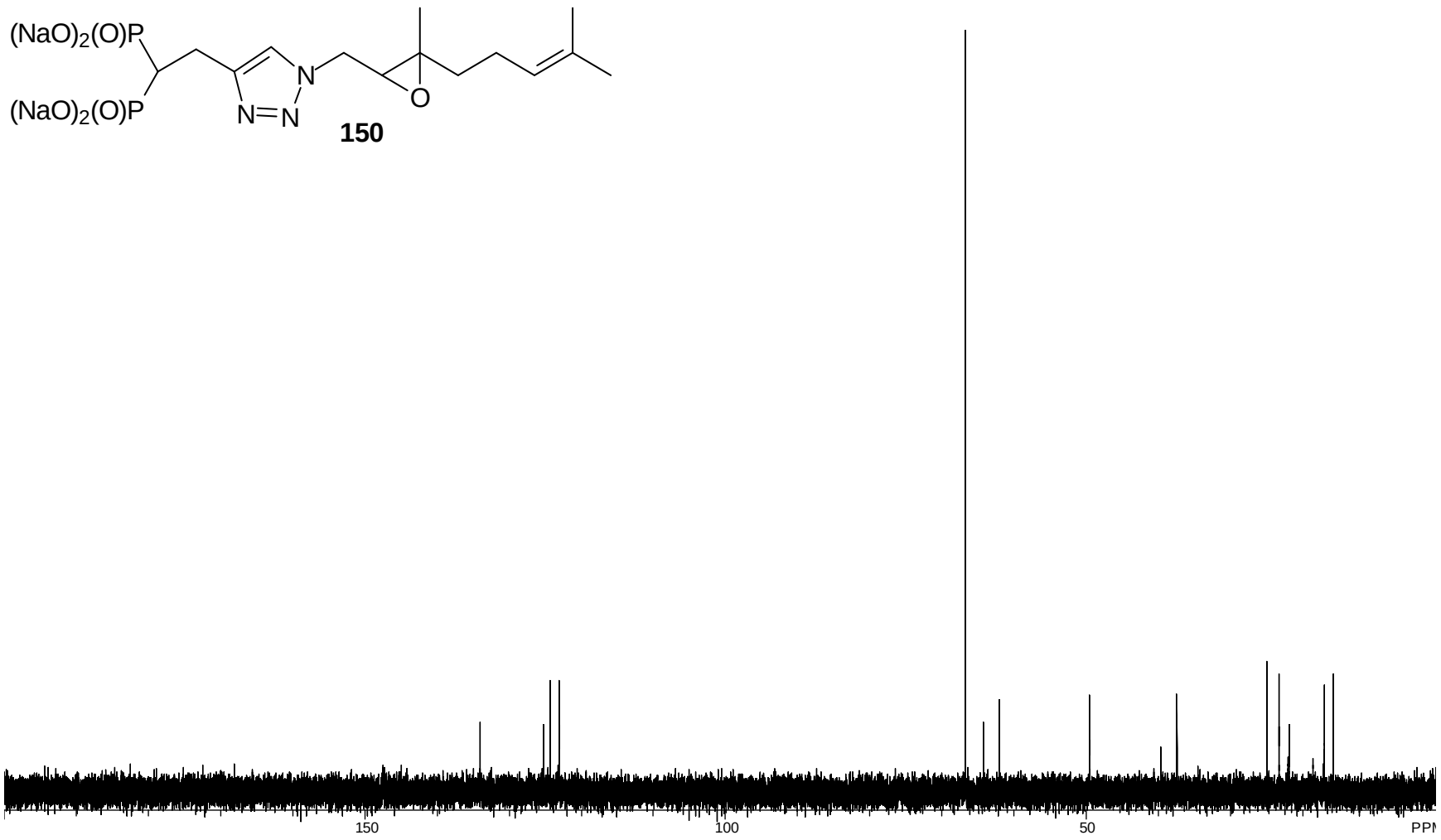

Figure A59. 125 MHz ^{13}C NMR Spectrum of Compound **150**.

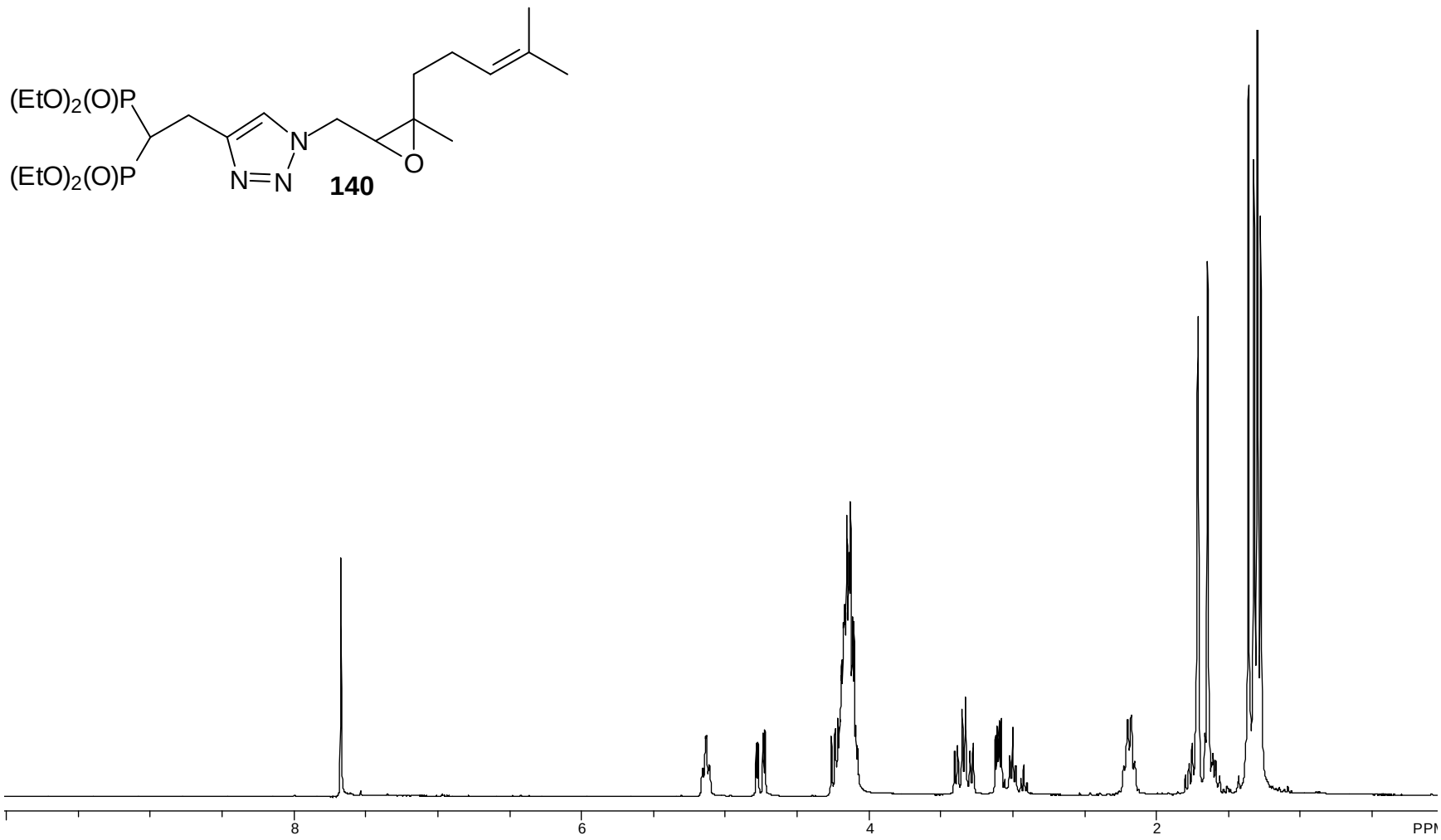

Figure A60. 300 MHz ^{1}H NMR Spectrum of Compound **140**.

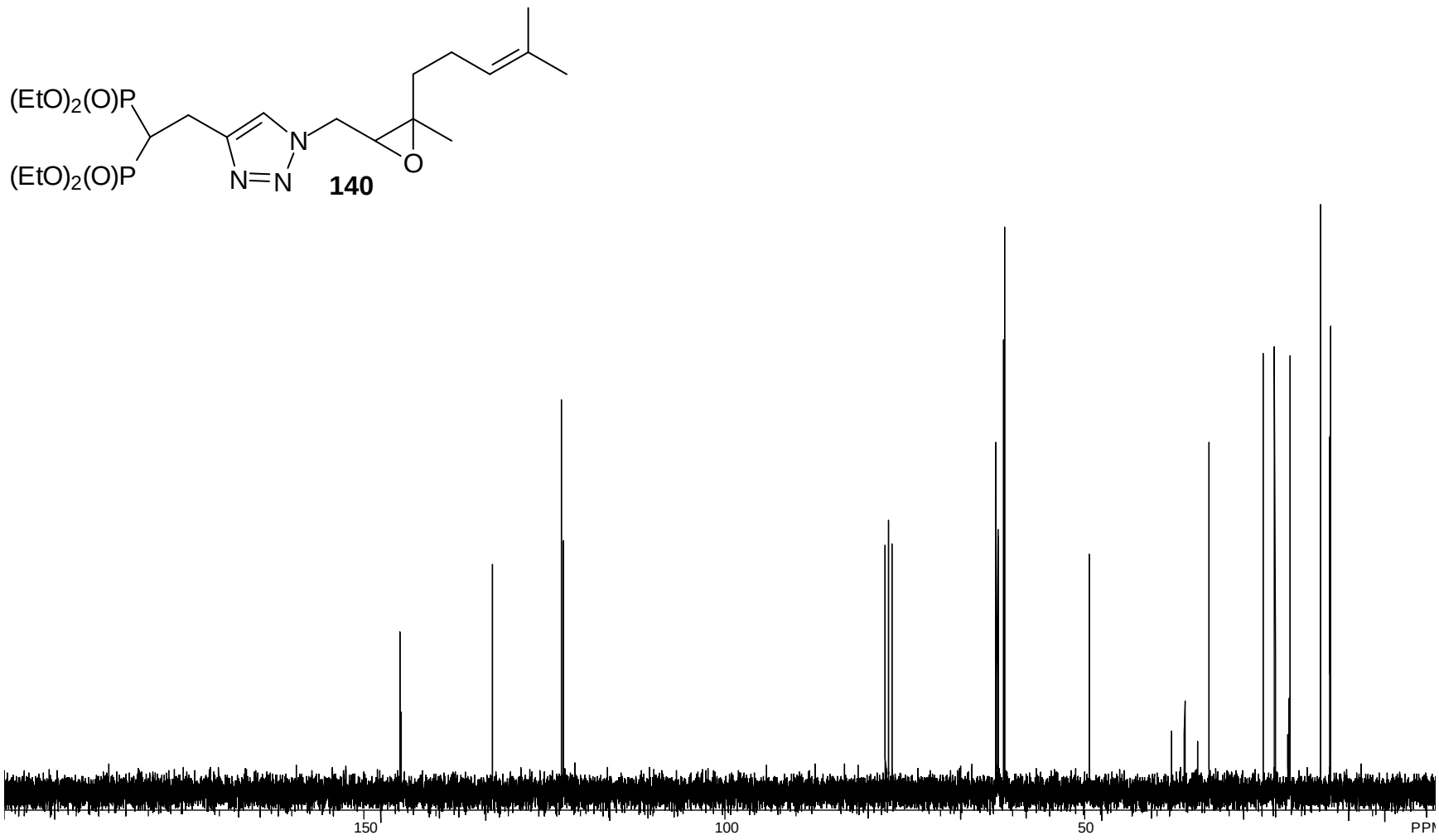

Figure A61. 75 MHz ^{13}C NMR Spectrum of Compound **140**.

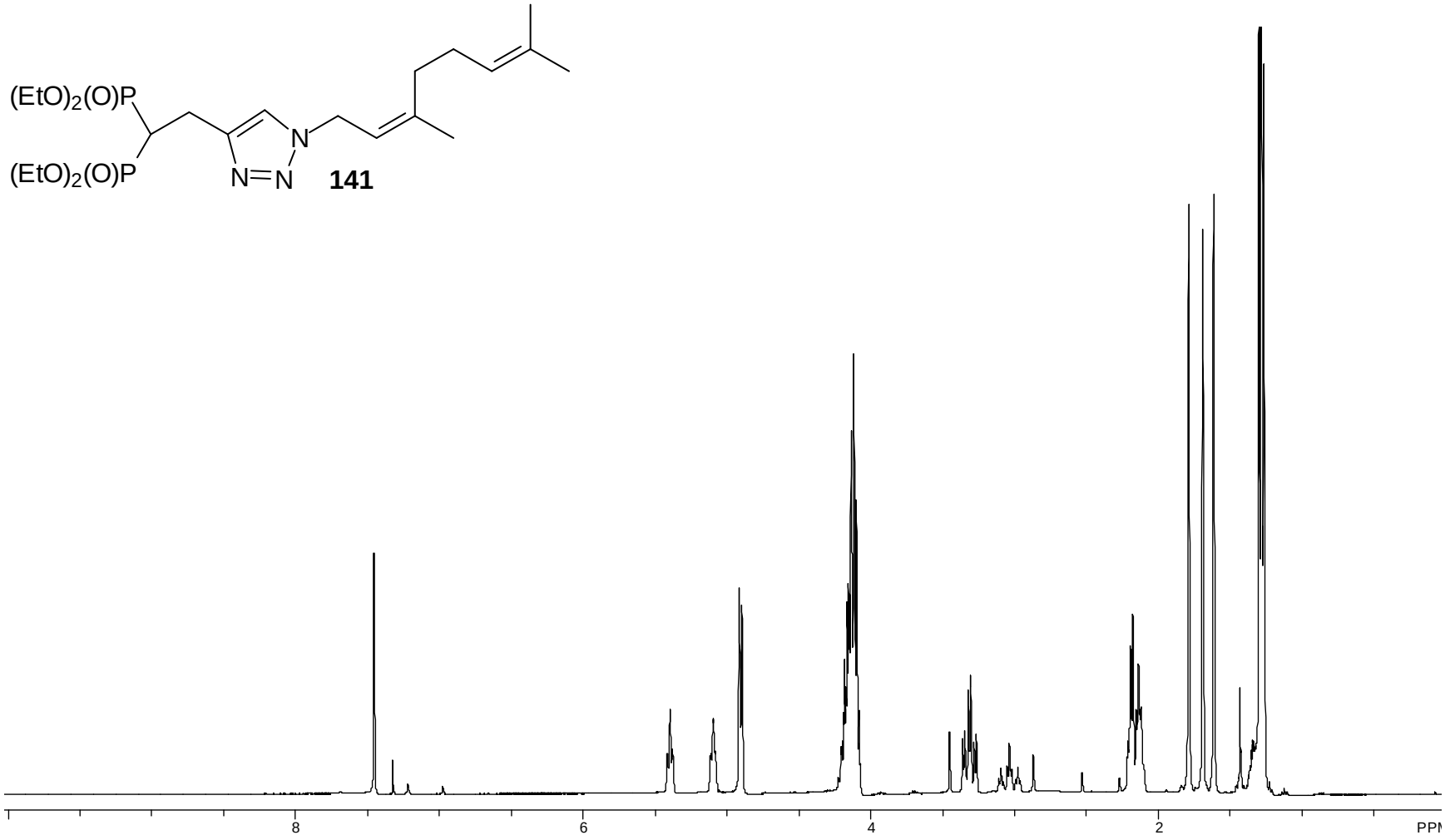

Figure A62. 400 MHz ^{1}H NMR Spectrum of Compound **141**.

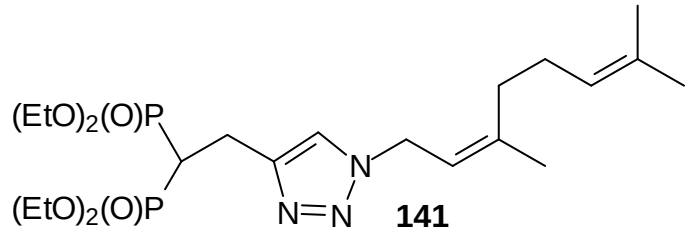

141

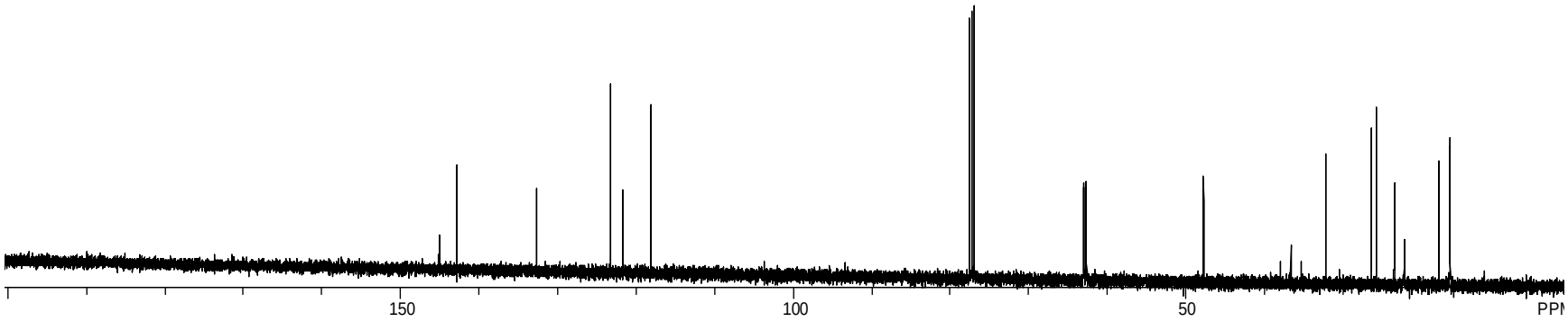

Figure A63. 100 MHz ^{13}C NMR Spectrum of Compound **141**.

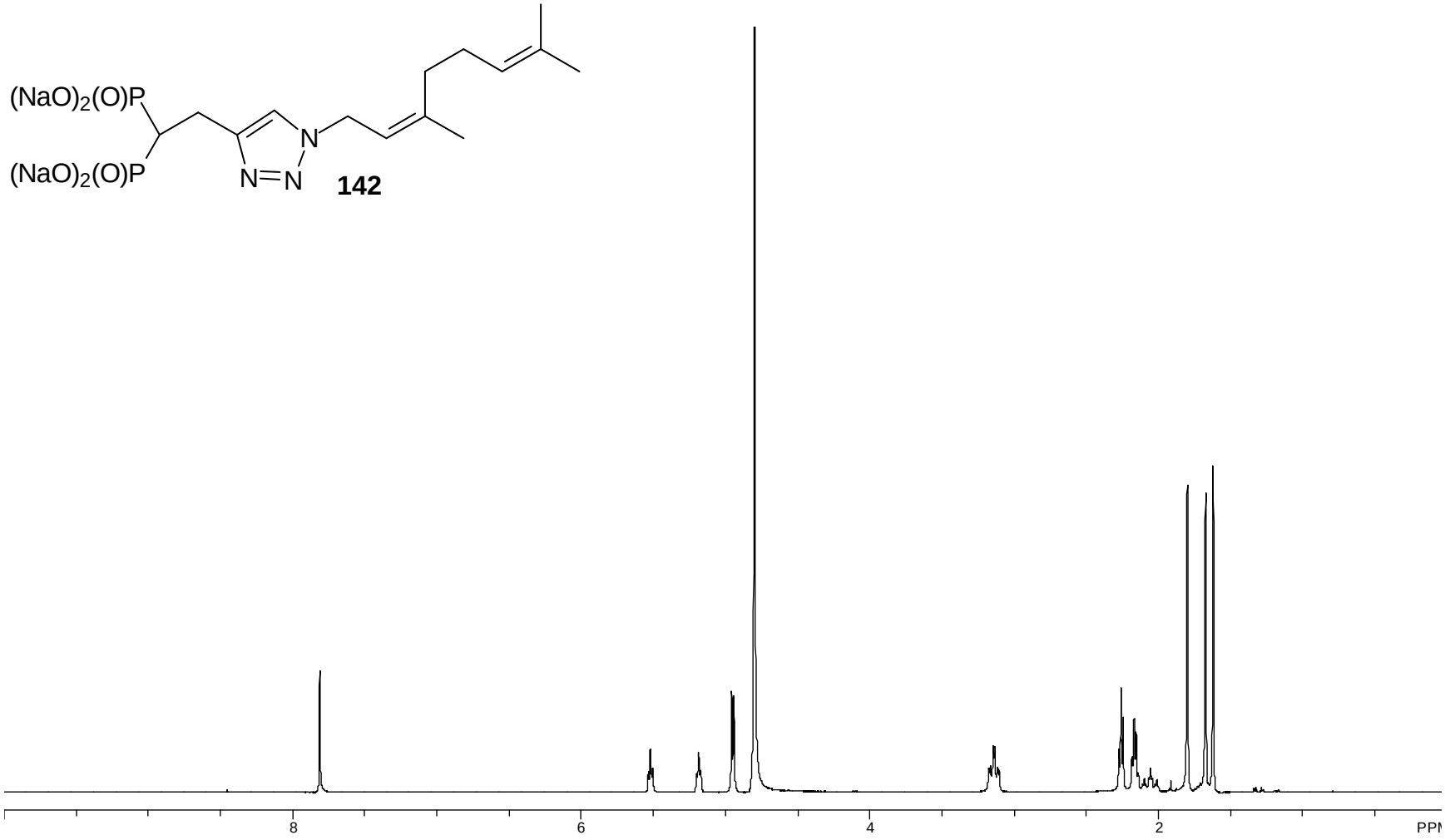

Figure A64. 500 MHz ^{1}H NMR Spectrum of Compound **142**.

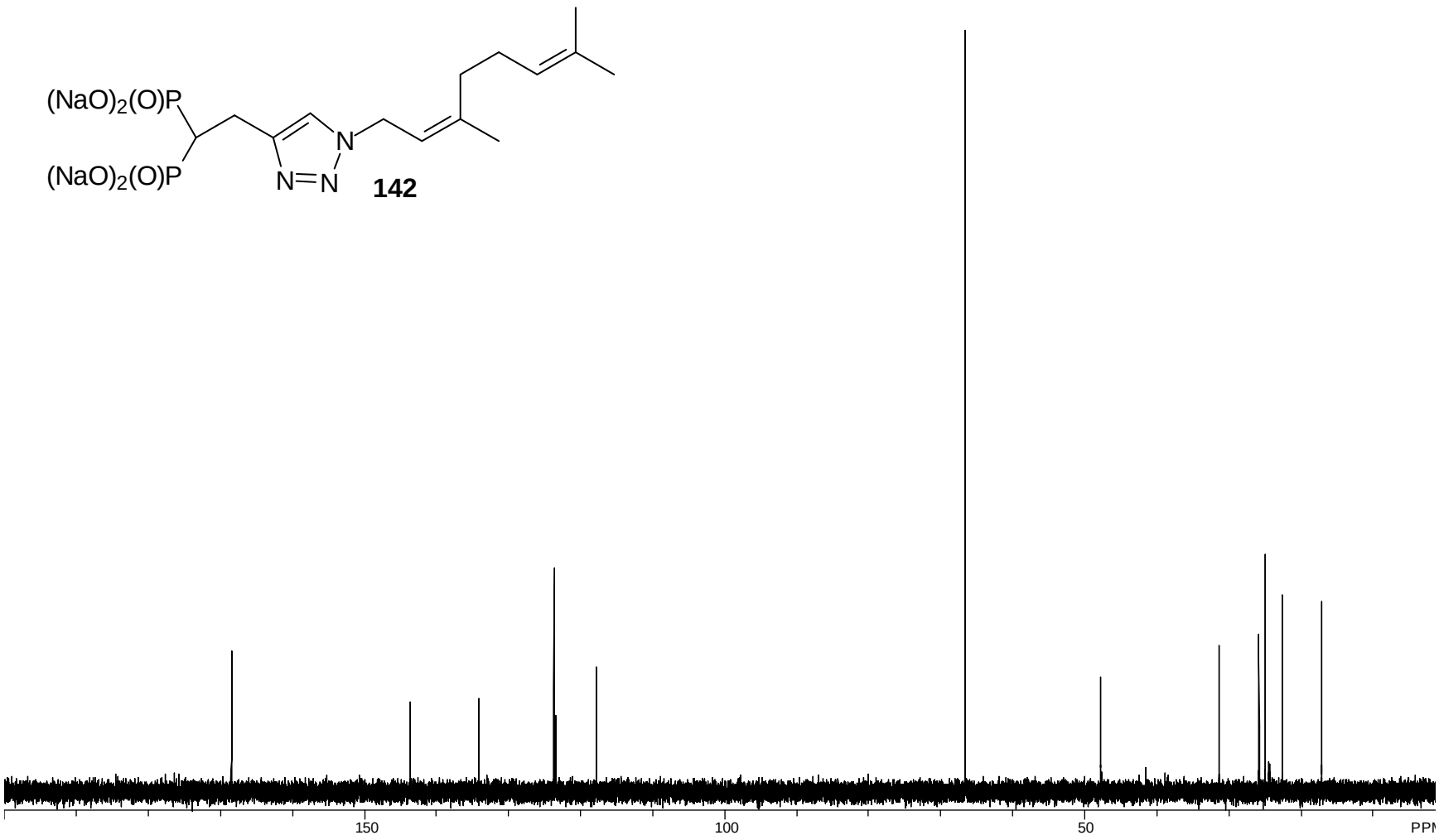

Figure A65. 125 MHz ^{13}C NMR Spectrum of Compound **142**.

Figure A66. 500 MHz ^{1}H NMR Spectrum of Compound **147**.

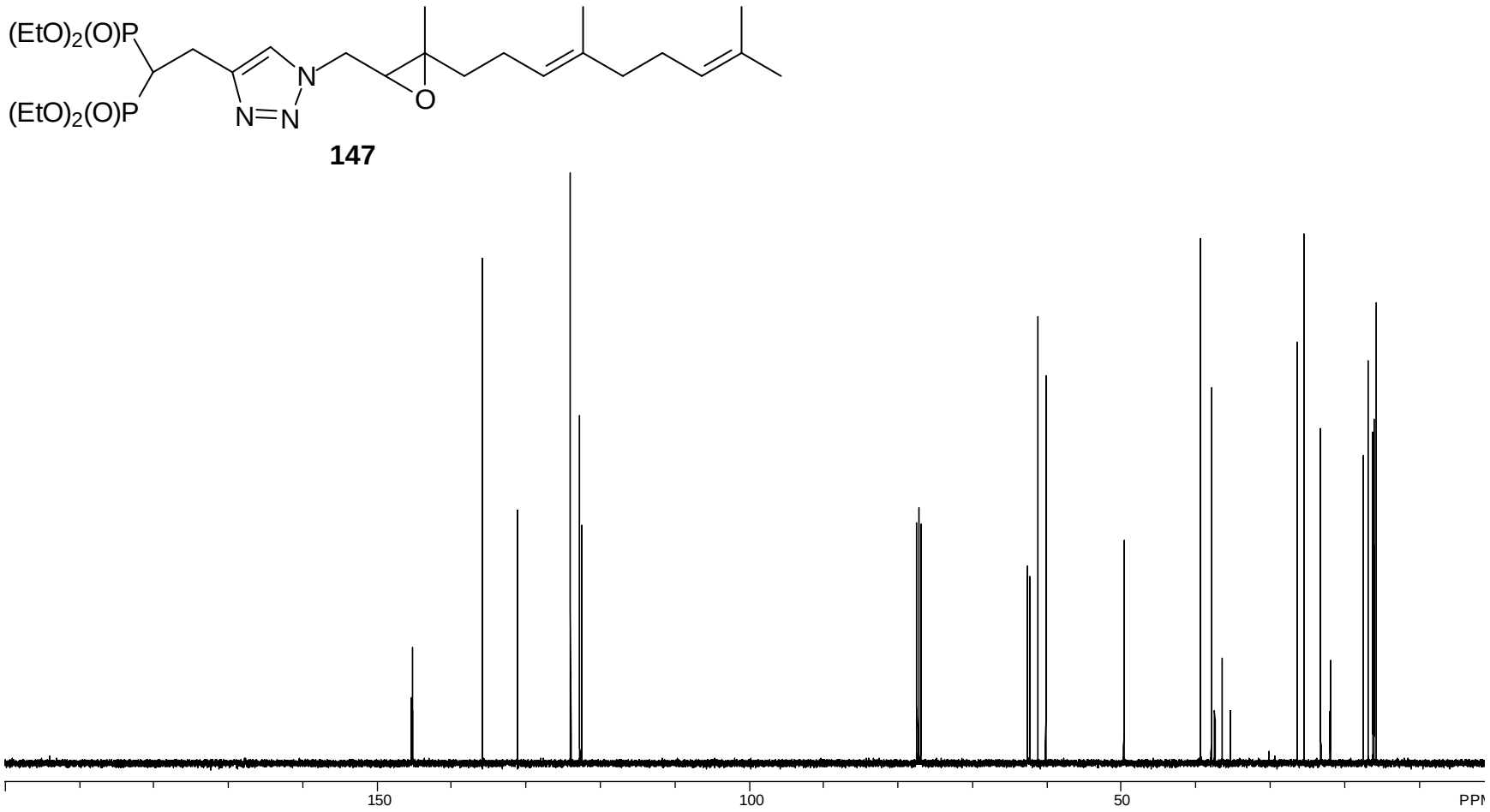

Figure A67. 125 MHz ^{13}C NMR Spectrum of Compound **147**.

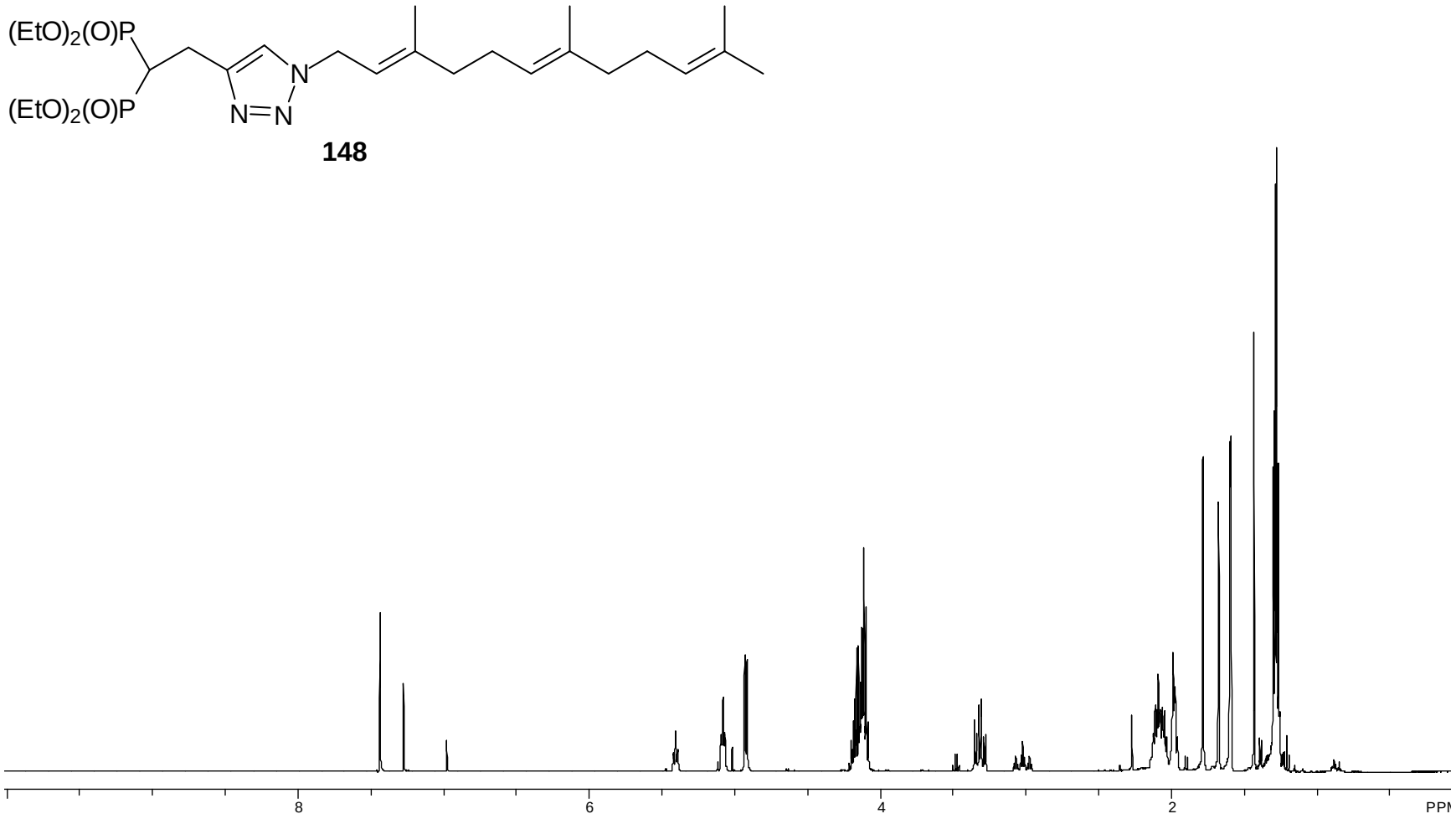

148

Figure A68. 500 MHz ^{1}H NMR Spectrum of Compound **148**.

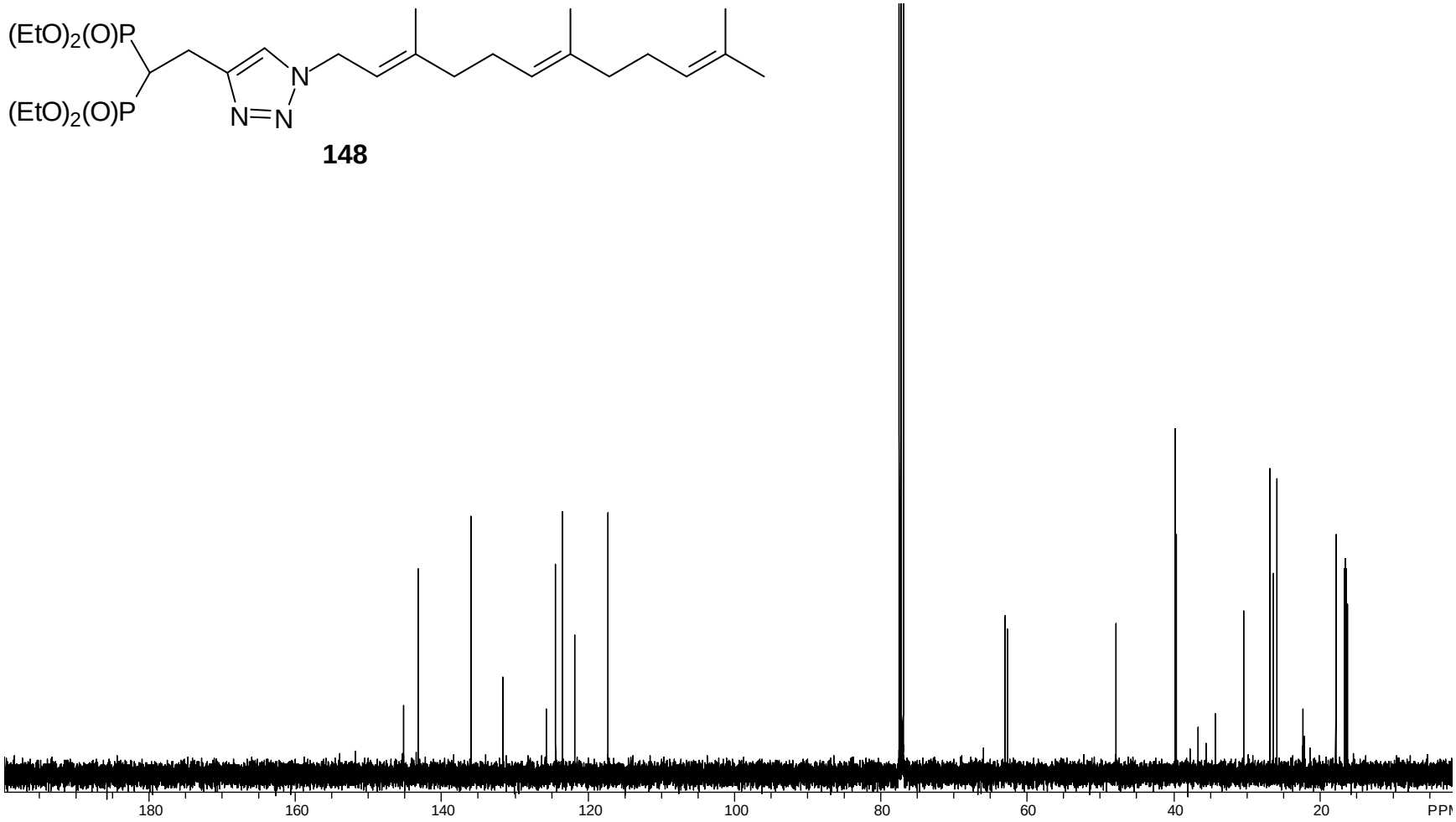

Figure A69. 125 MHz ^{13}C NMR Spectrum of Compound **148**.

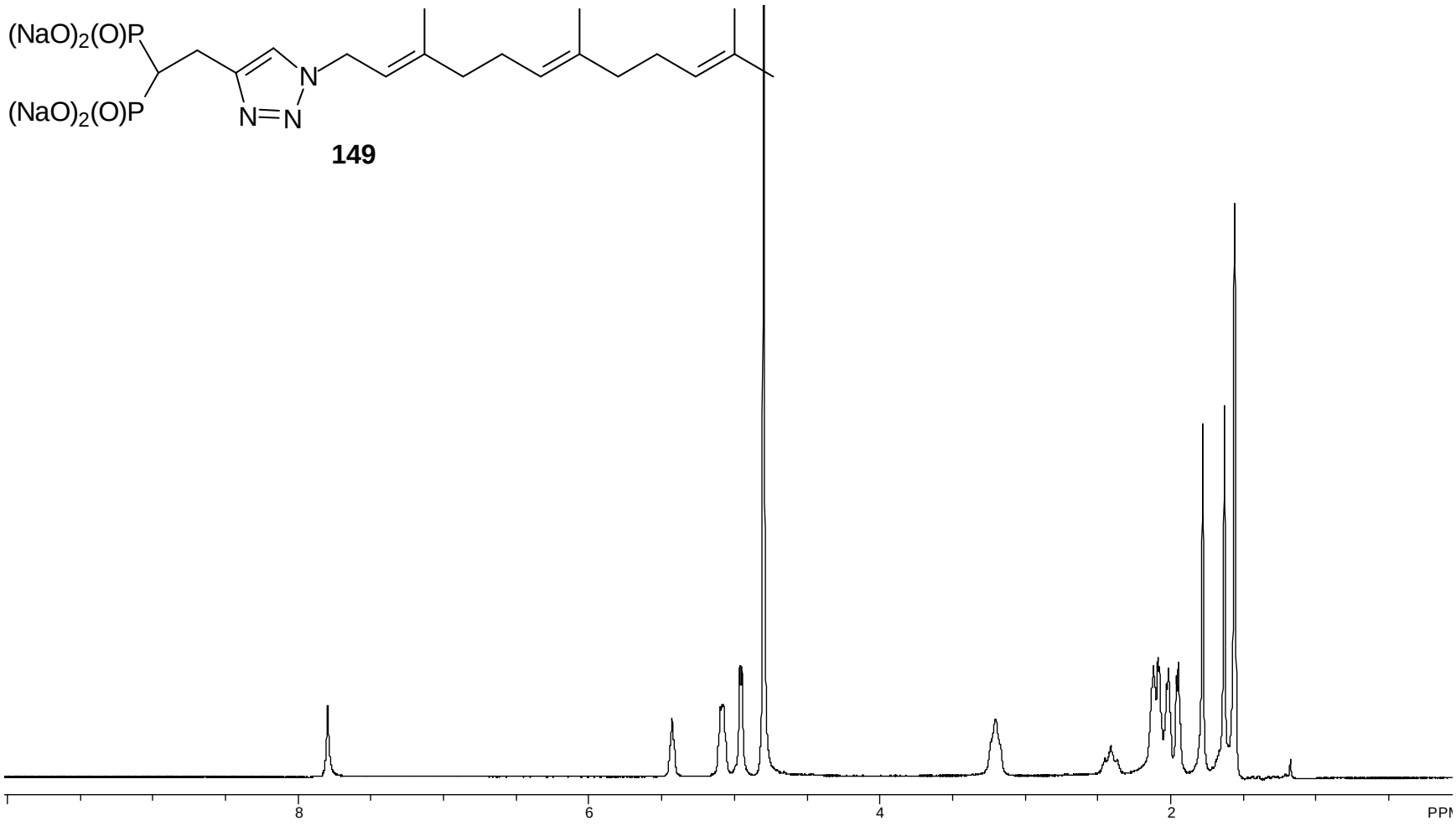

149

Figure A70. 500 MHz ^{1}H NMR Spectrum of Compound **149**.

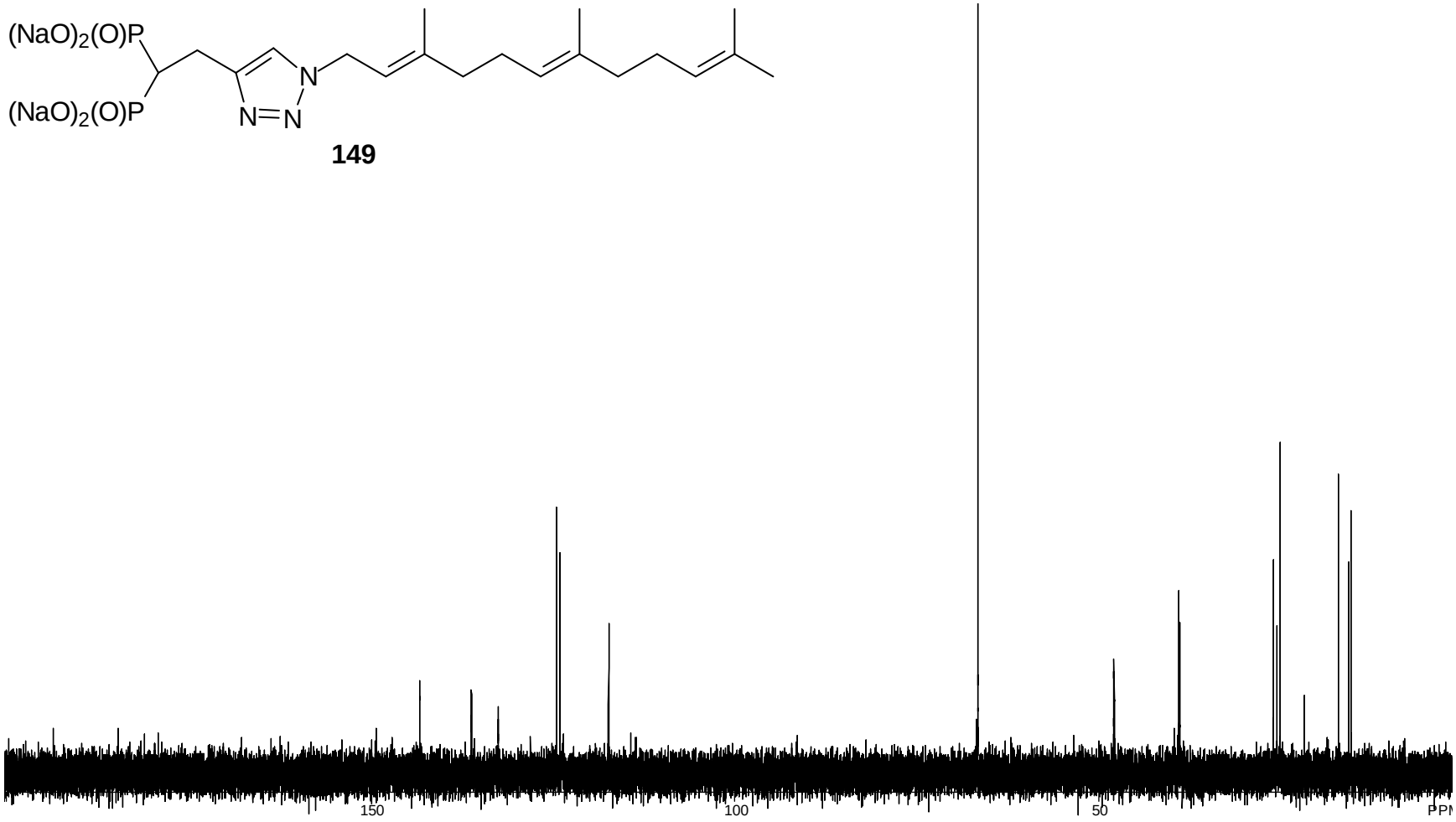

Figure A71. 125 MHz ^{13}C NMR Spectrum of Compound **149**.

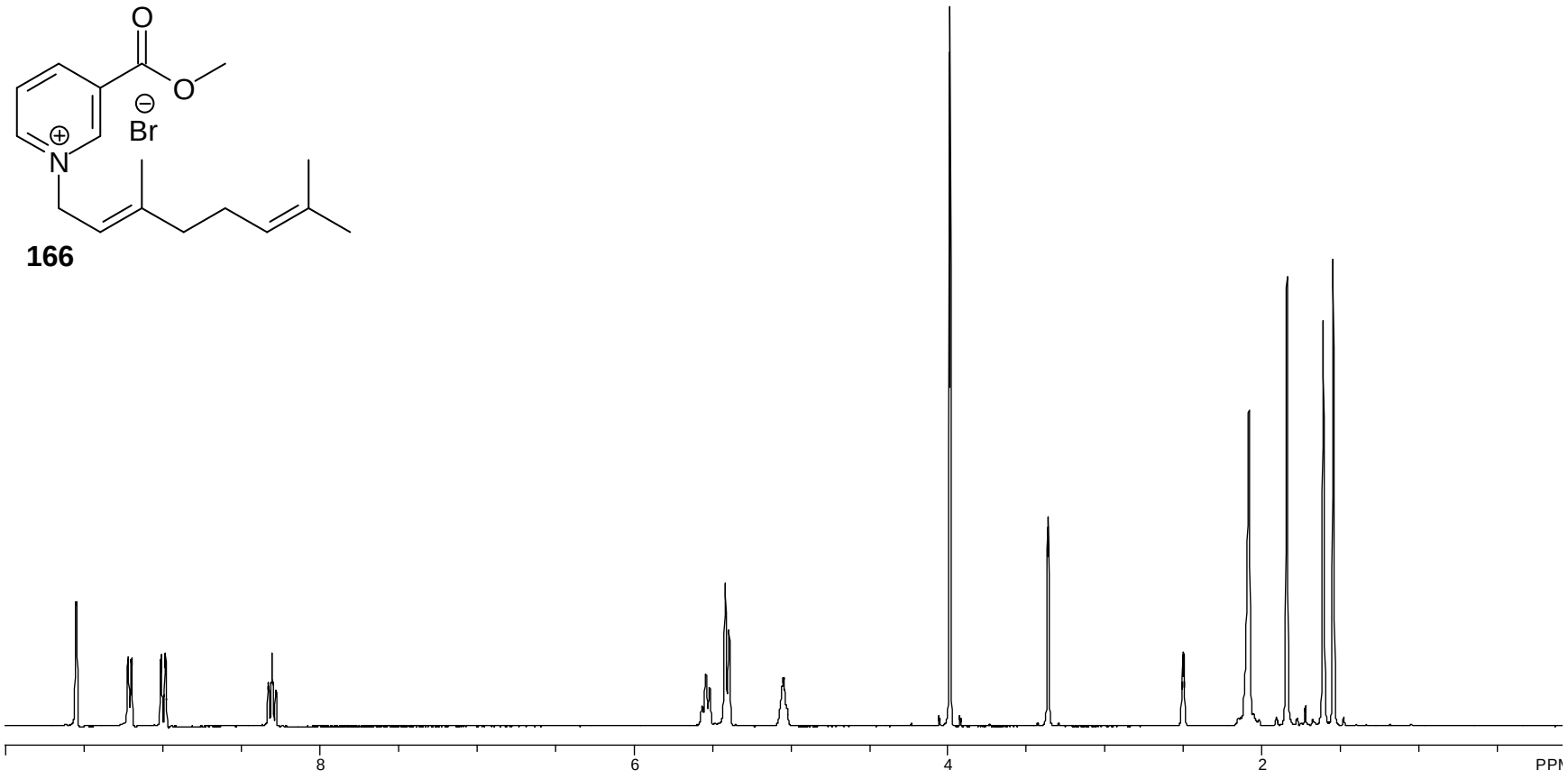

Figure A72. 300 MHz ^{1}H NMR Spectrum of Compound **166**.

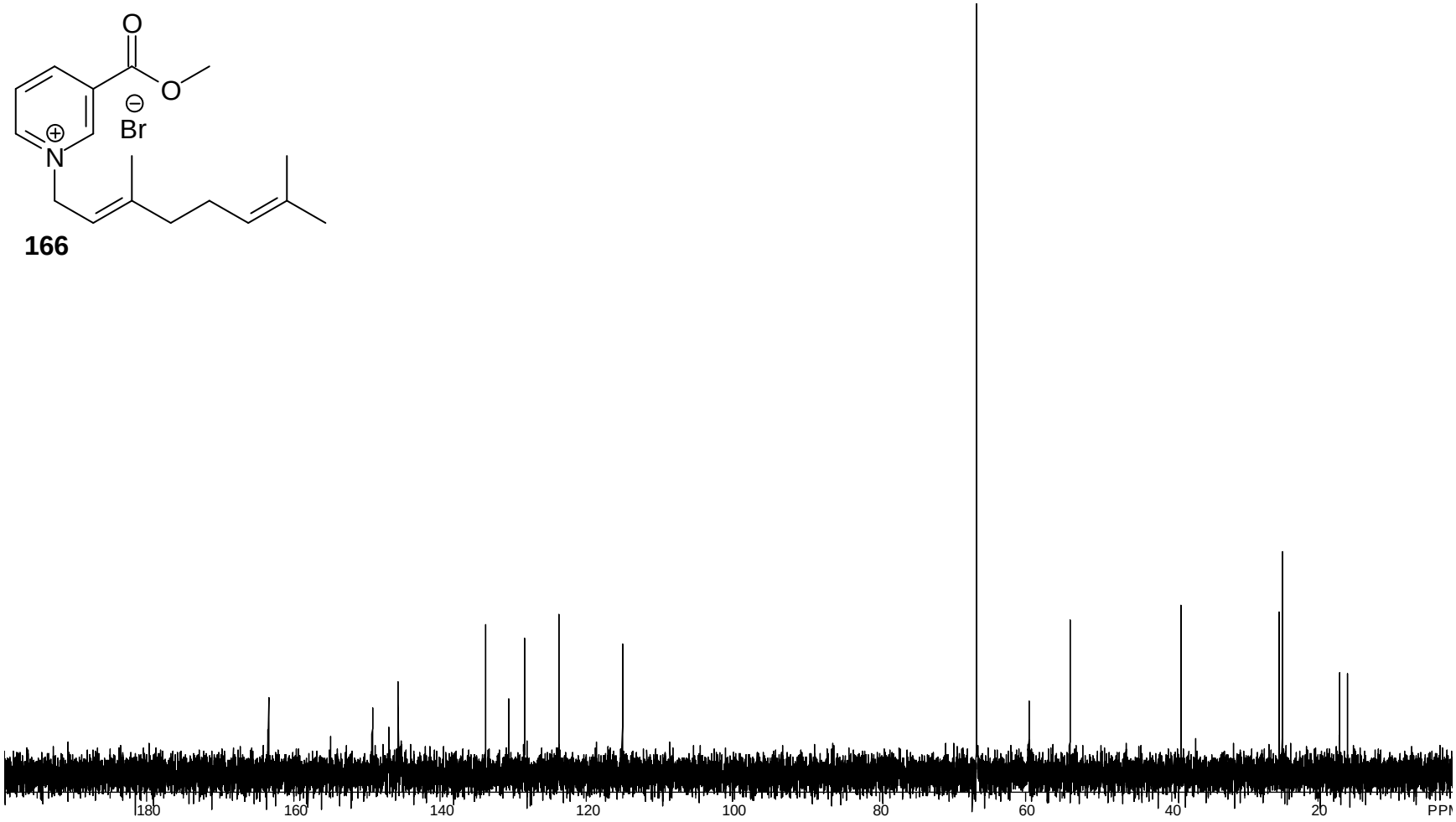

Figure A73. 75 MHz ^{13}C NMR Spectrum of Compound **166**.

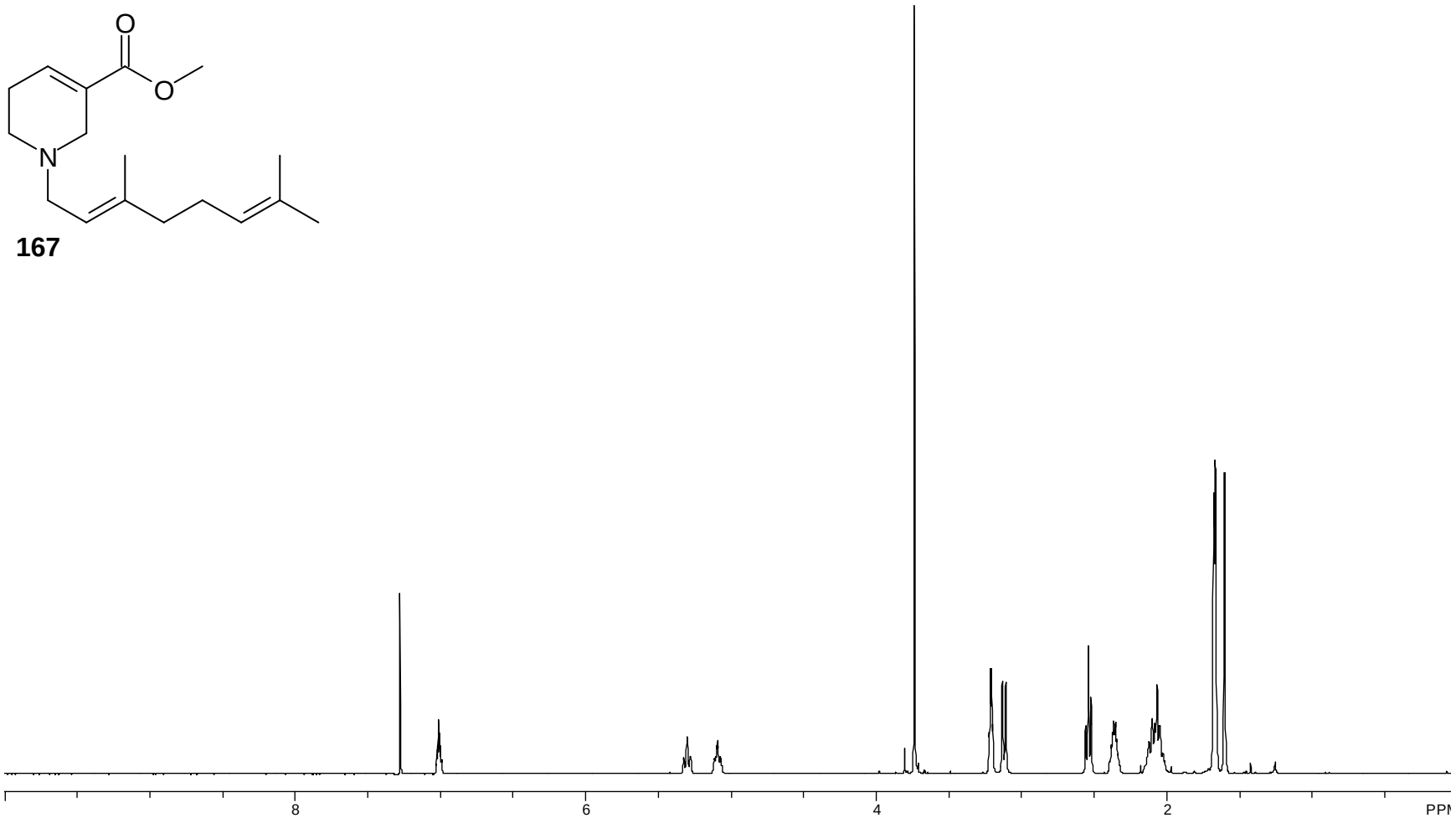

167

Figure A74. 300 MHz ^{1}H NMR Spectrum of Compound **167**.

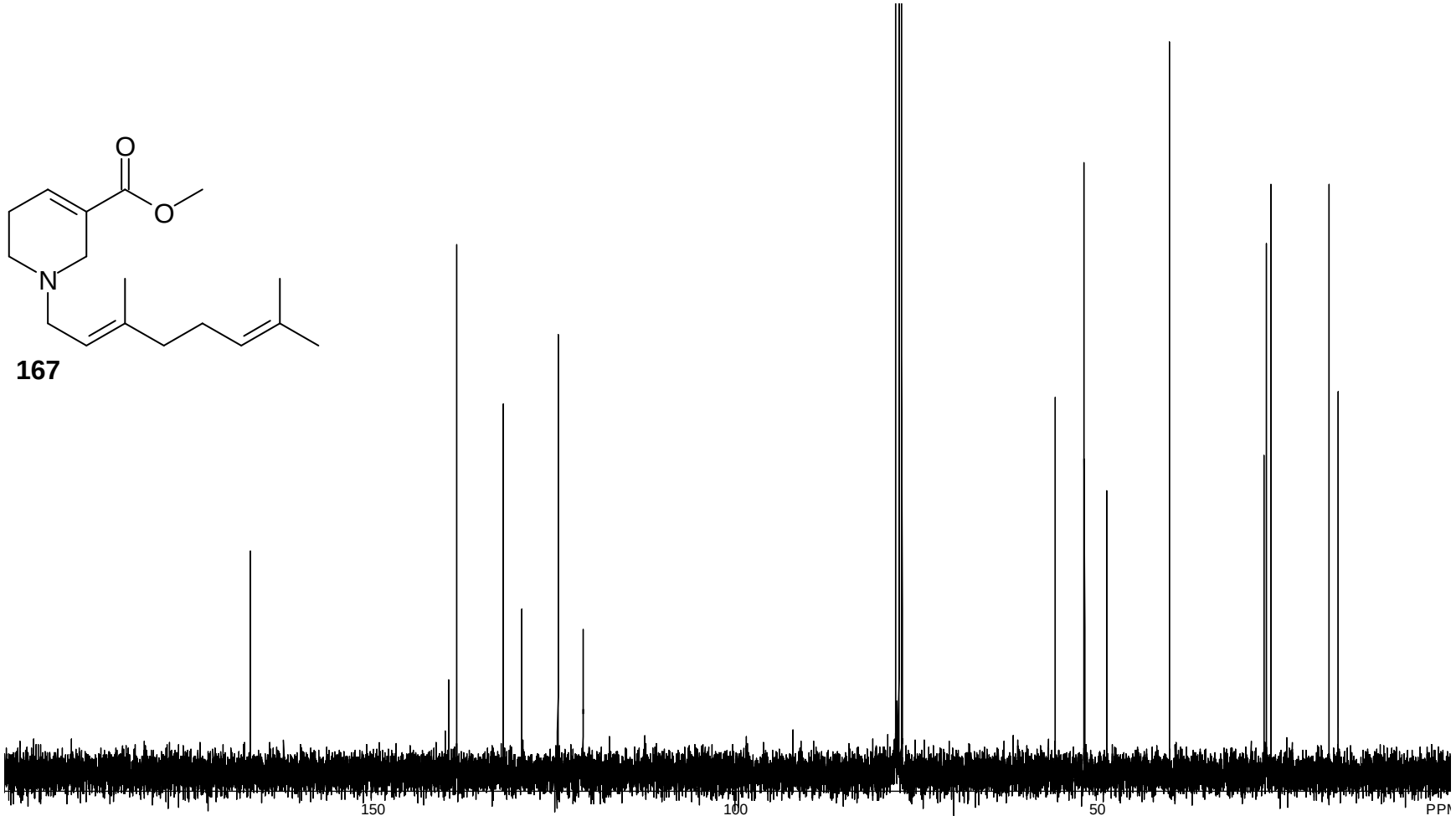

Figure A75. 75 MHz ^{13}C NMR Spectrum of Compound **167**.

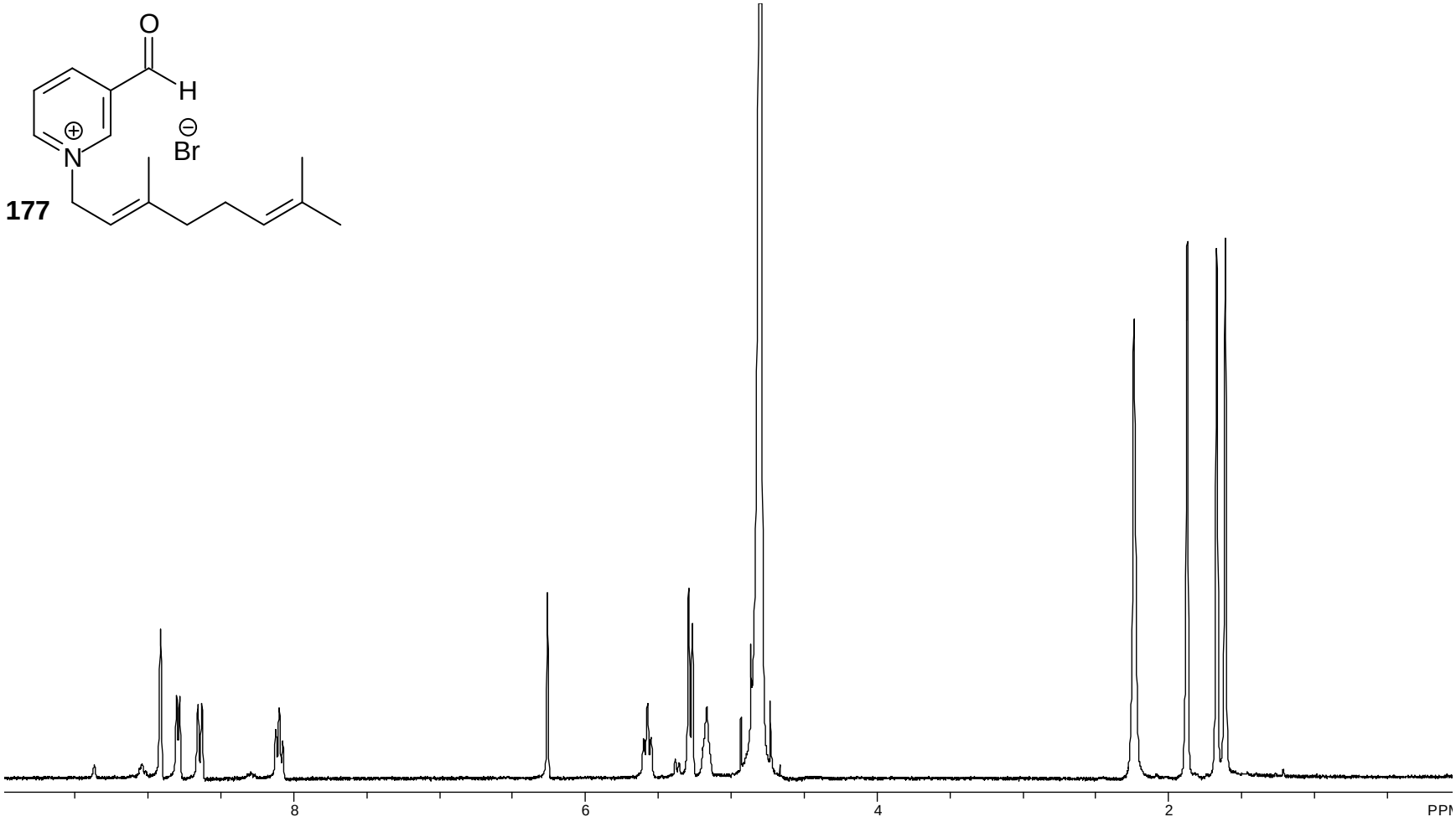

Figure A76. 300 MHz ^{1}H NMR Spectrum of Compound **177**.

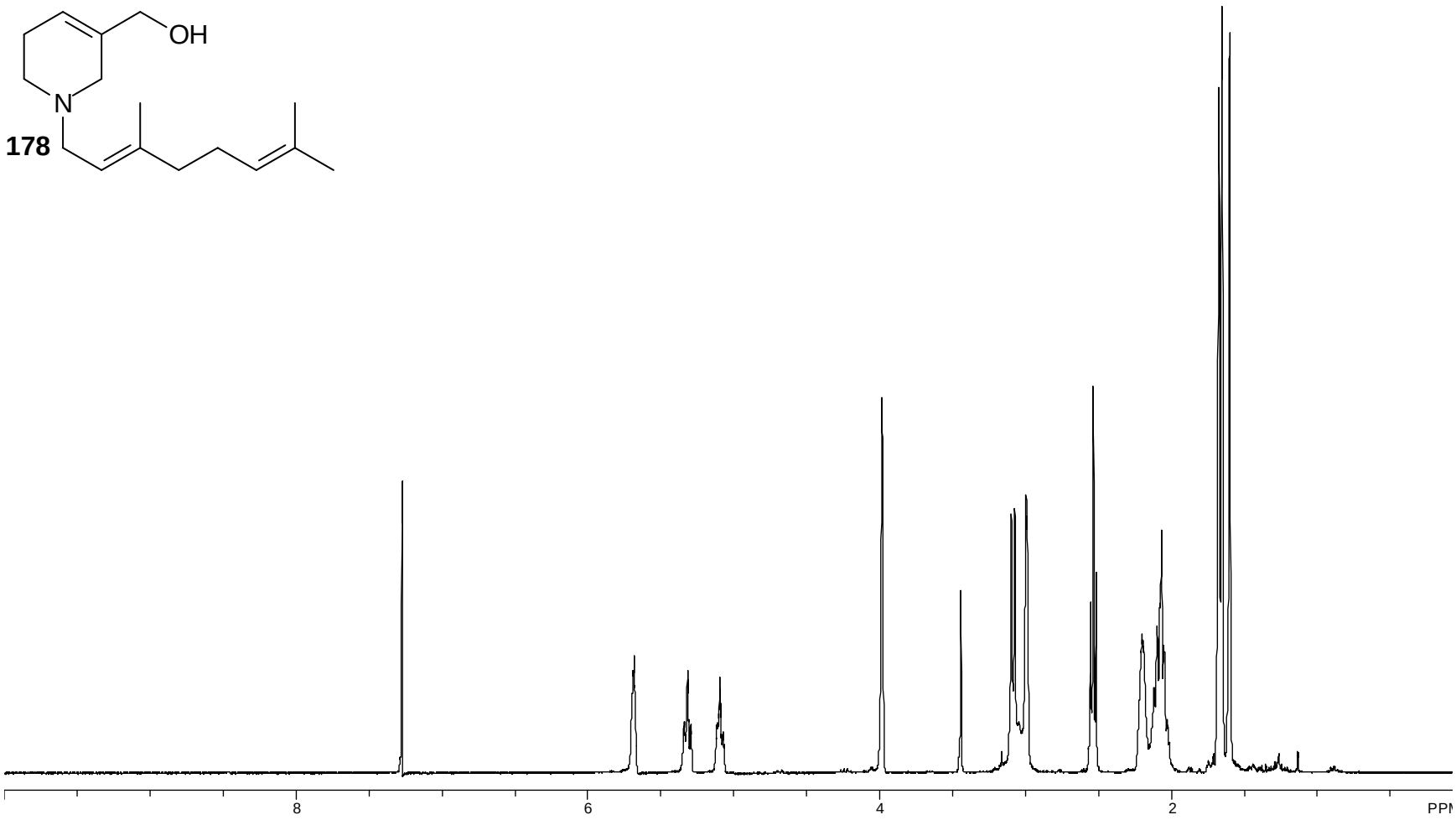

Figure A77. 300 MHz ^{1}H NMR Spectrum of Compound **178**.

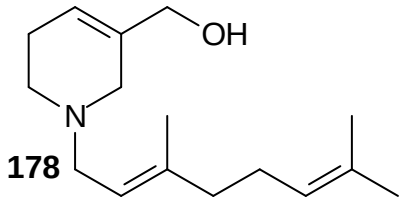

178

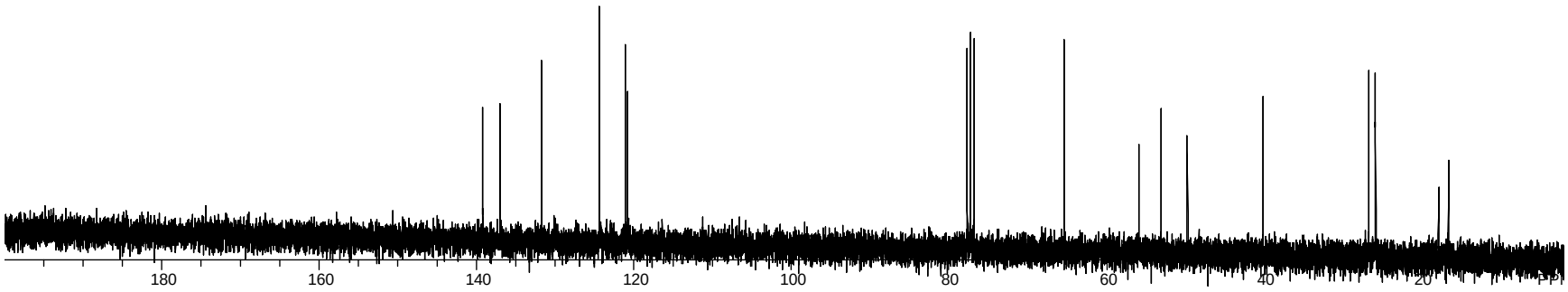

Figure A78. 75 MHz ^{13}C NMR Spectrum of Compound **178**.

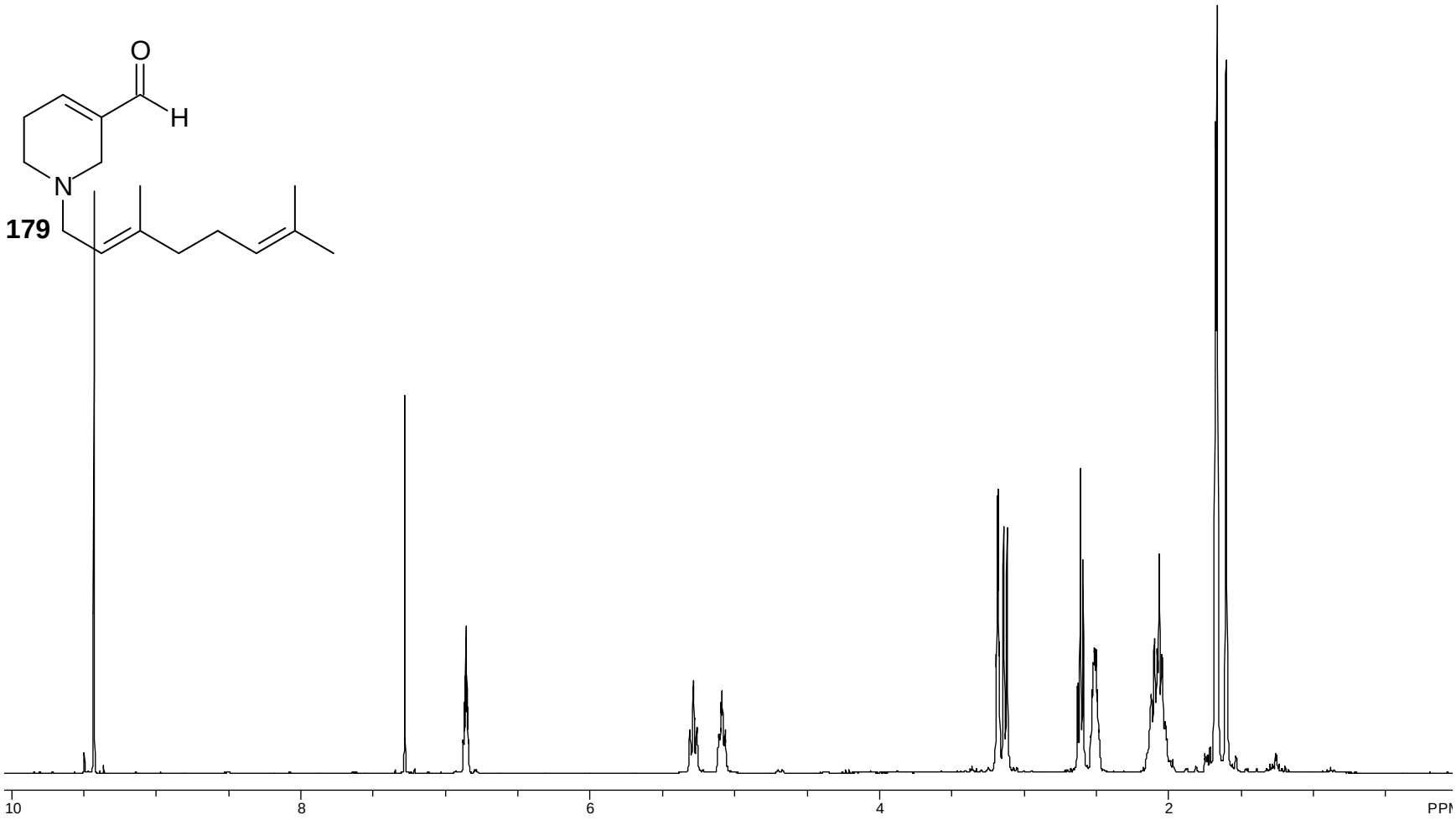

Figure A79. 300 MHz ^{1}H NMR Spectrum of Compound **179**.

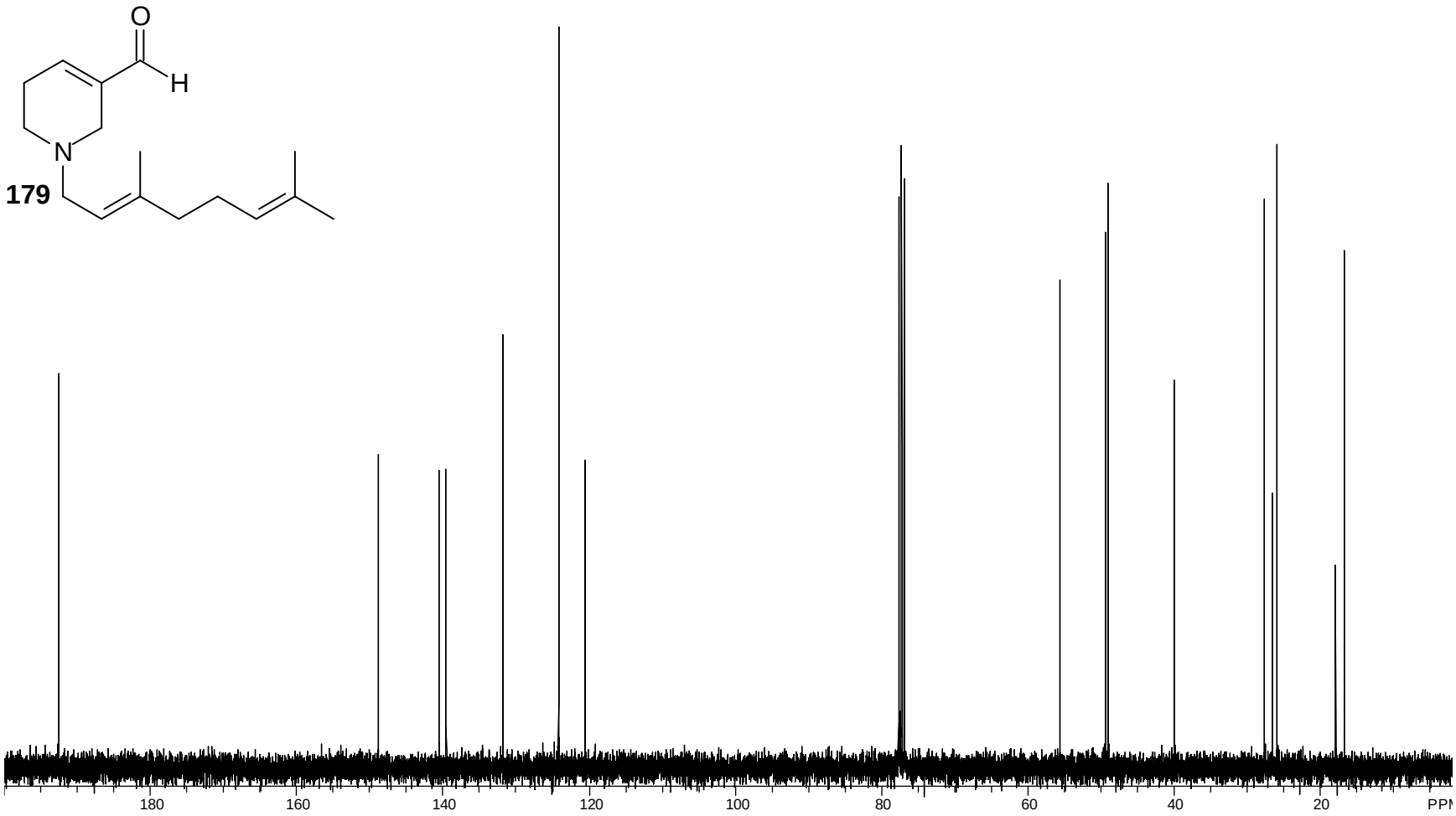

Figure A80. 75 MHz ^{13}C NMR Spectrum of Compound **179**.

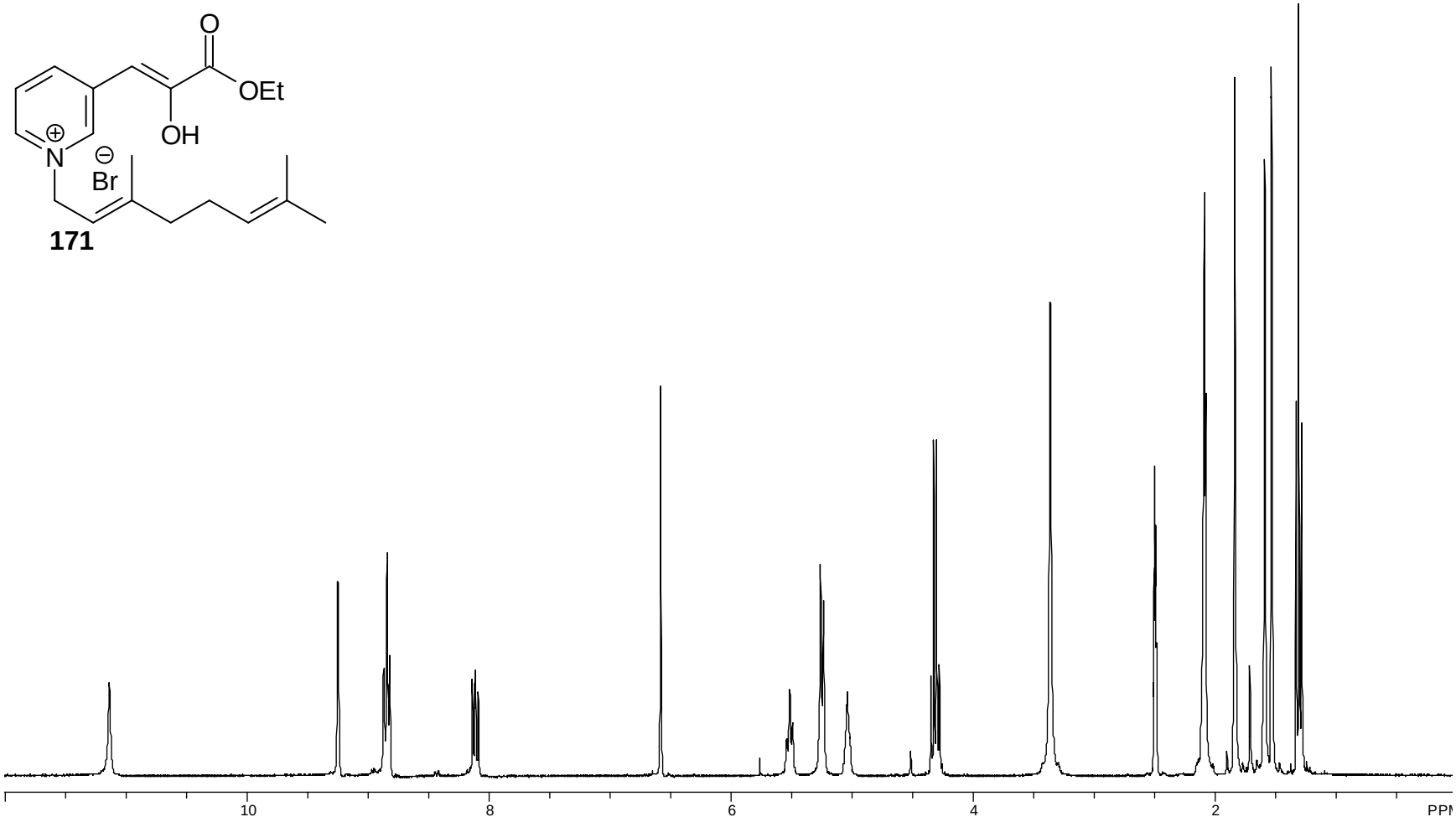

Figure A81. 300 MHz ^{1}H NMR Spectrum of Compound **171**.

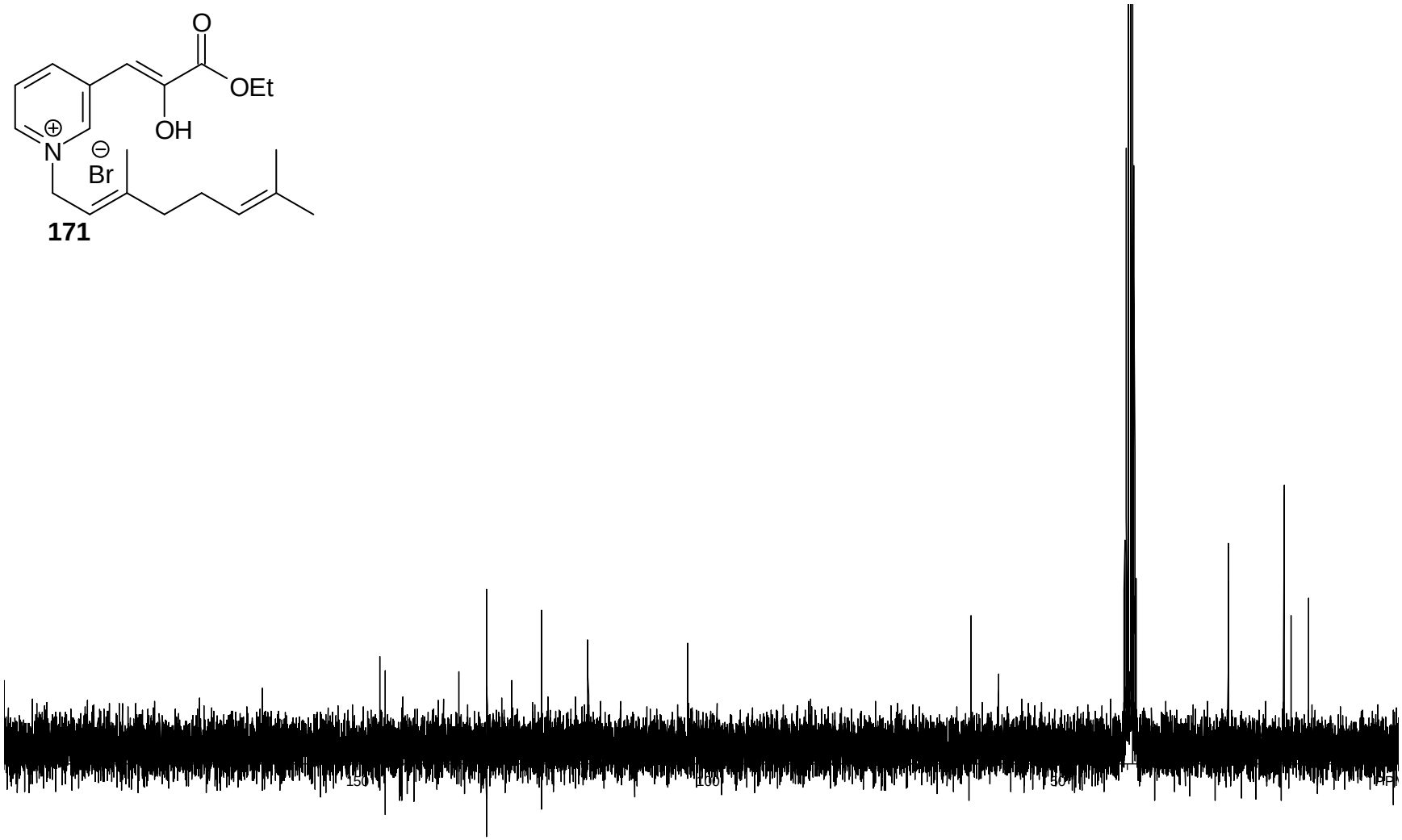

Figure A82. 75 MHz ^{13}C NMR Spectrum of Compound **171**.

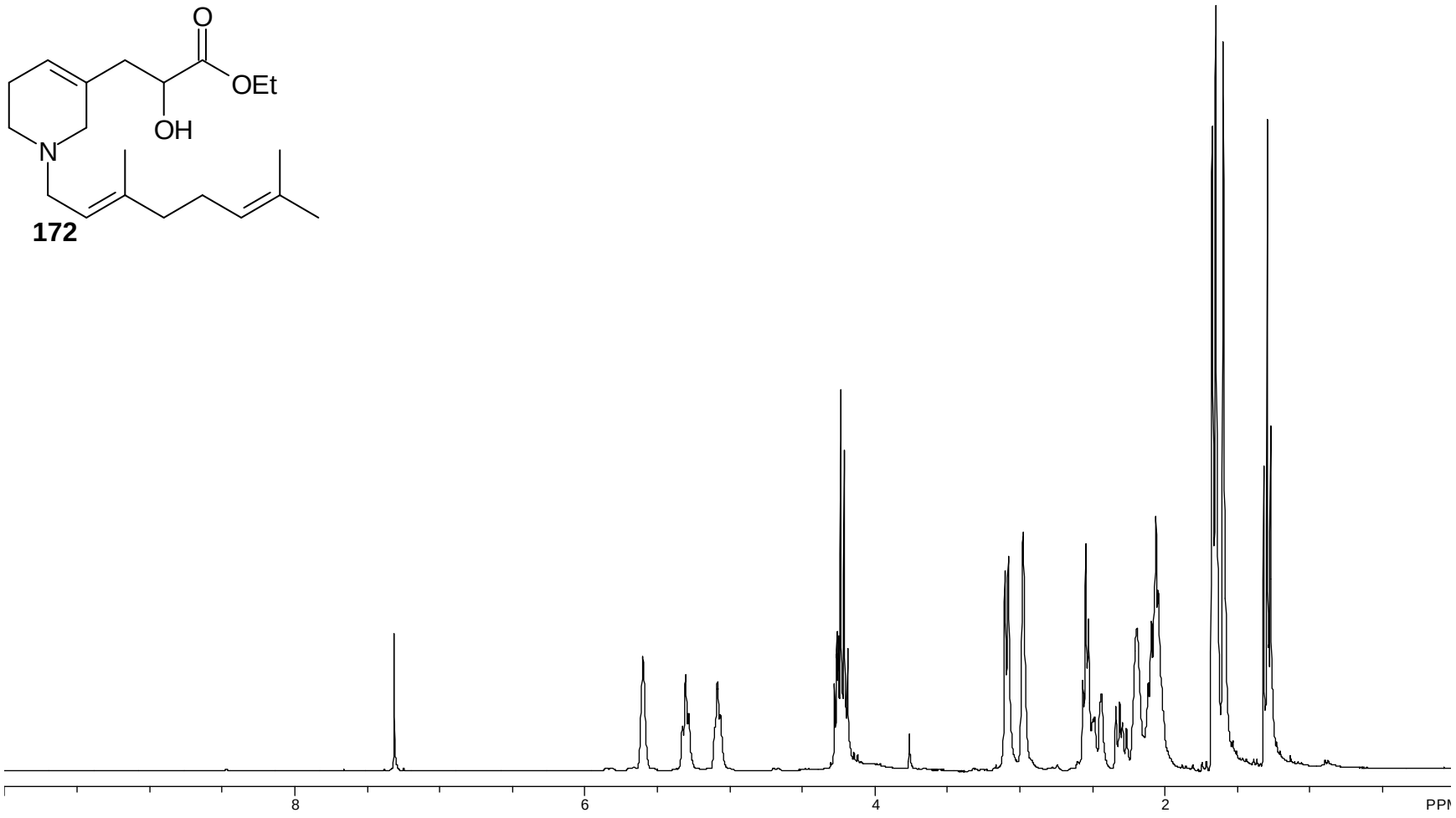

Figure A83. 300 MHz ^{1}H NMR Spectrum of Compound **172**.

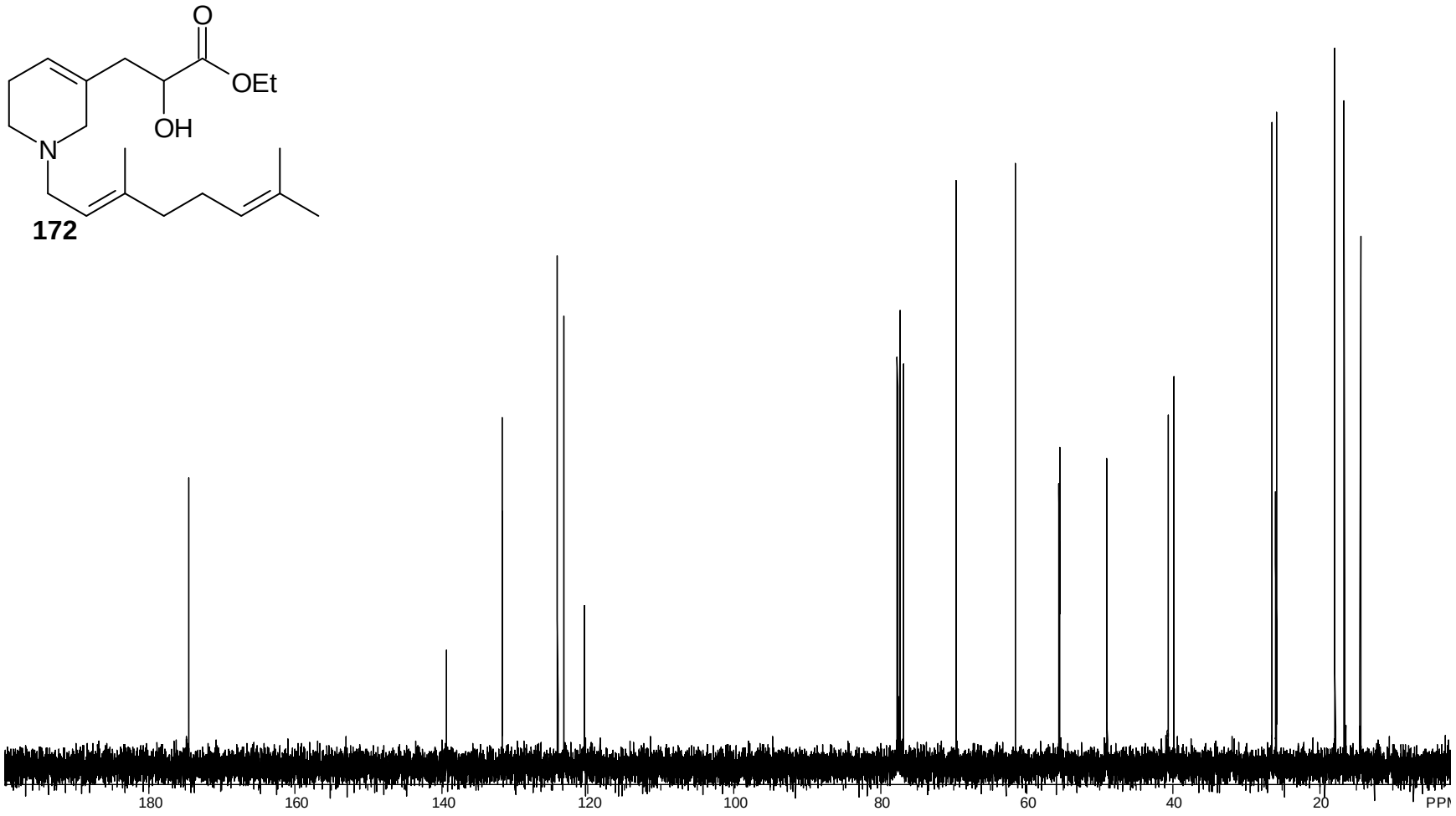

Figure A84. 75 MHz ^{13}C NMR Spectrum of Compound **172**.

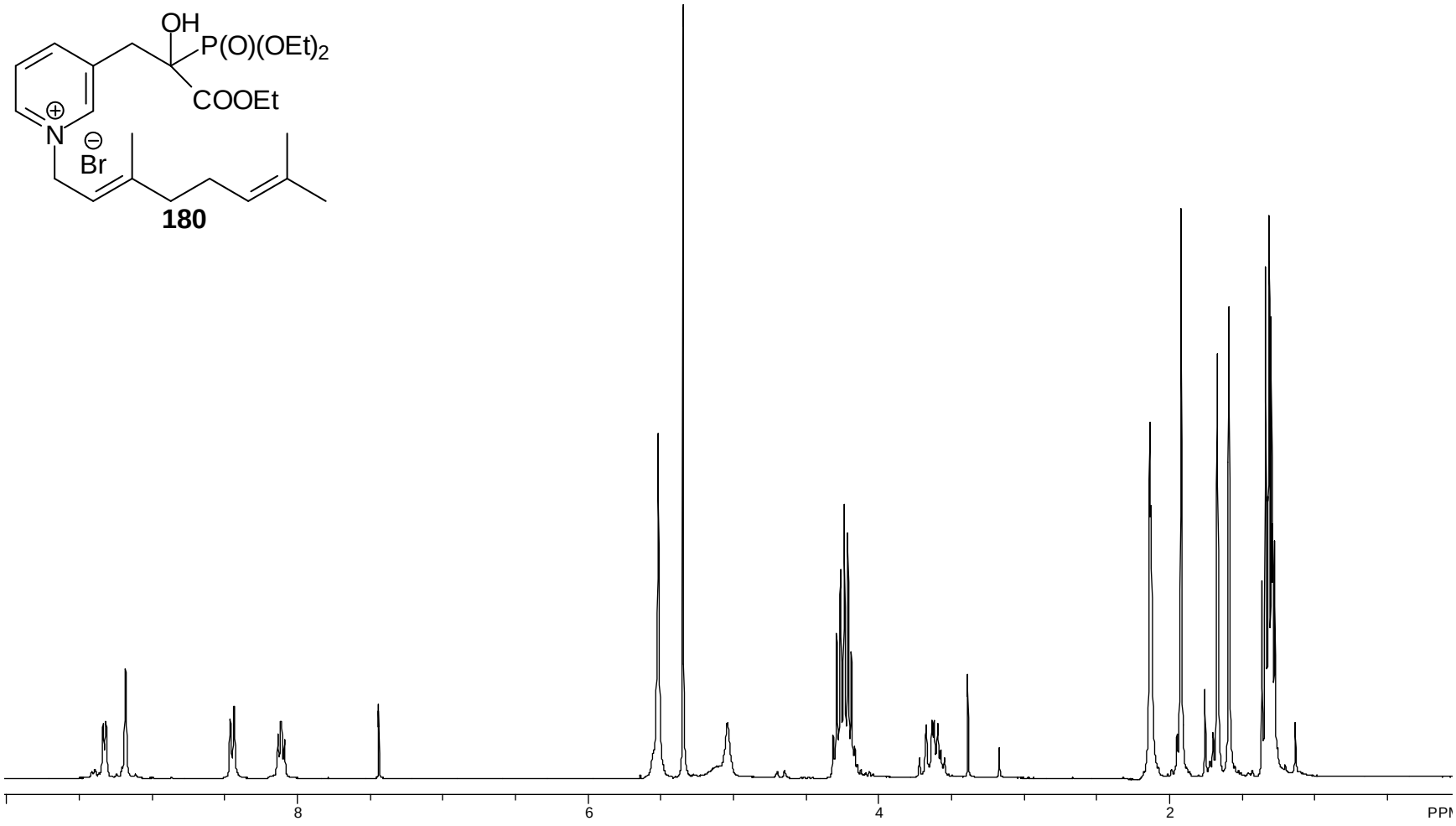

Figure A85. 300 MHz ^{1}H NMR Spectrum of Compound **180**.

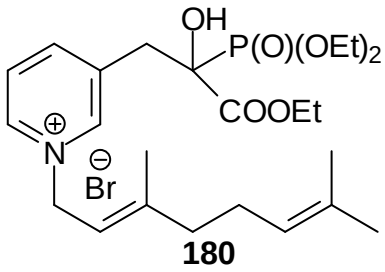

180

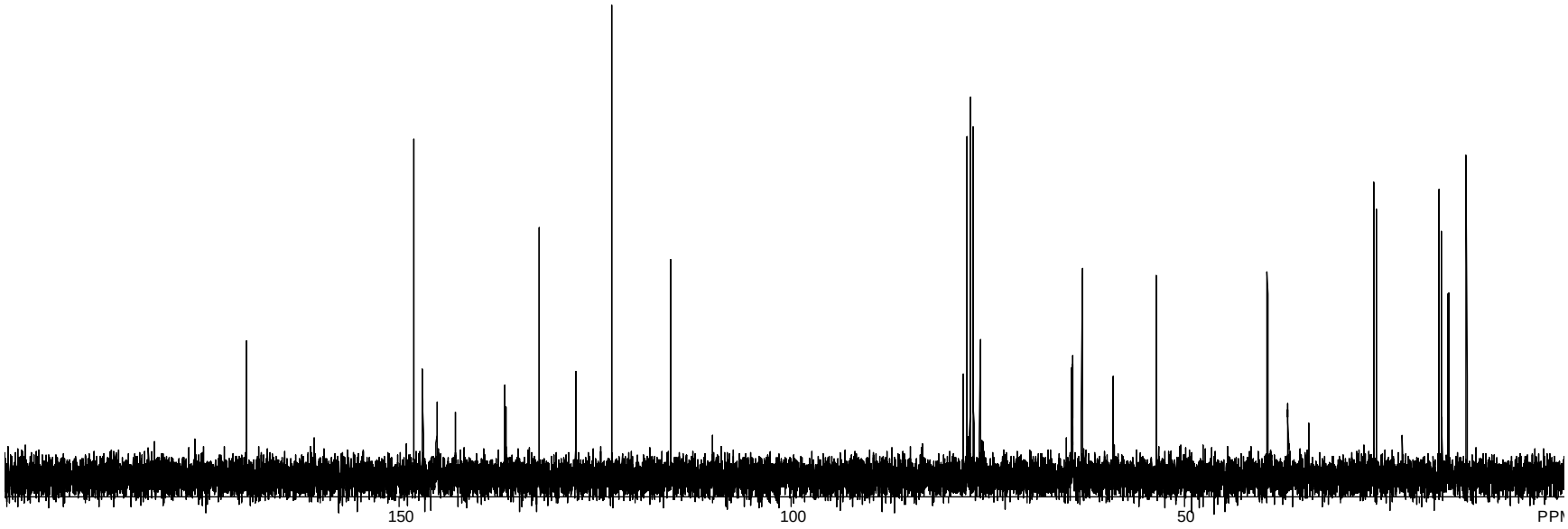

Figure A86. 75 MHz ^{13}C NMR Spectrum of Compound **180**.

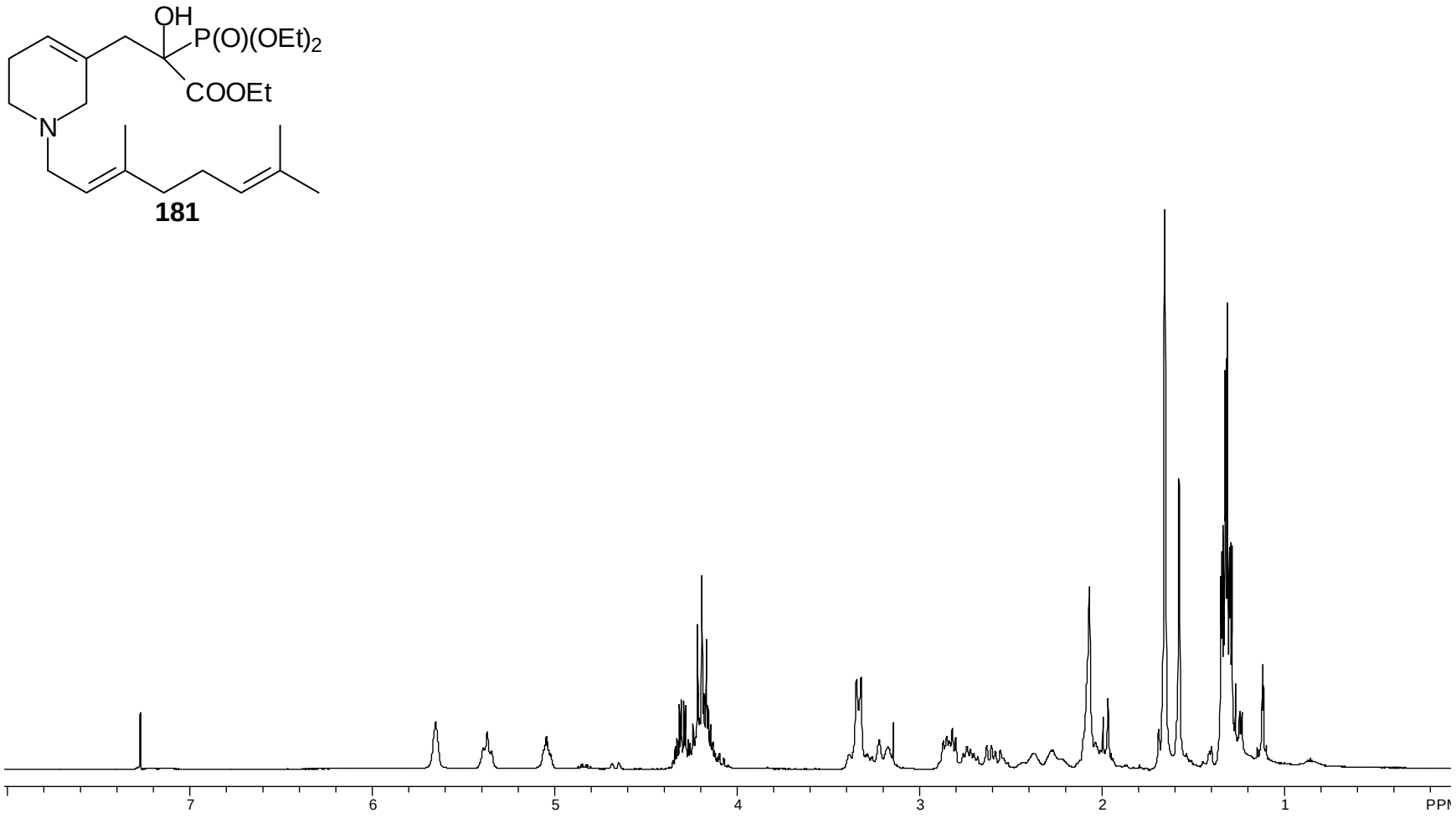

Figure A87. 300 MHz ^{1}H NMR Spectrum of Compound **181**.

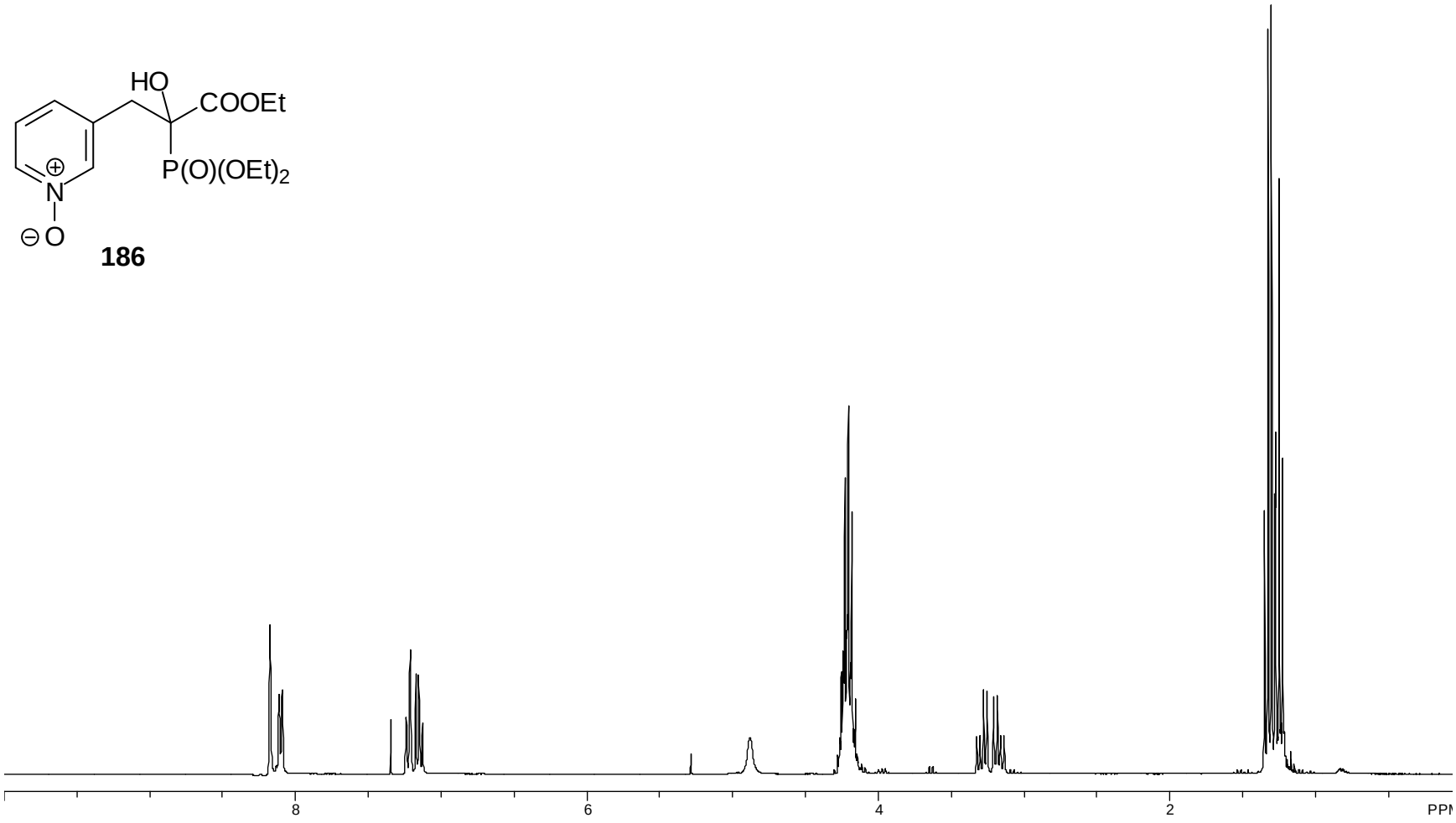

Figure A88. 300 MHz ^{1}H NMR Spectrum of Compound **186**.

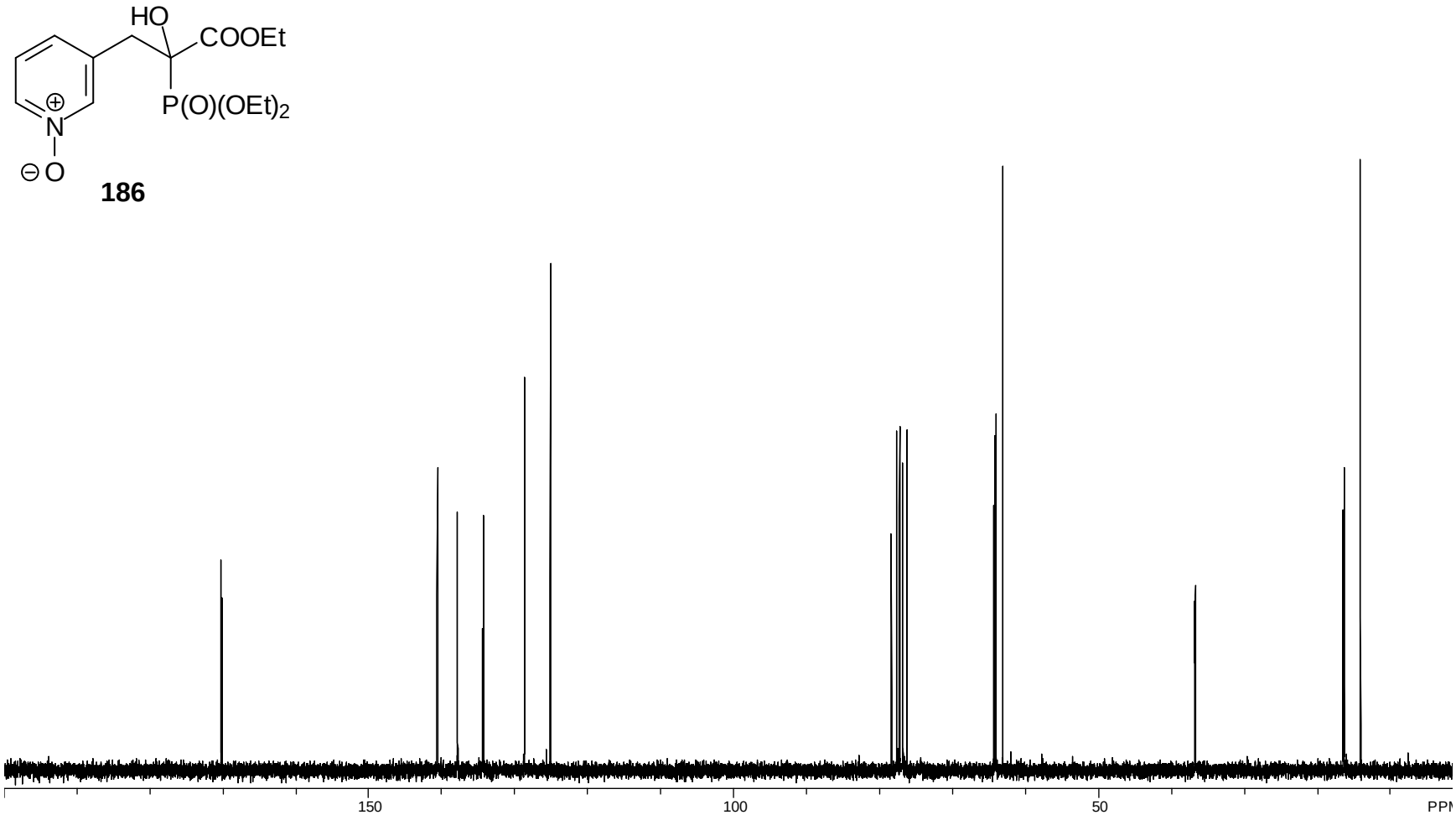

Figure A89. 75 MHz ^{13}C NMR Spectrum of Compound **186**.

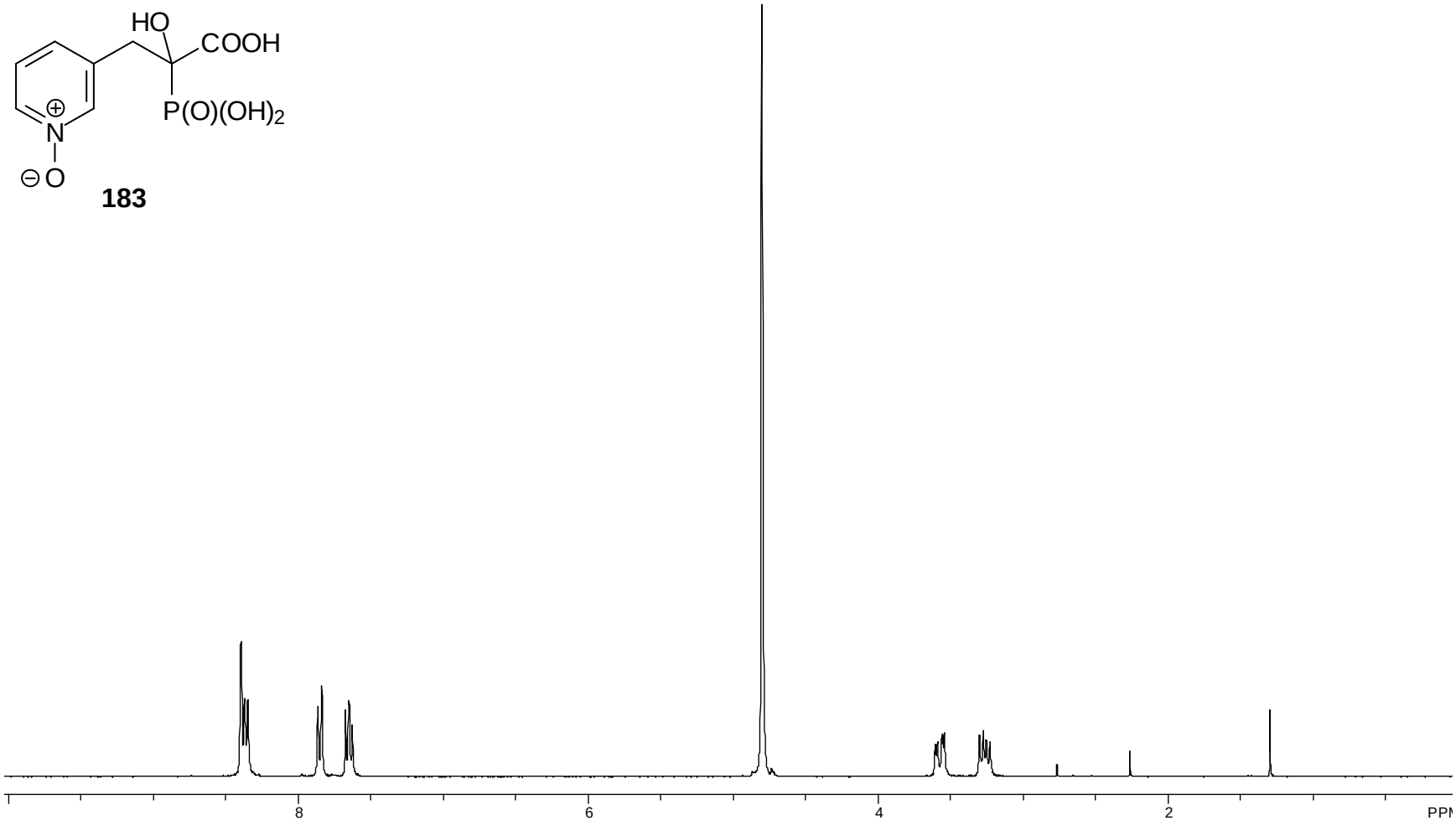

Figure A90. 300 MHz ^{1}H NMR Spectrum of Compound **183**.

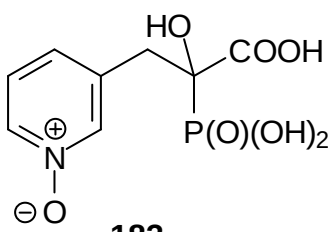

183

Figure A91. 75 MHz ^{13}C NMR Spectrum of Compound **183**.

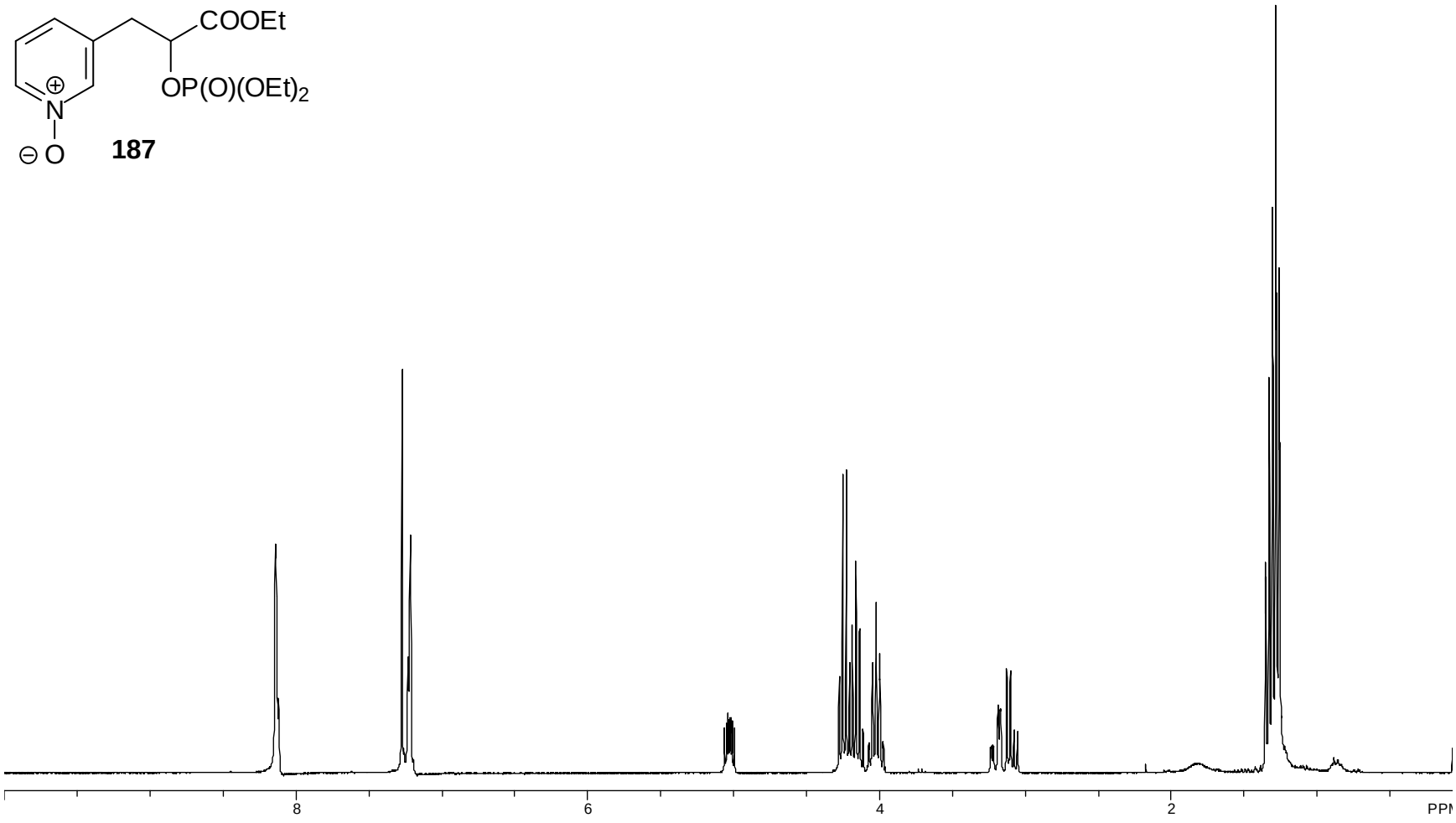

Figure A92. 300 MHz ^{1}H NMR Spectrum of Compound **187**.

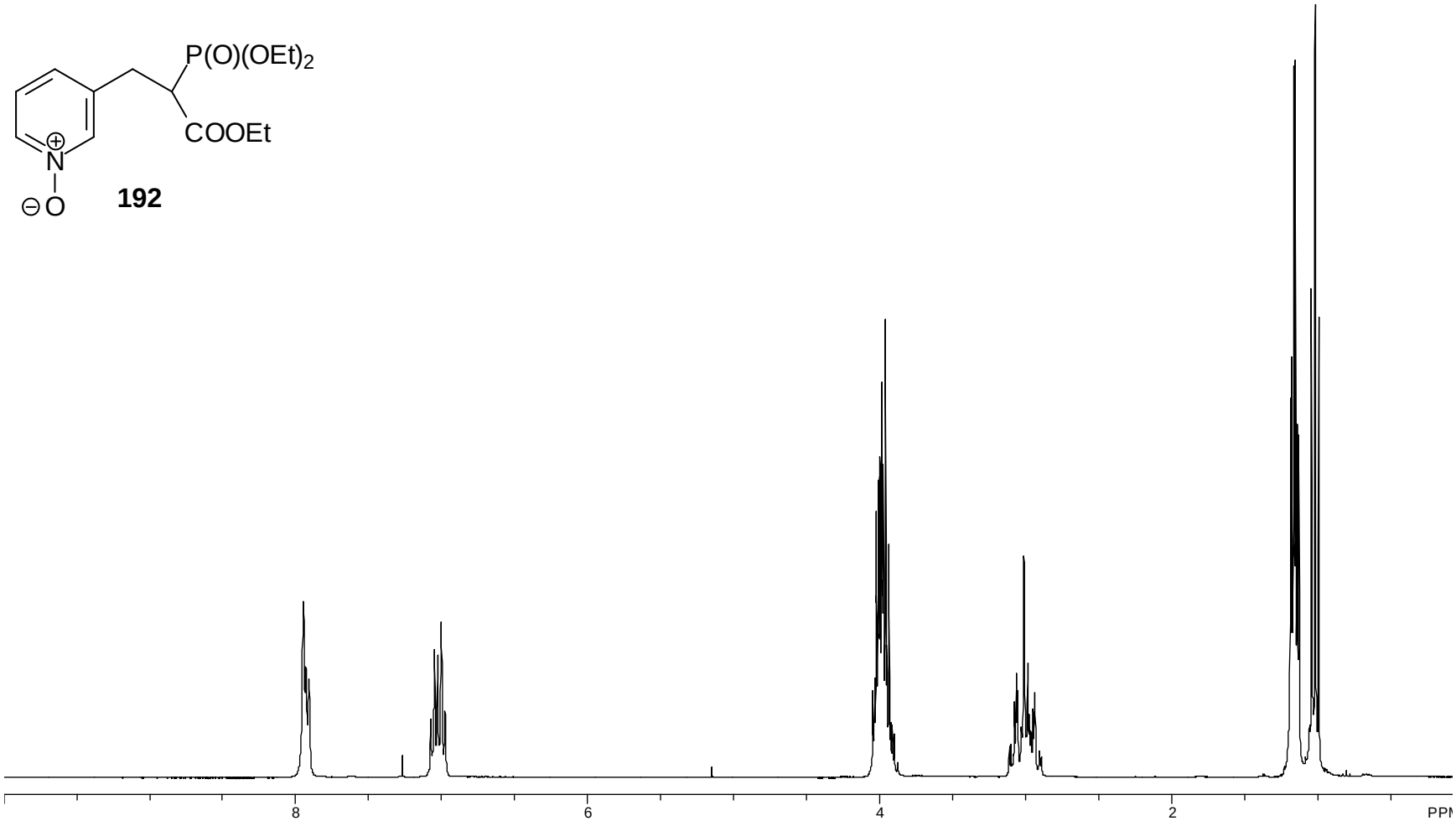

Figure A93. 300 MHz ^{1}H NMR Spectrum of Compound **192**.

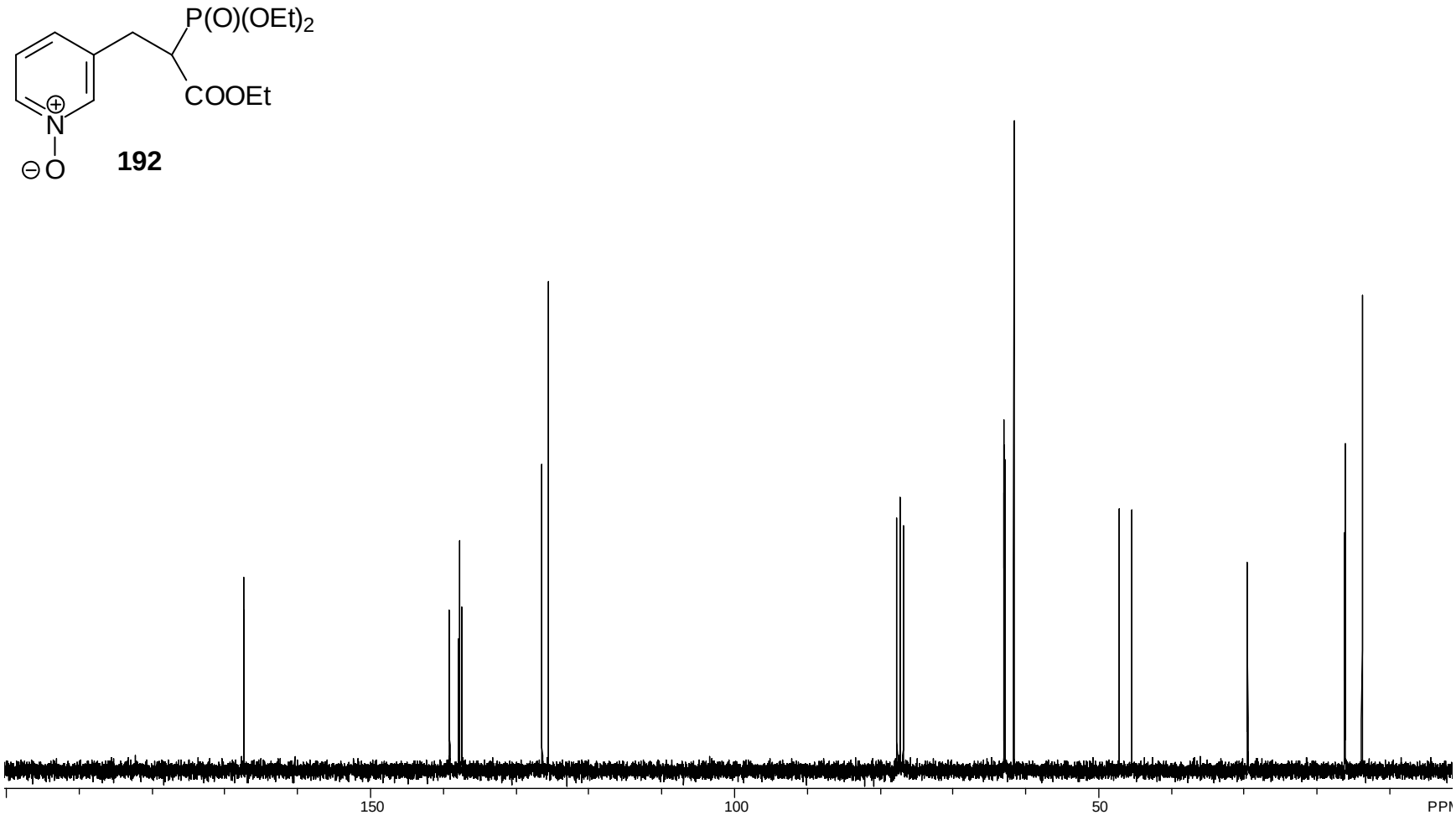

Figure A94. 75 MHz ^{13}C NMR Spectrum of Compound **192**.

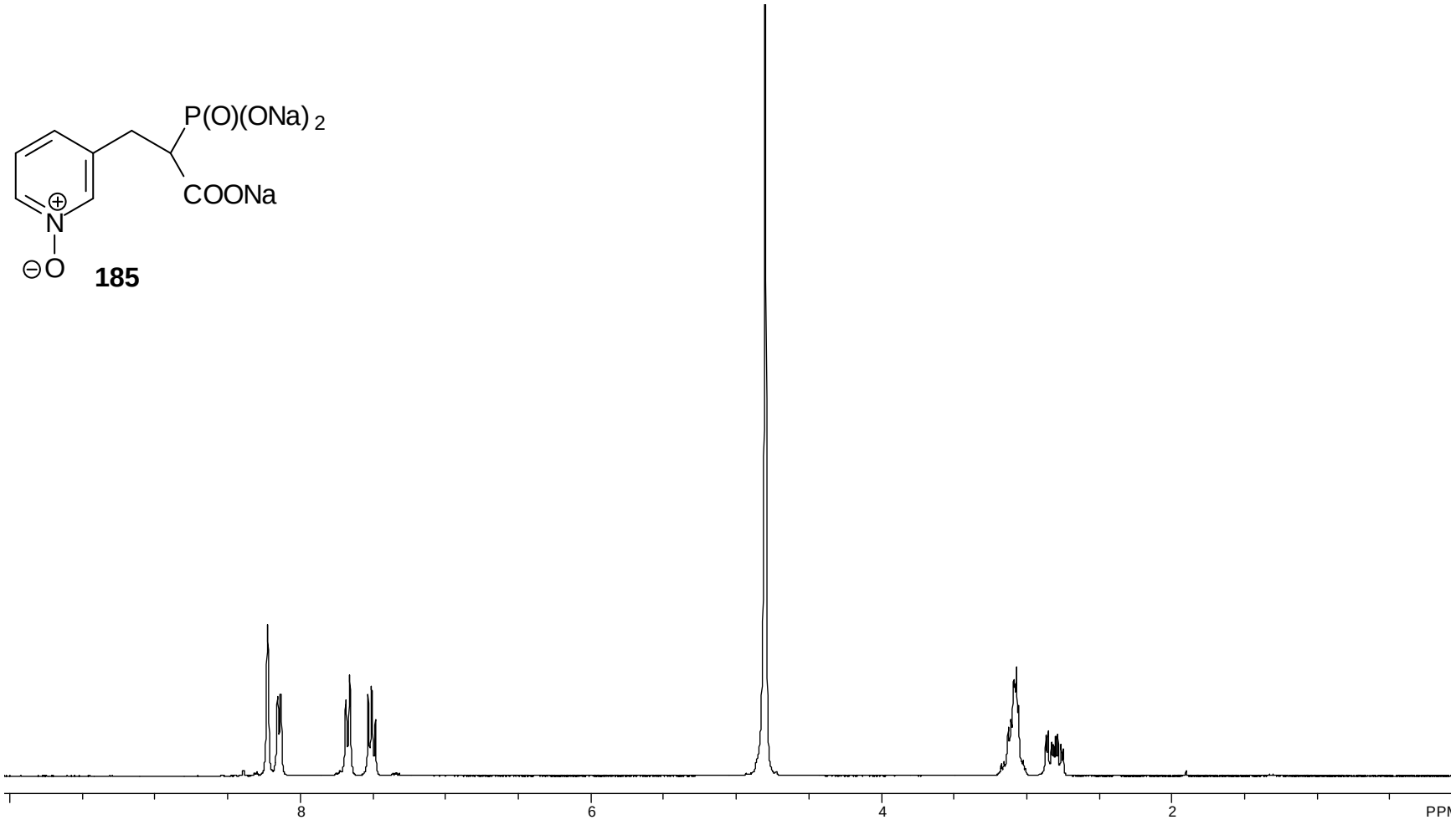

Figure A95. 300 MHz ^{1}H NMR Spectrum of Compound **185**.

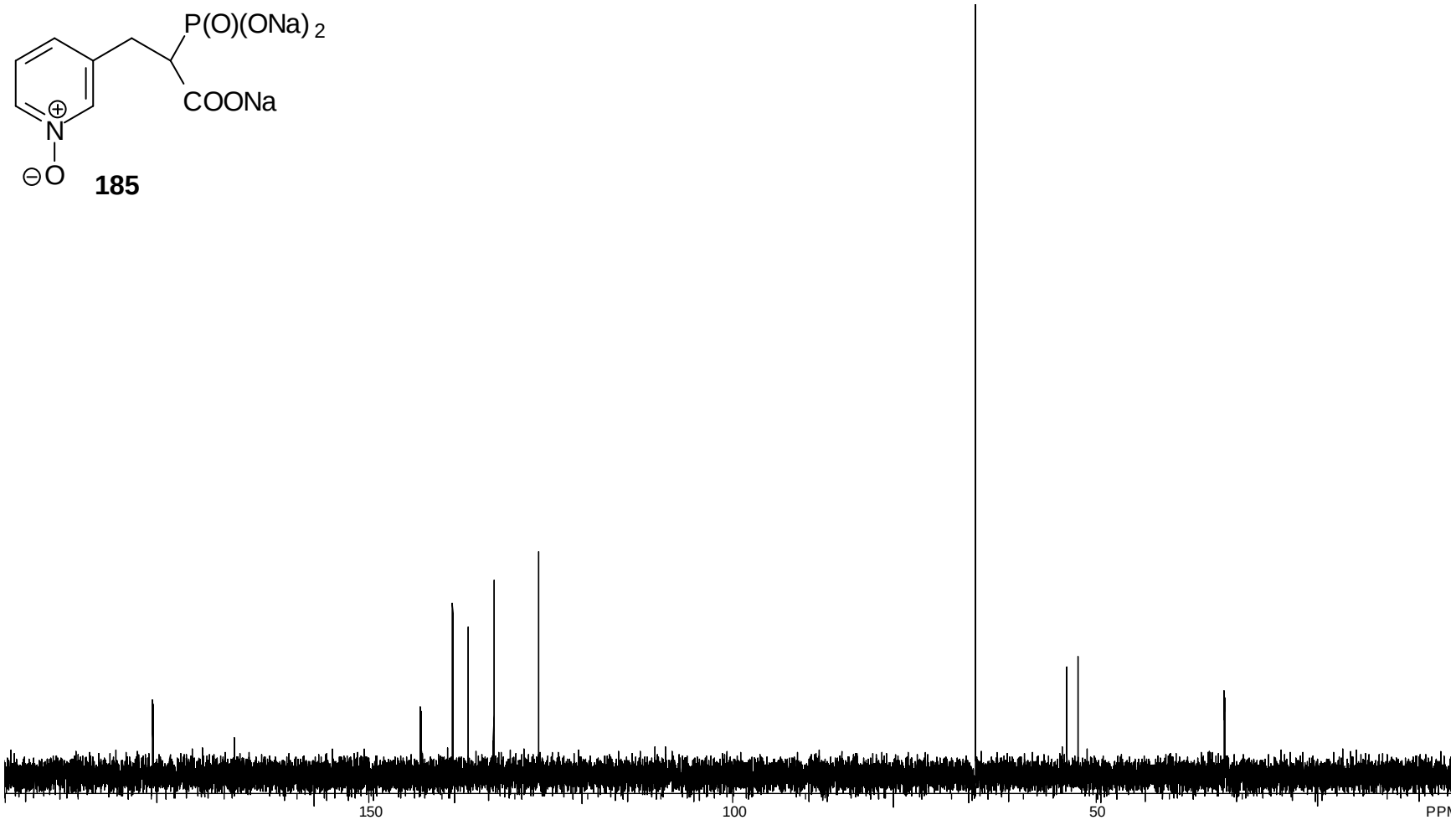

Figure A96. 75 MHz ^{13}C NMR Spectrum of Compound **185**.

REFERENCES

(1) Weeks, M. E. *Journal of Chemical Education* **1933**, *10*, 302.

(2) Gleason, W. *The Journal of The Minerals, Metals & Materials Society* **2007**, *59*, 17.

(3) McQuarrie, D. A.; Rock, P. A.; Gallogly, E. B.; Kelvin, G. V.; Muller, L. *General Chemistry*; WH Freeman, 1984.

(4) Thomson, R. D. *Dictionary of chemistry with its applications to mineralogy, physiology and the arts*; Rich. Griffin and Company, 1870.

(5) Wikipedia: http://en.wikipedia.org/wiki/Phosphorus; Vol. 2014.

(6) Campbell, N. A.; Williamson, B.; Heyden, R. J. *Biology: Exploring Life*; Recording for the Blind & Dyslexic, 2006.

(7) Berg, J. M.; Tymoczko, J. L.; Stryer, L. *Biochemistry, Fifth Edition*; W.H. Freeman, 2002.

(8) Buhaescu, I.; Izzedine, H. *Clinical Biochemistry* **2007**, *40*, 575.

(9) Hinson, D. D.; Chambliss, K. L.; Toth, M. J.; Tanaka, R. D.; Gibson, K. M. *Journal of Lipid Research* **1997**, *38*, 2216.

(10) Goldstein, J. L.; Brown, M. S. *Nature* **1990**, *343*, 425.

(11) Buss, J. E.; Quilliam, L. A.; Kato, K.; Casey, P. J.; Solski, P. A.; Wong, G.; Clark, R.; McCormick, F.; Bokoch, G. M.; Der, C. J. *Molecular and Cellular Biology* **1991**, *11*, 1523.

(12) Yu, J. S. C. Ph.D. thesis, The University of Iowa, 2007.

(13) Tansey, T. R.; Shechter, I. *Biochimica et Biophysica Acta (BBA) - Molecular and Cell Biology of Lipids* **2000**, *1529*, 49.

(14) Wiemer, A. J.; Wiemer, D. F.; Hohl, R. J. *Clinical Pharmacology & Therapeutics* **2011**, *90*, 804.

(15) Kuzuguchi, T.; Morita, Y.; Sagami, I.; Sagami, H.; Ogura, K. *Journal of Biological Chemistry* **1999**, *274*, 5888.

(16) Chen, C. K. M.; Hudock, M. P.; Zhang, Y.; Guo, R.-T.; Cao, R.; No, J. H.; Liang, P.-H.; Ko, T.-P.; Chang, T.-H.; Chang, S.-c.; Song, Y.; Axelson, J.; Kumar, A.; Wang, A. H. J.; Oldfield, E. *Journal of Medicinal Chemistry* **2008**, *51*, 5594.

(17) Connor. A.M., B. S., Narendran. A., Keystone, E. C. *Arthritis Research & Therapy* **2006**, *8*, R94.

(18) Resh, M. D. *Cellular Signalling* **1996**, *8*, 403.

(19) Park, H.-J.; Kong, D.; Iruela-Arispe, L.; Begley, U.; Tang, D.; Galper, J. B. *Circulation Research* **2002**, *91*, 143.

(20) Bifulco, M. *Life Sciences* **2005**, *77*, 1740.

(21) Endo, A. *International Congress Series* **2004**, *1262*, 3.

(22) Guijarro, C.; Blanco-Colio, L. M.; Ortego, M.; Alonso, C.; Ortiz, A.; Plaza, J. J.; Díaz, C.; Hernández, G.; Egido, J. *Circulation Research* **1998**, *83*, 490.

(23) van de Donk, N. W. C. J.; Schotte, D.; Kamphuis, M. M. J.; van Marion, A. M. W.; van Kessel, B.; Bloem, A. C.; Lokhorst, H. M. *Clinical Cancer Research* **2003**, *9*, 5735.

(24) Casey, P. J.; Solski, P. A.; Der, C. J.; Buss, J. E. *Proceedings of the National Academy of Sciences* **1989**, *86*, 8323.

(25) Hancock, J. F.; Magee, A. I.; Childs, J. E.; Marshall, C. J. *Cell* **1989**, *57*, 1167.

(26) Shipman, C. M.; Rogers, M. J.; Apperley, J. F.; Russell, R. G. G.; Croucher, P. I. *British Journal of Haematology* **1997**, *98*, 665.

(27) Licata, A. A. *Annals of Pharmacotherapy* **2005**, *39*, 668.

(28) Body, J. J.; Bartl, R.; Burckhardt, P.; Delmas, P. D.; Diel, I. J.; Fleisch, H.; Kanis, J. A.; Kyle, R. A.; Mundy, G. R.; Paterson, A. H.; Rubens, R. D. *Journal of Clinical Oncology* **1998**, *16*, 3890.

(29) Ebetino, F. H.; Hogan, A.-M. L.; Sun, S.; Tsoumpra, M. K.; Duan, X.; Triffitt, J. T.; Kwaasi, A. A.; Dunford, J. E.; Barnett, B. L.; Oppermann, U.; Lundy, M. W.; Boyde, A.; Kashemirov, B. A.; McKenna, C. E.; Russell, R. G. G. *Bone* **2011**, *49*, 20.

(30) Van Beek, E.; Löwik, C.; Van Der Pluijm, G.; Papapoulos, S. *Journal of Bone and Mineral Research* **1999**, *14*, 722.

(31) Wiemer, A. J.; Tong, H.; Swanson, K. M.; Hohl, R. J. *Biochemical and Biophysical Research Communications* **2007**, *353*, 921.

(32) Wiemer, A. J.; Yu, J. S.; Lamb, K. M.; Hohl, R. J.; Wiemer, D. F. *Bioorganic & Medicinal Chemistry* **2008**, *16*, 390.

(33) Wittig, G.; Schöllkopf, U. *Chemische Berichte* **1954**, *87*, 1318.

(34) Hoffmann, R. W. *Angewandte Chemie International Edition* **2001**, *40*, 1411.

(35) Maryanoff, B. E.; Reitz, A. B. *Chemical Reviews* **1989**, *89*, 863.

(36) Horner, L.; Hoffmann, H.; Wippel, H. G. *Chemische Berichte* **1958**, *91*, 61.

(37) Wadsworth, W. S. In *Organic Reactions*; John Wiley & Sons, Inc.: 2004.

(38) Horner, L.; Hoffmann, H.; Wippel, H. G.; Klahre, G. *Chemische Berichte* **1959**, *92*, 2499.

(39) Neighbors, J. D.; Buller, M. J.; Boss, K. D.; Wiemer, D. F. *Journal of Natural Products* **2008**, *71*, 1949.

(40) Topczewski, J. J.; Neighbors, J. D.; Wiemer, D. F. *The Journal of Organic Chemistry* **2009**, *74*, 6965.

(41) Hartung, A. M.; Beutler, J. A.; Navarro, H. A.; Wiemer, D. F.; Neighbors, J. D. *Journal of Natural Products* **2014**, *77*, 311.

(42) Topczewski, J. J.; Kodet, J. G.; Wiemer, D. F. *The Journal of Organic Chemistry* **2011**, *76*, 909.

(43) Claridge, T. D. W.; Davies, S. G.; Lee, J. A.; Nicholson, R. L.; Roberts, P. M.; Russell, A. J.; Smith, A. D.; Toms, S. M. *Organic Letters* **2008**, *10*, 5437.

(44) Umezawa, T.; Seino, T.; Matsuda, F. *Organic Letters* **2012**, *14*, 4206.

(45) Michaelis, A.; Kaehne, R. *Berichte der deutschen chemischen Gesellschaft* **1898**, *31*, 1048.

(46) Zhou, X.; Ferree, S. D.; Wills, V. S.; Born, E. J.; Tong, H.; Wiemer, D. F.; Holstein, S. A. *Bioorganic & Medicinal Chemistry* **2014**, *22*, 2791.

(47) Zhou, X.; Hartman, S. V.; Born, E. J.; Smits, J. P.; Holstein, S. A.; Wiemer, D. F. *Bioorganic & Medicinal Chemistry Letters* **2013**, *23*, 764.

(48) Zhou, X.; Reilly, J. E.; Loerch, K. A.; Hohl, R. J.; Wiemer, D. F. *Beilstein Journal of Organic Chemistry* **2014**, *10*, 1645.

(49) McKenna, C. E.; Higa, M. T.; Cheung, N. H.; McKenna, M.-C. *Tetrahedron Letters* **1977**, *18*, 155.

(50) Barney, R. J.; Richardson, R. M.; Wiemer, D. F. *The Journal of Organic Chemistry* **2011**, *76*, 2875.

(51) Richardson, R. M.; Wiemer, D. F. *Organic Syntheses* **2013**, 145.

(52) Richardson, R. M. Ph.D. thesis, The University of Iowa, 2012.

(53) Coxon, F. P.; Helfrich, M. H.; Van't Hof, R.; Sebti, S.; Ralston, S. H.; Hamilton, A.; Rogers, M. J. *Journal of Bone and Mineral Research* **2000**, *15*, 1467.

(54) Fisher, J. E.; Rogers, M. J.; Halasy, J. M.; Luckman, S. P.; Hughes, D. E.; Masarachia, P. J.; Wesolowski, G.; Russell, R. G. G.; Rodan, G. A.; Reszka, A. A. *Proceedings of the National Academy of Sciences* **1999**, *96*, 133.

(55) Shull, L. W.; Wiemer, A. J.; Hohl, R. J.; Wiemer, D. F. *Bioorganic & Medicinal Chemistry* **2006**, *14*, 4130.

(56) Sarro, A.; Minutoli, L. In *Bisphosphonates and Osteonecrosis of the Jaw: A Multidisciplinary Approach*; De Ponte, F. S., Ed.; Springer Milan: 2012, p 13.

(57) Lalinde, N.; Tropp, B. E.; Engel, R. *Tetrahedron* **1983**, *39*, 2369.

(58) Cooperman, B. S.; Chiu, N. Y. *Biochemistry* **1973**, *12*, 1670.

(59) Hounslow, A. M.; Carran, J.; Brown, R. J.; Rejman, D.; Blackburn, G. M.; Watts, D. J. *Journal of Medicinal Chemistry* **2008**, *51*, 4170.

(60) Nancollas, G. H.; Tang, R.; Phipps, R. J.; Henneman, Z.; Gulde, S.; Wu, W.; Mangood, A.; Russell, R. G. G.; Ebetino, F. H. *Bone* **2006**, *38*, 617.

(61) Jung, M. E.; Min, S.-J. *Journal of the American Chemical Society* **2005**, *127*, 10834.

(62) Karaman, R.; Goldblum, A.; Breuer, E.; Leader, H. *Journal of the Chemical Society, Perkin Transactions 1* **1989**, 765.

(63) Fitch, S. J.; Moedritzer, K. *Journal of the American Chemical Society* **1962**, *84*, 1876.

(64) Turhanen, P. A. V., J. J. *Synthesis* **2005**, 2119.

(65) Turhanen, P. A. V., J. J. *Synthesis* **2004**, 992.

(66) Turhanen, P. A. A., M. J.; Jarvinen, T.; Vepsalainen, J. J. *Phosphorus, Sulfur Silicon Relat. Elem.* **2001**, *170*, 115.

(67) Vachal, P.; Hale, J. J.; Lu, Z.; Streckfuss, E. C.; Mills, S. G.; MacCoss, M.; Yin, D. H.; Algayer, K.; Manser, K.; Kesisoglou, F.; Ghosh, S.; Alani, L. L. *Journal of Medicinal Chemistry* **2006**, *49*, 3060.

(68) Kolodyazhnaya, O. O.; Kolodyazhnyi, O. I. *Russian Journal of General Chemistry* **2009**, *79*, 862.

(69) Kolodyazhnaya, O. O.; Kolodyazhnyi, O. I. *Russian Journal of General Chemistry* **2011**, *81*, 307.

(70) Haelters, J.-P.; Couthon-Gourvès, H.; Le Goff, A.; Simon, G.; Corbel, B.; Jaffrès, P.-A. *Tetrahedron* **2008**, *64*, 6537.

(71) Smits, J. P.; Wiemer, D. F. *The Journal of Organic Chemistry* **2011**, *76*, 8807.

(72) Calogeropoulou, T.; Hammond, G. B.; Wiemer, D. F. *The Journal of Organic Chemistry* **1987**, *52*, 4185.

(73) Hammond, G. B.; Calogeropoulou, T.; Wiemer, D. F. *Tetrahedron Letters* **1986**, *27*, 4265.

(74) Ollivier, R. S., G.; Legendre, J. M.; Jacolot, G.; Turzo, A. *Eur. J. Med. Chem.* **1986**, *21*, 103.

(75) Biller, S. A. S., M. J.; Abt, J. W.; Delange, B.; Dickson, J. K.; Forster, C.; Gordon, E. M.; Harrity, T.; Magnin, D. R.; Marretta, J.; Rich, L. C.; Ciosek, C. P. *ACS Symp. Ser.* **1992**, *497*, 65.

(76) Tong, H.; Holstein, S. A.; Hohl, R. J. *Analytical Biochemistry* **2005**, *336*, 51.

(77) Bergman, J. A.; Hahne, K.; Song, J.; Hrycyna, C. A.; Gibbs, R. A. *ACS Medicinal Chemistry Letters* **2011**, *3*, 15.

(78) Wiemer, A. J.; Hohl, R. J.; Wiemer, D. F. *Anti-Cancer Agents in Medicinal Chemistry* **2009**, *9*, 526.

(79) Holstein, S. A. In *The Enzymes*; Christine A. Hrycyna, M. O. B., Fuyuhiko, T., Eds.; Academic Press: 2011; Vol. Volume 30, p 279.

(80) Seabra, M. C.; Goldstein, J. L.; Südhof, T. C.; Brown, M. S. *Journal of Biological Chemistry* **1992**, *267*, 14497.

(81) Anant, J. S.; Desnoyers, L.; Machius, M.; Demeler, B.; Hansen, J. C.; Westover, K. D.; Deisenhofer, J.; Seabra, M. C. *Biochemistry* **1998**, *37*, 12559.

(82) Lerner, E. C.; Qian, Y.; Blaskovich, M. A.; Fossum, R. D.; Vogt, A.; Sun, J.; Cox, A. D.; Der, C. J.; Hamilton, A. D.; Sebti, S. M. *Journal of Biological Chemistry* **1995**, *270*, 26802.

(83) McGuire, T. F.; Qian, Y.; Vogt, A.; Hamilton, A. D.; Sebti, S. M. *Journal of Biological Chemistry* **1996**, *271*, 27402.

(84) Coxon, F. P.; Helfrich, M. H.; Larijani, B.; Muzylak, M.; Dunford, J. E.; Marshall, D.; McKinnon, A. D.; Nesbitt, S. A.; Horton, M. A.; Seabra, M. C.; Ebetino, F. H.; Rogers, M. J. *Journal of Biological Chemistry* **2001**, *276*, 48213.

(85) Baron, R. A.; Tavaré, R.; Figueiredo, A. C.; Błażewska, K. M.; Kashemirov, B. A.; McKenna, C. E.; Ebetino, F. H.; Taylor, A.; Rogers, M. J.; Coxon, F. P.; Seabra, M. C. *Journal of Biological Chemistry* **2009**, *284*, 6861.

(86) Huang, S.; Clark, R. J.; Zhu, L. *Organic Letters* **2007**, *9*, 4999.

(87) Nguyen, D. M.; Frazer, A.; Rodriguez, L.; Belfield, K. D. *Chemistry of Materials* **2010**, *22*, 3472.

(88) Himo, F.; Lovell, T.; Hilgraf, R.; Rostovtsev, V. V.; Noodleman, L.; Sharpless, K. B.; Fokin, V. V. *Journal of the American Chemical Society* **2004**, *127*, 210.

(89) Skarpos, H.; Osipov, S. N.; Vorob'eva, D. V.; Odinets, I. L.; Lork, E.; Roschenthaler, G.-V. *Organic & Biomolecular Chemistry* **2007**, *5*, 2361.

(90) Simoni, D.; Gebbia, N.; Invidiata, F. P.; Eleopra, M.; Marchetti, P.; Rondanin, R.; Baruchello, R.; Provera, S.; Marchioro, C.; Tolomeo, M.; Marinelli, L.; Limongelli, V.; Novellino, E.; Kwaasi, A.; Dunford, J.; Buccheri, S.; Caccamo, N.; Dieli, F. *Journal of Medicinal Chemistry* **2008**, *51*, 6800.

(91) Smits, J. P. Ph.D. thesis, The University of Iowa, 2011.

(92) Yu, J. S.; Kleckley, T. S.; Wiemer, D. F. *Organic Letters* **2005**, *7*, 4803.

(93) Grisé, C. M.; Rodrigue, E. M.; Barriault, L. *Tetrahedron* **2008**, *64*, 797.

(94) Hansen, J. B.; Bjerring, P.; Buchardt, O.; Ebbesen, P.; Kanstrup, A.; Karup, G.; Knudsen, P. H.; Nielsen, P. E.; Norden, B.; Ygge, B. *Journal of Medicinal Chemistry* **1985**, *28*, 1001.

(95) Seabra, M. C.; James, G. L. *Methods in molecular biology (Clifton, N.J.)* **1998**, *84*, 251.

(96) Holstein, S. A.; Hohl, R. J. *Leukemia Research* **2001**, *25*, 651.

(97) Boren, B. C.; Narayan, S.; Rasmussen, L. K.; Zhang, L.; Zhao, H.; Lin, Z.; Jia, G.; Fokin, V. V. *Journal of the American Chemical Society* **2008**, *130*, 8923.

(98) Feldman, A. K.; Colasson, B.; Sharpless, K. B.; Fokin, V. V. *Journal of the American Chemical Society* **2005**, *127*, 13444.

(99) Caputo, R.; Mangoni, L.; Neri, O.; Palumbo, G. *Tetrahedron Letters* **1981**, *22*, 3551.

(100) Sharpless, K. B.; Michaelson, R. C. *Journal of the American Chemical Society* **1973**, *95*, 6136.

(101) Lempers, H. E. B.; Ripollès i Garcia, A.; Sheldon, R. A. *The Journal of Organic Chemistry* **1998**, *63*, 1408.

(102) Gash, R. C.; Maccorquodale, F.; Walton, J. C. *Tetrahedron* **1989**, *45*, 5531.

(103) Limberg, G.; Lundt, I.; Zavilla, J. *Synthesis* **1999**, *1999*, 178.

(104) Sonnet, P. E. *The Journal of Organic Chemistry* **1978**, *43*, 1841.

(105) Bohlmann, F.; Zeisberg, R.; Klein, E. *Organic Magnetic Resonance* **1975**, *7*, 426.

(106) Holstein, S. A.; Hohl, R. J. *Leukemia Research* **2011**, *35*, 551.

(107) Holstein, S. A.; Cermak, D. M.; Wiemer, D. F.; Lewis, K.; Hohl, R. J. *Bioorganic & Medicinal Chemistry* **1998**, *6*, 687.

(108) Wiemer, A. J.; Yu, J. S.; Shull, L. W.; Barney, R. J.; Wasko, B. M.; Lamb, K. M.; Hohl, R. J.; Wiemer, D. F. *Bioorganic & Medicinal Chemistry* **2008**, *16*, 3652.

(109) Holstein, S. A. In *The Enzymes*; Christine A. Hrycyna, M. O. B., Fuyuhiko, T., Eds.; Academic Press: 2011; Vol. 30, p 279.

(110) Barney, R. J. Ph.D. thesis, The University of Iowa, 2010.

(111) Lyle, R. E.; Boyce, C. B. *The Journal of Organic Chemistry* **1974**, *39*, 3708.

(112) Showell, G. A.; Gibbons, T. L.; Kneen, C. O.; MacLeod, A. M.; Merchant, K.; Saunders, J.; Freedman, S. B.; Patel, S.; Baker, R. *Journal of Medicinal Chemistry* **1991**, *34*, 1086.

(113) Raucher, S.; Bray, B. L.; Lawrence, R. F. *Journal of the American Chemical Society* **1987**, *109*, 442.

(114) Huang, S.-T.; Huang, W.-L.; Zhang, H.-B. *CHINESE JOURNAL OF PHARMACEUTICALS.* **2004**, *35*, 265.

(115) Okamura, T.; Kikuchi, T.; Nagamine, A.; Fukushi, K.; Sekine, T.; Arano, Y.; Irie, T. *Free Radical Biology and Medicine* **2005**, *38*, 1197.

(116) Huang, S. H., W.; Zhang, H. *Zhongguo Yiyao Gongye Zazhi* **2004**, *35*, 265.

(117) Tang, Z.; Mayrargue, J.; Alami, M. *Synthetic Communications* **2007**, *37*, 3367.

(118) Topczewski, J. J.; Wiemer, D. F. *Tetrahedron Letters* **2011**, *52*, 1628.

(119) Corey, E. J.; Suggs, J. W. *Tetrahedron Letters* **1975**, *16*, 2647.

(120) Lian, H.; Whitman, C. P. *Journal of the American Chemical Society* **1993**, *115*, 7978.

(121) Van der Steen, M.; Stevens, C. V.; Eeckhout, Y.; De Buyck, L.; Ghelfi, F.; Roncaglia, F. *European Journal of Lipid Science and Technology* **2008**, *110*, 846.

(122) Becht, J.-M.; Marin, S. D. L.; Maruani, M.; Wagner, A.; Mioskowski, C. *Tetrahedron* **2006**, *62*, 4430.

(123) Reddy, G. V.; Jacobs, H. K.; Gopalan, A. S.; Barrans, R. E.; Dietz, M. L.; Stepinski, D. C.; Herlinger, A. W. *Synthetic Communications* **2004**, *34*, 331.

(124) Artyushin, O. I.; Osipov, S. N.; Röschenthaler, G.-V.; Odinets, I. L. *Synthesis* **2009**, *2009*, 3579.

(125) Coxon, F. P.; Ebetino, F. H.; Mules, E. H.; Seabra, M. C.; McKenna, C. E.; Rogers, M. J. *Bone* **2005**, *37*, 349.

(126) Marma, M. S.; Xia, Z.; Stewart, C.; Coxon, F.; Dunford, J. E.; Baron, R.; Kashemirov, B. A.; Ebetino, F. H.; Triffitt, J. T.; Russell, R. G. G.; McKenna, C. E. *Journal of Medicinal Chemistry* **2007**, *50*, 5967.

(127) Taber, D. F.; Raciti, D. M. *Tetrahedron* **2011**, *67*, 10229.

(128) Romanenko, V. D.; Kukhar, V. P. *Beilstein Journal of Organic Chemistry* **2013**, *9*, 991.

(129) Kashemirov, B. A.; Bala, J. L. F.; Chen, X.; Ebetino, F. H.; Xia, Z.; Russell, R. G. G.; Coxon, F. P.; Roelofs, A. J.; Rogers, M. J.; McKenna, C. E. *Bioconjugate Chemistry* **2008**, *19*, 2308.

(130) Singh, A. P.; Zhang, Y.; No, J.-H.; Docampo, R.; Nussenzweig, V.; Oldfield, E. *Antimicrobial Agents and Chemotherapy* **2010**, *54*, 2987.